eman ta zabal zazu

Universidad del País Vasco

Euskal Herriko Unibertsitatea

UNIVERSITÉ DE PAU ET DES PAYS DE L'ADOUR

Fireproofing biosourced-phenolic resins for the protection of wood and wood composites

A dissertation presented by

Pedro Luis de Hoyos Martínez

In Fulfillment of the Requirements for the Degree
Doctor of Phylosophy in Renewable Materials Engineering
by the University of the Basque Country UPV/EHU

Under the co-joint supervision of

Dr. Jalel Labidi

Dr. Fatima Charrier-El Bouhtoury

Chemical and Environmental Engineering Department
Engineering School of Gipuzkoa

Institute of Analytical Sciences and Physico-Chemistry for
Environment and Materials (IPREM), IUT des Pays de l'Adour

Donostia-San Sebastián

2019

I. Preface

The research work presented in this manuscript is enclosed within a Thesis done in joint collaboration between the Universities of the Basque Country UPV/EHU (Spain) and of Pau and Pays de l'Adour UPPA (France) during the period 2015-2019. On the Spanish side, the actions were carried out in Donostia San Sebastian within the Chemical and Environmental Engineering department. On the French side, the research activities were performed at the Institute of Analytical Sciences and Physico-Chemistry for Environment and Materials (IPREM), UMR 5254 CNRS/UPPA, in Pau and Mont de Marsan. Meaningful contributions should be highlighted from the Research & Innovation Forest-Wood group Xylomat platform as well.

I would like to thank the University of the Basque Country UPV/EHU and the University of Pau and Pays de l'Adour for their financial support, which has allowed me to develop this work. I would also like to thank the COST Actions 1306 and 1407 for giving me the opportunity to attend different conferences and workshops, which have helped to increase my knowledge and research competences in the field of renewable materials and to get in contact with the corresponding scientific community.

I would like to express my gratitude towards both my thesis supervisors Dr. Fatima Charrier-El Bouhtoury and Dr. Jalel, whose efforts have allowed me to pursue the doctoral studies. For welcoming me from the beginning in both research groups, for guiding me when I was lost and providing me with different opportunities to progress in my research career.

I want to thank to all my colleagues from the Biorefinery Process group, which have been with me during this whole process. Especially to *"La Banlieu"*, those who have to bear with me day after day within 3 m^2, have helped me when I needed them and have shared moments, travels and experiences.

I also want to mention the colleagues from other international institutions in Italy, Germany or Tunisia with whom I had the pleasure to be in different moments along this journey.

I do not want to forget of course, all my colleagues from the IUT in the "*bureau des doctorants*" and those from the laboratory Xylomat/IPREM in France, thank you for being so nice with me from the beginning of my arrival in Mont de Marsan. Especially to Arsene and Peguy my Gabonese friends, who made my stay in this *"petite ville landaise"* a year to remember.

Last but not least, I cannot express enough all my gratitude to my family and friends. My parents who made me the person I am today, supported me in all my decisions and gave me the strength even from the distance in my weak moments. My brother who always understands me and knows how to cheer me up, being an essential part of my life. My friends, whom I do not see as much as I would like and however, even from 700 km of distance, are there for me.

Finally, a mentioned apart deserves this very important person in my life. She the reason why I ended up in the Basque Country doing this thesis. She has lived this whole jouney with me 24/7. We have laughed, we have cried and yet without you nothing would have been the same, I love you *"txikitxu"*.

Pedro Luis de Hoyos Martínez

Donostia-San Sebastián, October 2019

II. Summary

In the current situation of depletion of fossil fuels, the switch towards the utilization of energy and material sources of renewable nature has become a necessary step to take to assure the sustainability of our system.

In this respect, when focusing into the field of materials, wood is known for being an alternative of significant importance in the building and construction sector, owing to its favourable environmental, structural and mechanical characteristics. Nevertheless, wood is also known for displaying several disadvantages such as its vulnerability to different agents. Within these agents, special attention should be paid to fire, which can provoke considerable damage over wood, jeopardizing its desirable above-mentioned characteristics. Accordingly, the market demands are being focused towards different wood fireproofing treatments lately. The utilization of synthetic resins accounts for one of the most employed solutions within the chemical industry. However, it brings along the present issues related to the raw materials derived from non-renewable sources.

In this context, the substitution of those synthetic resins for other biosourced ones with a similar performance could fulfil the same function of the existing resins but lowering their impact over the environment.

This work is therefore trying to address the previous topic and for that purpose, it has been distributed into five chapters.

In the first one, the current background related to renewable raw materials vs. non-renewable raw materials is discussed with focus on the valorisation of lignocellulosic biomass, the biorefinery process and two of the most important natural phenolic compounds present in nature namely lignin and tannins.

In the second chapter the selection of the raw materials and the extraction processes of lignin and tannins are discussed, along with their characterization.

The third chapter addresses the process of lignin modification to achieve an enhancement of its properties and the combination lignin and tannins in the synthesis of the biosourced resins, together with their chemical characterization.

In the fourth chapter, the actual application of the biosourced resins as element to achieve wood protection against fire is carried out by using two different methods and the assessment of their performance in this respect is done.

The work ends with the fifth chapter in which the main conclusions, remarks and future perspectives of this research are drawn. The scientific publications and works derived from this thesis are listed as well.

III. Research goals and methodology

The general objective of this project is to develop a formulation of a biosourced resin that can be used for the protection of wood and wood composites against fire and to evaluate its performance and effectiveness for the mentioned application. With this purpose, the following specific sub-objectives are proposed:

- Valorisation of agricultural residues and wood and pulp industry by products, as source of phenolic compounds such as lignin and tannins.
- Extraction of the lignin by means of a process, which assures a high yield and purity of the mentioned compound and a low environmental impact.
- Characterization of the lignin extracted and the tannins supplied to get a clear picture of their chemical and reactivity.
- Development of different formulations of biosourced phenolic resins based on lignin and tannins (phenolic raw materials) and inorganic nanoparticles.
- Characterization of the biosourced phenolic resins to evaluate their chemical and thermal properties.
- Application of the synthetized resins as coatings for the protection of wood against fire.
- Assessment of the performance and efficiency of the coatings in wood fireproofing protection field.

With the aim of achieving the previous objectives, the following methodology, which was distributed in several tasks corresponding to different chapters of the thesis, was implemented:

In the second chapter, the lignocellulosic residues coming from the agroforestry sector (almond shells and maritime pine wood) were

characterized according to the TAPPI standards to assess their valorisation as source of lignin. Moreover, a multistage sequential organosolv process was carried out with the purpose of increasing the extraction yields of lignin. The mass balance of the process was performed to evaluate its efficiency and the liquors and solid products from each stage were characterized. The lignins obtained from the organosolv extraction were analysed to elucidate their composition and main structural characteristics. In this same chapter, commercial tannins (mimosa tannins) were characterized chemically to evaluate their composition and reactivity. Thereby, it can be inferred whether they represent a suitable raw material for the synthesis of the biosourced phenolic resins afterwards.

In the third chapter, the functionalisation of lignins isolated in the previous step was performed by means of a process of glyoxalation followed by another process of hybridization with inorganic nanoparticles. The former, was aimed to enhance the reactivity of the lignins, whereas the latter was intended to improve their thermal properties. The lignins were structurally characterized by using several techniques of analysis such as FTIR, GPC, ^{1}H-NMR, XRD and TGA. The process of functionalisation of the lignins was the previous stage to the resin synthesis, which was achieved after the combination of the modified lignins and the above-mentioned tannins. Once the resins were synthetized, they were analysed for several chemical parameters and thermal properties.

In the fourth chapter, the application of the biosourced phenolic resins for the protection of wood against fire was tested. Two different wood types, namely softwood and hardwood were employed to analyse the differences between them. Furthermore, two different wood applications were assessed i.e. surface treatment (coating) and impregnation.

Once the resins were used for the each application, the wood samples were conducted several analysis techniques to assess the wood performance under fire exposure. First, a calorimetry pump was utilized to measure the high calorific values of the wood samples and thus determine their flammability. Secondly, a fireproofing test based on the standard UL 94-HB was implemented to evaluate parameters such as the flame propagation and extinction and the actual fire protection gravimetrically. Finally, a Hot Disk Thermal Conductivity Analysis was performed to see the influence of the resins applied onto the wood in terms of heat conduction compared to wood unprotected.

Table of contents

1. Introduction

1.1 Context and motivation

At this very moment from the XXIth, the main repercussions from our current economic system based on the exploitation of non-renewable sources of materials and energy are becoming increasingly evident. Thereby, the depletion of oil and the greenhouse gas emissions are not upcoming problems anymore. Moreover, taking into consideration the ongoing population growth worldwide, which has experienced a growth of 33% in the last 20 years (from 6 to 8 billion) according to the United Nations Prospects[1], the lives of our future generations are in real danger. Fortunately, in the last years different environmental actions are being implemented. For example in Europe, from the 3rd March 2010 a plan called *"Europe 2020 strategy"* is being carried out. This 10 year-plan, is aiming several objectives in different areas such as employment, research and development, climate change and energy, education and poverty and social exclusion. In the environmental field, it is pursuing the reduction of greenhouse emissions to levels a 20% lower than in 1990, a 20% of energy coming from renewable sources and an increment of the 20% in the energy efficiency[2]. With these purposes, the implementation of various financial instruments such as "*Horizon 2020"* are taking place. The mentioned programme is the biggest European investment ever in Research and Development[3], with a contribution of 80 billion € for a period of 7 years (2014-2020). These policies are showing their influence and thus indicators such as the greenhouse emissions are displaying a decreasing tendency in the last years (Figure 1). This does not mean that the problem of greenhouse emissions is solved. In fact, more efforts would be needed to remove this issue from the picture in the medium-long term. However, the fact that these type of policies are showing a positive effect should encourage more world countries to embrace them.

Figure 1. This indicator measures all emissions of greenhouse gases for the average of the 28 European countries, which includes carbon dioxide (CO_2), methane (CH_4), nitrous oxide (N_2O), and the hydrofluorocarbons, perfluorocarbons, nitrogen triflouride (NF_3) and sulphur hexafluoride (SF_6). They are integrated into a single indicator expressed in units of CO_2 equivalents by employed the individual global warming potential (GWP) of each gas[4].

Worldwide, another agreement that can be highlighted is the one reached at the *"21th Conference of Parties (COP)"* held in Paris in December 2015 and enclosed under the United Nations Framework Convention on Climate Change (UNFCCC). In the mentioned agreement and for the first time, all nations are brought into a joint objective to embrace demanding efforts, which can tackle climate change. These efforts are majorly focused towards a central aim, which consists in maintaining the global temperature increment during this century "*well below 2°C above preindustrial levels and pursuing efforts to limit the temperature increase to 1.5°C above pre-industrial levels"*[5]. This goal is related to requirement that all the signing countries should work united to reduce to zero the greenhouse emissions by the second half of this century. Despite these well-intentioned actions, an opposite party exists as well, which can dangerously undermine and hinder these necessary efforts. The so-call "climate-change deniers" are represented by those countries, companies and/or administrations, which express their doubts and even question the principles of climate change.

Consequently it is time to double efforts and take this environmental crisis very seriously to switch our present system to a more equal and sustainable one.

1.2 Circular economy and biorefinery concept

When talking about a change of the system, it is implied a full change of mindset. Therefore, this new model should aim towards a sustainable development. This requires an equitable and concurrent consideration of several parameters at different levels (economic, social, environmental and technological) and the interrelation between them[6]. To address the topic of sustainable development, the concept of Circular Economy (CE) has appeared in the recent years. This is not a completely new concept but it has attracted a great deal of attention lately, not only around the policymakers[7] but also within the academic research with a significant increment in the number of publications (Figure 2).

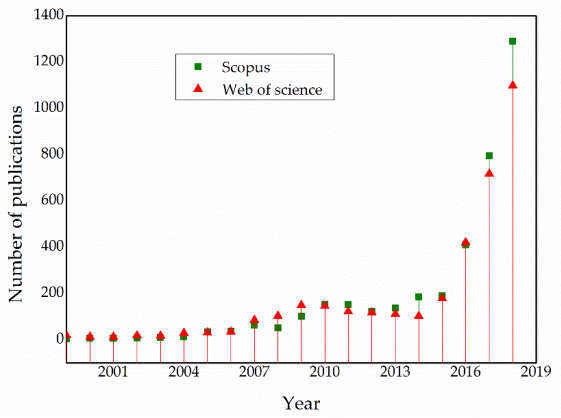

Figure 2. Evolution of scientific publications related to the topic of circular economy along the last 20 years.

The concept of Circular Economy was originated in the late 1970s and its current formulation is attributed to Pearce and Turner (1989). They based on a precedent study of an ecological economist called Boulding (1966), which presented the earth as a close-circular system in which the economy and the environment should be in perfect balance[8].

Concerning the theoretical framework of this concept, Pearce and Turner introduced the need for switch from the traditional linear and open-ended economic system *"Take, make, dispose"* to a circular model based on the principle of cradle-to-cradle, regenerative design or industrial ecology amongst others. The opposite nature of both systems is displayed in Figure 3.

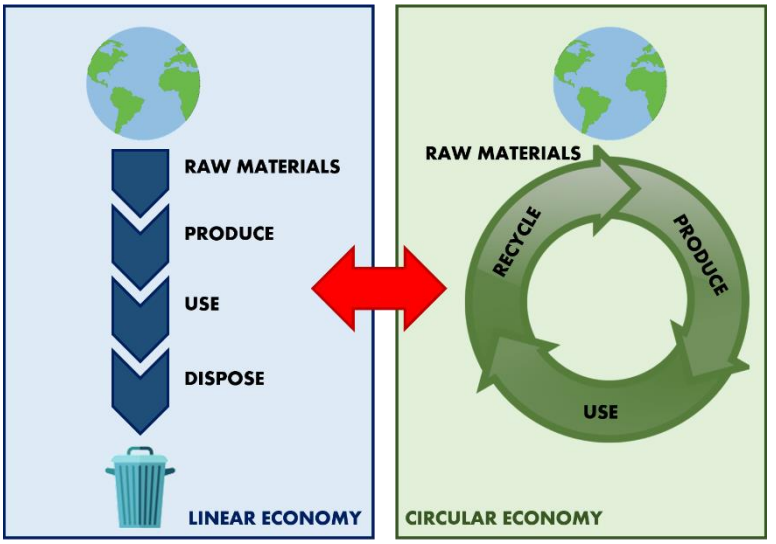

Figure 3. Comparison between the concepts of linear and circular economy.

The concept of circular economy has evolved along the years thanks to contributions made by different authors. Nowadays, the most extended definition has been stated by the Ellen MacArthur Foundation, which introduces circular economy as *"an industrial system that is regenerative by intention and design. It replaces the end-of-life concept with restoration, shifts towards the use of renewable energy, eliminates the employment of toxic chemicals, which impair reuse, and aims for the elimination of waste through the superior design of materials, products, systems, and, within this, business models"*[9]. In summary, circular economy can be described as a model that focuses on keeping products, components and materials at their highest utility and value at all times[10].

Circular economy is sustained on three main principles called "the 3Rs", namely reduction, reuse and recycle[11,12].

- Reduction: this principle is pursuing the minimization of the inputs of energy, raw materials and waste by maximizing the efficiency in the production and consumption processes[13].
- Reuse: this principle is defined as *"any operation by which products or components that are not waste are used again for the same purpose for which they were conceived"*[14].
- Recycle: this principle is referred to *"any recovery operation by which waste materials are reprocessed into products, materials or substances whether for the original or other purposes. It includes the reprocessing of organic material but it does not include energy recovery and the reprocessing into materials that are to be used as fuels or for backfilling operations"*[15].

From the above-listed principles, the ones playing the major roles are the former ones (reduce and reuse). They are the most sustainable solutions compared to the latter one in terms of resource efficiency and profitability[16]. Consequently, those ones should be the first considered, since it is known that recycling is limited by the demand and nature of the materials involved. The implementation of the Circular Economy in our current world is an arduous task since it needs from profound changes at so many different levels (industrial, business, societal etc.). However, new approaches are being taken to embrace the transition towards this more sustainable model, especially at the industrial production level. These approaches are based on the idea of Circular Economy of *"closing the loop"*. This means, that the final objective is the transformation of low value side streams, residues or wastes into more valuable products[17]. In this context, arises the concept of biorefinery. The mentioned concept appear as a useful tool that can help to the transition from a linear towards a circular economy and contribute to the improvement of the public health and environment[18]. A biorefinery presents certain similarities to the traditional refinery but in this case, petroleum is substituted by biomass as feedstock.

There are also other various divergences between them that influence considerably the way in which they operate (Table 1).

Table 1. Comparison between the traditional oil refineries and the biorefineries in terms of several parameters[19].

	Refinery	**Biorefinery**
Feedstock	-Homogeneous nature. -Low oxygen content. -Presence of suphurous compounds. -The weight of the product is incremented with processing.	-Heterogeneous nature. -High oxygen content. -Raw materials in polymeric form. -The weight of the product is decreased after processing.
Building blocks	-Ethylene, propylene, methane, BTX isomers	-Glucose, xylose, fatty acids
Processes	-Mainly chemical processes -Relative homogeneous nature. -Broad range of conversion chemistries.	-Combination of chemical and biochemical processes. -Relative heterogeneous nature. -Narrow range of conversion chemistries.
Intermediates at commercial scale	-Abundant.	-Few but with an increasing trend.

Concerning the biorefinery concept, there are two widely employed definitions. On the one hand, the IEA Bioenergy Task 42 states that *"biorefining is the processing of biomass into a spectrum of marketable products (food, feed, materials, chemicals) and energy (fuels, power and heat)*[19]. On the other side, the National Renewable Energy Laboratory (NREL) defines biorefinery as *"a facility that integrates biomass conversion processes and equipment to produce fuels, power and chemicals from biomass"*[20].

As seen from the previous definitions, it is clear that the major goal of a biorefinery is the production of a range of different products, using all kinds of biomass as feedstock and by means of different process technologies. Ideally, this approach should be able to compete with the traditional oil refineries but providing considerable environmental and technological advantages. Therefore, an important feature is the level of integration, which could assure the complete employment of all the resources. The energy demands of the process of transformation of biomass should be provided internally by the heat or electricity obtained from the valorization of the residues through of a combination of processes and technologies suitable designed[21].

Traditionally biorefineries have been classified according only to several individual parameters such as the type of feedstock employed, the level of integration, the type of conversion process used and the type of main intermediates produced. Nevertheless, since 2008 the IEA Bioenergy Task 42 developed a more precise and specific biorefinery classification system[22]. As described by Gnansounou and Pandey, 2017[23] this new classification system is pursing the next goals:

- To avoid ambiguity for the stakeholders in the biorefinery field.
- To provide accuracy concerning the feedstocks, platforms and final products.
- To display the complexity of the biorefinery facility
- To be appropriately accurate and specific in naming each biorefinery.

With these aims, the classification system is based on the illustrative representation of the chain from the full biomass to the end-products. Thus, this approach consists in the combination of four main features displayed in Table 2.

Table 2. Features considered for the description of the different biorefineries configurations.

Parameter	Description
Platform	Intermediates that can be used as link between biorefinery systems and their processes (e.g. C5/C6 sugars).
Product	The two main biorefinery groups are energy (e.g bioethanol or biodiesel) and products (e.g. chemicals or materials respectively).
Feedstock	The main groups within the biorefineries are energy crops (e.g. starch crops or short rotation forestry) and biomass residues (e.g. straw, bark or waste streams from biomass processing).
Process	Divided in four conversion processes such as biochemical (e.g. fermentation), thermochemical (e.g. pyrolysis), chemical (e.g. acid hydrolysis) and mechanical (e.g. pressing).

With the combination of the previous parameters, any type of biorefinery can unambiguously depicted by quoting the involved platforms, products and feedstocks and the process e.g. *oil biorefinery using oilseed crops for biodiesel, glycerin, and feed by means of pressing, esterification and distillation*[24].

1.3 Biomass and feedstock selection

A change of the system could not only be achieved by switching to new economic and production models such as the described in the previous section. Consequently, it is also necessary a swift towards new energy and material resources of renewable nature. Within all these renewable sources, a great deal of attention has been attracted specially by biomass.

This is motivated by several factors or strengths of this raw material[25]:

- It is an abundant and renewable source, which can be produced anywhere and that represents an option to decrease the dependency to oil.
- It provides a solution to poverty in under developed and developing countries, promoting the rural employment.
- It contributes to the reduction of the carbon dioxide (CO_2) emissions.

Concerning the biomass concept, there is not an only agreed definition. Generally, it can be defined as *"organic matter originated from living, or recently living microorganisms"*[26]. Nevertheless, other definitions can be found based on the context in which the concept is treated. On the one side in the field of bioenergy, biomass has been defined by the Directive 2009/28/EC as the *"biodegradable fraction of products, waste and residues from biological origin from agriculture, forestry and related industries including fisheries and aquaculture, as well as the biodegradable fraction of industrial and municipal waste"*[15]. On the other side, in the area of bioeconomy it has been stated that *"biomass consists of the renewable biological resources for their conversion along with other waste streams into value-added products such as food, feed, bio-based products and bioenergy"*[27].

Different biomass classifications can be found through the literature, according to the criteria used. Here two classifications are presented based on the chemical composition and origin of the biomass. Thereby the different types of biomass can be observed[28] as showed in Table 3.

Table 3. Types of biomass according to principle used for its classification.

Criteria	Types
Origin	Agricultural biomass
	Forest biomass
	Residues, wastes and by-product biomass (includes sewage and solid municipal wastes)
	Aquatic biomass
Chemical composition	Lignocellulosic biomass (with a predominance of cellulose, hemicellulose and lignin)
	Sugar-rich biomass
	Starch-rich biomass
	Oil-rich biomass
	Protein-rich biomass

In the present work, biomass is employed as the starting raw material from which the phenolic compounds are extracted. Nevertheless, a necessary previous step was the selection of the type of biomass to be used. For this purpose, it was considered the fact this is a research in joint collaboration between universities of two different countries (France and Spain). Accordingly, one type of biomass was selected from each country. The main factors contemplated to choose the type of biomass were the availability and potential economic impacts that could be derived from the valorization of these resources in both countries.

In the French side, the research was located in Mont Marsan in the French department of "Landes", which is enclosed within the region of "Nouvelle Aquitaine" at the south-west of France. In this region, the forestry resources are of significant importance, since they represent the major surface of forest in France with 2803±43 x1000 ha[29]. Within this forest surface, there is a predominance of resinous wood species, which triplicate the number of non-coniferous species[30].

Between the resinous species, maritime pine (*Pinus pinaster*) is the most representative one especially in the French department of "Landes" as it can be observed in Figure 4. Consequently and considering the previous data, it was decided to select forestry residues from maritime pine (*Pinus pinaster*) as the biomass source coming from the French part.

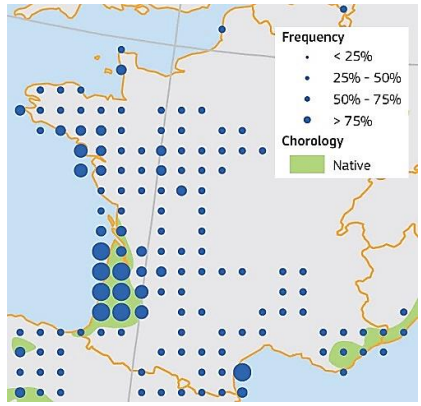

Figure 4. Plot distribution of the frequency of *Pinus pinaster* occurrence in France[31].

In the Spanish side, the research was situated in San Sebastian, within the region of the Basque Country in the north of Spain. Here the type of biomass selected was almond shells, which is a residue coming from the agriculture. Spain is the second world's major producer of almonds (0.2 million tons) after the USA according to FAOSTAT. Almond shells, which are the lignocellulosic material forming the husk of the almond tree fruit, are ranging 35-75% of the total fruit weight[32]. Hence, between 70-150 million kg of this waste are remaining annually in Spain and accordingly, almond shells valorization as a potential source of and materials is of great interest. Normally almond shells are burned owing to their higher heating value (HHV) which is comparable to that of forest residues[33]. Nevertheless, this generates problems such as air pollution, soil erosion and decrease of soil biological activity[34]. Consequently, the valorization of almond shells through their lignocellulosic components (cellulose, hemicellulose and lignin) appears as a more environmentally friendly solution.

1.4 Lignocellulosic biomass

Between the different types of biomass, the lignocellulosic counts as the most abundant group representing almost 70% of the total plant biomass[35]. Moreover, it is the most abundant organic material present in nature[36] with an estimated annual production worldwide of over $200 \cdot 10^9$ tons approximately[37]. For these reasons, it presents an excellent potential as renewable feedstock for energy and materials. Furthermore it does not compete with food and animal feed[38].

Lignocellulosic biomass can come from different sources such as agricultural and forestry residues, grasses and woody materials. Chemically, they are composed of two different components namely non-structural and structural[39]. In Figure 5, a schematic representation of the cell wall in lignocellulosic feedstocks is presented.

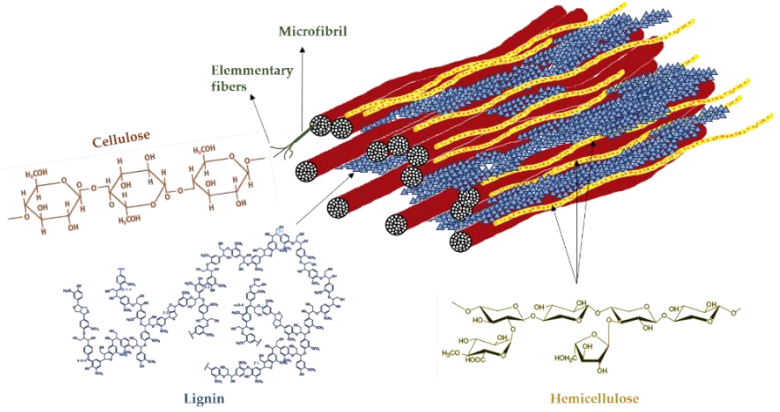

Figure 5. Diagram of the main component present in the plant cell wall.

The *non-structural components* are present in a minor extent in the lignocellulosic biomass. They are a variety of compounds non-chemically attached or attached by low-energy bonds (Van der Waals, hydrogen and electrostatic bonds) to the lignocellulosic cell wall including ashes, water, extractives and proteins[40]. On the other side, the *structural components* represent the most prominent group in lignocellulosic biomass.

They can be divided into two main groups namely cell wall polysaccharides and phenolic compounds[41].

- Cell wall polysaccharides: Within this group, two main fractions can be distinguished i.e. the cellulose and hemicellulose. **Cellulose** is the major component of the plant cell wall structure. It is defined as a complex polysaccharide formed by D-glucose moieties linked via β-(1→4) glycosidic bonds (Figure 6).

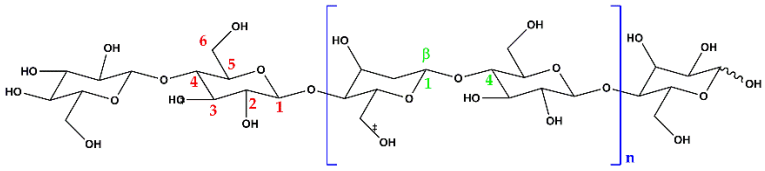

Figure 6. Chemical structure of cellulose.

It represents the most abundant organic polymer in nature and it is constituted of crystalline parts together with amorphous regions. Cellulose is a straight-chain polymer, which presents a rigid and extended structure with a rod-like conformation[42]. **Hemicellulose** is the second renewable polymer in abundance of the world after cellulose. Opposite to cellulose, it is a heterogeneous polymer based on pentoses (xylose, arabinose), hexoses (glucose, mannose and galactose) and/or uronic acids (glucuronic, methylgalacturonic and galacturonic acids) (Figure 7).

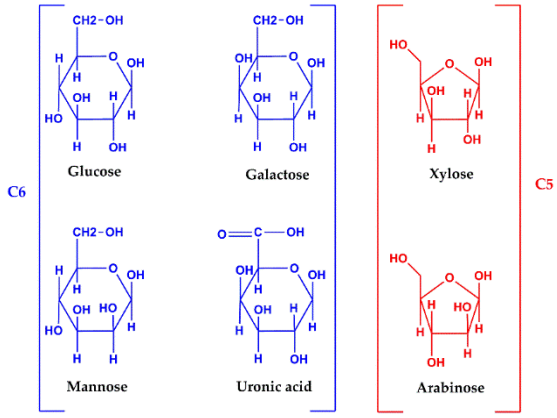

Figure 7. Main monomeric moieties of hemicellulose.

It is usually bound to other compounds in the cell wall, acting as linkage between cellulose and lignin. Its composition relies considerably on the vegetal source but also on plant tissue and geographical location. Thus, for instance in hardwood species they are mainly composed of xylans, whereas in softwood species the more prominent units are glucomannans.

- Phenolic compounds: Within the plant cell walls, three different types of phenolic compounds can be differentiated such as lignin, tannins and phenolic acids[41]. **Lignin** is the third natural polymer in abundance in the lignocellulosic biomass. It is known for being a heterogeneous polymer with a marked crosslinked and aromatic nature. It confers to the lignocellulosic biomass excellent structural and mechanical properties. **Phenolic acids** are majorly structural components of the lignin core, such as carboxyl and phenolic groups, which permit the bonds between lignin and carbohydrates via ester and ether linkages.

  Tannins are not structural components but they are also important group of phenolic compounds within lignocellulosic biomass. They are a family of compounds also characterized by their structural heterogeneity and aromatic nature. In the cell wall, they can be found linked to protein or polysaccharides[43].

  Lignin and tannins are two families of compounds being subject of a considerable number of researches lately (Figure 8). This is due to their phenolic nature, which is of great potential for partial or total replacement of fossil materials. For this reason, these compounds were chosen as the main raw materials to be used from biomass within the present work. In the following sections, a more profound description of both families of compounds will be provided.

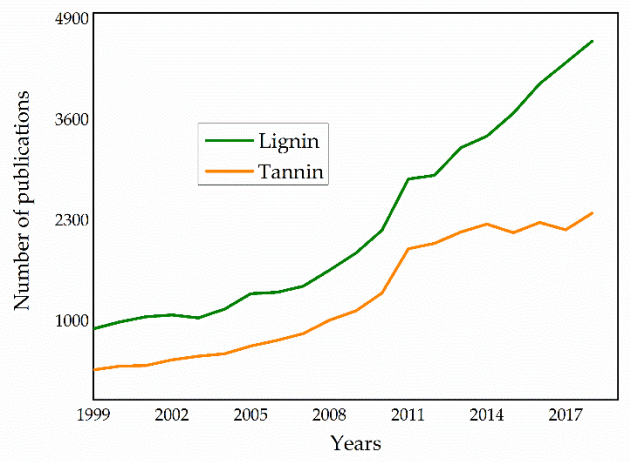

Figure 8. Works find in the literature regarding lignin and tannin-derived research.

1.5 Lignin

Lignin is defined as an amorphous-tridimensional biopolymer derived from the polymerization of phenylpropanoid moieties with hydroxyl and methoxy substituents[44]. It is known for being the most abundant organic aromatic polymer in nature.

1.5.1 Lignin chemistry and structure

Chemically, lignin is an irregular and heterogeneously crosslinked polymer, which is composed of three major precursors (monolignols) namely p-coumaryl, coniferyl and sinapyl alcohols[45]. From these precursors, radicals are formed during the lignin biosynthesis, which incorporated into the lignin polymer. These are called p-hydroxyphenyl (H), guaiacyl (G) and syringyl (S) moieties respectively[46] (Figure 9)

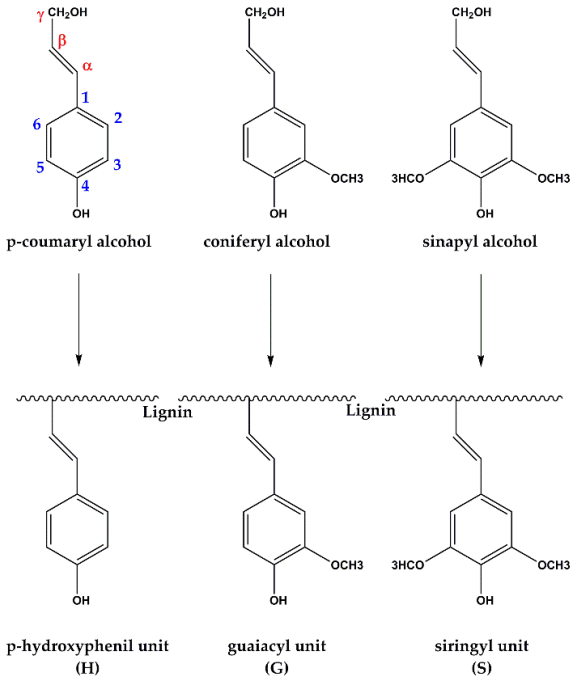

Figure 9. Types of precursors and monomeric units of lignin.

All the monomeric units of lignin have a hydroxyl group in C4 but they differ on the methoxyl groups substituted in the positions C3 and C5, with none, one or two of groups. The side chain carbons are identified as α, β and γ, being Cα linked to aromatic C1. During lignin polymerization, these moieties are linked between each other via condensed bonds (C-C) and ether (C-O-C) linkages. The most reactive positions are the Cβ, which easily turns into aryl-ether bonds and the phenoxy oxygen[47]. The most common interunit linkages between lignin moieties are presented in Figure 10.

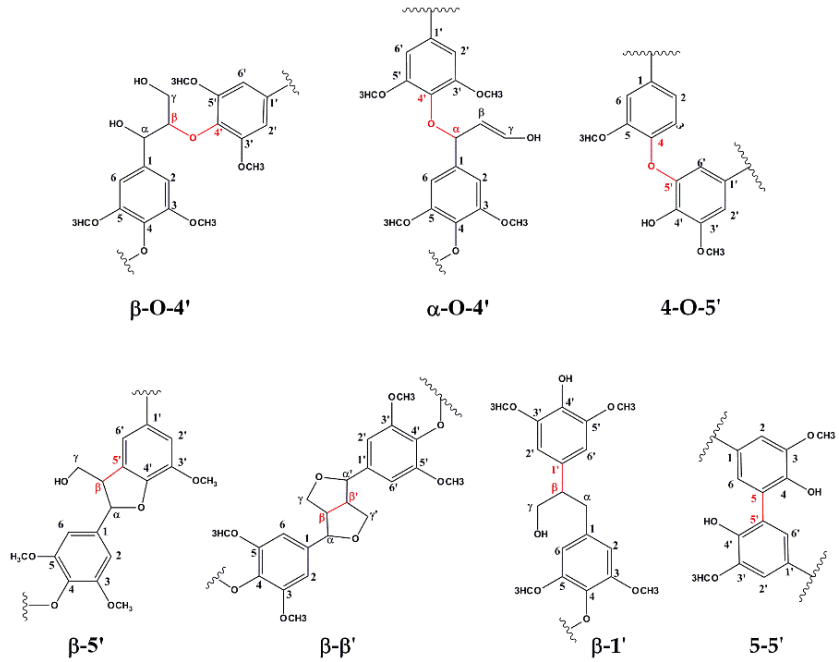

Figure 10. Main types of linkages between units in lignin structure.

The structure of the lignin molecules is seen to display several functional groups, which have a significant influence on its reactivity[48]. According the current knowledge on lignin structure and chemistry, the most typical functional groups present are phenolic and aliphatic hydroxyl groups and carbonyl and carboxylic groups in a smaller extent, along with the aromatic metxoyl groups previously commented[49]. The distribution of these functional groups rely on different parameters such as the lignin origin and the isolation process.

1.5.2 Lignin in nature: function, origin and abundance in plants

The term lignin is derived from the latin *"lignum"*, which means wood. It has been already introduced as one of the main components of the cell wall in plants.Particularly, lignin is an essential compound for the cohesion of the secondary cell walls, since it provides fundamental mechanical properties to the cells, needed for functions such as water transportation and structural support[50].

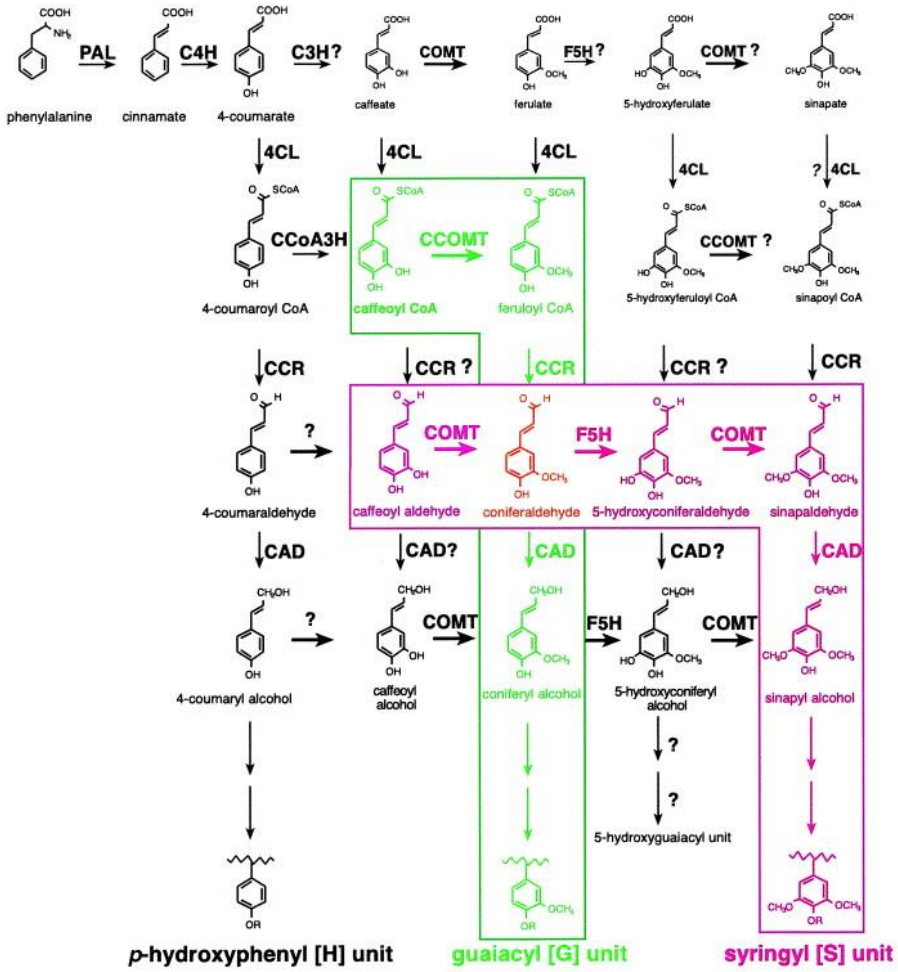

PAL: phenylalanine ammonia lyase, C4H: cinnamate 4-hydroxylase, C3H: p-coumarate3-hydroxylase, COMT: caffeic acid O-methyltransferase, F5H: ferulate 5-hydroxylase, 4CL: 4-coumarate coenzyme A ligase, CCoA3H: 4-coumaroyl-coenzyme A 3-hydroxylase, CCOMT: cafeoyl-coenzyme A O-methyltransferase , CCR: cinnamoyl-coenzyme A reductase, CAD: cinnamyl alcohol dehydrogenase.

Figure 11. General phenylpropanoid pathway to monolignols. All enzyme reactions shown with a solid arrow have been demonstrated to occur in vitro. Reactions shown in smaller type may not occur in vivo. The reactions shown in green seem the most likely route to G lignin in vivo. The reactions in red represent those reactions consistent with both in vivo and in vitro evidence for being involved specifically in S lignin biosynthesis. The intermediate in orange is common to both G and S lignin pathways. (Reproduced from Dixon et al., 2001[54] with permissionof Elsevier via Copyright Clearence Center).

The formation of lignin in the secondary cell wall follows the general phenylpropanoid pathway (Figure 11) and starts with the biosynthesis of monolignols. These monolignols are originated from phenylalanine through a sequence of reactions in which several enzymes are involved[51] e.g. phenylalanine ammonia lyase, cinammat-4-hydroxylase, ferulate-5-hydroxylase etc. Once the monolignols are synthetized, they are oxidized to the corresponding radicals. This oxidation reaction is mediated by different enzymes such as peroxidases and/or laccasses[52]. Then, the obtained radicals are polymerized by means of various reactions with free-radical coupling mechanisms, leading to the final phenylpropanoid units[53].

The lignin content and its composition generally varies consistently between different plants species. For instance in hardwood species, lignin content can range 15-25%, while in softwoods it can represent up to 25-35%[55]. Concerning lignin composition, significant differences are also observed (Table 4). Gymnosperm species (softwood), display lignins with a prominence of guaiacyl units (G). On the other hand, angiosperms (hardwood) present a more complex structure since in this case, lignin is derived from the polymerization of both coniferyl and sinapyl alcohols. Thereby, syringyl (S) and guaiacyl (G) units can be found within the lignin structure, with approximately equal amounts of each one[56]. In both of the previous species (softwood and hardwood), p-hyxroxyphenyl (H) moieties can be present as well, but in very small amounts. These units are prominently encountered in non-woody species such as grasses[57].

Table 4. Composition of the lignin depending on the source.

	Presence of lignin units		
Species	**p-Hydroxyphenyl units (H)**	**Guaiacyl units (G)**	**Syringyl units (S)**
Hardwood		X	X
Softwood		X	
Grass	X	X	X

1.5.3 Lignin applications

Lignin displays a great potential for different application owing to its aromatic polymeric structure[58]. The lignin properties also have a considerable influence over its potential applications in various areas.

Table 5. Applications of lignins in different areas of the industry according to the literature.

Applications		Area	Reference
Synthesis of carbon fibers			59
Enhancement of cement performance			60
Synthesis of polymer composites from lignin.	Thermoplastic polymers	Materials	61
	Thermosetting polymers		62
	Rubbers		63
	Biodegradable polymers		64
	Nanocomposites		65
Fuel source (production of char, syngas, hydrogen and aromatic hydrocarbons)		Energy	66
Energy storage			67
Synthesis of resins	Substituent of phenol in phenol-formaldehyde resins.	Chemicals	68
	Epoxy resins.		69
	Substituent of polyols in polyurethanes for the production of foams.		70
Additive to animal and human food.		Food	71
Scavenger or sequestering agent for water treatment.		Environment	72
Synthesis of bionanoparticles to be used as delivery systems such as drug release.		Biomedicine	73
Additive in healthcare products.		Cosmetics	74

For example, in the field of materials, lignin-derived ones (Table 5) present several advantages over the synthetic ones due to properties such as its biodegradability, availability, abundance in industrial wastes or low cost[75]. In other sectors such as medical and cosmetic industries, features like its antioxidant and antimicrobial nature make lignin the perfect candidate for several uses. In the following table the range of different applications studied for lignin in the last years are presented.

1.6 Tannins

Tannins are the most abundant components extracted from biomass, after cellulose, hemicelluloses and lignin[76]. Besides, they represent the second most extensive source of phenolic compounds after lignins[77]. The "tannin" definition has its origin in the primary function of this group of compounds i.e. tanning. The tanning process has been important along history since it allowed the protection of animal skins turning them into leather by means of plant extracts. The first species reported for tanning leather was oak, which was actually designated with the name "tann" among the Celts[78]. One of the first tannins definitions was given by A. Seguin in 1796, who described them as substances in vegetable extracts used for converting animal skins into stable leather[79]. Nevertheless, it was not until the early 1960s that a more accurate definition of tannin was introduced by Swain and Bate-Smith in 1962. They defined tannins as "*naturally occurring water soluble polyphenolic compounds having a molecular weight between 500 and 3000, capable of precipitating alkaloids as well as gelatin and other proteins from aqueous solutions*"[80]. This definition is the one most frequently found and cited within the literature.

1.6.1 Tannins in nature: abundance, occurrence and function in plants

Tannins are well distributed among the vegetal kingdom being present in both terrestrial and aquatic environments.

Their content is majorly dependent on the species considered. In terrestrial environments, tannins are found in high concentrations in several species such as *Schinopsis balansae* (quebracho wood), *Acacia mearnsii* (black mimosa bark), *Pinus radiata* and *Pinus nigra* (pine species), *Quercus spp* (oak bark.) and *Castanea sativa* (chestnut wood). On the other hand, in aquatic environments they are present in non-vascular plants (primitive non flowering plants without roots, stems or leaves), emergent salt marsh vegetation[81] and mangroves[82]. Nevertheless, within the same species the tannin content is reported to vary between the different parts of the plant with special abundance in barks, leaves, seeds, roots and rhizomes[79]. In the literature, there are several works in this respect, remarking the influence of the different species and parts of the plants on the tannin content[83,84]. For instance, it was reported by Cheng et al., ,2012 that the variety of the grape employed significantly influenced the amount of tannins quantified in the extracts[85]. They found that the extracts of the variety *Pinot Noir* presented higher amount of tannins than *Pinot Meunier*. This was attributed to the different viticulture practices and environmental conditions. Moreover, the amount of tannins was higher in the seeds compared to skin and pomace.

In addition, tannin content can also vary with seasonal and environmental factors e.g. water availability, temperature, light intensity and soil quality[86]. Thus, their concentrations can change between seasons owing to the different stage of growth of the plant and demand for nutrients[87]. For example, during the growth period, when plants produce a lot of biomass, few resources are available for synthesis of phenolic compounds (low tannin content). However, at the time of flowering, the plant growth decreases and an excess of carbon is produced. This carbon is then available for the synthesis of tannins (high tannin content).

Respecting tannins function in plants, they are known for being secondary metabolites[88]. This means that they are not essential for the growth and the development but they play a major role in the plant survival owing to their defensive properties against insects and herbivores[89].

1.6.2 Tannins classification and chemistry

The categorization of tannins based on their structural aspects and chemical characteristics is the most extended, since it offers a proper framework for further study. Traditionally, tannins were divided into two major classes namely condensed and hydrolysable tannins. However, currently two other types are also considered i.e. complex tannins and phlorotannins.

Condensed tannins are defined as polymeric flavonoids[90]. However, they can appear as oligomers as well, when they are composed of two to ten monomeric units[91]. In the form of polymeric flavonoids they have limited to no solubility in water, whereas in oligomeric form they are water soluble[92]. Within the flavonoids group, condensed tannins are considered as flavanols, since they are composed of flavan-3-ol moieties[93] (Figure 12).

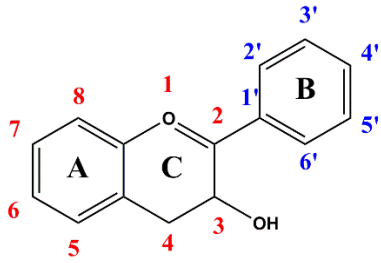

Figure 12. Flavan-3-ol structure and its nomenclature.

The flavan-3-ols units can display different structures depending on the type of "A" and "B" rings present. "A" ring can appear as a phloroglucinol or resorcinol moieties, whereas "B" ring can be arranged as a catechol or pyrogallol units. These combinations lead to the formation of several monomers of condensed tannins. The compounds showed in table 6 are the precursors of various types of condensed tannins. In this sense, the tannins whose structure is exclusively composed of (epi)catechins are designated as procyanidins, which are the most abundant type of condensed tannins present in plants.

On the other part, those tannins mainly formed by (epi)fisetinidol, (epi)robinetinidol and (epi)gallocatechin units, are labelled as profisetinidin, prorobinetidin and prodelphindin respectively.

Table 6. Structures of the most common flavan-3-ol monomers of condensed tannins.

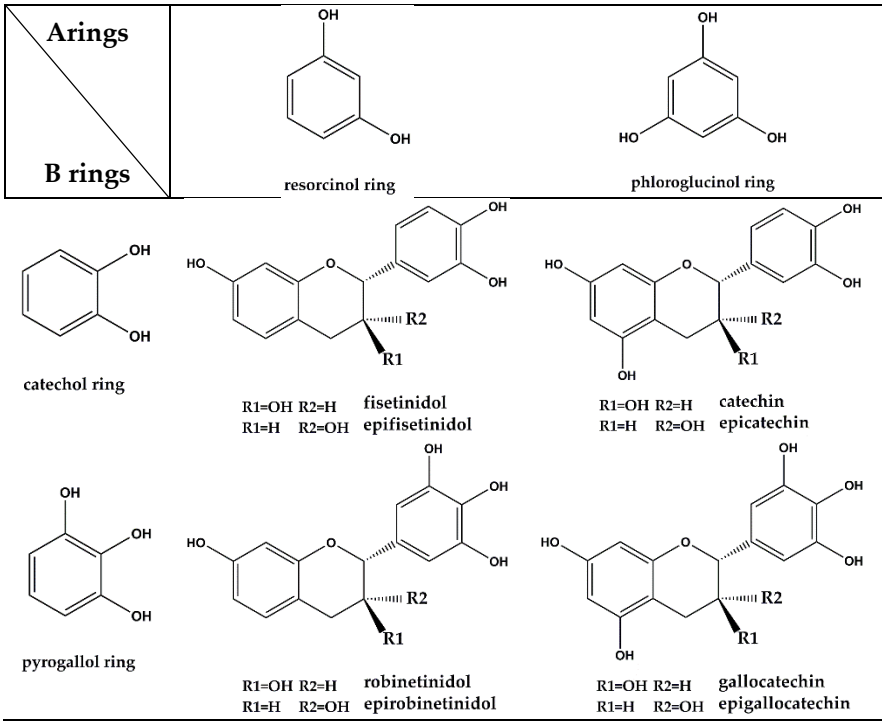

Condensed tannins monomeric units are joined via interflavonoid bonds, which are mainly C-C (either C4-C8 or C4-C6) and occasionally C-O-C[94]. In the C4-C8 linkages, the C4 carbon corresponds to the extender and the C8 carbon to the terminal unit. This type of bonds usually lead to linear structures, whereas the C4-C6 bonds induce the formation of branched polymers and oligomers (Figure 13).

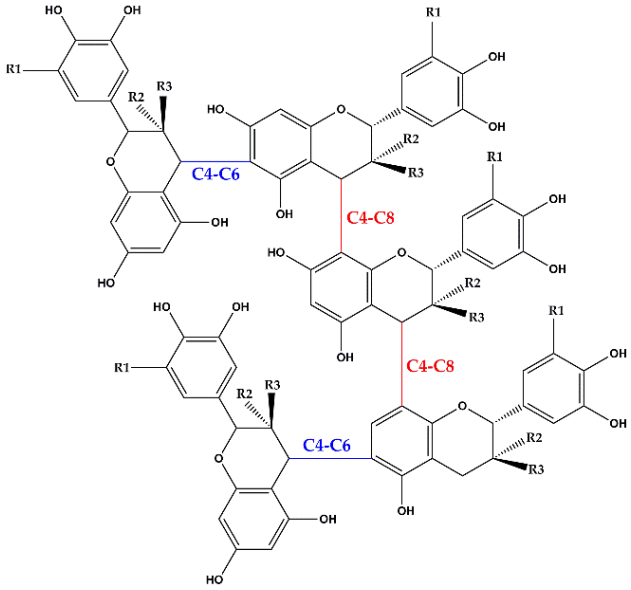

Figure 13. Major links between monomeric units in condensed tannins polymers and oligomers.

Hydrolysable tannins are heteropolymers composed of polyphenolic acids and their derivatives, esterified to a polyol[95]. This polyol, generally a carbohydrate, forms a central core to which several polyphenolic acid units are attached via ester bonds (Figure 14).

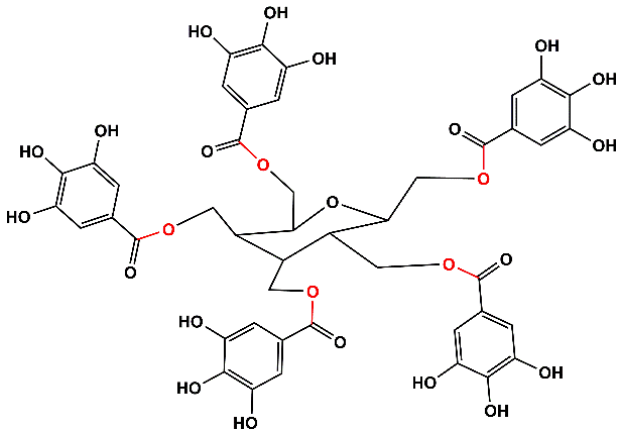

Figure 14. Example of a hydrolysable tannin unit and the linkages present (e.g. pentagalloyl glucose structure linked via ester bonds).

Gallic acid (GA) is the most basic block attached to the core of the monomeric units. Gallic acid moieties can yield other derivatives such as hexahydroxydiphenic acid units (HHDP), via oxidative coupling of two or more molecules. In turn, the HHDP units can spontaneously lactonize to ellagic acid (EA) moieties upon hydrolysis[96]. In Figure 15, the transformation between the different polyphenolic acids, which can be present in hydrolysable tannins structure are showed.

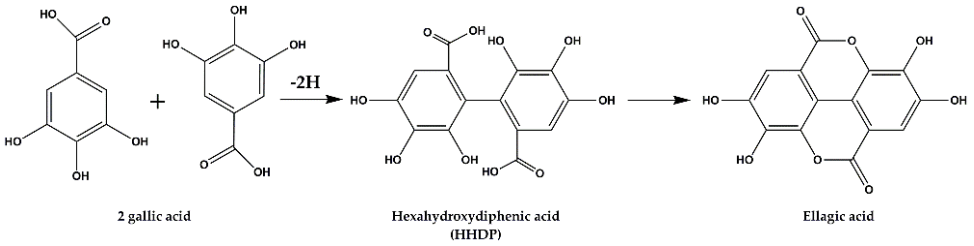

Figure 15. Transformation between the main polyphenolic acids and derivatives present in the structure of hydrolysable tannins.

The distinctive property of hydrolysable tannins is their ability of being fractionated hydrolytically into their basic components[97]. This is due to their ester bonds, which are susceptible to break via hydrolysis under acidic and basic conditions. Thererby, they are usually classified into two main subcategories i.e. gallotanins and ellagitannins.

- Gallotannins: they represent the simplest kind of hydrolysable tannins and consist of galloyl or digalloyl units linked to a polyol core. The hydroxyl groups of the core can be either completely or partially substituted by galloyl units[76]. They have the ability to yield gallic acid from the hydrolysis reaction.
- Ellagitannins: this kind of tannins are characterized by having one to several HHDP units attached to a polyol core. Upon hydrolysis, ellagitannins are able to produce HHDP free units, which spontaneously turn into the dilactone (ellagic acid).

Another type of tannins recently considered within the literature is **complex tannins**. This kind is characterized by the presence of monomeric units of hydrolysable and condensed tannins[98]. They are composed of a gallotannin or ellagitannin moiety and a flavan-3-ol building block connected through a carbon-carbon linkage. This type represents a minoritary group within the tannins family. A typical example of this kind of compounds is accutisim A (Figure 16).

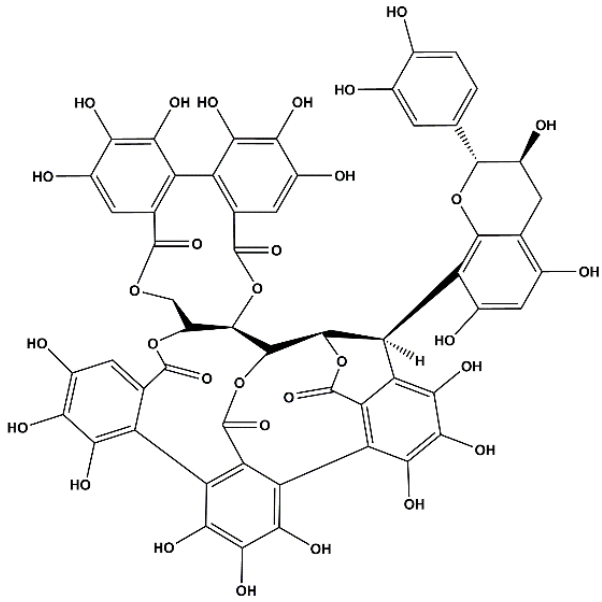

Figure 16. "Accutisim A", a typical example of complex tannins group.

Phlorotannins are another type of tannins discovered in the recent years. This group is prominently found in brown algae and is composed of phloroglucinol units (1,3,5-trihydroxybenzene). The research carried out lately on this group of tannins, has led to the structural elucidation of more than 150 compounds with a large range of molar masses between 126-625000 g·mol^{-1} [99–101]. Structurally phlorotannins form dehydro-oligomers and polymers of phloroglucinol moieties linked via aryl-aryl (C-C) and diaryl ether bonds (C-O)[102]. Thus, they can be divided in different subgroups, according to the kind of linkage between the monomers (Table 7).

Table 7. Different types of phlorotannins regarding the linkages between units.

Denomination	Linkages	Structure
Fuhalol (a) Phloroethol (b)	Ether (-C-O-C-)	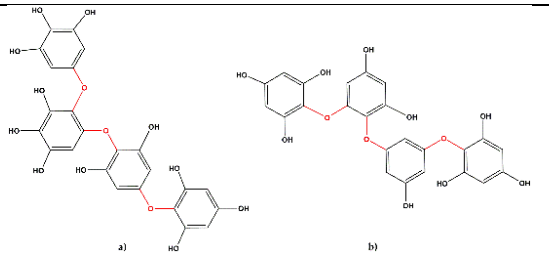
Fucol	Phenyl (-C_{Ph}-C_{Ph}-)	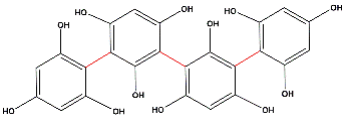
Fucophloroethol	Ether (-C-O-C-) + Phenyl (-C_{Ph}-C_{Ph}-)	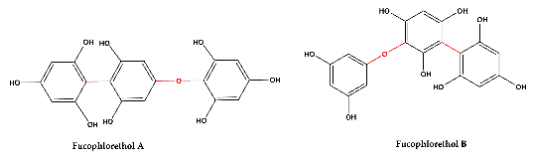
Eckol (a) and carmalol (b)	Dibenzodiox in	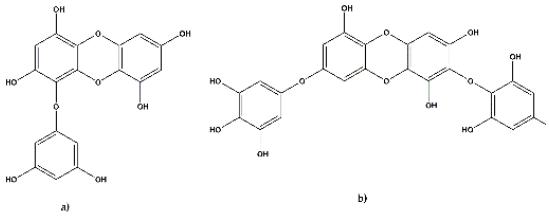

1.6.3 Tannins applications

Historically the first tannins application was related to the tanning of leather. This was thanks to their ability of precipitating proteins in animal hides to obtain a non-putrescible material. Nowadays, with the advances in the tannins chemistry, their utilization has developed and spread to a wide variety of areas and industries. The main areas of application of tannins are presented in the following points:

- Food industry: tannins have been used within this field lately, following the current trend towards the utilization of natural functional ingredients owing to the demand of consumers for cleaner labels. Thus, they are being employed in several food products and beverages, due to their desirable colour and health benefits[103]. Their more representative application relies on the wine industry and oenology, where they are utilized as additives during the process of fermentation[104].
- Medical industry: the utilization of tannins in medicine is not new, since some herbs whose active principles are astringent tannins have long been used for medicinal purposes. Their antioxidant nature is the main feature regarding their applications in this field. This is linked to the phenolic rings present in their structure, which can act as electron scavenger to trap different anions and radicals. Thus, tannins have proved interesting outcomes in several studies within this area regarding their antimicrobial[105], antibacterial[106], anti-inflammatory[107], antimutagenic or anticarcinogenic[108,109] properties.
- Chemical industry: they have started to play a major role in this sector in the last years as potential renewable source of products e.g. phenolic resins. In this respect, they can provide a good substituent of "greener nature" to phenol, thanks to their polyhydroxylated aromatic structure. As part of phenolic resins, several application can be listed according to literature such as adhesives[110] or foam products[111] for insulation, heat exchange or adsorption purposes. They have also been used as reinforcement in biobased materials such as composites[112].

2. Extraction and characterization of raw materials

This second chapter is devoted to the characterization of the lignocellulosic biomass from which the phenolic raw materials used, are extracted and extraction and to the characterization of the specific phenolic raw materials used for the synthesis of the biosourced resins. The phenolic raw materials are referred to the lignins extracted from these lignocellulosic biomass sources and the tannins selected. The chapter is divided into three sections A, B and C. Part A is focused on the chemical characterization of the two lignocellulosic biomasses to assess their suitability as lignin source. The second section (B) is centered on the justification of the type of lignin, which was selected, compared to the rest lignin types available, the process of extraction of the lignin from the two different sources of biomass and finally the characterization of the lignins extracted. In the final part (C), the central topics are the argumentation about the selected type of tannins as phenolic raw material and the characterization of the mentioned tannins in terms of composition and reactivity.

Part A. Characterization of the sources of lignocellulosic biomass selected

A.1 Motivation

The selection of the types of lignocellulosic biomass was based on the availability and significance of the raw materials. These points were assessed for the regions where this research was carried out, namely "Basque Country" (north Spain) and "Landes" (south France). Thereby, the raw materials chosen were almond shells (Spanish side) and maritime pine wood residues (French side). In this section, a chemical characterization of the mentioned biomass was performed to elucidate their composition and therefore evaluate their suitability as raw materials, especially as source of lignin.

The almond shells employed, were coming from almond trees (*Prunus amygdalus*) of the variety "Marcona" and they were provided by local farmers of the nearby area. Concerning the maritime pine wood (*Pinus pinaster*) residues, they were composed of leftovers from wood industry activities such as small pieces of wood, parts of wood panels or wood chips.

A.2 Experimental procedure

The raw materials namely almond shells and maritime pine residues were pretreated prior to any characterization analysis. During the pretreatment the two types of lignocellulosic biomass were milled and sieved to particle size lower than 0,25 mm to assure an intimate contact with the reagents utilized and therefore proper characterization results (no over- or underestimations). Once both almond shells and the maritime pine wood residues had the desired size, they were subjected to moisture (TAPPI T264-cm-97), ethanol-toluene extractives (TAPPI T204-cm-97) and ashes (TAPPI T211 om-02) quantification. The elucidation of the insoluble lignin content was performed by quantitative acid hydrolysis with 72% H_2SO_4 (TAPPI T222-om-98). Besides the hemicellulose and cellulose content were determined according to methods proposed by Wise et al., 1946 [113] and Professor R. Rowell, 1984 [114] respectively. All these characterization methods of the materials chemical composition are described in the section Annex I.

A.3 Results and discussion

Following the procedures mentioned above, the main parameters concerning the chemical composition of the two raw materials were determined. The results are shown next in table 8.

Table 8. Chemical composition on dry basis (% w/w) of the raw materials selected.

Component	Raw material	
	Almond shells	**Maritime pine residue**
Cellulose	18.19±0.19	34.05±0.05
Hemicellulose	35.99±1.23	18.07±0.22
Lignin	31.24±0.29	30.36±0.68
Extractives	3.11±0.32	5.40±0.14
Ashes	0.81±0.09	0.32±0.11

The composition of the almond shells was in general in accordance with the values of other works from the literature[115,116]. Nevertheless, some differences were observed derived from the characterization technique, the grain size of the material employed or the composition, which can vary from one year to another. In this study quantitative acid hydrolysis (TAPPI T249-em-85) was performed instead of other TAPPI norms used generally for wood characterization (since almond shells are not exactly woody materials). Moreover, in our work the almond shells were milled and sieved to a size small enough (0.25 mm) to assure the intimate contact with the reagents used in the characterization. The differences encountered, are especially marked in the lignin content (e.g. 31.24% compared to 52.59%). Such a big value for lignin can be derived from an overestimation of this component when the grain size of almond shells is not small enough for an intimate contact with the characterization reagents.

In the case of maritime pine wood residues, the values obtained for each component were within the ranges of other works[117,118], without any significant divergences.

A4. Conclusions

In both cases, it was seen that lignin is one of the major components concerning its abundance. The values range around 30% of the sources of lignocellulosic biomass. This content of lignin, in addition to local availability of these resources, was consistent with a favorable valorization of both raw materials as a source of lignin for further applications.

Part B. Lignin extraction and characterization

B.1 Motivation

A key point in lignin valorization is the method employed for its extraction. In this respect, several process are utilized nowadays with this purpose displaying different advantages and disadvantages. In this section, the distinct lignin extraction processes are first presented and the one selected for performing the lignin isolation is properly justified, highlighting its importance and advantages against the other processes. Furthermore, a case of study of a multistage process for the lignin extraction is introduced. In the final part a comparison is carried out for the single extraction process and the latter characterization between the lignins obtained from the two lignocellulosic biomass selected in the previous section.

B.2 Background

Traditionally lignin is produced as a by-product of the pulp and paper industry. Thereby the most common processes employed industrially for isolating lignin are Kraft and sulfite methods[119]. However, they exhibit some disadvantages derived from environmental aspects of the process and the heterogeneity of the extracted lignins. This has triggered a growing interest on the sulfur-free delignification processes such as organosolv, alkaline and ionic liquid pretreatments[120]. In this point, the above-mentioned processes are described with their main strengths and weak points.

B.2.1 Kraft process

This is the most implemented industrially pulping process in the world[121]. Furthermore, it is responsible for the majority of the lignin produce in the industry (about 85% of the worldwide production)[122].

This chemical process consist in the treatment of the wood chips at elevated conditions of temperature (140-170ºC) and pressure with an alkali solution of sodium hydroxide (NaOH) and sodium sulfide (Na_2S) known as "*white liquor*"[123]. The pulping reactions allows the solubilisation of lignin in the pulping liquors. Due to reaction with the hydroxide and hydrosulphite anions, the lignin undergoes several structural changes such as the breakage of the ether linkages between units, which decreases its molecular weight; the increment of the condensed C-C bonds and phenolic hydroxyl groups[124] and the introduction of thiol groups within its structure[125]. The lignin dissolved through this process leads to a so-called "*black liquor*", which is generally concentrated via evaporation and burned to recover heat and chemicals. The isolation of the Kraft lignin from the black liquor requires from its acidification by means sulfuric acid (H_2SO_4) or carbon dioxide (CO_2)[126]. As a result of that, the pH is lowered and the lignin precipitated. Then, it can be recovered by filtration and washing. The isolated Kraft lignin is reported to display a sulfur content, which ranges 1-3% (w/w)[127].

B.2.2 Sulphite process

This treatment is based on the process patented by Tilghman in 1867 for the manufacture of paper, where wood was decomposed by means of sulphur salts and acids[128]. Currently, in the sulphite pulping process lignin reacts with sulphite (SO_3^{-2}) or bisulphite (HSO_3^-) ions yielding lignosulfonates as by-products[129]. The conditions of the pulping process can confer different properties to the lignosulfonates obtained. Generally, the treatment is performed at acidic pH (1-5) or neutral (5-7) and the cations mostly employed are sodium and calcium (Na^+, Ca^{2+}) but others can also be used such as magnesium or ammonium (Mg^{2+}, NH_4^+)[130].

During the process, the lignin undergoes two main reactions, namely sulfonation and hydrolysis[131]. As a result of these reactions sulfonate groups (SO_3) are integrated into the lignin structure, which conduces to an increase of their solubility[132]. After the pulping, the lignosulfonates can be isolated from the spent liquor via filtration.

Within this spent liquour, lignosulfonates account for 50-80% (w/w) but other components are present such as carbohydrates and residual chemicals[133]. For this reason, lignosulfonates usually display a high content of impurities (around 30%) and wide distribution of molecular weights[134]. Concerning their average molecular weights, they are usually high and even higher than those of Kraft lignins[125].

B.2.3 Alkali process

Alkaline treatment is the oldest pulping method[135] and it is based on the employment of reagents of strong alkaline nature. Currently, it is implemented especially on non-woody biomass such as annual plants or agricultural residues. In this process, the biomass is reacting with different alkali reagents at high temperatures and pressures[136]. Along alkaline treatment two main reactions are taking place, the dissolution of lignin and hemicellulose and the rupture of the of the ester linkages between moieties (saponification)[137]. The reagent most typically used is sodium hydroxide (NaOH), but other agents have been reported for performing this treatment such as sodium carbonate (Na_2CO_3), ammonium (NH_4^+), calcium hydroxide ($Ca(OH)_2$) and hydrazine[138,139]. From the previous reagents, sodium hydroxide is generally used for being the strongest one. It allows the effective cleavage of lignin-carbohydrate linkages, the ester bonds previously commented and the condensed carbon linkages between lignin units[139]. The lignins isolated by this method display the advantage of being sulphur free. Nevertheless, they can present a high ash content derived from the presence of soda in the reaction[124].

B.2.4 Ionic liquids process

This type of process is receiving a great deal of attention lately. It is based on the utilization of ionic liquid as solvents for the treatment of the biomass and isolation of the lignin. The ionic liquids are a novel kind of solvents compose of ions with favorable conditions such as low melting point (below 100ºC), high polarity and thermal stability and insignificant vapor pressure[140].

During the reaction, the ionic liquids are said to compete for the H linkages with the other components, thus breaking the lignocellulosic network[141]. With this process, a high purity lignin can be extracted from the biomass by properly selecting the ionic liquid. Moreover, the lignins extracted are also sulphur free and the solvent can be recovered and reused, reducing the amount of wastes of the process[142]. Nonetheless, they display some disadvantages such as their high cost and the difficulty of implementing the recovery and recycling processes[143].

B.2.5 Organosolv process

Organosolv extraction method is an efficient technique for delignification based on the employment of a mixture formed by an organic solvent and water[144]. The most typical organic solvents are alcohols (methanol or ethanol) or organic acids (formic and acetic acid)[123]. The pretreatment can be carried out at a broad range of temperatures (100-250ºC) and high pressure. During the process, the lignin is solubilized into the solvent and the washing liquor and then it can be precipitated by lowering the pH. Several reactions are generally occurring during this pretreatment. The most relevant for lignin extraction, is the hydrolysis of the lignin-hemicellulose linkages and internal lignin bonds via cleavage of the 4-O-methylglucuronic acid ester bonds and α and β-O-aryl ether linkages[145]. It is known that the cleavage of these aryl ether bonds is responsible for the break-down of lignin. The α-O-aryl ether are separated more easily, while the β-O-aryl ether linkages need more severe conditions[146]. Through this solubilization, lignin and lignin-carbohydrate compounds (in lower

extent) can be precipitated from the liquid phase whereas cellulose and some hemicellulose remain in the solid residue. The organosolv pulping is generally considered more efficient and environmentally friendly compared to other methods such as Kraft and sulphite processes but it also displays several advantages against sulphur free methods like alkali or ionic liquid processes (table 9). Furthermore, it is the most effective alternative to extract lignin without altering its native structure[149].

Table 9. Advantages of the organosolv-lignin-extraction process against the rest of the processes.

Extraction processes		Comparison points
Organosolv process	Kraft process	Organosolv process is sulphur-free avoiding air and water pollution. A green solvent can be employed in organosolv process. The purity of the lignins obtained is higher in the organosolv process.
	Suphite process	The organosolv lignins present lower molecular weight and higher hydrophobicity.
	Alkali process	Organosolv process yields high purity lignins avoiding the significant salt amount formed in alkali process. The water consumption in organosolv process is lower.
	Ionic liquids process	The recovery of the lignin and the regeneration of the ionic liquid is difficult and presents a high cost. The organosolv process provide an easier and less expensive recovery of the solvents by means of evaporation and condensation.

Sources: Fernandez et al., 2019 [123]; Chaturvedi and Verma, 2013 [147]; Kumar and Sharma, 2017 [143]; Lora and Glasser, 2002 [148].

Taking into account the previous points, the process selected for performing the lignin extraction from the lignocellulosic biomass was the organosolv pretreatment.

B.3 Case of study: sequential multistage organosolv extraction process

In this part, a case of study consisting in the implementation of a multistage organosolv system composed of three sequential extraction stages is shown. The purpose of this process was the study of the maximization of the lignin extraction yield. The lignins obtained from each extraction stage were characterized to evaluate if significant chemical or structural changes existed between them. The proposed system was firstly applied to the lignin extraction from the almond shells to assess (in base to the results) if it could be extrapolated to the other source of lignocellulosic biomass.

B.3.1 Experimental procedure

In the following points, the reagents and equipment employed in the implementation of the process are detailed along with the presentation of the multistage process and the description of the parameters (solvent, temperature, pressure, time etc.) selected for the organosolv extraction.

B.3.1.1 Raw materials and equipment

The almond shells, which were provided by local farmers, were coming from almond trees (*Prunus amygdalus*) of the variety *Marcona*. These almond shells were crushed and sieved by means of a Retsch Hammer mill to chips with a size lower than 1 cm prior to the extraction process. Thus, impurities such as little stones, soil or dust could be removed. The chemical reagents employed for the extraction process and chemical assays were kindly supplied by Sigma-Aldrich.

B.3.1.2 Process set up

A multi-step extraction process was developed to maximize the delignification of the almond shells. Thereby three sequential organosolv pulping cycles were carried out resulting in highly pure lignins from each cycle. The diagram displayed in figure 17 show the different streams derived from the process. In the first cycle (C1), the almond shells (AS) underwent organosolv pulping process yielding two different streams i.e. black liquor (BL1) and almond shells pulp (ASP1) from the first cycle. The former was used for the precipitation of the lignin from the first cycle (L1) whereas the almond shells pulp (ASP1) was employed as raw material for the second cycle (C2). In this second cycle, the almond shells pulp (ASP1) went through another organosolv pulping process. Again, two separate products were obtained namely black liquor (BL2) and almond shells pulp (ASP2) from the second cycle. The lignin from the second cycle (L2) was anew precipitated from the black liquor (BL2) and the almond shells pulp (ASP2) was utilized as the starting material from the third cycle (C3). This last cycle was implemented analogously to the previous ones resulting in black liquor (BL3) and precipitated lignin (L3) from the third cycle and almond shells pulp (ASP3).

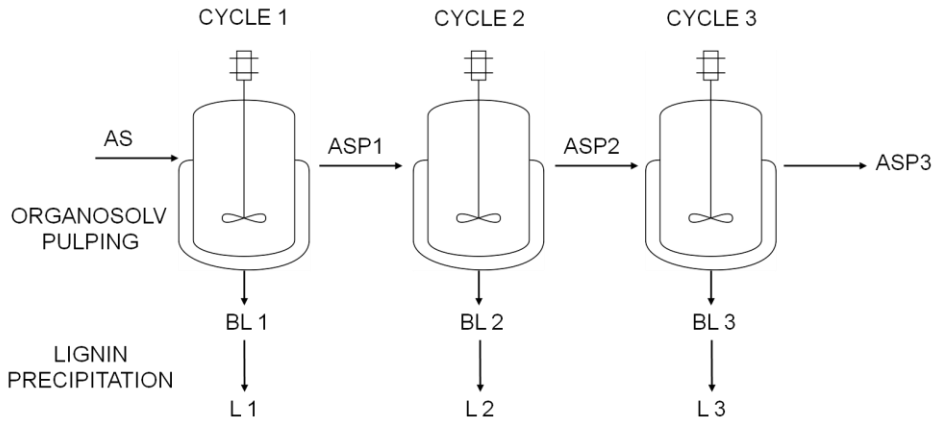

Figure 17. Diagram representing the process set up of the multistage system for the organosolv extraction of lignin.

B.3.1.3 Organosolv extraction process

The organosolv process used in each stage of the system to extract the lignin is described next. The process was carried out employing a mixture of ethanol/water (70:30 v/v) at 200 ºC during 90 minutes with a ratio solid to liquid 1:6. It was implemented in a 1.5 L stainless steel Parr Reactor under constant agitation. The liquid phase was separated from the almond shells pulp remaining via filtration. This pulp was washed several times with a mixture of ethanol/water and dried at 50 ºC until all the moisture was removed. The liquid phase (black liquor) went through a precipitation step to extract the dissolved lignin. The procedure was done using two volumes of acidified water (pH around 2) per volume of black liquor obtained. The suspension was left to settle overnight to allow a better lignin precipitation. After that, the precipitated lignin in suspension was filtered using polyamide filters (0.22 μm pore size) under vacuum and washed with distilled water until neutral pH was achieved. Finally, the recovered lignin was dried at 50 ºC for three days.

B.3.1.4 Characterization methods

As presented in section A for the two sources of lignocellulosic biomass, here the chemical composition of the solid pulps remaining after each stage was determined (cellulose, hemicellulose, lignin, extractives and ashes).

The methods used were also based on the TAPPI standards and they are described in the corresponding sections of Annex I. For the characterization of the liquors and the lignins obtained from each stage of the system several methods were employed, which are described in the Annexeses II and III and summarized in table 10.

Table 10. Characterization methods used for the analysis of the chemical composition of de liquors and lignins and their structure

Component	Analysis	Technique	Annex	Section
Liquor	Physico-chemical parameters	pH	Annex II	II.1.1
		Density		II.1.2
	Composition	TDS[A], IC[B], OC[C], LC[D]		II.2
	Chemical composition	Klason lignin		III.1.1
		Acid soluble lignin		III.1.2
		Ashes		III.1.3
		Carbohydrates		III.1.4
Lignin	Total hydroxyl groups	Folin Ciocalteau assay	Annex III	III.2
	Molecular weight	HPSEC[E]		III.3
	Structural units (S/G ratio)	Py-GC/MS[F]		III.4
	Thermal properties	TGA[G]		III.5

[A]TDS: total dissolved solids, [B]IC: inorganic compounds content, [C]OC: organic compounds content, [D]LC: lignin concentration, [E]HPSEC: High performance size exclusion chromatography, [F]Py-GC/MS: *Pyrolysis-gas chromatography/Mass spectrometry analysis and [G]TGA: Thermogravimetric analaysis.*

B.3.2 Results and discussion

Here are presented the main results from the previous experiments, to assess the changes in the composition of the starting materials (almond shells and pulps) and the liquors; and the structural characteristics of the lignins extracted.

B.3.2.1 Chemical composition of the raw materials

The characterization of the raw materials used in the subsequent extraction stages was performed to know their initial composition. The results are enclosed in Table 11 and presented in terms of percentages of cellulose, hemicelluloses, lignin, extractive and ashes.

Table 11. Initial composition of the raw material utilized in this work and the pulps remaining after each extraction step.

	Cellulose (%)	Hemicelluloses (%)	Lignin (%)	Extractives (%)	Ashes (%)
AS	18.19±0.19	35.99±1.23	31.24±0.29	3.11±0.32	0.81±0.09
ASP1	42.97±0.61	29.21±0.33	15.97±0.78	4.42±0.41	ND[(A)].
ASP2	48.06±0.75	23.83±0.41	15.02±0.63	1.68±0.21	ND[(A)]
ASP3	48.63±1.27	22.15±0.26	14.85±0.40	0.93±0.05	ND[(A)]

[(A)]*ND: non detectable*

As it can observed in the previous table, the content of the different components in the almond shell pulps (ASPs) varied substantially from that of the raw material. Indeed the content of the two main components (hemicelluloses and lignin) was considerably reduced. In the case of hemicellulose, such a decrease was caused by the harsh conditions of pressure and temperature employed, which led to its degradation. On the other side, the lignin reduction was expected since it was the goal of the organosolv treatment. Respecting to the content of cellulose and extractives, an increasing tendency was observed. Nonetheless, the content of the former underwent a substantial boost whereas the percentage of the latter grew slightly. These rises do not imply that the amounts of cellulose and extractives were bigger in the ASPs than in AS but that they diminished less than hemicellulose and lignin contents. This is confirmed in the mass balance afterwards.

When comparing the content of the different components in the ASPs, two clear tendencies could be regarded. On the one hand, the content of cellulose was increasing, mainly from the ASP1 to the ASP2. On the other hand, the content of the rest of the components tended to decrease. The amount of ashes in the ASPs was negligible and therefore it was too low to be detected.

B.3.2.2 Efficiency of the process extraction cycles

The effectiveness of the different cycles was assessed in terms of lignin extraction yields (overall, relative, total amount extracted yield) and yields of ASPs (Table 12).

Table 12. Parameters for the evaluation of the efficiency of the different extraction cycles

Cycle	Overall yield[A] (% w/w)	Relative yield[B] (% w/w)	ASP yield[C] (% w/w)	Total amount of lignin extracted[D] (% w/w)
C1	16.75±0.29	79.95±1.16	39.21±0.79	79.95±1.16
C2	3.27±0.14	27.14±1.52	77.43±1.12	85.39±0.72
C3	0.96±0.09	15.86±2.75	85.05±2.19	87.73±0.34

(A)– Amount of lignin extracted related to mass of used biomass

(B)- Amount of lignin extracted related to the lignin content in the biomass used

(C)- Amount of pulp remaining after each extraction cycle

(D)- Percentage of lignin extracted after each cycle related to the initial amount of lignin in biomass

From the previous results, it can be observed that high extraction yields were obtained in the first cycle, whereas lower efficiencies were achieved in the second and third ones. The reason for that was that after each extraction cycle the amount of lignin available was lower and therefore less lignin could be extracted. On the contrary, the yields of ASP were increasing as the cycles passed by, owing to the reduction of the pulp solubility.

These two tendencies were interrelated and hence, the fact that in each cycle less amount of pulp was dissolved, resulted in less amount of lignin transferred from the pulp to the liquor and therefore less amount of lignin recovered. After the three consecutive extraction cycles, 87.73% of the total lignin present in the almond shells at the beginning was recovered. This yield was comparable to that obtained in a precedent work (89.40%)[119].

B.3.2.3 Mass balance of the process

Once the chemical characterization of the raw material and pulps was known and their yields elucidated, a mass balance of the whole system was carried out. Thereby, the variations in the amounts of different components through the cycles could be monitored. The mass balance was based on the quantity of almond shells fed into the reactor at the beginning of cycle 1 (100 g). The results of the mass balance are presented in table 13.

Table 13. Mass balance of the whole process of organosolv delignification of the almond shells presented by steps.

	Cycle	Initial amount (g)	Amount dissolved (%)	Cellulose (g)	Hemicellulose (g)	Lignin (g)	Extractives (g)	Ashes (g)
AS		100		18.19	35.99	31.24	3.11	0.81
	C1		60.79					
ASP1		39.21		16.85	11.45	6.26	1.73	N.D[a]
	C2		22.57					
ASP2		30.36		14.59	7.23	4.56	0.51	N.D[a]
	C3		14.95					
ASP3		25.82		12.55	5.71	3.83	0.24	N.D[a]

In regards to these data, it was proved that the majority of the lignin was extracted after the first cycle. Similar to lignin, more than the half of the hemicellulose amount was degraded in this stage. On the other hand, the amount of cellulose remained almost intact between AS and ASP1. Considering these previous tendencies, it can be explained the great increase of cellulose percentage displayed in Table 11.

The reason for that was that the amounts of hemicellulose and lignin decreased highly after first extraction cycle and hence cellulose became the major component in the pulps. Concerning the second extraction cycle, it was not as effective to the lignin as the first one was. Thereby, no big differences were encountered in the composition between ASP1 and ASP2. The bigger reduction was regarded in the hemicellulose content, although again it was much lower than that of the first cycle. This was a result of the pulp degradation, owing to the high temperature and pressure underwent during the extraction. The amount of the rest of the components slightly decreased, because of these conditions. Third cycle showed only a small reduction in the extraction efficiency for all the components. The reason for this loss of efficiency compared to the other cycles was that the pulp was already too degraded and saturated from the previous extraction processes at such severe conditions. Regarding the total extraction of the different components, lignin (which was recovered) and hemicellulose were majorly extracted by the end of the third stage. On the other hand, the amount of cellulose did not go through a significant change, since almost 70% of the initial content remained after the whole extraction process.

B.3.2.4 Liquors characterization

The main physico-chemical parameters of the liquid fraction obtained from the delignification processes were assessed and summarized in table 14.

Table 14. Parameters for the chemical characterization of liquors: pH, density, total dissolved solids (TDS), organic compounds (OC), inorganic compounds (IC) and lignin content in the liquor (LC)

	pH	Density (g/cm^3)	TDS (%)	IC (%)	LC (g/L)
Liquor C1	4.09±0.03	0.89±0.00	6.62±0.18	ND[(a)]	35.17±0.32
Liquor C2	4.29±0.01	0.86±0.00	2.20±0.10	ND[(a)]	8.34±0.38
Liquor C3	4.27±0.01	0.88±0.00	1.13±0.19	ND[(a)]	2.29±0.33

The values of the pH and density were similar for all the liquor samples since the conditions used in each stage of the almond shells delignification were the same. Concerning the TDS and LC, a reduction was observed from the liquor C1 to the liquor C3. It must be noted that the TDS content was almost completely associated to the OC content, since no inorganic matter was detected in the liquors. Focusing on the OC and LC contents it was concluded that both parameters were highly related since it was expected that the lignin in the liquor accounted for the majority of the organic compounds. For this reason, both parameters were reduced after the sequential extractions. The main reduction was observed between the first and the second extraction cycle (from 35.17 to 8.34 g·L-1). This was in agreement with the reduction of the lignins extraction yields mentioned in the previous part (especially between the two first delignification steps). Thus, as the lignin content in the liquor, was dramatically diminished there was a lower amount of lignin available to be extracted resulting in a much lower yield.

B.3.2.5 Lignins characterization

Within this part are presented the results from the different analysis carried out for the lignins extracted (chemical composition and structure).

Chemical composition of lignins

The characterization of all the lignins samples was determined for elucidating their chemical composition (Table 15).

Table 15. Parameters measuring the chemical composition of lignin samples: klason lilgnin (KL), acid soluble lignin (ASL), total sugars (TS) and ashes.

	KL (%)	**ASL (%)**	**TS (%)**	**Glucose (%)**	**Xylose (%)**	**Ashes**
L1	89.30±0.44	2.18±0.25	1.49±0.18	---	0.98±0.18	4.04±0.49
L2	92.07±0.89	2.05±0.80	1.62±0.07	---	1.62±0.07	3.59±1.31
L3	89.14±1.51	1.38±0.03	3.83±0.05	2.15±0.05	1.68±0.04	3.69±0.69

The different lignin samples showed high KL percentage and therefore high purity (≈ 90%), as was expected for organosolv lignins[150]. The values were similar and within a narrow range, since they were extracted from the same feedstock under analogous circumstances. This implies that sequential extraction process did not jeopardize the purity of the lignins extracted. Respecting to the acid soluble lignin content, the values tended to slowly decrease from extraction stage to extraction stage due to the delignification processes. On the other side, lignin was also said to yield lignin carbohydrate complexes (LCC) owing to non-covalent interactions and oxidative reactions with polysaccharides[151]. These compounds represented certain percentage in the lignin content, considered impurities, which was assessed by measuring the sugar content. The sugar content in the lignin samples was low proving once more their high purity. This content was increasing following the delignification processes. The reason for that was that the lignins from the different steps were gradually becoming more condensed and with stronger linkages. Thus, the removal of the remaining sugars impurities was hindered as the stages went by. Xylose was the main sugar from the hemicellulose fraction found in the lignins. This was in agreement with that reported by Gordobil et al., 2014[152]. This trend was not observed in the lignin from the last extraction cycle, which had a higher amount of glucose. In this case, the bigger presence of glucose could indicate that at the last stage some cellulose was removed from the ASP. The harsh conditions underwent by the pulp sample after 3 cycles, would have caused the dissolution of cellulose along with the lignin.

<u>High performance size exclusion chromatography (HPSEC)</u>

Through this technique, the main parameters measured were the weight average, number average molecular weights and polydispersity index (Table 16).

Table 16. Variation of the weight average (Mw), number average molecular weights (Mn) and polydispersity index (Mw/Mn) of lignins.

	M_w (g/mol)	M_n (g/mol)	M_w/M_n
L1	6371	1286	4.96
L2	6606	1491	4.43
L3	6730	1775	3.79

As shown in the previous table no significant differences were observed between the lignins concerning their average and number average molecular weights. The values were low and within the typical range of organosolv lignins[144]. Nevertheless, they slightly increased following the successive lignin extraction steps. This tendency might point out that at the beginning, the lignin structure was more branched and the linkages were broken more easily. Therefore, the remaining fragments had a bit lower molecular weight. However, as the delignification stages moved forward, the lignin structure became more condensed and the linkages were more difficult to break leading to a slightly higher molecular weight lignin.

Respecting to the polydispersity index, the tendency was the opposite to that of the molecular weights. This could be because the lignins obtained in the final stages had a more condensed structure owing to the increase of the C-C bonds and were more stable.

Total Hydroxyl content (Folin-Ciocalteau Assay)

The quantification of the relative content of hydroxyl groups in the different lignin samples was done using the Folin Ciocalteau assay. This is important, since the content of hydroxyl groups is reported to be a good indicator of the reactivity of the lignins[153], providing a point of comparison between them concerning their potential applications. The results were calculated in terms of concentration of gallic acid equivalents (CGAE), percentage of gallic acid equivalents (%GAE) and percentage of hydroxyl groups (%OH) and were presented in Figure 18.

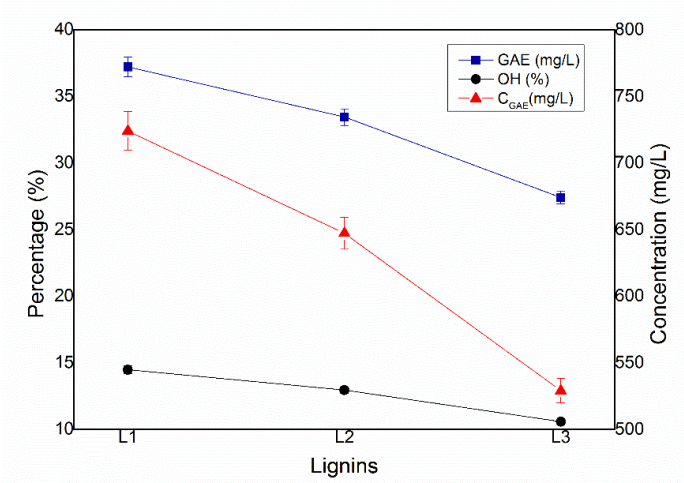

Figure 18. Variation of the different parameters calculated for the phenolic content of the lignin samples.

The values obtained for the previous parameters were comparable to those reported in other works in the literature for organosolv lignins[154,155].

Besides, it was observed that these parameters were decreasing following the sequential delignification steps. This fact would indicate a degradation of the phenolic compounds owing to the extraction steps at harsh conditions. The reduction of hydroxyl groups proved as well that the lignins extracted after the consecutive cycles presented a more condensed structure. On the contrary, the higher content of hydroxyl groups in the lignin extracted in the first cycle compared to the others highlighted its higher reactivity.

Analysis of lignin composition by Py-GC/MS

The pyrolysis analysis yielded a huge and heterogeneous number of compounds (phenols, acids, esters and ketones), from which the phenolic ones were the most abundant group. Phenols are related to the lignins reactivity and they can play an important role in potential applications. For this reason, special focus was put on this group and they were properly evaluated. The mentioned phenols were classified into different subcategories, depending on the substituents as reported by Chen et al., 2015[156].

Thereby five groups of compounds namely benzene type (B), phenol type (P), catechol type (C), guaiacol type (G) and syringol type (S) were defined. The identification and characterization of the main phenolic compounds and derivatives produced during the pyrolysis is included in Table 17.

Table 17. Compounds identified and quantified in the different lignin samples

Molecule	m/z	Origin	Retention time (min)	Content (%)		
				L1	L2	L3
Styrene	104/103/78	B	5.894	0.02	---	---
Phenol	95/66/65	P	7.361	0.16	0.12	0.07
4-methyl-Phenol	108/107/77	P	8.908	0.2	0.13	0.08
Guaiacol	109/124/81	G	9.209	1.82	1.53	0.89
4-Ethyl-phenol	107/122/77	P	10.556	0.2	---	---
4-Methyl-Guaiacol	138/123/95	G	11.23	2.28	1.74	1.39
Catechol	110/64/81	C	11.397	0.13	---	---
3-methoxy catechol	140/125/97	C	13.124	0.47	0.35	0.25
4-ethyl guaiacol	137/152/122	G	13.615	1.02	0.55	0.47
4-vinylguaiacol	150/135/107/77	G	14.834	3.21	4.06	2.5
p-allyl phenol	134/133/107	P	15.55	0.07	0.06	0.02
Syringol	154/139/111/96	S	15.908	3.6	2.85	1.62
Eugenol	164/149/131/77	G	16.035	0.79	0.74	0.46
4-Propylguaiacol	137/166/122	G	16.266	0.31	0.16	0.12
Vanillin	151/152/81	G	17.086	1.71	2.02	1.23
cis-isoeugenol	164/149/77/131	G	17.225	0.48	0.41	0.23
4-methyl syringol	168/153/125	S	18.114	8.01	3.32	2.58
trans-eugenol	164/149/77/103	G	18.097	---	3.52	1.4
4-Propylguaiacol	137/166/122	G	18.299	0.19	0.84	0.61
acetoguaiacone	151/166/123	G	18.825	0.82	1.34	0.77
4-ethyl syringol	167/182/168/77	S	19.489	1.71	1.05	0.81
Guaiacyl acetone	137/180/122	G	19.604	0.92	0.46	0.889
4-vinylsyringol	180/137/165	S	20.147	4.2	5.1	2.93
Propioguaiacone	151/180/123	G	20.413	0.53	0.48	---
4-allylsyringol	194/91/119	S	20.696	1.66	1.4	0.68
4-Propylsyringol	167/196//168	S	20.777	0.67	---	---
cis-4-allylsyringol	194/91/179	S	21.377	1.59	1.4	0.85
syringaldehyde	182/181/167	S	21.568	3.08	3.02	1.79

Molecule	m/z	Origin	Retention time (min)	Content (%)		
				L1	L2	L3
trans-4-allylsyringol	194/91/179	S	22.082	8	8.75	4.12
Acetosyringone	181/196/153	S	22.498	3.22	3.11	1.85
Syringylacetone	167/210/168	S	22.931	2.07	2.64	1.74
Propiosyringone	181/210/182	S	23.543	1.66	1.37	---
Synaphaldehyde	208/165/137	S	25.212	---	---	2.71
Synapaldehyde	208/165/137	S	25.535	2.4	---	---
Total benzene derivatives				0.02	---	---
Total phenol derivatives				0.63	0.31	0.17
Total catechol derivatives				0.6	0.35	0.25
Total guaiacyl derivatives				14.08	17.85	10.95
Total syringyl derivatives				41.87	34.78	21.99
Ratio S/G				2.97	1.95	2.01

From the previous results it was seen that the amount of phenolic compounds identified and quantified in the L1 and L2 was similar (small reduction from 57,18% L1 to 53,29% L2). Nevertheless, the relative content of phenolic units identified in the L3 was much lower compared to the previous ones (decrease from 53,29% L2 to 33,37% L3). Concerning the different phenolic groups, it could be remarked that no considerable amount of benzene derivatives was found in the different lignin samples. Phenol and catechol derivatives presented comparable contents and tendencies. In respect to guaiacyl and syringyl derivatives, there was a global reduction following the consecutive delignification steps. Besides the content of syringyl type compounds was higher than the guaiacyl one in all the lignin samples, yielding S/G ratios higher to one. Considering this point, it was concluded that despite being a non woody lignin source, almond shells could be considered as a hard wood, since the selectivity to syringyl type units was higher than that of guaiacyl ones[157,158]. On the other side, the highest S/G ratio was obtained for the L1, whereas the L2 and L3 ones were lower and similar.

This was in accordance to the work by Lourenço et al., 2012[159] who reported that the syringyl-rich lignins were more easily cleaved and solubilised. Moreover, since high S/G ratios were known to induce high lignin reactivity[160], L1 was said to be the more reactive. In addition to that, the fact that the L2 and L3 showed lower S/G ratios than L1, confirmed the more condensed structure of those lignins as reported by Sun et al., 2016[161]. Finally when comparing L2 and L3 samples the latter was said to have a more condensed structure because the selectivity to phenolic derivatives after pyrolysis presented a strong reduction.

Thermogravimetric analysis (TGA/DTGA)

The thermal stability of the different lignins and their decomposition was studied and thus the thermogravimetric (TG) and the first derivative thermogravimetric (DTG) curves were determined and presented in figures 4A and 4B.

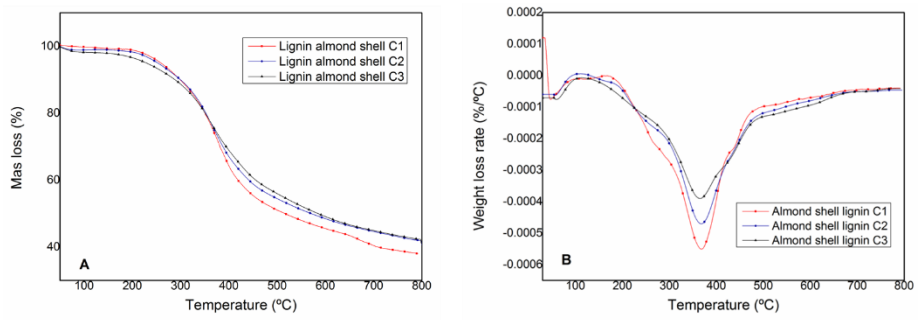

Figure 19. Thermogravimetric (A) and derivative thermogravimetric (B) curves for the lignins extracted from the different cycles.

Figure 19A showed that the lignins degradation took place throughout a broad range of temperatures, due to the complexity of the lignins structure[162]. This was also explained by the fact that lignins presented several functional groups containing oxygen, which have different thermal stabilities[163]. Consequently, the degradation of the lignins occurred through several stages. The first weight loss was due to the moisture evaporation of the lignins below 100 ºC[164].

A second stage was regarded within the range 325-400 ºC related to the cleavage of ether inter-units linkage[165], which constituted the main degradation step. Following that, the split of the aliphatic side chains and other structural units occurs as well[166]. Finally, at 800 ºC a char residue remained because of the rearrangement of lignin structure at high temperatures. Figure 19B showed that lignins decomposition presented a wide peak due to their polydispersity. Indeed, it was noted that the wideness of the peak was decreasing as lignin sequential extraction moved forward. This was in agreement with their polydispersity, which was also decreasing from L1 to L3. The thermal stability of the samples was evaluated by several parameters presented in Table 18, namely initial degradation temperature ($T_{5\%}$), maximum degradation temperature (T_{max}) and char residue remaining at the final temperature.

Table 18. Thermogravimetric parameters of the different lignin samples

	$T_{5\%}$ (ºC)	T_{max} (ºC)	Residue at 800ºC (wt.%)
L1	221.97	385.82	38.73
L2	212.50	379.52	42.35
L3	208.91	363.48	42.68

It can be seen from these results that the L1 and L2 presented similar behavior concerning the initial and the maximum degradation temperatures and higher than L3. However, all these temperatures were within a narrow range, showing that all the different lignins presented a similar thermal behavior. Regarding the char residue remaining, the percentages of L2 and L3 were similar and higher compared to the L1.

B.3.3 Conclusions

The implementation of a multistage-organosolv-extraction system with three sequential stages was carried aiming the enhancement of the extraction yield. In this respect, it was observed that a significant extraction efficiency was achieved after the first cycle (≈80%).

Nonetheless, the extraction effectiveness of the second and third cycles was low and in the end, the total extraction yield was only improved to an 87%. On the other hand, the lignins extracted from each cycle did not display considerable divergences in terms of structure or composition (similar purities and molecular weights). Moreover, the thermal properties of the lignins were analogous. It can only be remarked a decreased in the amount of hydroxyl groups and phenolic derived units (lower S/G ratios) as the delignification stages moved forward. These facts result in a decrease of the lignin reactivity from that of the first cycle (L1) to the others (L2 and L3). It was also considered the fact that the structure of the lignin became slightly more condensed as the extraction steps went by. Consequently, it was concluded that the implementation of the multistage-organosolv-extraction system do not provide any significant advantage neither in terms of extraction efficiency nor in terms of lignins with a more suitable structure of composition. Therefore, it was decided that a single-stage-organosolv extraction process would be sufficient to obtain lignins with suitable an extraction yield and interesting properties for further applications.

B.4 Single-stage-organosolv extraction process and characterization of lignins

In this section, the process of extraction of lignin from the two lignocellulosic biomass sources is evaluated. Moreover, the lignins obtained from both sources of biomass are comprehensively analyzed and compared concerning their main structure characteristics.

B.4.1 Experimental procedure

In the following subsections, the raw materials and apparatus used during the extraction are detailed, as well as the single-stage-extraction of lignin and the techniques of analysis employed for the characterization of the lignins.

B.4.1.1 Raw materials and equipment

The former raw materials was the same described in the case of study of section B.3.1.1. The latter consisted of leftovers from wood products manufacture and wood industry activities such as small pieces of wood, parts of wood panels, wood chips etc. In both cases, the residues were milled and sieved to chips of 5 mm prior to the isolation of the lignins. The reactor used in the process of delignification was the same depicted in section B.3.1.1.

B.4.1.2 Organosolv extraction process

The organosolv pretreatment used for the lignin extraction was analogous in terms of reaction conditions (pressure, temperature, time etc.) and procedure to that introduced in section B.3.1.3. Nevertheless, contrary to the case of study, this time a single-stage-extraction process was implemented for the source of biomass.

B.4.1.3 Characterization methods

The lignins extracted from the two different sources of biomass, were characterized by means of the techniques of analysis displayed in Table 19.

Table 19. Characterization methods used for the analysis of the chemical composition of lignins and their structure.

Component	Analysis	Technique	Annex	Section
Lignin	Chemical composition	Klason lignin	Annex III	III.1.1
		Acid soluble lignin		III.1.2
		Ashes		III.1.3
		Carbohydrates		III.1.4
	Molecular weight	HPSEC[A]		III.3
	Structural units (S/G ratio)	Py-GC/MS[A]		III.4
	Thermal properties	TGA[C]		III.5
	Chemical structure	FTIR[D]		III.6.1
		^{1}H-NMR[E]		III.6.2

[A]HPSEC: High performance size exclusion chromatography, [B]Py-GC/MS: *Pyrolysis-gas chromatography/Mass spectrometry analysis and* [C]*TGA: Thermogravimetric analysis,* [D]*FTIR: Fourier Transformed Infrared Spectroscopy analysis,* [E] *^{1}H-NMR: Proton Nuclear Magnetic Resonance Spectroscopy analysis.*

B.4.2 Results and discussion

The main outcomes derived from the lignin extraction and characterization and their analysis are presented in the next points.

B.4.2.1 Chemical composition of the lignins

The main chemical characteristics of the lignin isolated from the almond shells (LAS) and maritime pine residues (LMP) are displayed in the following table.

Table 20. Major parameters regarding the chemical composition of the lignins. (KL: klason lignin, ASL: acid soluble lignin and TS: total sugars)

Source	KL (%)	ASL (%)	TS (%)	Ashes (%)
Almond shells	89.30±0.44	2.18±0.25	1.49±0.18	4.04±0.49
Maritime pine	90.69±0.60	1.98±0.18	0.98±0.06	4.80±0.23

It can be seen from the previous table that both lignins presented similar compositions, since they were extracted using the same process and conditions. The content of insoluble lignin (KL) in both cases was high and in the typical range of organosolv lignins reported in literature[167,168]. This highlights the high purity of the lignins isolated by this pretreatment. Concerning the sugar content, both displayed low values, a bit higher in the case of that from almond shells. The amount of inorganic compounds was slightly high (4-5%). This behavior has also been observed in another work by Fernández-Rodríguez et al., 2017 [119] for almond shells organosolv lignin (≈4%). This ash content may be due to some remaining sulfuric acid from the acidified water used to precipitate the lignin, which was not washed completely after the filtration.

B.4.2.2 Analysis of the composition of the lignins via Py-GC/MS

The two lignins extracted, namely LAS and LMP, were analyzed by means of Py-GC/MS analysis, to determine the different types of phenolic moieties yielded after pyrolysis. In Table 21 the phenolic derivatives, originated are displayed.

Table 21. Compounds identified and quantified in the different lignin samples subjected to pyrolysis

Molecule	m/z	Origin	Retention time (min)	Content (%)	
				LAS	LMP
Toluene	91/92/65	B	4.081	---	0.88
Ehtylbenzene	91/106/65	B	5.518	---	0.12
Styrene	104/103/78	B	5.894	0.02	0.32
Phenol	95/66/65	P	7.361	0.16	0.35
2-methyl-Phenol	107/108/78	P	8.683	---	0.50
4-methyl-Phenol	108/107/77	P	8.908	0.20	1.04
Guaiacol	109/124/81	G	9.209	1.82	4.46
2,4-dimethyl-phenol	107/122/121	P	10.341	---	1.01
4-Ethyl-phenol	107/122/77	P	10.556	0.20	0.21
4-Methyl-Guaiacol	138/123/95	G	11.230	2.28	17.64
Catechol	110/64/81	C	11.397	0.13	---
2,4,6-trimethyl phenol	121/136/91	P	12.198	---	0.18
3-methoxy catechol	140/125/97	C	13.124	0.47	0.20
3-methyl catechol	124/78/123	C	13.153	---	1.96
4-ethyl guaiacol	137/152/122	G	13.615	1.02	3.41
4-vinylguaiacol	150/135/107	G	14.834	3.21	7.98
p-allyl phenol	134/133/107	P	15.55	0.07	---
Syringol	154/139/111	S	15.908	3.6	---
Eugenol	164/149/131	G	16.035	0.79	---
Allylguaiacol	164/77/103	G	16.272	---	3.26
4-Propylguaiacol	137/166/122	G	16.266	0.31	1.00
Ethyl Catechol	123/138/91	C	16.797	---	1.51
Vanillin	151/152/81	G	17.086	1.71	3.04
cis-isoeugenol	164/149/77	G	17.225	0.48	1.69
4-methyl syringol	168/153/125	S	18.114	8.01	---
4-Propylguaiacol	137/166/122	G	18.299	0.19	0.49
4-propyl catechol	123/152/67	C	18.680	---	0.41
acetoguaiacone	151/166/123	G	18.825	0.82	1.74
4-ethyl syringol	167/182/168	S	19.489	1.71	---
Guaiacyl acetone	137/180/122	G	19.604	0.92	0.75

Molecule	m/z	Origin	Retention time (min)	Content (%)	
				LAS	LMP
4-methyl-syringol	178/91/163	S	19.919	---	0.1
4-vinylsyringol	180/137/165	S	20.147	4.2	---
Propioguaiacone	151/180/123	G	20.413	0.53	1.01
1-hydroxy-eugenol	137/180/124	G	20.436	---	0.59
4-allylsyringol	194/91/119	S	20.696	1.66	---
4-Propylsyringol	167/196//168	S	20.777	0.67	---
cis-4-allylsyringol	194/91/179	S	21.377	1.59	---
Methyl homovanillate	137/182/138	G	21.481	---	1.48
syringaldehyde	182/181/167	S	21.568	3.08	---
Propenylsyringol	192/177/131	S	21.741	---	---
trans-4-allylsyringol	194/91/179	S	22.082	8	---
Acetosyringone	181/196/153	S	22.498	3.22	---
Coniferyl aldehyde	178/135/77	G	22.602	---	1.14
Syringylacetone	167/210/168	S	22.931	2.07	0.27
Propiosyringone	181/210/182	S	23.543	1.66	---
Synaphaldehyde	208/165/137	S	25.212	---	---
Synapaldehyde	208/165/137	S	25.535	2.4	---
Total benzene derivatives				0.02	1.32
Total phenol derivatives				0.63	4.54
Total catechol derivatives				0.6	9.04
Total guaiacyl derivatives				14.08	59.29
Total syringyl derivatives				41.87	0.37
Ratio S/G				2.97	0.01

From the Py-GC/MS analysis it was seen that the relative content of phenolic units derived from LAS was lower compared to that of LMP (57.2% and 74.56% respectively). The most relevant difference between both lignins was encountered in the S/G ratio. In this respect, the value was considerably higher in the LAS compared to the LMP.

This was because maritime pine (*Pinus pinaster*), is a softwood species which generally presents a very low content or even lacks syringyl units, typical from hardwood species[169]. Thereby, the guaiacyl units are predominant within the LMP lignin structure, resulting in low S/G ratios. On the other hand, the almond shells, which are not strictly a woody source of lignin, were considered in section B.3.2.5 as pseudo-hardwood lignin source owing to their preferential selectivity towards syringyl type units. Accordingly, the S/G ratio in this case is significantly higher due to a majority of syringyl type moieties compared to guaiacyl ones. This difference in the relative content of syringyl and guaiacyl type units between the two lignins (reflected on the S/G ratio), results in an important impact over the structure of both lignins. Moreover, it is the origin of several divergences detected in the rest of the analyses discussed in the following sections.

B.4.2.3 Fourier transformed Infrared spectroscopy analysis (FTIR)

The two lignins were analyzed by FTIR spectroscopy to elucidate their major structural differences. The FTIR spectra of the lignins LAS and LMP is showed in Figure 20. The main bands detected in both lignins and the assignations to the peaks from the spectra are listed in Table 22. Both lignins were characterized by a broad band at 3400 cm^{-1} of hydroxyl groups, another intense band around 3000 cm^{-1} linked to methyl and methylene groups and two narrow bands between 1600-1500 cm^{-1} typical of aromatic rings vibrations of lignin. Nevertheless, several differences were observed within the structure of the lignins depending on their provenance. In fact, it is known that the origin of the lignin influences its structure[170].

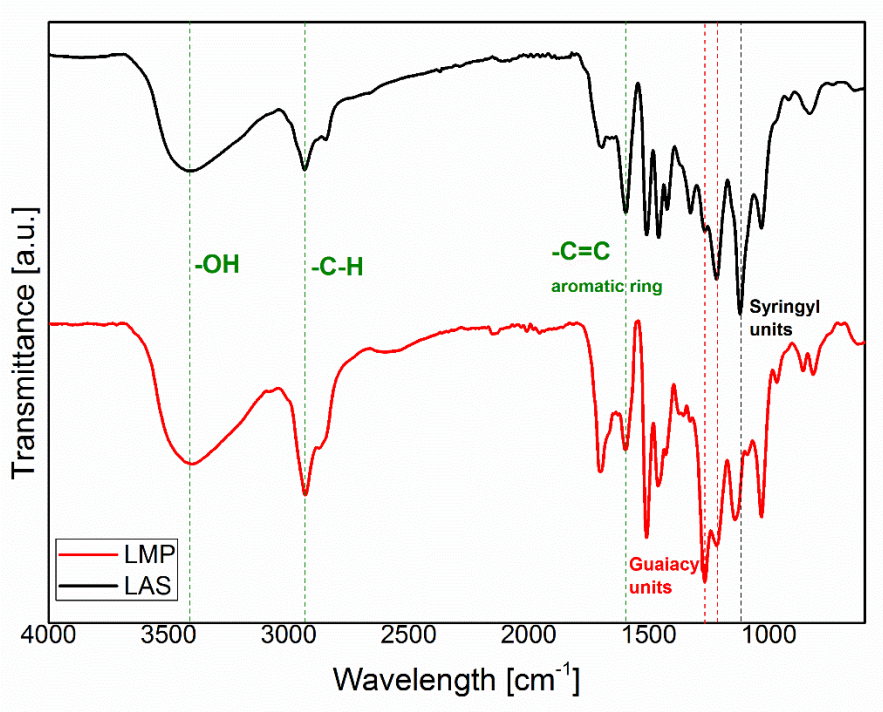

Figure 20. FTIR spectra of the lignins extracted from almond shells (LAS) and maritime pine residues (LMP).

Hence, the lignin obtained from almond shells (LAS), which presented a higher S/G ratio, displayed an intense band related to syringyl structures at 1119 cm^{-1}. This peak did not appear in the lignin extracted from maritime pine residues (LMP), as maritime pine is a softwood species with prevalence of guaiacyl groups. Accordingly, two bands related to guaiacyl rings appear in LMP (1266, 1139 cm^{-1}). From these bands only the former one was present in the spectra of LAS, but with low intensity. This was in agreement with the higher relative content of syringyl units compared to the guaiacyl ones observed in the Py-GC/MS analysis. In general, the major difference between the lignins, highlighted from the spectra was the prevalence of syringyl groups in LAS and of guaiacyl groups in LMP. This is concurrent with the S/G ratios determined in the characterization of lignins via Py-GC/MS in the previous point.

Table 22. Assignments of the major bands found in the FTIR spectra of the lignins extracted

Range of wavelength (cm^{-1})	Assignments	Identified bands (cm^{-1})	
		LAS	LMP
3410-3400	O-H stretching	3408	3401
3000-2850	C-H stretch methyl and methylene groups	2933	2930
1710-1680	C=O stretching	1697	1701
1600-1500	C=C vibration aromatic ring	1596, 1508	1597, 1508
1460-1440	C-H bending in methyl and methylene groups	1458	1458
1430-1420	C-H deformation vibrations aromatic ring	1423	1423
1270-1260	C-O stretching in guaiacol ring	1272	1266
1230-1210	C-C, C-O and C=O stretching	1218	1218
1150-1140	C-H deformation in guaiacol ring		1139
1120-1110	C-H deformation in syringyl ring	1119	
1035-1030	C-H aromatic in plane deformation	1031	1030
850-815	C-H aromatic out of plane deformation in G and S groups	829	857, 815

B.4.2.4 ^{1}H-NMR spectroscopy analysis of the lignins

This structural analysis was performed to confirm the results obtained in the Py-GC/MS and FTIR analyses. After this analysis, the peaks were normalized to the highest intensity prior to the discussion of the results. In Figure 21, the ^{1}H-NMR spectra of the lignins extracted are shown and in Table 23, the assignations to the main signals detected are presented. In the spectra of LAS and LMP, different signals appeared in the range 0.7-3.0 ppm, which correspond majorly to CH_3 and CH_2 from saturated aliphatic chains. According to Oliveira et al., 2009 [171], this suggests the presence of aliphatic compounds linked to the lignin structure.

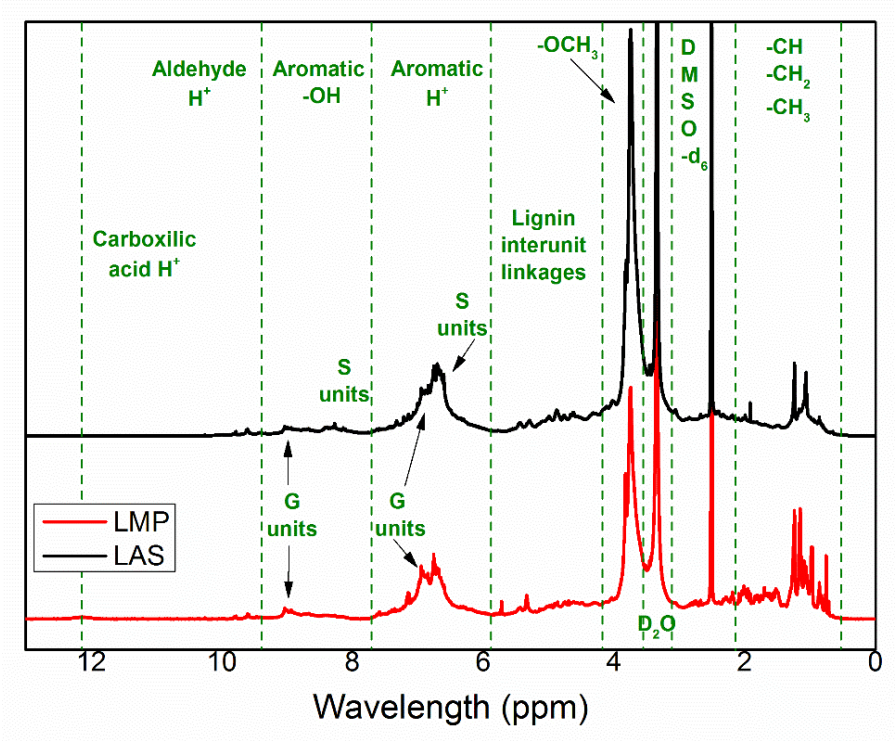

Figure 21. Comparison of the ^{1}H-NMR spectra of LAS and LMP.

At 3.7 ppm a strong signal was seen in both pristine lignins, which is related to the protons of methoxyl groups. In this signal, a significant difference was found between the spectra of LAS and LMP. Thus, its intensity in the case of the former lignin was higher compared to the latter, indicating that a higher abundance of this type of protons is present in LAS respect to LMP. This was attributed to the fact that LAS displayed a majority of syringyl type units within its structure, whereas in LMP there was almost an absence of these moieties. Moreover, since each syringyl unit is normally composed of two methoxyl groups with their corresponding protons, it can be expected that the intensity of the peak for these protons would be lower in the lignin where syringyl moieties were not present or were present in a lower extent. Some mild to small signals were found in the range between 4-6 ppm attributed to the protons from the typical lignin interlinkages β-O-4, β-β, β-5.

Table 23. Assignation of the main signals detected in the ^{1}H-NMR spectra of the lignins.

Chemical shift (ppm)	Assignation
0.8-1.6	Aliphatic protons of saturated chains
1.24	Aliphatic protons of oxidized lignin
2.5	DMSO
3.35	Water
3.75	Protons from methoxyl groups
4.6	Protons H_β from β-O-4 structure
4.7	Protons H_α from β- β structure
4.85	Protons H_α from β-O-4 structure
5.3-5.4	Protons H_α from β-5 structure
6.6-6.7	Aromatic protons from syringyl units
6.9-7.0	Aromatic protons from guaiacyl units
8.1-8.3	Phenolic proton from syringyl units
8.7-9	Phenolic proton from guaiacyl units
9.6	Formyl proton from cinnamaldehyde
9.8	Formyl proton from benzaldehyde
12.13	Proton from carboxylic acid derived groups

In the range 6-8 ppm, more intense signals were present corresponding to aromatic protons as reported in other works[172,173] and differences were encountered between LAS and LMP. The former lignin displays higher intensity within this region compared to LMP and its band was also wider, highlighting a bigger amount and a greater variety of aromatic protons. In LAS, proton signals corresponding to syringyl and guaiacyl moieties were seen, whereas in LMP only guaiacyl-derived signals. This is in accordance with the S/G ratios previously discussed in section B.4.2.2. Between 8 and 9 ppm protons derived from phenolic hydroxyl groups are normally reported[174,175]. To confirm the presence of the mentioned groups, a method for the determination of hydroxyl groups was followed, which is described in Annex III (section III.6.2.1).

Thereby, several hydroxyl signals were detected in the range 8-9 ppm. Again, differences were found regarding the content of guaiacyl and syringyl units. In LAS samples, signals related to hydroxyl groups from syringyl and guaiacyl moieties were detected while in LMP only the latter ones were seen. Beyond 9 ppm, few signals were observed such as a couple of peaks related to aldehyde protons and a weak broad peak around 12 ppm associated to protons from carboxylic acids.

B.4.2.5 High performance size exclusion chromatography analysis (HPSEC)

With this technique of analysis, different lignin-size-related parameters were determined, such as the average weight and number molecular weights (M_w, M_n) and the polydispersity index (Table24).

Table 24. Parameters calculated from the analysis of the size of the lignins

	M_w (g/mol)	M_n (g/mol)	M_w/M_n
LAS	6598.50±43.13	1244.45±149.20	4.91±0.05
LMP	4782.50±153.59	1038.75±101.72	4.63±0.31

Although both lignins were isolated by means of the same extraction process, they presented divergences in terms of the molecular weights. This was attributed to their different origin. Thus, it was observed that the lignin extracted from the maritime pine residues (LMP) displayed lower values of the molecular weights (M_w and M_n) compared to that obtained from almond shells (LAS). This means that in LMP the moieties taking part of the lignin structure were smaller than those of LAS. The size differences in organosolv lignins based on their distinct origin have also been reported in another work by Gordobil et al., 2015 [176].

Here, a higher molecular weight was found for organosolv lignin derived from hardwood species compared to organosolv softwood-derived lignin.

B.4.2.6 Thermogravimetric analysis of the lignins

The two lignins from different origin were subjected to thermal analysis, to assess their distinct thermal characteristic and performance. In Figure 22 are presented the curves from the thermogravimetric and derivative thermogravimetric analyses. On the other side, the main thermal parameters determined from these analyses are shown in Table 25.

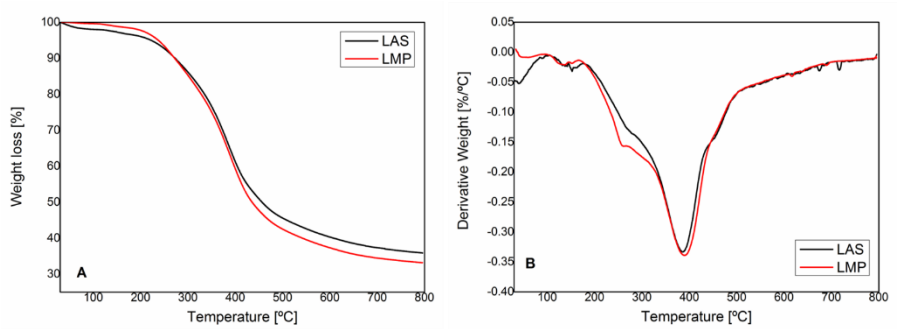

Figure 22. Graphs from the thermogravimetric (A) and derivative thermogravimetric (B) analyses.

From the previous figure, it was observed that the degradation of the lignins followed various steps. In this respect, some divergences can be seen between LAS and LMP. The first stage of degradation (until 100ºC), related to the evaporation of moisture and volatiles, occurred analogously in both lignins. Between 100-325ºC, a second stage of degradation appeared, which was attributed to the decomposition of the carbohydrates linked to the lignin structure (LCC), since they are usually degraded within this range of temperatures[177] (e.g. hemicellulose 200-280ºC). In this rage of temperatures, the lignin with a higher thermal performance was LMP as seen in Figure 22A. This may be because it presented a lower carbohydrate content (Table 20). The third step (325-400ºC) corresponded to the main stage of degradation, which was related to the decomposition of the lignin structure. Here, small divergences were identified between both lignins, such as the slightly higher temperature of maximum degradation of LMP. This is due to the higher thermal stability of guaiacyl units reported in other works[178,179].

Above the third stage of degradation (400-800 ºC), the thermal performance of the lignin from almond shells (LAS) was higher to that derived from maritime pine residues (LMP). This may be attributed to the higher molecular weight of LAS. Since larger units were present in this case, the recalcitrant structure formed by the rearrangement of lignin structure at higher temperatures (after lignin decomposition) could result a higher thermal resistance (Figure 22A). By this same reason, the char residue remaining at the end (800ºC) was a bit higher in the case of LAS compared to LMP.

Table 25. Thermogravimetric parameters determined for the lignins from almond shells (LAS) and maritime pine residues (LMP)

	$T_{5\%}$ (ºC)	T_{max} (ºC)	Residue at 800ºC (wt.%)
LAS	221.97	385.82	38.73
LMP	237.23	389.83	33.18

B.4.3 Conclusions

After performing the organosolv-lignin-extraction in a single-stage process, it was observed the significant influence of the source of biomass employed. Thereby, the lignins isolated from almond shells (LAS) and maritime pine residues (LMP) displayed several differences, especially concerning their chemical structure.

By Py-GC/MS, FTIR and ^{1}H-NMR analyses it was confirmed that both lignins presented opposite contents of syringyl and guaiacyl type units, owing to their different origin (pseudo-hardwood for LAS and softwood for LMP).

Divergences were seen as well in respect to the size of the lignins. Thus, despite the fact that they were extracted by means of the same pretreatment, their molecular weights were significantly different. This was also said to influence their thermal properties and performance as pointed out in the thermogravimetric analysis.

B.5 General conclusions

Considering the result and discussion provided the following conclusion were extracted:

- The different pretreatments employed currently for lignin isolation were assessed through the literature. It was concluded that organosolv method was the one that better fitted the characteristic desired for the process of extraction and the lignin.
- Although a multistage-organosolv extraction process was tested, it was concluded that it did not provide significant advantages compared to the single-stage-organosolv extraction process.
- The organosolv pretreatment implemented for both sources of biomass achieved to isolate highly pure lignins efficiently.
- The different origin of the biomass sources used resulted in lignins with considerable structural differences. Thereby almond shells lignin (LAS) presented a higher content of syringyl derived units, whereas maritime pine lignin (LMP) displayed a higher abundance of guaiacyl derived moieties.

Part C. Tannins selection and characterization

C.1 Motivation

It was already introduced in chapter 1, the current interest and the potential of tannins as phenolic raw material for different applications such. However, these interest and potential application applications are highly dependent on several aspects such as the process of extraction and the type of tannins used. Accordingly, within this part, the wide spectra of methods available for tannins extraction is first presented and the pertinent discussion and comparison is carried out. Following to that, the selection of the tannins employed for this work is justified, remarking the strong points of the type of tannins chosen compared to other tannin species. In the final part, a brief chemical characterization is included to address some important points such as their purity and reactivity.

C.2 Background

One important aspect of tannins is their heterogeneous nature, which makes impossible to settle a universal method for their extraction[180]. Accordingly, the yield, purity and composition of the extracts generally rely on several parameters such as the vegetal source, technique employed, extraction time, temperature etc.[181]. Within these aspects, the process of extraction of tannins constitutes a crucial keypoint for their reuse and valorisation in different applications. In this respect, since 17th century, a great number of techniques have emerged. Accordingly, old methods such as soxhlet extraction coexist nowadays with more recent techniques like extraction assisted by microwaves or ultrasound.

C.2.1 Solid-liquid extraction (SLE)

This is the simplest and most traditional method employed for tannins extraction. During this kind of extraction, the solvent penetrates into the cell wall of the feedstock containing the tannins. Then, they are dissolved and taken out in the form of extracts[182]. A variety of solvents can be used in this method, but generally organic solvents, water or aqueous solutions are employed. Concerning the use of organic solvents and their aqueous solutions, the extraction is commonly carried out by means of a soxhlet apparatus whose experimental extraction procedure has been described in several works[183,184]. On the other hand, the extraction with water can be carried out under reflux or through simple infusion or maceration in flasks or vessels. In this extraction method, the polarity of the solvent is an important parameter, which can increase the extraction yield[185]. Consequently, methanol, ethanol, water and their aqueous mixtures are typically selected as solvents for their high extraction efficiencies towards tannins[186]. At the industrial scale, it is the most widespread technique, especially by using water as solvent (more environmentally friendly). In this case, small amount of alkaline compounds and salts are reported to increase highly the extraction efficiency[187,188].

C.2.2 Supercritical fluid extraction (SFE)

The principle of this method is based on the concept of critical point, which is defined as the highest temperature and pressure at which a pure substance can exist in a vapor-liquid equilibrium[189]. Above this point, a fluid shares properties between a gas and a liquid, such as the typical weight of liquids with the penetration power of gases[190]. The most widely employed solvent for this type of extraction is carbon dioxide (CO_2). This is due to its desirable properties such as non-toxicity, non-flammability, non-corrosive nature, availability and low critical temperature and pressure[191].

Generally, a co-solvent is utilized as well (e.g. ethanol or methanol) owing to the non-polar nature of CO_2 and the polar nature of most of the tannin compounds. This helps ameliorating the solvating power of CO_2 towards tannins and improving the extraction yields.

C.2.3 Pressurized water extraction (PWE)

This extraction method is based on the use of water as solvent at high pressures and temperatures, generally at subcritical conditions i.e. between its atmospheric boiling point (100°C, 0.1 MPa) and its critical point (374°C, 22.1 MPa). Within this range water is maintained in the liquid state but properties such as the polarity, viscosity, surface tension and disassociation constant are considerably lowered compared to water at ambient conditions[192]. The reduction of these parameters enhances the mass transfer of the tannins from the feedstock matrix[193]. The main difference to traditional solid-liquid extraction, is that here the temperature is kept above the boiling point and the pressure above the atmospheric to maintain water in liquid state. The temperature plays a major role in this extraction method. Thereby, its increment until certain point (avoid sample degradation) can lead to enhanced extraction yields[194].

C.2.4 Microwave assisted extraction (MAE)

This method is based on the combination of the traditional solvents employed for tannins extraction and the fast heating in the microwave field. In this case, the extraction process is ameliorated because both the solvent and the sample can be rapidly heated by direct interaction with electromagnetic radiation (depending on their dielectric characteristics).

The effect of heating on the solvent increases its solubility, whereas on the material it improves porosity allowing an easier penetration of the solvent[195]. Both phenomena provide an eased extraction of tannins from the cell wall of the feedstock. Accordingly, the microwave power displays a considerable influence over the process efficiency.

Hence, it can increment the amount of tannins extracted[196]. Besides this parameter, the polarity of the solvent is also of great importance, as it was already reported for the traditional solid-liquid extraction.

C.2.5 Ultrasound assisted extraction (UAE)

The extraction of tannins by this technique is based on the formation, growth and collapse of micro bubbles inside a liquid phase submitted to ultrasonic cavitation[197]. The bubbles are induced by sound waves, with frequencies above 20 kHz, which cause mechanical vibrations into the plant matrix. These mechanical vibrations can rupture cell wall tissues ameliorating the penetration of the solvent into the matrix and achieving higher amounts of tannins extracted[198]. The power of sonication has a direct influence over the extraction results as it was commented in the previous case of MAE for the microwave power. The polarity of the solvent employed is a decisive parameter as well, which can provide improved extraction yields.

C.2.6 Assessment of the different extraction methods

The methods listed before for tannins extraction are based on different principles and therefore they can yield different results concerning the amount of tannin extracted and the extraction efficiency. In the following table, their main strengths and weaknesses are presented and compared. As presented in Table 26, each method of extraction of tannins presented different strengths and weak points. Currently, there is a trend towards the switch from the most traditional extraction of tannins (SLE) to the most state of the art techniques (PWE, MAE or UAE). In the literature it can be found an increasing number of works where similar tannin extraction results are obtained by the most modern techniques[199–202].

Table 26. Evaluation and comparison of the most used extraction methods for tannins.

Extraction method	Advantages	Disadvantages
Solid-liquid extraction	-Simplicity, efficiency and low cost. -Available at industrial scale.	-High amount of solvent needed. -Long time of extraction (1h-72h).
Supercritical fluid extraction	-Mild temperatures are used.	-Considerably high investment costs. -Necessity of a co-solvent.
Pressurized water extraction	-Low time of extraction (15-30 minutes). -No-toxic solvent.	-Harsh conditions needed (high pressure and temperature). -Expensive equipment is required.
Microwave assisted extraction	-Low time of extraction (1-5 minutes). -Lower amount of solvent needed.	-Possibility of thermal degradation of the sample. -High cost of the equipment.
Ultrasound assisted extraction	-Low time of extraction (15-30 minutes). -No too high cost of the equipment.	-Lack of uniformity of the ultrasound intensity. -Reduction of the ultrasound power with the time.

Nevertheless, they still remain at the laboratory scale rather than moving to a higher scale. Their constraints are mostly related to the operational complexity of the processes and equipment and reagents investments. Furthermore, even in the laboratory scale the amounts of tannins extracted by these methods are limited to provide enough availability for further applications. For this reason, the traditional solid-liquid extraction continues to be the extraction method for tannins preferred among the industry[203].

C.3 Tannins selection

In this section, the choice of the tannins to be used a phenolic raw material later on is presented and justified. In this respect, two aspects are discussed: the election between a tannin extracted in the small-scale in the laboratory and a commercial tannin extract coming from the industrial scale and provided by a company and the decision between the different tannin species. Concerning the former point, it was decided to select a commercial tannin extract supplied by a company rather to perform the tannin extraction in the laboratory. These extracts were obtained via solid-liquid extraction with hot water, which is the dominant method within the industry (as commented in the previous section), under optimized conditions. The decision for the commercial tannin extract was based on two reasons namely the amount and availability of the tannin powder needed and the quality of the extract. One of the weak points of the extraction of tannins in the laboratory is that on average, the extraction yields achieved are low-moderate (ranging 10-40%)[186,187,204,205]. Add to this, the fact that the mass of raw material fed into the reactor is generally low. Accordingly, the amount of extracts obtained may not be sufficient to satisfy the availability requirements. This would be a limiting factor (numerous batches would be needed) for the utilization of the tannin as raw material in a further synthesis of phenolic resins. The other major reason is that the commercial extracts coming from the industry can provide a high tannin purity and reactivity, whereas those produced at the laboratory scale generally lack from these conditions. For instance, in some cases where the yields achieved are significant, the actual amount of tannins in the extracts are low[206–208]. In other cases, the extracts can display a good tannin content but then a high reactivity cannot be assured[209,210] . For this reason the selection of a tannin extract, which is commercialized at the industrial scale will assure these points. Another point playing a significant role is the species of the tanins, as it will determine the chemical composition and structure of the tannins.

Between the two main types of tannins, namely condensed and hydrolysable, the former one displays a higher commercial availability. In fact, this type represent more than the 90% of the tannin production worldwide[211]. Moreover, condensed tannins present a higher reactivity than hydrolysable type owing the low level of phenol substitution and nucleophicity of the latter[188]. Consequently, a specie with a majority of condensed tannin moieties was preferred. Within, the species with prominence of this type of tannins, mimosa (*Acacia mearnsii*) is responsible for the most common commercial condensed tannins, with a production of 220000 ton/year[212]. This is due to the high content of condensed tannins in mimosa compared to other species and owing to the significant yield obtained in the extraction process. The tannins are typically extracted from the mimosa bark, as it is reported to have the highest content of tannins compared to other parts of the plant[213]. This is an advantage because it is preferable to extract the tannins from the bark, which may not have any other further specific application, rather than for example the wood. Furthermore, this may also promote the protection of wood as a source. Taking all this points into consideration, a commercial tannin extract from mimosa bark (*Acacia mearnsii*) was selected as the other phenolic raw material for the later synthesis of the resins. Since it was a commercial product, a fully comprehensive characterization, as the one carried out for the lignins, was not necessary. Nevertheless, a brief analysis of the chemical composition, reactivity and structure was performed to confirm the desired characteristics of the commercial tannin extract. The mentioned analysis is showed in the following section.

C.4 Tannins characterization

The tannin extract selected as phenolic raw material for the further synthesis the biosourced phenolic resins, is briefly characterize in this part concerning their general composition and other chemical and structural parameters.

C.4.1 Experimental procedure

In this subsection, the description of the tannin selected as phenolic raw material and the main techniques for its characterization are described.

C.4.1.1 Raw material

The raw material selected was a commercial tannin extract from mimosa (*Acacia mearnsii*) with the name Tanfood, which was provided by Tanacinc (Brazil).

C.4.1.2 Characterization methods

The techniques of analysis employed for the characterization of the tannin extract are listed within this section and displayed in Table 27.

Table 27. Characterization methods used for the analysis of the chemical composition of the tannin selected and its structure.

Component	Analysis	Technique	Annex	Section
Tannin	Chemical composition	OC[A] and IC[B]	Annex II	II.1.2
	Total phenolic content	Colorimetric method (GAE[C])	Annex III	III.2
	Molecular weight	HPSEC[D]		III.3
	Chemical structure	FTIR[E]		III.6.1
	Total carbohydrate content	Anthrone method	Annex IV	IV.1
	Total flavonoid content	Colorimetric method (QE[F])		IV.2
	Total condensed tannin content	Colorimetric method (CyE[G])		IV.3
	Reactivity	Stiasny Index assay		IV.4

[A]OC: organic content, [B]IC: inorganic content, [C]GAE: gallic acid equivalents, [D]HPSEC: High performance size exclusion chromatography, [E]FTIR: Fourier Transformed Infrared Spectroscopy analysis [F]QE: quercetin equivalent, [G]CyE: Cyanindin equivalents.

C.4.2 Results and discussion

In this section, the results derived from the techniques of analysis implemented for the characterization of the tannin selected are displayed.

C.4.2.1 Chemical composition and reactivity of the tannin

Several parameters related to the composition and the reactivity of the commercial tannin extract were determined (Table 28), to confirm its suitability as phenolic raw material for the synthesis of the resins in the following chapter.

Table 28. Parameters determined for assessing the composition and reactivity of the mimosa tannin extract.

Parameters measured		Value
Purity	Organic content (%)	97.10±0.22
	Char content (%)	31.35±0.04
	Total carbohydrate content (%)	2.892±0.07
	Inorganic content (%)	2.90±0.23
Composition	Total phenolic content ($mg_{GAE}/g_{extract}$)	582.67±50.66
	Total flavonoid content ($mg_{QE}/g_{extract}$)	552.15±17.42
	Total condensed tannin ($mg_{CyE}/g_{extract}$)	537.59±58.75
Reactivity	Stiasny number (%)	89.46±2.46

First, it was confirmed the purity of the commercial extract since, the content of inorganic compounds (ashes) represented less than 3% of the total and the amount of carbohydrates detected in the extract displayed a low value compared to the total amount of organic compounds.

This was expected, as carbohydrates are more likely to appear in extracts with a predominance of hydrolysable tannins and mimosa extracts are composed mainly of prorobinetinidin and profisetinidin, which are monomeric units typical from condensed tannins[214].

Concerning the content of total phenolic compounds, the value obtained was in accordance with other works from the literature[196,215]. On the other hand, the content of flavonoids and condensed tannins was high compared to the values reported in other works for the extraction of tannins from *Acacia mearnsii*[216,217]. This was attributed to the fact that the selected mimosa extract is obtained from an industrial process optimized to allow its commercialization. Nevertheless, the tannins extraction performed at the small-scale generally lacks from this optimization, which has a direct influence over the final amount of actual tannins in the extracts. The content of flavonoids represented the most part of the phenolic compounds determined in the extracts. Likewise, the same tendency was observed for the content of condensed tannins, which accounted to almost the majority of the flavonoid compounds. Thereby, it was confirmed (as expected) the predominance and availability of condensed tannin compounds in the commercial mimosa extract. This was concurrent with the decision of selecting a commercial tannin extract, instead of carrying out the extraction of the tannins as it was done for the lignin.

The Stiasny Index assay showed that the reactivity to aldehydes of the selected tannin extract was high, as compared to mimosa extracts reported in other works from the literature[218,219]. This is a point of great significance, since tannins with lower reactivity would not be suitable for their utilization in the synthesis of phenolic resins of the phenol-formaldehyde type. Besides, the value obtained for the Stiasny Index (SI) was around 90% and according to Rosales et al. 2002 a tannin extract with a SI higher than 65 is a suitable source of condensed tannins for its utilization in other applications e.g. adhesives formulation[220].

C.4.2.2 High performance size exclusion chromatography analysis (HPSEC)

This technique was carried to evaluate the size and heterogeneity of the compounds forming part of the tannins extract. The curve obtained for size distribution of the mimosa tannin extract and the main parameters calculated from the analysis concerning the molecular weights and distribution are presented in Figure 23 and Table 29 respectively.

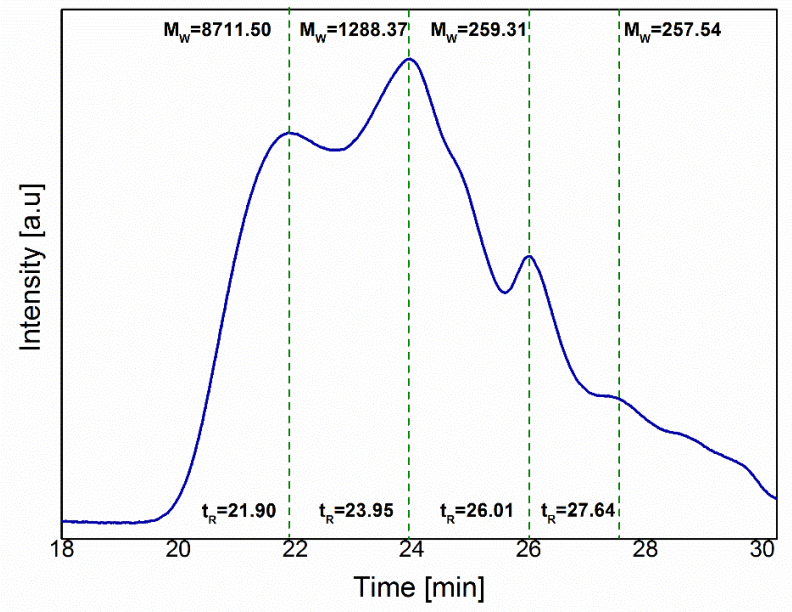

Figure 23. Curve for the size distribution of the mimosa tannin extract.

In the previous figure, several peaks were detected at different retention times. Accordingly, it could be concluded that the commercial mimosa tannin extract was composed of various molecules of different molecular weights. This was expected, since the tannins from mimosa extracts are considered as oligomers formed by several flavan-3-ol units, mainly fisetinidol and robinetinidol[221].

The molecular weights displayed in each section of Figure 23 could be associated to various flavonoid monomers, dimers, trimers or other oligomers. Robinetinidol ($C_{15}H_{14}O_6$) and fisetinidol ($C_{15}H_{14}O_5$) have molecular weights of 290.26 g/mol and 274.26g/mol respectively.

That means that the peaks appearing at the longer retention times could be associated to these monomers or their radicals, since the molecular weight are similar. Thereby the main peak, obtained for the mimosa tannin extract may be attributed to an oligomer composed of 4-5 units, considering its molecular weight (1288.37 g/mol). This would be in agreement with Pasch et al., 2001 [222], who evaluated the composition of monomers and oligomers of a mimosa tannin extract by MALDI-TOF and found the higher intensities for the tetramers and pentamers. These oligomers have been also reported in other works[223,224]. The first peak with a higher molecular (weight might be related to a more condensated and polymerized formed of the tannins.

Average results were extrapolated from the analysis regarding different parameters and pointing out a molecular weight within the typical range of tannins[225]. Moreover, the polidispersity index confirmed the presence of several monomeric units for the extract that was already presented in the previous figure. Besides the value was within the expected range for mimosa tannins[226]. The low value of the average molecular weight is of great interest, since it would ease a further chemical polymerization with other components, avoiding steric hindrance.

Table 29. Parameters calculated from the analysis of the size of the mimosa tannin extract

M_w (g/mol)	M_n (g/mol)	M_w/M_n
3402±2.72	702±5.84	4.85±0.04

C.4.2.3 Fourier transformed Infrared spectroscopy analysis (FTIR)

This technique was employed to characterize briefly the main functional groups and linkages, present within the structure of the commercial mimosa tannin extract. In Figure 24 the spectra of the mimosa tannin extract is presented and the assignations to the main bands and peaks detected in the spectra are listed in Table 30.

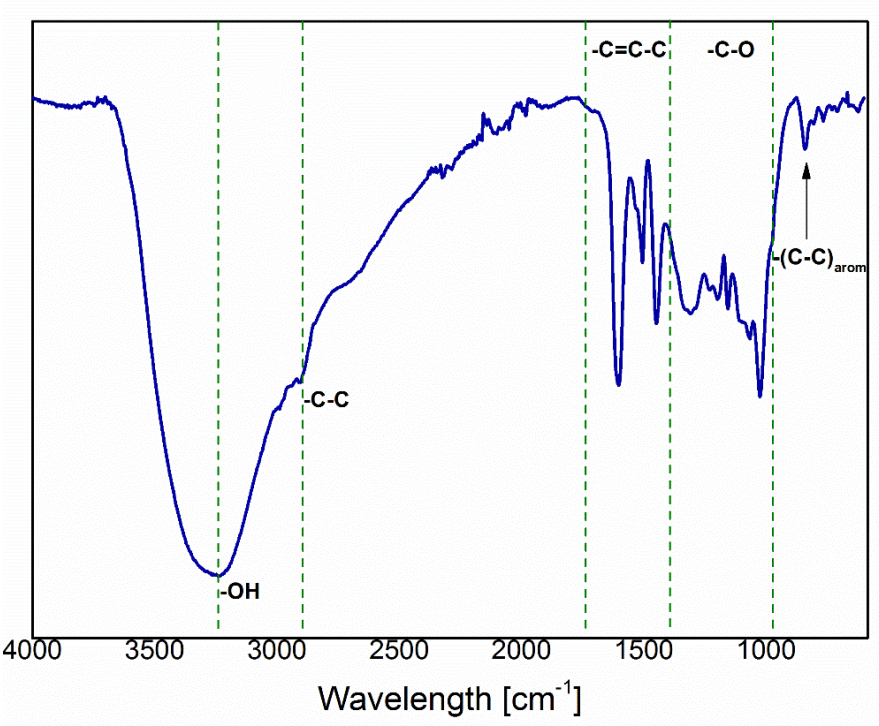

Figure 24. FTIR spectra of the commercial tannin extract of mimosa.

From the previous spectra, a wide intense band was observed between 3500-3100 cm^{-1} attributed to the hydroxyl groups of the tannin molecules. Since tannin are polyphenolic molecules with high content of different types of hydroxyl groups[227], it was expected that this band presented such an important contribution to the spectra. Around 3000 cm^{-1}, stretching vibrations of CH, CH_2 and CH_3 groups were seen, related to the C-ring of mimosa tannin monomers[228]. In the range 1600-1450 cm^{-1}, some signals were detected attributed to aromatic ring stretching vibrations[229]. In the next region (1300-1020 cm^{-1}), several peaks were distinguished, especially that at 1024 cm^{-1}, associated to the ether linkages of the heterocyclic ring of flavonoids[230].

A final peak around 850 cm^{-1} was found derived from the distortion vibrations of aromatic carbon double bonds from benzene rings[231].

Table 30. Assignments of the major bands found in the FTIR spectra of the commercial tannin extract selected.

Wavelength (cm^{-1})	Intensity	Assignments
3239	VS	O-H stretching
2900	VW	C-H stretching vibrations
1603	S	C=C-C aromatic stretching vibrations
1505	W	
1450	M	
1311	M	C-O-C stretching of pyran heterocyclic ring of flavonoids
1231	VW	
1195	VW	
1158	VW	
1110	VW	
1064	VW	
1024	S	
838	W	C-C vibrations in benzene ring

VS: very strong, S: strong, M: medium, W: weak and VW:very weak

The bands detected from the spectra confirmed that the commercial mimosa tannin extract presents the expected structure of this type of tannins (high amount of hydroxyl groups and heterocyclic ring typical of flavonoid moieties).

C.4.3 Conclusions

It was confirmed that the commercial mimosa tannin extracts display a suitable composition, reactivity and structure for their use as phenolic raw material. On the one hand, a significant content of phenolic and more specifically condensed tannins in the extracts was found. This proves its purity and assures the predominance of these desired components in the extract.

The reactivity as assessed by the Stiasny Index (SI) was high as well. Moreover, the extended presence of hydroxyl groups within its structure, as seen in the FTIR structural analysis, confirmed the high reactivity of the tannins.

C.5 General conclusions

Within this section, various points related to the selection of the process of extraction for tannins and the most suitable type of tannins were discussed. Furthermore, a general characterization of the tannin extract selected was provided. Taking into consideration the previous assessment and results provided the next conclusions were drawn:

- A commercial tannin extract obtained at industrial scale was selected to avoid the main limitation from the laboratory-scale extraction of tannins, namely low quantity and purity of the tannins extracted.
- After the literature review carried out on tannins, it was concluded that mimosa tannins display advantages compared to tannins from other species, especially regarding their abundance and commercial availability. Therefore, a commercial extract of this kind of tannins was selected.
- The characterization carried out, confirmed the suitability of the composition, reactivity and structure of the tannin extract for its utilization in further chemical synthesis reactions (raw material in the formulation of biosourced phenolic resins).

3. Functionalization of raw materials and synthesis of biosourced phenolic resins

The third chapter of this work is focused on the synthesis of biosourced phenolic resins from the raw materials extracted and characterized in the previous chapter, namely organosolv lignins and mimosa tannin extract. The chapter was split into two different sections A and B. On the one hand, section A is devoted to the process of chemical modification to which lignins were subjected prior to their utilization as raw materials for the synthesis of the phenolic resins. Furthermore, the effects of the chemical modification of the lignins were determined by several chemical and structural characterization techniques. In the end, the enhancements achieved for both lignins after the process of modification in terms of structure and performance were assessed. On the other hand, part B was dedicated to the process of synthesis of the biosourced phenolic resins and to the characterization of the resin formulation obtained. They were evaluated for several physical-chemical parameters and for their thermal performance. They were compared based on these characteristics to resins reported in other works from the literature.

Part A. Chemical modification of the lignins

A.1 Motivation

It has already been presented previously the interest on lignin in the recent years, owing to its potential use in several industrial applications, especially in the field of materials. Nevertheless, lignin as raw material also displays various limitations derived from its complex and recalcitrant structure.

For instance, compared to other synthetic compounds such as phenol, lignin presents less active sites within its structure. Therefore, its reactivity it is considerably lower, which can hinder its use as phenol alternative[232]. Similarly, properties of lignins such as its structure and thermal stability need to be improved as well for specific applications.

For these reasons, the chemical modification of lignin is generally employed aiming the increment of its reactivity and/or the improvement of certain characteristics and/or performance.

In this section, first a general revision of the main process utilized within the literature for lignin chemical modification are displayed. Then, the process implemented in this work for achieving the activation of the lignins and the improvement of their thermal properties is presented. The main effects derived from the process at chemical and structural level were evaluated as well.

A.2 Background

Despite the many application of lignin among different areas, its utilization in its original state, that is as it is obtained in the industry, entail several difficulties such as the low reactivity, the brittle and rigid structure and low replacement ratio[233]. The reactivity is one of the most important issues to face when handling lignin. Although lignin displays a considerable number of phenolic oxygen within its structure, the majority of them are hindered as interunit ether bonds and methoxyl groups[234]. Therefore the actual amount of free phenolic hydroxyl groups is reduced compared to other compounds. Since it is known that the presence of hydroxyl groups within the lignin structure is related to its reactivity, the increase of this functional group is desired to enhance the reactivity of the lignins.

In the recent years, several works have studied the enhancement of lignin reactivity via different methods such as methylolation or hydroxymethylation[235], demethylation[234], amination[236] and phenolation[237]. From the previous techniques, methylolation is one of the most employed, especially for the use of lignin in the synthesis bio-based resins[238,239]. This method consists in the reaction of lignin with formaldehyde in alkaline medium to introduce hydroxymethyl groups (-CH_2OH) into its structure.

The major problem of this modification lies on the non-renewable nature of formaldehyde and its toxicity. Accordingly, there have been efforts towards the utilization of a more environmentally friendly aldehyde. Glyoxal, which is composed of two aldehyde groups, is a non-toxic aldehyde classified as non-volatile (NTIS2005). Furthermore, it can be directly obtained from various natural sources e.g. lipids oxidation and as side product of some biological processes[240]. Considering this, there has been a tendency towards the replacement of formaldehyde by glyoxal for lignin modification[241–243]. On the other side, the issue of its rather rigid and brittle structure in its original state poses a challenge in certain areas like building and construction industry, in which certain properties (mechanical strength, thermal stability or fire resistance) need to be improved[244]. In this case, the combination of lignins with inorganic compounds like silicates or silicate clays appears as an alternative to overcome this issue. The mentioned combination leads to a novel topic recently discussed in the literature and refer to as hybrid materials. The International Union of Pure and Applied Chemistry (IUPAC) define hybrid materials as "*materials composed of an intimate mixture of inorganic components, organic components or both types in which these components usually interpenetrate on scales less than 1μm*"[245]. This kind of modification presents various advantages such as the combination of properties of organic and inorganic materials into one material and the introduction of several functional groups, creating multifunctional materials[246].

Moreover, a synergistic effect in organic-inorganic materials is reported, owing to the properties of the different components present[247]. Lately the process of grafting of inorganic compounds in the nanoscale to different organic matrices has been used in the elaboration of clay or silicate-polymer nanocomposites or hybrid materials. In fact, the dispersion of nanoscale clay layers into polymeric matrices is said to block the diffusion of volatile decomposition products during thermal degradation, improving the thermal resistance of the materials[248].

Besides, this type of hybrids shows enhanced mechanical properties, flame retardancy and barrier properties at the nanoscale level[249] compared to the typical only organic-based materials. Nanoclays and nanosilicates are currently widely utilized in the formulation of the organic-inorganic hybrid materials.

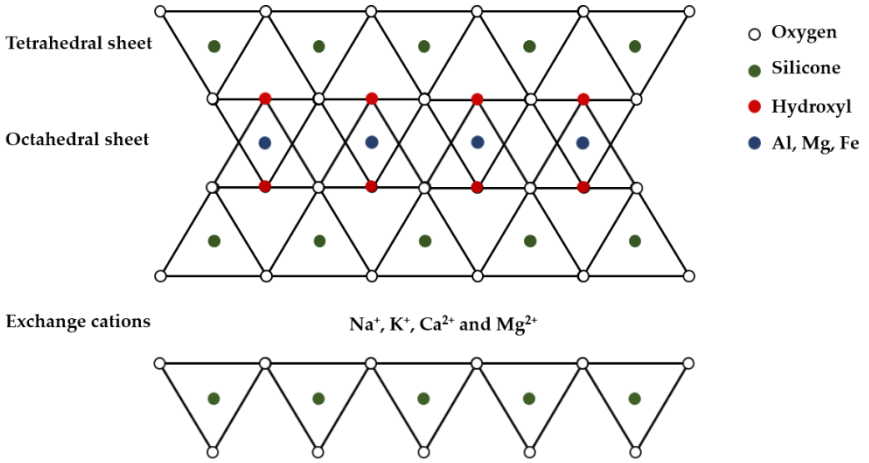

Figure 25. General clay structure composed of negatively charged sheet and positively charged cations.

The former group is composed of nanostructured compounds belonging to family of clays. Clay minerals are hydrous silicates defined as fined-grained particles with a structure composed of sheet stacked one over another[250].

Clay minerals can display different geometries and therefore several arrangements for the individual layers exist: two, three or four sheet of either $[SiO_4]^{4-}$ tetrahedral (T) or $[AlO_3(OH)_3]^{6-}$ octahedral (O). These sheets are organized one over another, with a Van der Waals interactions between them. The negative layer charge is compensated by the cations (Na^+, K^+, Ca^{2+} and Mg^{2+}), which occupied inter-lamellar space (Figure 25). Concerning the number and arrangements of sheets in each clay layer, different types of clay minerals can be distinguished as shown in Table 31

Table 31. Kinds of clay minerals depending on the arrangement of sheets in the layers (T: tetrahedral and O: octahedral)

Number of sheets per layer	Arrangement	Clays examples
2	1:1 [T:O]	Kaolinite, halloysite
3	2:1 [T:O:T]	Vermiculite, smectite, pyrophyllite
4	(2:1):1 [(T:O:T):O]	Chlorite

One of the most used nanoclays in this type of nanocomposites is montmorillonite (MMT), a natural 2:1 sheet phyllosilicate belonging to the family of smectites[251]. It displays various advantages such as low price and rich intercalation chemistry, providing the possibility of being chemically modified to increase the compatibility with the polymeric matrices[252].

On the other hand, among the nanosilicates polyhedral oligomeric silsesquioxanes (POSS) are a group receiving a great deal of attention in the recent years[253]. Structurally, POSS are characterized by a silica cage core with organic functional groups attached to the corners of the structure (Figure 26). Hence, they present the general formula $(RSiO_{1.5})_n$ where R can be an hydrogen atom or any organic functional group[254]. The availability of several R groups within the structure allows the introduction of various functional groups to increase the compatibility with various polymers.

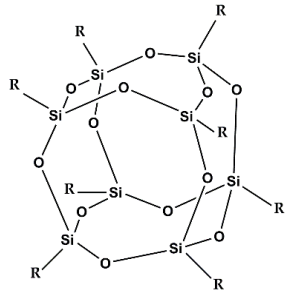

Figure 26. Molecular structure of polyhedral oligomeric silsesquioxanes (POSS).

Different types of polyhedral oligomeric silsesquioxanes (POSS) can be distinguished, based on the level of functionality and reactivity.

- Molecular silica: is the case in which all the functional groups attached to the Si-O cage are non-reactive (R=H).
- Monofunctional POSS: in this case, only one reactive group is present among the functional groups attached (one R=organic functional group).
- Multifunctional POSS: in this case, two or more reactive groups are attached to the Si-O cage (more than one R=organic functional group).

This kind of nanoparticles displays several advantages such as the fact that they can reduce the viscosity in the case of highly filled resins[255] and that they can provide various organic functional groups attached to their structure, being compatible to multiple polymers[256].

A.3 Experimental procedure

In the next subsections, the description of the raw materials and the processes of functionalization of the raw materials are presented.

A.3.1 Raw materials and reagents

The raw materials employed in this part were the organosolv lignins obtained from almond shells (LAS) and the residues from maritime pine (LMP), which were characterized in the previous chapter (Chapter 2, section B.4.2). The process carried out for their extraction, was detailed in chapter 2, section B.4.1.2. Within this section, these lignins are referred to as pristine or unmodified lignins. The reagents employed during the process of lignin modification were glyoxal (40% aqueous solution) and sodium hydroxide pellets, which were purchased from Sigma Aldrich.

Concerning the nanoparticles used in for the synthesis of the organic-inorganic nanohybrids, a nanoclay and nanosilicate were employed. The nanoclay employed was Dellite® 43B, which was kindly provided by LAVIOSA Advance Mineral Solutions (Italy). It was derived from naturally occurring montmorillonite purified and modified with a quaternary ammonium salt (dimethylbenzylhydrogenated tallow ammonium) as presented in Figure 27.

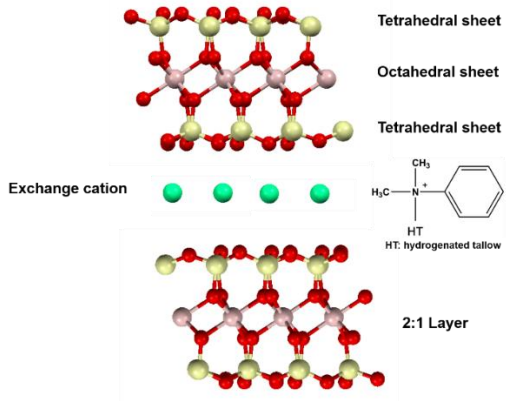

Figure 27. Structure of the organically modified montmorillonite employed in this work (Dellite 43B).

The nanosilicate used was SO1458-TriSilanolPhenyl POSS®, purchased from Hybrid Plastics® Inc. (USA). It consisted of a polyhedral oligomeric silsexquioxane core modified with organic phenyl groups and three active silanol functionalities as showed in figure 28.

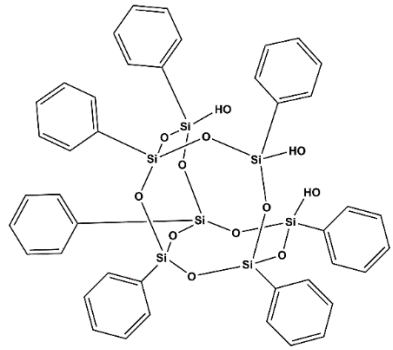

Figure 28. Structure of the nanosilicate trisilanol phenyl polyhedral oligomeric silsesquioxanes (SO1458-TriSilanolPhenyl POSS®).

A.3.2 Processes of functionalization

The lignins were functionalized by the means of two different processes namely glyoxalation and hybridization with inorganic nanoparticles.

A.3.3.1 Glyoxalation of lignins

The reaction of lignin with glyoxal was carried out according to a procedure published in another previous work with some modifications[257]. Here different formulations of glyoxalated lignins were prepared by varying the amounts of water and glyoxal used (Table 32).

Table 32. Molar ratios of the components for the different formulations of glyoxalated lignins and the lignin concentration (w/w).

Formulation	Origin	Lignin	Water	Glyoxal	Lignin concentration
LG1	Almond shells	1	13.93	0.25	26.18
LG2		1	13.93	0.58	24.86
LG3		1	10.44	0.58	29.80
LG4	Maritime pine wood	1	13.93	0.25	26.18
LG5		1	13.93	0.58	24.86
LG6		1	10.44	0.58	29.80

Thereby the influence of these components in the process of lignin modification can be studied and the lignin formulation with the highest activated structure selected. Shortly, 15 g of organosolv lignin were added to different amounts of water. Then, an aqueous solution of sodium hydroxide (30%) was added to the suspension until a pH in the range 12-12.5 was obtained. When the desired pH was reached, different amounts of glyoxal (40% in water) were added and the mixture was heated at 58 ºC during 8 h. During the reaction, mechanical agitation was employed (450 rpm).

Afterwards, small samples of the liquid glyoxalated lignins were dried following the procedure described in the ASTM D4426-96 standard, to determine the solid content of the modified lignins. The values obtained for this parameter ranged between 32-35±1.70.

A.3.3.2 Hybridization of the lignins or modification with inorganic nanoparticles

This process was carried out by using the glyoxalated lignins obtained from the previous modification and the inorganic nanoparticles. The glyoxalated lignins were homogeneous brown solutions to which the organically modified montmorillonite (OMMT) and polyhedral oligomeric silsesquioxanes (POSS®) were added.

The amount of these nanoparticles used for the reaction was 5% (w/w) respect to solid lignin in solution. The mixture was left overnight at 40 ºC with magnetic agitation (550 rpm). After this period, it was observed that no particles were remaining floating on the surface of the solution and that no particle agglomerates were settled at the bottom. Hence, a homogeneous solution was obtained where the nanoparticles were properly dissolved and dispersed. Once the lignin modification was carried out, the samples were dried at 50ºC during 24h to remove the liquid phase. Then the solid was recovered and crushed into powder (mesh size ≤ 0.25 mm) to be ready for further analyses. This procedure was also employed with the glyoxalated lignins for the same purpose. The formulations containing OMMT were designated with the letter A (LGiA) while those with POSS® were labeled as B (LGiB). The conditions of the different lignins modified with these inorganic compounds are described in Table 33.

Table 33. Conditions used for the different formulations of the lignins modified with inorganic nanoparticles.

Formulation	Glyoxalated lignin	Inorganic phase (%)[A]		Mixture conditions
		Dellite 43B	SO1458-Trisilanol phenyl POSS®	
LG3A	LG3	5	---	40ºC
LG3B		---	5	1 atm
LG6A	LG6	5	---	550 rpm
LG6B		---	5	12-15h

[A]*Content of inorganic phase expressed in percentage respect to lignin amount*

A.3.3. Characterization methods

The techniques of analysis employed for the characterization of the lignins modified by the previous processes are displayed in the following table.

Table 34. Characterization methods used for the analysis and evaluation of the main structural changes derived from the processes of modification of the lignins.

Component	Analysis	Technique	Annex	Section
Lignin	Molecular weight	HPSEC[A]	Annex III	III.3
	Thermal properties	TGA[B]		III.5
	Chemical structure	FTIR[C]		III.6.1
		^{1}H-NMR[D]		III.6.2
	Hybrid organic-inorganic structure	XRD[E]		III.7

[A]*HPSEC: High performance size exclusion chromatography,* [B]*TGA: Thermogravimetric analysis,* [C]*FTIR: Fourier Transformed Infrared Spectroscopy analysis,* [D] ^{1}*H-NMR: Proton Nuclear Magnetic Resonance Spectroscopy analysis and* [E]*XRD: X-ray diffraction analysis.*

A.4 Results and discussion

In the next points, the main results obtained from the functionalization and chemical modification of the lignins are shown with the corresponding analysis.

A.4.1 Fourier transform infrared spectroscopy analysis (FTIR)

This technique was employed to assess the main structural changes in the lignin after the process of glyoxalation.

In figure 29, the spectra corresponding to the pristine or unmodified lignins (LAS and LMP) and the different formulations of glyoxalated lignins (LG1-LG6) are shown. Several differences were observed in the structure of the lignins before and after the reaction with glyoxal.

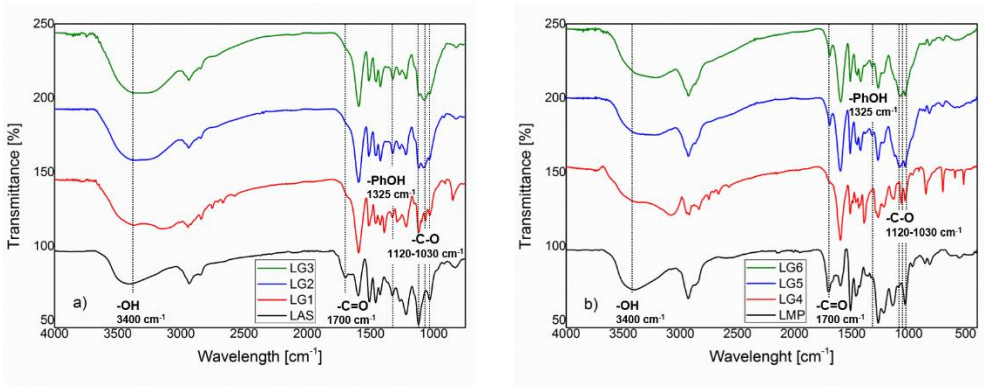

Figure 29. Comparison of the spectra from pristine and glyoxalated lignins: a) almond shells lignin b) maritime pine lignin.

First, the band of hydroxyl groups at 3400 cm^{-1} increased after glyoxalation becoming wider, especially as the amount of glyoxal used was incremented. The band at 1700 cm^{-1} linked to carbonyl groups, which appeared in both lignins, displayed different tendencies after the process of modification. On the one hand, in the glyoxalated LAS the intensity of the band decreased considerably and became broader and less intense. On the other side, in the case of glyoxalated LMP the band intensity decreased in a small extent.

This may be associated to a different reaction path of the carbonyl groups present in both types of pristine lignins (LAS and LMP) during glyoxalation. Another band around 1325 cm^{-1} was seen, which was related to phenolic hydroxyl groups. Nevertheless, the major changes after glyoxalation were detected in the region between 1120 and 1030 cm^{-1}. Here three main bands appeared at 1117 cm^{-1}, 1060-1080 cm^{-1} and 1030 cm^{-1}, corresponding to C-O stretching of secondary alcohol and C-O stretching and deformation of primary alcohol respectively. The major band was located in the region between 1060 and 1080 cm^{-1}, which became broader as the amount of glyoxal in the reaction increases. From the previous analysis, a glyoxalation index was determined to assess the degree of modification of each formulation. To calculate the glyoxalation index (GI), the absorbance spectra were obtained and normalized to the maximum absorbance values. Then, the resulting curve was fitted using PeakFit 4.12 signal processing software, to elucidate the absorbance wavelengths of each band by integrating the area under the fitted curves. The numerical fitting was performed with a correlation of 0.999 ± 0.015. With the values of absorbance of each band, relative absorbance ratios (equations 1-3) were calculated based on the work by Malutan et al., 2007 [258]. The GI was calculated as the quotient of the means of these ratios.

$$\text{OH-total groups} = \text{Average}\ (A_{3400}, A_{1325}, A_{1117}, A_{1076}, A_{1030}) \quad (1)$$

$$\text{Phenolic OH-groups} = A_{1325} \quad (2)$$

$$\text{GI} = \text{OH-Aliphatic / OH-Aromatic} = [(\text{OH-total / OH-Aromatic})-1] \quad (3)$$

The ratios previously defined are shown in table 35. With regard to the results, it was confirmed that both the total hydroxyl groups and the glyoxalation index presented the same increasing tendency. This was because during the glyoxalation reaction, hydroxymethyl groups (-CH_2OH) were introduced into the lignin structure as reported by Younesi-Kordkheili and Pizzi, 2017 [259]. Thereby, the GI was taken as indicator to assess the degree of activation of the lignins.

Table 35. Ratios of relative absorbance for the different glyoxalated lignins

Samples	OH-aromatic*	OH-total*	GI
LG1	1.95	6.04	2.09
LG2	3.24	10.44	2.31
LG3	3.44	12.11	2.53
LG4	1.78	5.32	1.99
LG5	2.54	10.37	3.09
LG6	2.13	11.28	4.29

**These ratios were expressed as percentage of area contribution to the total area under the spectra curves*

Regarding the amount of aromatic hydroxyl groups (OH-aromatic), two trends were observed. In the glyoxalation of LAS, this ratio increased, whereas it remained within a smaller range in the case of LMP. This indicated that LMP presented a higher amount of aliphatic OH compared to LAS after glyoxalation. For this reason, the GI of glyoxalated LMP was considerably higher than that of LAS, since the GI is defined as the ratio between aliphatic and aromatic OH. This index outlined that the introduction of hydroxymethyl groups (–CH_2OH) in the lignin structure was more evident in the LMP, and therefore the degree of modification was higher for this type of lignin. The reason for that was related to the S/G ratios of both pristine lignins (Chapter 2, section B.4.2.2). The fact that LMP has a low S/G ratio underlines a majority of guaiacyl units within its structure (one methxoyl group in the aromatic ring), whereas the higher S/G ratio of LAS highlights a preponderance of syringyl moieties (two methoxyl groups in the aromatic ring). Thus, it is clear that a major amount of free positions in the aromatic rings will be available in LMP compared to LAS. In the reaction between lignins and glyoxal and formaldehyde, the hydroxymethyl (-CH_2OH) groups are normally introduced in the C3 and/or C5 position of the aromatic rings[259,260]. Accordingly, the LMP lignins with more free spaces in their aromatic rings would facilitate the process of activation, leading to a higher extent of glyoxalation.

Besides, it was evidenced in both cases that the formulations with higher amounts of glyoxal added (LGS3 and LGS6) were the ones with a higher degree of glyoxalation and thus more activated. Accordingly, these formulations were selected for performing the process of modification with inorganic nanoparticles. The process of hybridization or modification of lignins with the inorganic nanoparticles was evaluated as well by FTIR analysis to determine the main structural differences between the activated lignins before and after the addition of the inorganic compounds. Thus, it was possible to elucidate whether the nanoclay (OMMT) and the nanosilicate (POSS®) were introduced into the lignin structure and whether the substitution of the functional groups happened. In figure 30, the spectra of the different formulation of lignins modified with the inorganic nanoparticles are shown.

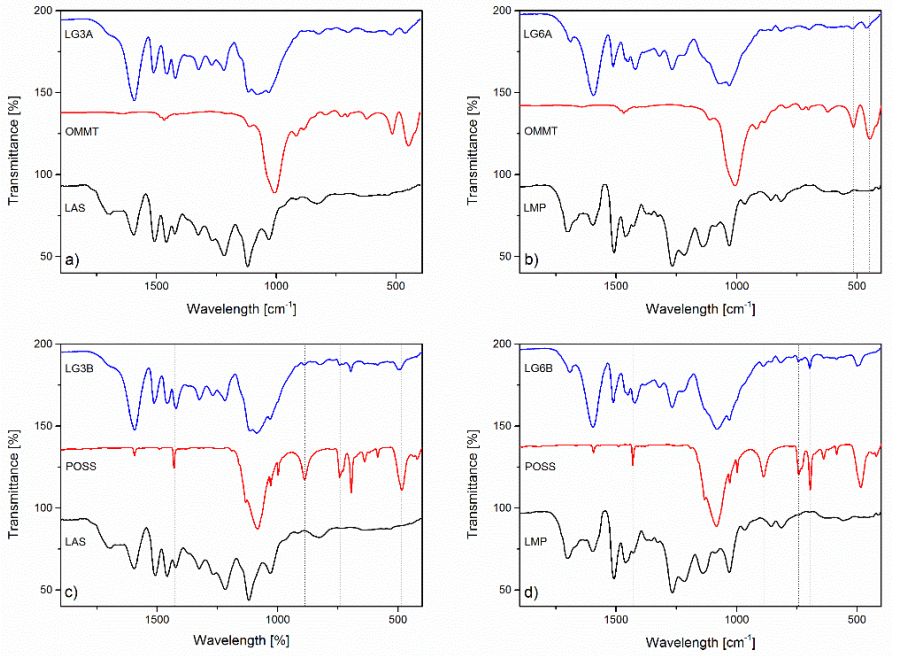

Figure 30. Comparison of the spectra from glyoxalated lignins before and after addition of inorganic nanoparticles: a) almond shells lignin with OMMT b) maritime pine lignin with OMMT, c) almond shells lignin with POSS® and d) maritime pine lignin with POSS®.

Additionally, the spectra of the nanoparticles are displayed as well and presented as reference. The spectra range selected was between 1900 and 400 cm^{-1} to highlight the bands showing the most significant changes.

It was seen in the previous figure that new bands derived from OMMT and POSS® appeared in the lignins after the process of hybridization. Nevertheless, some differences were observed depending on the type of nanoparticles used. In the case of lignins modified with OMMT, two main bands were highlighted at 460 cm^{-1} and 520 cm^{-1}. The first one corresponds to deformation of Si-O-Si bonds[261] whereas the second band to Si-O-Al linkages of montmorillonite layered-structure[262]. On the other hand, the lignins modified with POSS® showed four new bands at 499 cm^{-1}, 695 cm^{-1}, 890-895 cm^{-1} and 1423 cm^{-1} associated to Si linkages. These are linked to Si-O bending[263], Si-C stretching[264], Si-OH bending[265] and Si-Ph stretching[266] vibrations respectively. Another new band was seen in the modified lignin spectra at 740-745 cm^{-1} related to C-H deformations of aromatic rings from POSS® structure. In all the lignins modified with inorganic nanoparticles, both OMMT and POSS ®, a strong band was observed at 1100-1000 cm^{-1}. This band, which corresponds to Si-O-Si symmetric stretching, was overlapped with that of glyoxalated lignins attributed to C-O stretching and deformation of primary and secondary alcohols. This phenomenon was also observed in another work by Zhang et al., 2013 [267]. Considering the mentioned variations in the spectra of the lignins modified with inorganic nanoparticles, a possible reaction between the glyoxalated lignins and the inorganic nanoparticles was presented. Thus, it was proposed that the components could be reacting through their hydroxyl groups by means of a condensation reaction. This was based on several observations from the spectra of the different lignins, OMMT and POSS®. On the one hand, the OMMT showed two small peaks at 917 and 885 cm^{-1} attributed to the in-plane vibration of the hydroxyl groups of AlMgOH and AlAlOH respectively[268] and those peaks disappeared from the original spectra to the lignin modified with this nanoparticle.

A similar tendency was seen for the band of POSS® related to the bending vibrations of hydroxyl groups linked to Si, whose intensity considerably decreased from the original POSS® spectra to the lignins modified with this nanoparticle. In another work by An et al., 2018 [269] an analogous explanation to the previous ones was described concerning the reaction of the hydroxyl groups between montmorillonite and a lignocellulosic compound to form a nanocomposite. Besides these facts, it was observed that the intensity of the band corresponding to the total hydroxyl groups (≈3400 cm^{-1}) decreased from the spectra of the glyoxalated lignins to the spectra of the lignins modified with OMMT and POSS®, as shown in Figure 31.

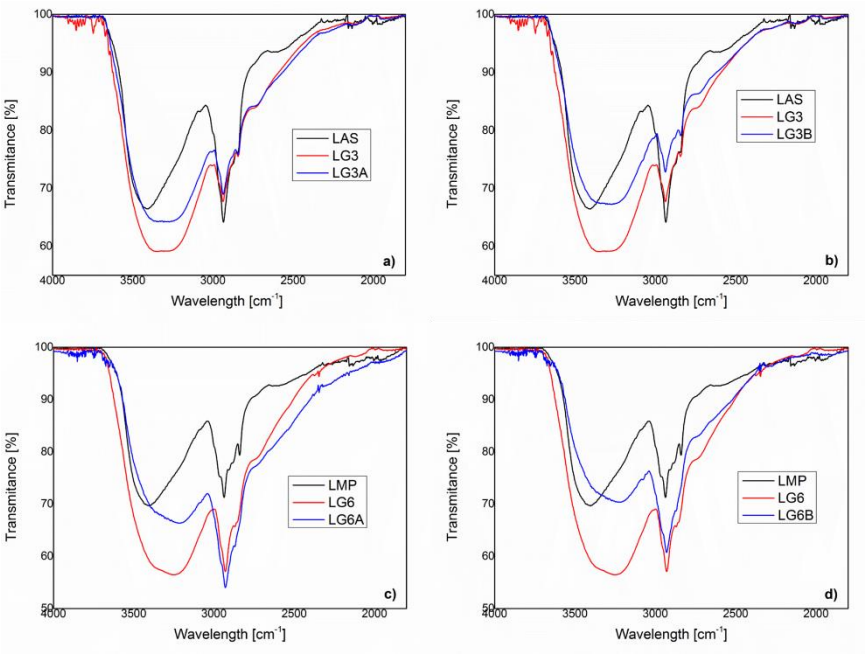

Figure 31. Comparison of the band corresponding to total hydroxyl groups between glyoxalated lignins and lignins modified with inorganic nanoparticles: LG3A-(a), LG3B-(b) and LG6A-(c), LG6B-(d).

This decrease in the intensity of the band from one spectra to the other was attributed to the above-mentioned condensation reaction between the lignins and the inorganic nanoparticles through the hydroxyl groups. Thus, when the OMMT and POSS® were linked to the lignin structure they may be attached to the different types of hydroxyl groups present in the glyoxalated lignins, lowering the amount of these functional groups and accordingly reducing the intensity of the band in the infrared spectra. From these results, it was confirmed that both OMMT and POSS® were introduced into the lignins structure and therefore the formation of organic-inorganic hybrid based on activated lignins and inorganic nanoparticles was achieved.

A.4.2 High performance size exclusion chromatography analysis (HPSEC)

The molecular weight of the pristine lignins and that of the lignins after glyoxalation and modification with inorganic nanoparticles was elucidated to evaluate the size variations of the lignin structures. The results derived from this analysis are displayed in figure 32. It was observed a clear difference between the molecular weights of the pristine lignins (PL) the glyoxalated (G1-3) and the hybridized lignins (M1-2). After the reaction with glyoxal, the molecular weights increased considerably since they were almost doubled in both cases. This was attributed to the condensation between cleaved and uncleaved lignin units through glyoxylene bridges as reported by Navarrete et al., 2012 [270].

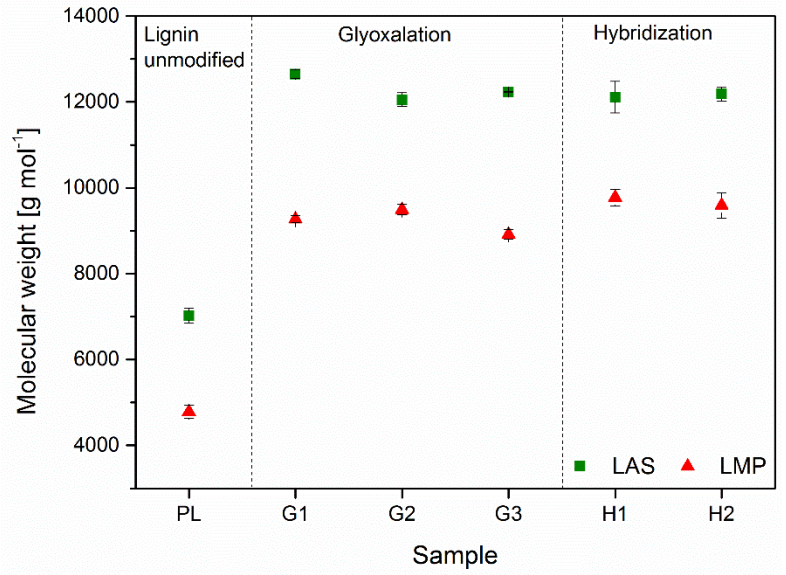

Figure 32. Molecular weights of the lignins before modification, after glyoxalation and after modification with inorganic nanoparticles. PL: pristine lignins, G1: glyoxalation conditions of LG1 and LG4, G2: glyoxalation conditions of LG2 and LG5, G3: glyoxalation conditions of LG3 and LG6, H1: hybridization with OMMT, conditions of LG3A and LG6A and H2: hybridization with POSS ®, conditions of LG3B and LG6B.

As it was stated in the previous section, during the glyoxalation reaction, hydroxylmethyl groups are introduced in the free positions of the aromatic rings from the lignin units. Then those lignin units can follow a condensation reaction through the hydroxymethyl groups forming methylene bridges, as reported by Hussin et al., 2019 [260]. A possible reaction path for these reactions is proposed in figure 33.

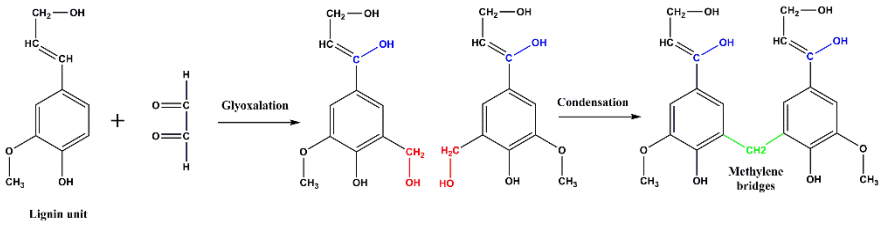

Figure 33. Mechanism proposed for the reaction between lignin units and glyoxal.

Concerning the different glyoxalated lignins, no significant differences are regarded between them in terms of molecular weights. Thus, the increment of the glyoxal content along the glyoxalated lignins might contribute mainly to the introduction of hydroxymethyl groups in the lignin units (e.g. blue groups in figure 33) rather than to further condensations, which could grow the molecular weights of the lignins. This would be in agreement with the increase of the OH groups proved with FTIR analysis.

Regarding the modified lignins with inorganic nanoparticles, none of the molecular weights showed any big differences compared to the glyoxalated lignins. This was because during the process of modification a 5% of nanoparticles were added based on the amount of lignin. Since these nanoparticles do not have big molecular weights, the values for the hybridized lignins remain almost constant.

A.4.3 ^{1}H-NMR spectroscopy analysis of the lignins

The structural changes of the lignins before and after the glyoxalation were regarded by analyzing their ^{1}H-NMR spectra. Before this analysis, the peaks were normalized to the highest intensity. In Figure 34, the spectra of the lignin samples before and after modification are shown. During the glyoxalation, some of the bands from the pristine lignins were modified owing to the structural changes induced by the reaction of lignins with glyoxal. The main differences in the spectra of the modified lignins were regarded specially in the range between 4-5.5 ppm. Within this region, a moderate to strong signal was observed at 4.5 ppm, which could be associated to the hydroxyl proton of hydroxymethyl groups (-CH_2OH). To confirm that this signal is due to a hydroxyl group, the same methodology mentioned in chapter 2, section B4.2.4 based on the addition of TFA (Annex III section III.6.2.1) was employed.

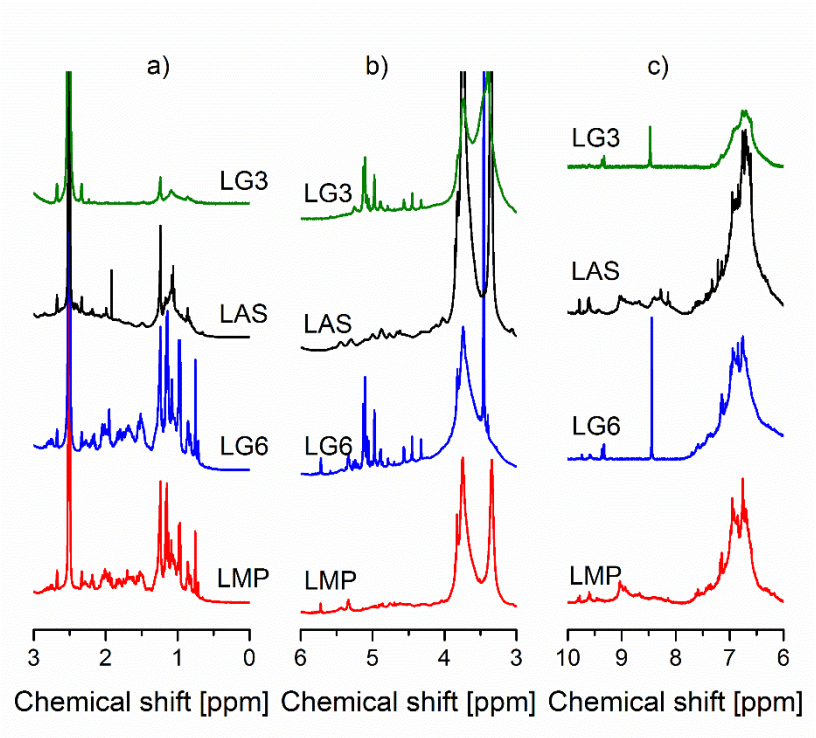

Figure 34. H-NMR curves of the original (LAS and LMP) and glyoxalated lignins (LG3 and LG6) focusing in the different parts of the spectra: a) aliphatic H^+ (range 0-3 ppm), b) methoxyl and lignin interunits linkages H^+ (range 3-6 ppm), and c) aromatic and hydroxyl H^+ (range 6-10 ppm).

Following this method, the previous hypothesis was proved as shown in Figure 35. This was in agreement with the introduction of hydroxyl groups mentioned in section A.4.1 and observed in the infrared spectra. The rest of the peaks detected within this section of the spectra, were related to the methylene or glyoxalene groups, both linked and non-linked to hydroxyl groups. The latter ones would be associated to linkages between lignin small fractions to form a bigger structure. This assumption was in accordance with the condensation of lignin moieties through glyoxalene bonds stated in section A.4.2.

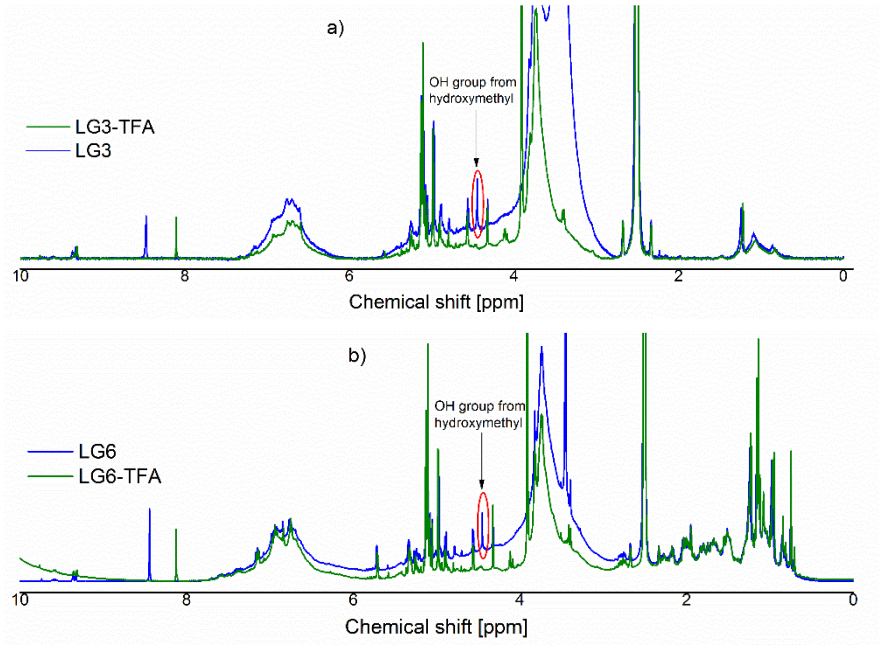

Figure 35. Determination of the peaks of protons from hydroxyl groups: a) glyoxalated lignin from almond shells (LG3) and b) pristine lignin from maritime pine (LG6).

The other major divergences were seen in the last part of the spectra (Figure 34c). Here it was observed that the width of the peak due to aromatic protons (6-8 ppm) was reduced after reaction with glyoxal. A similar tendency was regarded for the signals of the aromatic hydroxyl groups (8-9 ppm), but in this case, they disappeared after glyoxalation. This can indicate that some of the linkages formed between lignin moieties via glyoxalene bridges may occur through the H and some of the OH of the aromatic rings. On the other hand, a narrow and intense peak appeared in both cases after glyoxalation at 8.4-8.5 ppm. This peak was related to the reaction of glyoxal and lignin. Capraru et al., 2012 [271] pointed out an analogous trend in the same range for the reaction of lignin and formaldehyde. Finally, peaks at 9.3 ppm and 9.4 ppm appeared after the lignin modification. These peaks, which have the typical shift of aldehyde protons[272], could be attributed to aldehyde compounds derived from some residual glyoxal or glyoxal oligomers remaining unreacted.

A.4.4 X-ray diffraction analysis of the lignins

The X-ray diffraction analysis was carried out for the lignin samples modified with inorganic nanoparticles to evaluate the introduction of the nanoparticles into the lignin structure. The diffractograms obtained from the XRD analysis were normalized to highest intensity prior to any assessment. Then the FitPeak 4.12 signal processing software was used to perform the fit of the curves from the diffractograms. The numerical fitting was done with a correlation of 0.999±0.012. In Figure 36, the normalized diffraction patterns of nanoparticles, pristine and modified lignins are displayed. Results from indexing and phase identification are presented in Tables 36 and 37.

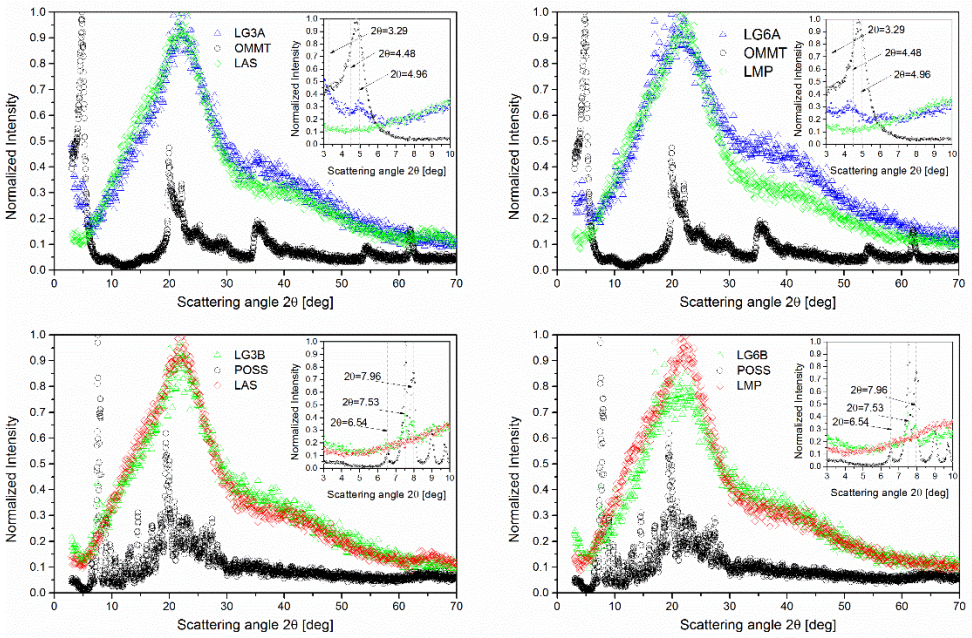

Figure 36. Diffractograms of the different lignins modified with inorganic nanoparticles: a) LAS modified with OMMT, b) LMP modified with OMMT, c) LAS modified with POSS® and d) LMP modified with POSS®.

Concerning the organically modified montmorillonite, the peaks with the highest intensities were regarded in the range 2θ between 0-10º.

Here it could be highlighted the peaks at 3.29º and 4.96º related to the silicate structure and the organic modifier present in the nanoclay (dimethylbenzylhydrogenated tallow ammonium) respectively[273,274]. In the next range (2θ between 10-30º), considerable intensities were observed as well. Within this region, the peaks at 20.04º and 22.04º were remarked, which were attributed to the planes 020 and -111 respectively. They are typical from the montmorillonite as reported in various works[275,276]. Beyond 2θ=35º, other important planes at -201 and -131 of monoclinic montmorillonite were seen.

Table 36. Indexing of the different peaks obtained from the DRX analysis for OMMT

2θ (º)	Amplitude a.u.	$d_{spacing}$ (Å)	h k l	Phase	Type of signal	Source
3.29	0.71	26.89	0 1 0	MMT[a]	S[B]	Calculated
4.48	1.00	19.70	0 1 0	43B[b]	VS[A]	Esposito et al., 2015 [277]
4.96	0.93	17.83	-1 0 0	MMT[a]	VS[A]	Calculated
5.79	0.20	15.25	0 0 1	MMT[a]	VW[D]	Calculated
6.66	0.07	13.27			VW[D]	
8.88	0.03	9.96	0 0 1		VW[D]	Calculated
15.62	0.03	5.67			VW[D]	
17.27	0.04	5.14	0 0 2		VW[D]	Calculated
18.38	0.08	4.83	1 1 0		VW[D]	
19.12	0.11	4.64			VW[D]	Calculated
20.04	0.64	4.43	0 2 0	MMT[a]	S[B]	Gournis et al., 2008 [275]
20.93	0.43	4.24	1 0 2		W[C]	Calculated
22.04	0.44	4.03	-1 1 1	MMT[a]	W[C]	Galimbeti et al., 2009 [276]
23.04	0.17	3.86			VW[D]	
23.81	0.13	3.74			VW[D]	
24.52	0.18	3.63			VW[D]	
25.29	0.18	3.52			VW[D]	
26.19	0.11	3.40			VW[D]	
26.91	0.07	3.31	0 2 2		VW[D]	Calculated
27.63	0.09	3.23			VW[D]	
28.52	0.11	3.13	1 2 2		VW[D]	Calculated

2θ (º)	Amplitude a.u.	$d_{spacing}$ (Å)	h k l	Phase	Type of signal	Source
29.41	0.08	3.04			VW[D]	
30.10	0.09	2.97			VW[D]	
31.26	0.04	2.86			VW[D]	
31.82	0.02	2.81			VW[D]	
33.07	0.03	2.71			VW[D]	
35.09	0.19	2.56	-2 0 1	MMT[a]	VW[D]	Calculated
35.53	0.03	2.53	-1 3 1	MMT[a]	VW[D]	Calculated
35.99	0.16	2.50		MMT[a]	VW[D]	Calculated
36.82	0.10	2.44		MMT[a]	VW[D]	
37.80	0.08	2.38	-2 0 2	MMT[a]	VW[D]	Calculated
38.90	0.07	2.32	-1 1 4	MMT[a]	VW[D]	Calculated
40.26	0.07	2.24	1 3 2	MMT[a]	VW[D]	Calculated
41.16	0.05	2.19	2 0 2	MMT[a]	VW[D]	Calculated
42.06	0.04	2.15		MMT[a]	VW[D]	
42.88	0.04	2.11	-2 2 2	MMT[a]	VW[D]	Calculated
43.80	0.03	2.07		MMT[a]	VW[D]	
44.46	0.02	2.04	0 4 2	MMT[a]	VW[D]	Calculated
45.20	0.03	2.01		MMT[a]	VW[D]	
46.96	0.01	1.93	2 0 3	MMT[a]	VW[D]	Calculated
54.23	0.06	1.69	1 5 0	MMT[a]	VW[D]	Calculated
54.97	0.04	1.67	3 1 1	MMT[a]	VW[D]	Calculated
55.65	0.01	1.65	0 0 6	MMT[a]	VW[D]	Calculated
57.06	0.01	1.61	-1 3 5	MMT[a]	VW[D]	Calculated
61.99	0.01	1.50	1 1 6	MMT[a]	VW[D]	Calculated

[a]MMT: planes related to monoclinic montmorillonite structure

[b]43B: plane related to the organic modifier (dimethylbenzylhydrogenated tallow ammonium)

[A]VS: very strong, [B]S: strong, [C]W:weak, [D]VW: very weak

In both modified lignins with OMMT (LG3A, LG6A), the contribution of the first peaks in the range 2θ=0-10º (owing to the silicates) was clearly visible. However, the peaks corresponding to the planes in the range 2θ=15-30º were only present in the modified lignin from maritime pine (LG6A) and not in that from almond shells (LG3A). This was observed specially in the peak of OMMT at 2θ=20.04º, which was shifted in the modified lignin (2θ ≈18.5º).

This may be caused by a better interaction between the lignin from maritime pine and the OMMT, owing to its structure with more free positions in the aromatic rings thus having higher activation. This tendency was also observed and explained in the lignin modified with POSS® presented afterwards. In the range 2θ=30-50º, the contribution of planes of the monoclinic montmorillonite were present in both modified lignins but it was again more perceptible in the case of LG6A.

Concerning the polyhedral oligomeric silsesquioxane, several peaks were observed in the region 2θ=0-10º. Weak signals at 6.54º and 8.99º and strong a one at 7.53º [278], corresponding to the triclinic structure of trisilanol phenyl (TS-Ph), were identified. Besides a peak at 7.96º attributed to the rhombohedral structure of POSS® was seen. In the range 2θ=10-20º, strong to weak signals were highlighted at 14.53º, 17.00º, 19.43º and 19.98º, which were associated to the trisilanol phenyl structure (TS-Ph) as well. Beyond 2θ=20º, the majority of the signals were attributed to rhombohedral planes of POSS® [279].

Table 37. Indexing of the different peaks obtained from the DRX analysis for POSS®

2θ (º)	Amplitude a.u.	$d_{spacing}$ (Å)	h k l	Phase	Type of signal	Source
6.54	0.10	13.52	1 -1 0	TS-Ph[a]	W[C]	Calculated
7.53	1.00	11.75	1 0 -1	POSS[b]	VS[A]	Barry et al., 1955 [278]
7.96	0.79	11.10	1 0 -1	POSS[b]	VS[A]	Calculated
8.99	0.31	9.83	1 1 0	TS-Ph[a]	W[C]	Calculated
9.75	0.19	9.07	1 1 -1		VW[D]	Calculated
10.59	0.12	8.35	1 1 0	POSS[b]	VW[D]	Fu et al., 2001 [279]
11.57	0.09	7.65	2 0 0	POSS[b]	VW[D]	Fu et al., 2001 [279]
12.26	0.08	7.22	2 0 -1	TS-Ph[a]	VW[D]	Calculated
12.91	0.11	6.86	2 0 0	POSS[b]	VW[D]	Fu et al., 2001 [279]
14.53	0.31	6.10	-2 2 1	TS-Ph[a]	W[C]	Calculated

2θ (º)	Amplitude a.u.	$d_{spacing}$ (Å)	h k l	Phase	Type of signal	Source
15.47	0.08	5.73	2 0 2	POSS[b]	VW[D]	Fu et al., 2001 [279]
17.00	0.23	5.22	2 2 0	TS-Ph[a]	W[C]	Calculated
17.93	0.14	4.95		POSS[b]	VW[D]	
18.57	0.23	4.78	2 2 1	POSS[b]	VW[D]	Barry et al., 1955 [278]
19.43	0.52	4.57	2 2 -2	TS-Ph[a]	S[B]	Calculated
19.98	0.26	4.44	3 0 2	TS-Ph[a]	W[C]	Calculated
20.89	0.23	4.25	3 1 -2	POSS[b]	VW[D]	Fu et al., 2001 [279]
22.33	0.19	3.98	2 3 0	TS-Ph[a]	VW[D]	Calculated
23.19	0.18	3.84	4 0 0	POSS[b]	VW[D]	Barry et al., 1955 [278]
23.67	0.18	3.76	4 -1 -1	POSS[b]	VW[D]	Fu et al., 2001 [279]
25.33	0.07	3.52	1 2 4	POSS[b]	VW[D]	Barry et al., 1955 [278]
26.37	0.17	3.38	3 2 1	POSS[b]	VW[D]	Barry et al., 1955 [278] Fu et al., 2001 [279]
27.93	0.02	3.20	3 2 2	POSS[b]	VW[D]	Barry et al., 1955 [278] Fu et al., 2001 [279]
29.58	0.06	3.02		POSS[b]	VW[D]	
31.39	0.07	2.85	4 0 -4	POSS[b]	VW[D]	Calculated
32.81	0.04	2.73		POSS[b]	VW[D]	

[a]*TS-Ph: planes related to triclinic trisilanol phenyl structure*

[b]*POSS: planes related to the rhombohedral polyoligomeric silsesquioxane structure*

[A]*VS: very strong,* [B]*S: strong,* [C]*W:weak,* [D]*VW: very weak*

Respecting to the lignins modified with POSS (LG3B and LG6B), in the range 2θ=0-10º the contribution of the signal corresponding to rhombohedral POSS structure was seen in both lignins. Nevertheless in the next region (2θ=10-20º), the contributions due to trisilanol phenyl (TS-Ph) at 19.43º and 19.98º were more evident (more pronounced signals at those scattering angles) in the case of modified lignin from maritime pine (LG6B).

Furthermore, the relative intensity of the broad curve associated to the amorphous structure of lignin was reduced around 15% in this same modified lignin. Thereby, in the case of the modified lignin from maritime pine (LG6B) there was a higher predominance of the organic-inorganic modified structure of lignin compared to the modified lignin from almond shells (LG3B). This would mean that the extent of insertion of the inorganic nanoparticles was higher in the LG6B than in LG3B. This tendency was attributed to the fact that pristine lignin from maritime pine presents more free positions in the aromatic rings than the lignin from almond shells; owing to the prevalence of guaiacyl units, as commented in the section A.4.1. Thereby a higher degree of activation was achieved during the glyoxalation for those lignins. For this reason, the introduction of the inorganic nanoparticles into the lignin matrix was higher compared to the almond shells lignin, which presents a lower degree of activation.

A.4.5 Thermogravimetric analysis of the lignins

This analysis was carried out to assess the thermal performance of the lignins after chemical modification with glyoxal and after the incorporation of the inorganic nanoparticles.

The curves from the thermogravimetric and derivative thermogravimetric analyses are presented in Figure 37. The main thermal parameters determined from the previous curves are listed in Table 38. After glyoxalation, it was clear that lignins structure was changed as new degradation stages, which were not present in the pristine lignins, appear. Thereby, in glyoxalated lignins four main events were regarded during the thermal degradation. The first one was associated to evaporation of moisture and volatiles and appeared at the same range of temperatures described for the pristine lignins (chapter 2, section B4.2.6). Nevertheless, the rate of degradation of this step was increased compared to that of unmodified lignins. Accordingly, the initial degradation temperature ($T_{5\%}$) considerably decreased compared to that of pristine lignins (Table 38).

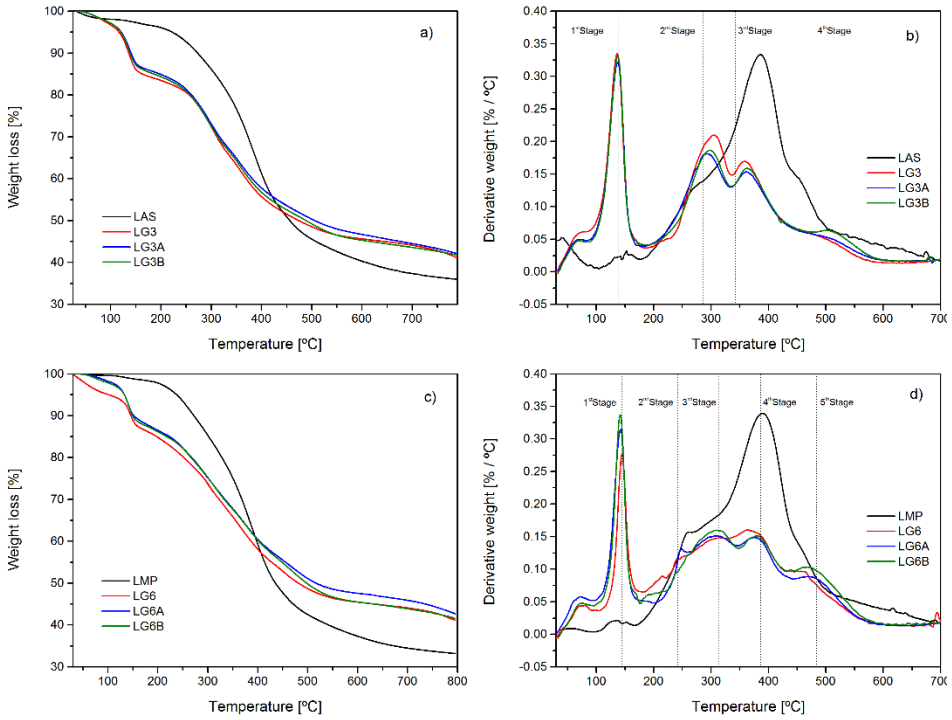

Figure 37. Curves from the thermal analysis of the different lignin samples before and after modification: a) thermogravimetric curves of lignins from almond shells, b) derivative thermogravimetric curves of lignins from almond shells, c) thermogravimetric curves of lignins from maritime pine, and d) derivative thermogravimetric curves of lignins from maritime pine.

This decrease observed in the glyoxalated lignins could be attributed to the presence of unreacted glyoxal and glyoxal dimers or trimers in a smaller percentage, which were not in the pristine lignins. The second stage of degradation was observed between 295-310 ºC. Since this step appeared only in the glyoxalated samples, it was related to the reaction between lignin and glyoxal. Thus, this step could be attributed to the formation of new lignin condensates of smaller molecular weight after the crosslinking between the lignin moieties by means of methylene bridges as reported by Ang et al., 2015 [280]. The third event (360-363 ºC) was linked to degradation of the glyoxalated lignin structure. In comparison to the pristine lignins, this temperature of degradation was decreased.

This may be due to the introduction of more hydroxyl groups, which would increase the susceptibility to thermal decomposition[281]. The last stage of degradation (450-500 ºC), was derived from the glyoxalation reaction and therefore it was again present only in the lignin samples modified with glyoxal. An extra step of decomposition at 240 ºC was regarded in LG6 following the same tendency of LMP mentioned in the previous chapter.

Table 38. Main thermal degradation parameters of the different lignins.

	TGA Analysis			DTGA Analysis (Temperatures of degradation ºC)				
	$T_{5\%}$ (ºC)	$T_{50\%}$ (ºC)	Residue (%)	1st Stage	2nd Stage	3rd Stage	4th Stage	5th Stage
LAS	221.97	456.22	35.89	148.18[A]	385.84[C]			
LG3	116.09	477.63	40.22	137.25[A]	303.94[B]	360.78[C]	503.79[D]	
LG3A	121.43	505.96	42.45	137.23[A]	293.49[B]	358.94[C]	510.78[D]	
LG3B	122.28	513.44	42.58	137.11[A]	298.64[B]	359.84[C]	507.85[D]	
LMP	237.23	435.30	33.18	137.05[A]	258.33	389.72[C]		
LG6	116.37	481.87	41.54	145.24[A]	239.15	308.01[B]	363.45[C]	458.80[D]
LG6A	129.89	509.65	42.55	141.02[A]	250.01	309.61[B]	376.14[C]	475.60[D]
LG6B	131.11	494.54	41.07	142.52[A]	256.54	309.46[B]	380.74[C]	468.85[D]

[A]*Stage of degradation related to the moisture and volatiles decomposition*

[B]*Stage of degradation related to the decomposition of lignin polymers of low molecular weight formed during the glyoxalation*

[C]*Stage of degradation related to the decomposition of the main lignin structure*

[D]*Stage of degradation related to the decomposition of the condensed structure formed after glyoxalation*

The lignins modified with inorganic nanoparticles displayed some differences concerning the thermal behavior, compared to the glyoxalated ones. Regarding the initial degradation temperature ($T_{5\%}$), an increment was observed after the addition of inorganic nanoparticles.

This was due to the hydrophobicity of the integrated inorganic nanoparticles, which incremented the temperatures of the first stage of degradation (moisture evaporation). Since $T_{5\%}$ was located within this stage an increase was observed in the values of these temperatures after the addition of the nanoparticles. This tendency was also seen for the temperature at which the half of the mass was lost ($T_{50\%}$). In this case, the increase in the $T_{50\%}$ was associated to the attachment of the inorganic nanoparticles to the lignin structure, which improved the thermal resistance of the modified lignins (up to 30ºC more in the most favorable case). These trends were regarded in both types of lignins. The residues remaining after thermal degradation were in the range 33-42% and slightly higher in the modified lignins than in the pristine ones. Concerning the stages of degradation, lignins modified with inorganic nanoparticles showed the same ones described for the glyoxalated lignins. Nonetheless, not the same results were obtained for both type of lignins. In the case of LAS, the temperatures of degradation remained constant or slightly increased from the glyoxalated lignin (LG3) to the lignins modified with inorganic nanoparticles (LG3A and LG3B). On the other hand, in the case of LMP the stages of degradation were delayed in the lignins modified with inorganic nanoparticles (LG6A and LG6B) compared to the glyoxalated one (LG6). This tendency was more noticeable in the last stages of degradation. In the step of degradation associated to the lignin structure (≈360 ºC), the temperature of decomposition was increased between 10-15 ºC. In addition to that, in the last stage of degradation (due to lignin modification with glyoxal) the degradation temperature was delayed 15-20 ºC. Thereby it was confirmed that the introduction of the nanoclay and nanosilicate particles did improve the thermal behavior of the lignins specially that of LMP. These results concur with those observed in the XRD patterns, linking directly proportionally the higher thermal stability to the presence of inorganic agents.

A.5 Conclusions

The results presented in this part displayed the structural modification of the lignins from different origin via glyoxalation and modification with inorganic nanoparticles. On the one hand, the glyoxalation reaction resulted in an increase of the amount of hydroxyl groups within the lignin structure and in the formation of condensates between lignin small units by means of methylene bridges.

These phenomena were verified mainly by the FTIR and ^{1}H-NMR analyses. On the other hand, the introduction of the nanoparticles and their substitution into the lignin structure was confirmed as well, as shown in the results from the FTIR and XRD analyses. Accordingly, it was observed that the activation of the lignin through the reaction with glyoxal succeeded aiding the incorporation of the inorganic phases into the organic polymer matrix. Moreover, these inorganic phases were proved to enhance the thermal behavior of the organic-inorganic hybrid by delaying the temperatures of degradation, especially in the case of lignin derived from maritime pine.

Part B. Synthesis of biosourced phenolic resins

B.1 Motivation

The current major role of the phenolic resins in the industry for many different applications is well known. These resins are traditionally obtained from compounds dependent on fossil fuel sources. Nevertheless, owing to industry strict limitations and environmental reasons, there is an ongoing tendency towards the utilization of biosourced phenolic resins. Accordingly, toxic and non-renewable raw materials e.g. phenol or formaldehyde, are switched by others with similar chemical compounds obtained from natural and renewable sources. In this part, the issue of the transition from synthetic to biosourced phenolic resins is introduced first. Then the process of synthesis of the biosourced resins from activated lignin and tannins is presented. The mentioned resins are chemically characterized by various parameters employed nowadays in the industry and a comparison to other synthetic resins is provided. Finally, a thermal analysis of the liquid resins is carried out, to assess the influence of the different components and evaluate the performance of the resins prior to and during the curing process.

B.2 Background

Phenolic resins have a long history with over 100 years since their discovery. They were the first synthetic resins obtained, by means of the polycondensation reaction between phenol and aldehydes. Over the years, several advances have taken place contributing to a better knowledge and the development of these systems (Table 39), which have allowed to their employment in several applications.

Table 39. Timeline of the most relevant events related to the phenolic resins since their discovery.

Years	Events
1872	**Bayer** first reported the reaction between phenol and aldehydes.
1894	**Lederer** and **Manasse** reported the formation of –ortho and –para phenols from the reaction of phenol and formaldehyde under basic conditions.
1902	Production of novolacs industrially via phenol resin condensation by **Blumer**.
1909	The production of the first plastic via polycondensation of phenol and formaldehyde is reported by **Baekeland**.
1910	Production of oil-soluble modified phenolic resins by **Behrends**, via addition of rosin to the general phenol-formaldehyde polycondensation.
1928-1931	Treatment of resol resins with fatty acids to obtain air-drying varnishes.
1930-onwards	Theoretical work on the mechanisms of formation of phenolic resins leading to the development of new application areas for phenolic resins.

Sources: Hesse et al., 2005 [282] *and Pilato et al., 2013* [283].

Nowadays, these resins play a prominent role among the chemical industry, being one of the most extensive commodity resin systems with a worldwide production of 6 million ton/year approximately[283]. In fact, within the European market of thermoset resins they are the most distributed just after urea formaldehyde resins (UF) for different applications, as shown in Figure 38.

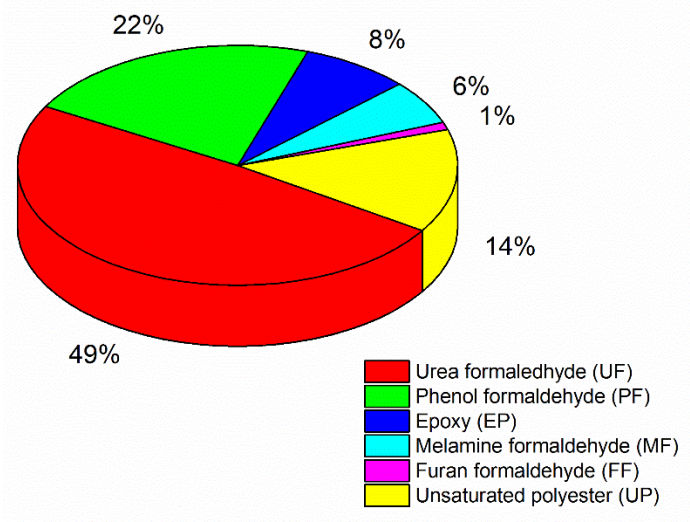

Figure 38. Distribution of the main thermoset resin systems along Europe[284].

They are commercialized in various areas of the industry, with a wide extent of product applications. Some examples are the use as composites and nanocomposites in the automotive and aircraft industry[284] ; agents in the paint, coating and adhesive industry[285]; binders in the processing of different materials[286,287]; insulators[288] and laminates[289].

Concerning their physical chemical properties, phenolic resins can present a coloration ranging from yellow to intense brown colour. They also display a wide range of solubility from water-soluble to naphta-soluble. They are generally classified into two different types, namely *resole* and *novolac* resins, based on the amount of the components and the reaction conditions (Figure 39). Apart from these general types other have been reported such as benzoxazines and cyanate esters[290].

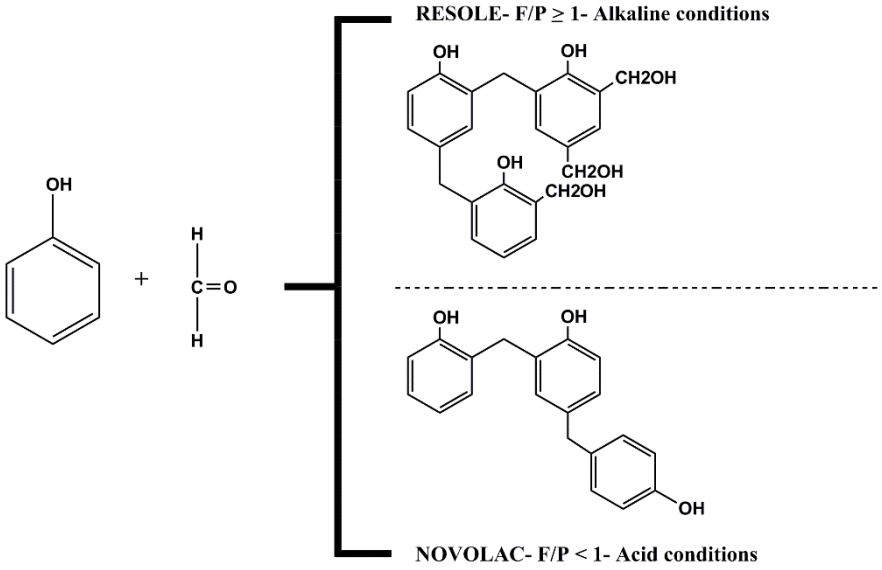

Figure 39. Types of phenolic resins depending on their synthesis.

- Resole resins: this type of phenolic resins are synthetized with excess of formaldehyde respect to phenol and under alkaline conditions. In this case, the characteristic groups formed after polycondensation are hydroxymethyl groups and dimethylene ether bridges. These resins can be polymerized with heat and with or without the action of a hardener.
- Novolac resins: this kind of resins are obtained with an excess of the phenol respect to formaldehyde and under acidic conditions. Unlike the previous type, they require a curing agent for the process of polymerization. After polymerization, the units are linked by means of alkylidene bridges.

From the above information, it is clear that the synthetic phenolic resins are well settled in the industry. Nontheless, in the recent years these synthetic resins are being subjected to rising limitations, partly owing to the strict exposure regulations but also because they are mainly derived from non-renewable sources.

Consequently there is a current growing tendency to promote the substitution of their components by other of natural origin and more environmentally friendly. These new phenolic resins in which the components are obtained from renewable, natural or non-oil-derived raw materials are referred to as biosourced phenolic resins[291]. Here two strategies are exploited at the present: the substitution of formaldehyde for aldehydes with less toxicity and similar performance and the use of natural or renewable compounds of phenolic nature[292]. In respect to the former point, glyoxal and glutaraldehyde are interesting alternatives as reported in various works from the literature[293,294]. Glyoxal is the substitute to formaldehyde generally used, owing to its low toxicity, low volatility and the possibility of being be produced from natural sources. Moreover, its bifunctionality makes it an efficient crosslinker and therefore a perfect candidate for the synthesis of formaldehyde-free resins[295]. Glutaraldehyde also represents another significant alternative, since it is able to react with several functional groups of proteins or cellulose[296,297]. Besides, it constitutes the second most important dialdehyde after glyoxal[296].

Table 40. Examples of the main compounds commercialized as phenol replacement in biosourced phenolic resins.

Origin	**Compound**
Woody plants and algae	Tannins
Woody plants and by-product from pulp and paper industry	Lignins
Woody plants	Carbohydrates (cellulose, starch and hemicellulose)
Cashew nut shell liquid	Cardanol and derivatives
Vegetal protein (soya and soybean)	Triglicerides (“Soyoil”)
Animal hide, bones and fish	Proteins (casein)

Concerning the latter point there are variety of phenolic compounds offering interesting possibilities as alternative to phenol (Table 40). From the previous examples, the ones more extensively used for biosourced phenolic resins are tannins and lignins. In the case of tannins-based resins, they are already established in the market for example as adhesives[298]. This is because tannins can provide similar interactions to aldehydes and reactivity, due to their structure[299]. On the other hand, the resins derived from lignin are on the slow way to commercialization. The reason for that is that lignin has a more complex structure compared to phenol with some of its functionalities impeded and therefore presents a lower reactivity. For this reason, although the use of lignins as phenol substitute in phenol-formaldehyde type resins has been widely studied[300,301], they generally need a step of functionalisation prior to their substitution[302].

It was mentioned before that biosourced phenolic resins derived from tannins are well studied, developed and have proved their efficacy in several applications. Nevertheless, they display the disadvantage of competing with other tannin application with higher added value in areas such as medicine or pharmacology. For this reason, in the recent years, the combination of tannins and lignin as substitute of phenol in biosourced phenolic resins has been reported[303–305]. The utilization of both compounds as alternative to phenol allows the utilization of lower amounts of tannins to avoid competition to other tannin applications) and the valorisation of lignin, which is nowadays an underutilized compound with a significant potential.

Considering the previous points introduced, in this part the synthesis of a biosourced phenolic resins was designed. Lignin and tannins were chosen as substitutes to phenol, whereas glyoxal was used as alternative to formaldehyde. The lignin from maritime pine residues (extracted and characterized in chapter 2) was selected for its favourable properties and performance after functionalization compared to the lignin from almond shells, as it was presented in part A of this chapter.

The tannins employed were those of commercial mimosa extract, introduced previously in the last part of Chapter 2. The biosourced phenolic resin synthetized was of resole type, since excess of glyoxal was used compared to the lignin (phenol alternative) and basic conditions (pH 12-12.5) were set. These alkaline conditions are reported to favour the reactivity of the tannins in the reaction medium as well[306]. Besides, hexamine was selected as hardener or curing agent to promote the reaction between both lignin and tannins.

B.3 Experimental procedure

In the next subsections the materials used, the process followed for the synthesis of the biosourced phenolic resins and the techniques of analysis are described.

B.3.1 Raw materials and reagents

For the synthesis of the biosourced phenolic resins, lignins and tannins were employed as main raw materials. The lignins employed was that extracted from maritime pine residues (Chapter 2, part B) and subjected to functionalization via glyoxalation a later hybridization with a nanoclay (OMMT) and a nanosilicate (POSS) (Chapter 3, part A). The tannins used were a commercial extract from mimosa (*Acacia mearnsii*), which were supplied Tanacinc (Brazil) under the commercial name Tanfood.

Hexamethylenetetramine (≥99%), sodium hydroxide pellets and acetone (≥99%), which were kindly provided by Sigma Aldrich, were utilized as well as reagent during the process of synthesis.

B.3.2 Synthesis of the biosourced phenolic resins

The biosourced phenolic resins were obtained by using lignins and tannins as substitutes to phenol. Hexamine was employed as curing agent for the reaction, owing to the reported efficiency towards mimosa tannins[307].

Alkaline medium was set for the reaction, since it is known that the stability of hexamine is favored at higher pH. Moreover, the solution of mimosa tannins and hexamine in alkaline medium displays the advantage of having a significant pot life at ambient temperature[308]. The process of synthesis was based in a previous work by Mansouri et al., 2011 [304]. Two phases were elaborated separately, namely functionalized lignin and tannins solution, prior to their mixture for the synthesis of the resin. Three different formulation were obtained based on the functionalization to which lignins were subjected (Table 41).

Table 41. Formulations of the biosourced phenolic resins obtained based on the type and amount of their components.

Formulation	Components (% w/w)		
	Lignin	Tannins	Nanoparticles
$R_{REFERENCE}$	50 glyoxalated	50	0
R_A	48.78 glyoxalated+hybridized	48.78	2.44 OMMT
R_B	48.78 glyoxalated+hybridized	48.78	2.44 POSS

The phase of the functionalized lignin was obtained by using the organosolv lignin extracted from the maritime pine residues and following the processes described in sections A.3.3.1 and A.3.3.2 for the glyoxalated and hybridized lignins respectively. For the phase of the tannins, a mimosa tannin solution was first prepared with a concentration of 45% (w/w) in aqueous acetone 70% (w/w). Then the pH of the solution was set between 10-10.5 by adding sodium hydroxide aqueous solution 33% (w/w). Then the hardener or curing agent was prepared as aqueous hexamine solution 30% (w/w). This solution of the hardener was added to the solution of the tannins at set pH, based on 5% hexamine solids per tannin solids. Once both the functionalized lignin phase and that of mimosa tannins were prepared, they were mixed in proportion *functionalized lignin: mimosa tannin* of 1:1 by weight at ambient temperature (25ºC) and left with magnetic agitation (550 rpm) during 45-60 min.

B.3.3. Characterization methods

The main techniques of analysis used for the characterization of the different formulations of biosourced phenolic resins are displayed in Table 42.

Table 42. Characterization methods used for the assessment of the main characteristics and performance of the synthetized resins.

Component	Analysis	Technique	Annex	Section
Resins	Physical-chemical parameters	ρ[A]	Annex II	II.1.1
		pH		II.1.2
		μ[B]		V.1.1
		NVC[C]		V.1.2
	Amount of hydroxyl groups	Hydroxyl number	Annex V	V.2
	Degree of acidity or alkalinity	Acid/Alkalinity number		V.3
	Thermal analysis of curing	DSC[D]	Annex III	V.4
		TGA[E]		III.5

[A]ρ: density, [B]μ: viscosity, [C]NVC: non-volatile content, [D]DSC: differential scanning calorimetry, [E]TGA: Thermogravimetric analysis.

B.4 Results and discussion

In the next sections, the results obtained from the characterization carried out for the different formulations of the biosourced phenolic resins are shown and discussed.

B.4.1 Chemical characterization of the resins

The resins were first characterized for the typical physical chemical parameters and the results are showed in table 43.

Table 43. Physical-chemical parameters determined for the different formulations of the biosourced phenolic resins.

Formulation	Density (g/cm^3)	pH	Viscosity* (mPa·s)	NVC % (w/w)
$R_{REFERENCE}$	1.128±0.017	8.575±0.007	73.000±3.677	36.810±0.367
R_A	1.144±0.002	8.875±0.007	73.750±3.182	37.420±0.068
R_B	1.142±0.023	8.82±0.011	73.800±5.727	37.408±0.032

**The values of the viscosity correspond to the fresh resins just after synthesis.*

In respect to the previous results, it was seen that the parameters determined presented values within a small range for the different formulations. Nevertheless slight differences were detected, which followed analogous tendencies for the mentioned parameters. The pH of the resins formulations showed rather alkaline values. This was expected since the pH of the tannins phase was set at 10.4. Besides the lignin, which was the other main raw material, was dissolved at an alkaline pH prior to the glyoxalation reaction. The fact that the pH was slightly reduced from that of the tannins phase was related to the acidic pH of glyoxal (2-3.5), which could have remained unreacted in the glyoxalated lignin phase. Concerning the densities of the different formulations, they were lower than the ones reported in the literature for other phenolic resins based on the phenol formaldehyde type[309,310].

This may be due to the considerable amount of solvents employed in the synthesis of the different formulations (ratio Liquid/Solid>1). This had also a direct influence over the percentage of non-volatile compounds, which was lower than 50%. The values determined for this parameter range 40% and presented a slight increase in the formulations were inorganic nanoparticles were added, owing to the little increment of the solid content.

The values of the NVC were lower compared to other works from the literature[311,312] and specially compared to the typical phenol formaldehyde resins[313]. The viscosity was another parameter displaying a similar tendency to the density and the non-volatile content, as all these parameters were interrelated and influenced by the solid content of the resins. Consequently, the values of the viscosity exhibited low values as well as compared to other similar phenolic resins reported in the literature[314,315]. On the hand, the evolution of the viscosity was monitored, since this parameter is of significant influence over the potential applications of the resins. The results are showed in figure 40. A clear tendency was observed concerning the viscosity of the different resins formulations during their pot-life. Thus, the values of this parameter tended to increase significantly after 1 and 2 weeks. This was attributed to the fact that as the time passed by the resins became more condensated, owing in part to the typical autocondensation reactions of the raw materials, especially tannins[316] and in part to further condensation reaction between the main components of the resins (tannins and glyoxalated lignin phases).

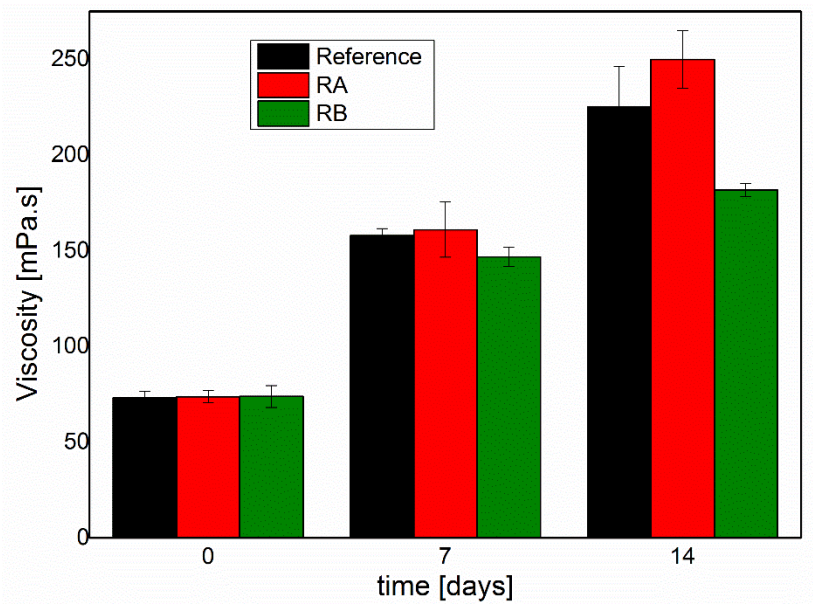

Figure 40. Evolution of the viscosity during the shelf-life of the resin.

The fact that the viscosity was increased to values near to 300 mPa·s would be interesting for applications such as wood adhesives[317]. However, in other cases a high viscosity could lead to problems of application of the resin over the wood surface[318]. In our case, the objective was to use the resins as coatings (superficial treatment) and accordingly a lower viscosity would facilitate to spread the resins along the surface of wood. Moreover, it would allow some penetration of the resin into the wood to promote the interaction between their functional groups. For these reason, it was decided to employ the resin directly after synthesis for further resin application as coating.

The resins were also characterized based on two important parameters namely hydroxyl value and alkalinity number. The former gives information about the number of free hydroxyl groups present in the material. The hydroxyl number is important since it is an indicative of the reactivity of the resins. Furthermore, the presence of hydroxyl groups in a resin is convenient to enhance the ability of forming a film for any coating material[319].

The latter gives a measure of the alkaline constituents of the resins. They are expressed in mg_{KOH}/g_{sample} and are determined by means of the equations (4-6). The results calculated for these parameters are shown in table 44.

$$\text{Hydroxyl number} = [(B-A)\cdot N\cdot 56.1]/W \quad (4)$$

where A=NaOH required for titration of the sample (mL)
B=NaOH required for titration of the blank (mL)
N=normality of the NaOH
W=weight of the sample

$$\text{Basic value} = [(A-B)\cdot N\cdot 56.1]/W \quad (5)$$

where A=KOH required for titration of the sample (mL)
B=KOH required for titration of the blank (mL)
N=normality of the KOH
W=weight of the sample

$$\text{Hydroxyl number (corrected)} = \text{Hydroxyl number} - \text{Basic value} \quad (6)$$

Table 44. Physical-chemical parameters determined for the different formulations of the biosourced phenolic resins.

Resin	Hydroxyl number (mg_{KOH}/g_{sample})	Alkalinity value (mg_{KOH}/g_{sample})	Hydroxyl $number_{corrected}$ (mg_{KOH}/g_{sample})
Reference	140.30±28.54	19.70±0.39	120.60±28.15
R_A	227.96±45.19	21.87±0.11	206.09±45.09
R_B	244.57±30.72	20.65±0.59	223.91±30.13

In regards to the previous results it was observed that the hydroxyl number incremented in the resins in which the inorganic nanoparticles were added. This may be attributed to the additional hydroxyl groups present in the structure of the POSS and the OMMT. In general, the hydroxyl number of the different resin formulation presented considerable values, which were comparable or even higher than those of other phenolic resins reported in the literature (Figure 41).

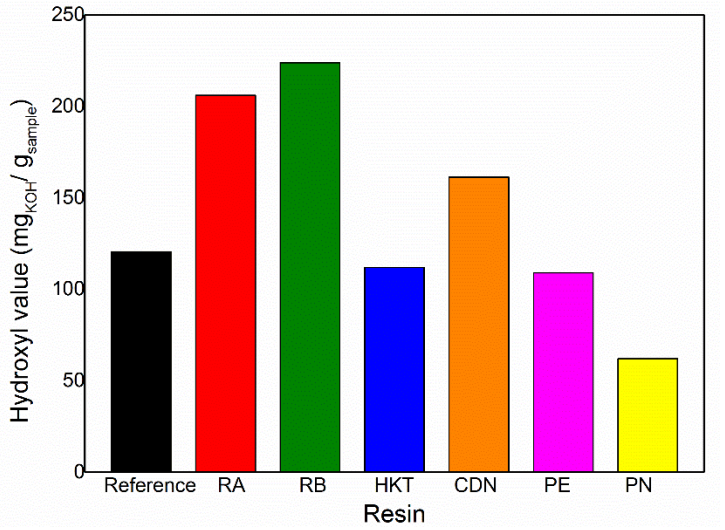

Figure 41. Hydroxyl values of the resins synthetized compared to other resins from the literature. HKT: hydroxylated ketonic resin, CDN: cardanol novolac resin, PE: polyester resin and PN: propargylated novolac resin. Information extracted from Marengo et al., 2004 [320];Sunitha et al., 2013 [321] and Uttaravalli et al., 2018 [322].

Special attention was put on the resins formulation R_A and R_B, which showed hydroxyl values significantly above the rest of the resins. These formulations would provide a considerable amount of these functional groups leading to a suitable compatibility with the hydroxyl groups from the wood structure. Therefore, these formulations would be appropriate for their application as coating.

B.4.2 Thermal analysis of the liquid resins

In this part, the liquid resins were subjected to differential scanning calorimetry analysis (DSC) to assess the curing process and evaluate the differences derived from each formulation. The thermogravimetric analysis was performed as well to evaluate the thermal resistance of the resins formulation during the process of heating.

B.4.2.1 Differential scanning calorimetry analysis (DSC)

The calorimetry analysis was performed for the different resins formulations, namely Reference, R_A and R_B, but also for their single components glyoxalated lignin (GL) and tannins solution (TS).

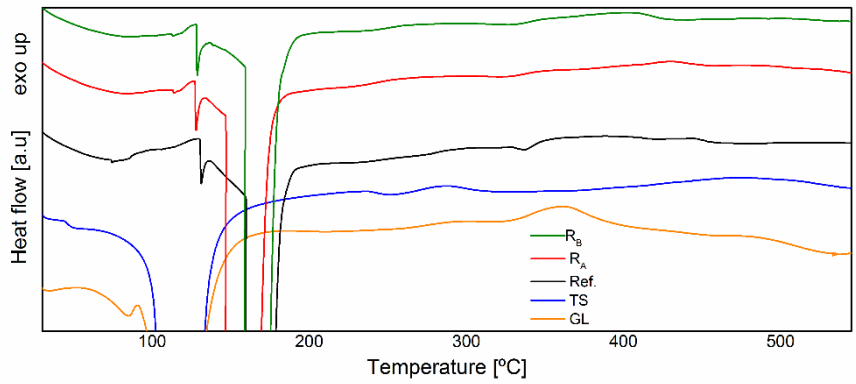

Figure 42. Diagrams of the calorimetry analysis for the resins formulations and components.

In figure 42, the whole diagram of the heating process is showed for the resins and their components. The same phenomena were observed for both. In the first range, the T_g was detected followed by an endothermic peak of great intensity, which was related to the evaporation of the liquid phase of both the components and the resins. Afterwards, moderate and wide exothermic signals were encountered, which were associated with the stages of curing and degradation. Although the single components of the resins (*GL* and *TS*) and the resins formulation (*Ref.*, R_A and R_B) displayed the same phenomena during the heating, discrepancies were found concerning the temperatures at which these appeared. For example, the T_g of the *TS* was lower compared to that of *GL*. This may be attributed to a faster reaction between tannins and hexamine compared to that of lignin and glyoxal. Consequently, the tannins solution would start to harden at a lower temperature than the glyoxalated lignin lignin. In the case of the resin *Ref.*, which is composed of both tannin solution and glyoxalated lignin, the glass transition temperature was detected at temperature in the range between the two previous components. However in the resins formulations composed of an inorganic phase (R_A and R_B), the value T_g was detected at a higher temperature as compared to the *Reference* resin. This was attributed to the fact that inorganic compounds were being intercalated within the organic polymeric matrix, thus delaying the start of the hardening process.

Concerning the process of curing, two wide peaks of moderate intensity were observed in all the resins formulations (Figure 43b). This two peaks were associated to the reticulation of the main components i.e. lignin and tannins. The fact that the signals related to the process of curing of the resins, appeared at different temperatures would be in agreement with the fact that tannins displayed a faster reaction than lignins did.

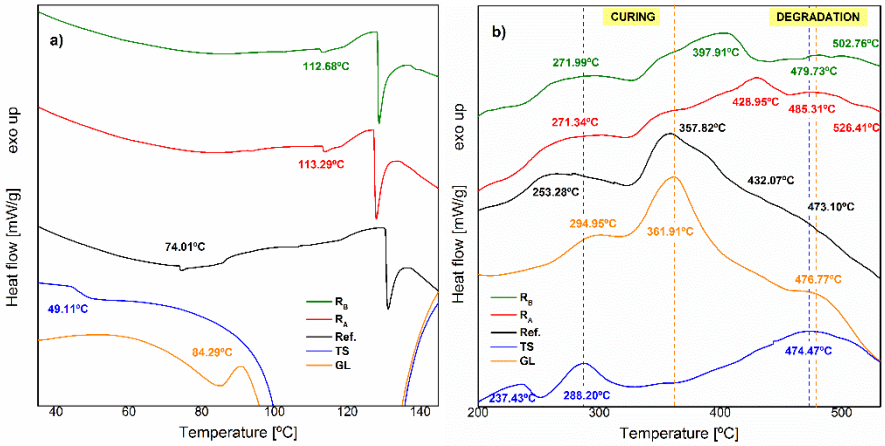

Figure 43. Study of different thermal phenomena during the heating of the resins formulations and components: a) Evolution of the T_g for the single components and resins formulations, b) Evolution of the curing and degradation processes for the single components and resins formulations.

After comparison of the curves of *GL* and *TS* with that of *Ref.* it was clear that the first exothermic signal (253.28 ºC) was derived from the reticulation of tannin, whereas the second one (357.82 ºC) was related to the reticulation of lignin. These exothermic signals related to the curing reaction of the main components of the resins, were also encountered in *RA* and *RB*. Nevertheless, in these formulations the temperatures for the reticulation were increased. This was again attributed to the inorganic nanoparticles. This was in accordance with the work of Corcione and Frigione, 2012 [323], in which the addition of a nanofiller (organically modified montmorillonite) affected to the polymerization by switching the beginning of the polymerization reactions to higher temperatures. This same tendency was seen for the degradation of the resins. Here the signals due to the decomposition appeared again at higher temperatures in the formulations *RA* and *RB*, which were composed of inorganic nanoparticles. This was because these particles would block the flux of degradation products and therefore resins would degrade at higher temperatures and more slowly. This was concurrent with the results presented in the part A of this same chapter (enhancement of the thermal performance of the lignins after addition of inorganic nanoparticles).

B.4.2.2 Thermogravimetric analysis (TGA)

This technique complemented the information obtained from the previous analysis, by evaluating the thermal performance of the liquid resins in the different stages of hardening, curing and degradation. Unlike other thermogravimetric analysis presented before, in this case the heating was performed in an oxidative atmosphere (O_2) to evaluate the behavior of the resins under harsh thermal conditions. The mass loss of the different resins during the heating process was assessed and it is showed figure 44. In this respect, a strong decrease was seen at beginning (25-180 ºC).

It represented the major mass loss (≈60%) and it was related to the evaporation of the liquid phase of the resins. This was in agreement with the percentage of non-volatile compounds determined in section B.4.1, which was around 40%. Besides, the mass loss appeared at a temperature within the range determined for the liquid phase vaporization in the DSC analysis.

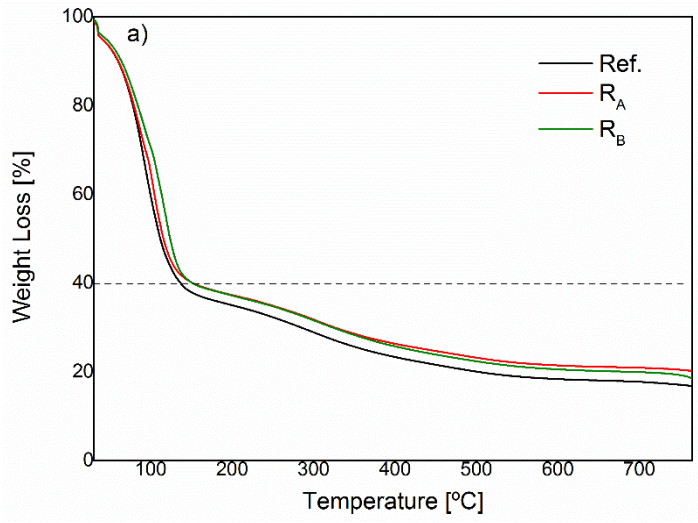

Figure 44. Curves from the thermogravimetric analysis of the liquid resins.

Between 200-800ºC, the mass loss showed by the resins was much lower, since they started to harden and reticulate and therefore they displayed a major resistance to heating decomposition. In this range, differences were observed between the formulations of the resins.

Thereby, the thermal degradation was delayed at higher temperatures in the resins R_A and R_B (about 40-50ºC of difference), which presented inorganic nanoparticle within their structure. This was in agreements with the results commented previously for the DSC analysis, showing that the addition of this inorganic phase did improve the thermal resistance of the resins.

B.5 Conclusions

Three resins formulations based on lignin, tannins and inorganic nanoparticles (POSS and OMMT) were successfully synthetized. From the chemical characterization, it was seen that the low values of the non-volatile content and viscosity would ease the application of the resins onto the wood surface. Moreover, the considerable hydroxyl values obtained, especially in the formulations R_A and R_B, proved their high reactivity. These features would be beneficial for their application as wood coating rather than to other e.g. wood adhesive. Concerning the thermal analysis of the resins, it was observed that the inclusion of inorganic nanoparticles into the resins formulation had a significant influence over the curing and degradation processes, by delaying both to higher temperatures. This would lead to an improvement of the thermal resistance of the resins and therefore would allow the utilization of these resins to protect wood against fire.

4. Application of the resins for the protection of wood against fire

The current chapter is centered on the employment of the resins synthetized in the previous chapter with a specific application. This application was the use of the mentioned resins as coating for wood protection against fire, as it was concluded in chapter 3. First and foremost, a brief discussion on the different components and methods used in this area is introduced and a special emphasis is placed on the coating treatment. Then, the experimental process of coating application, drying and curing of the resin onto the wood surface was comprehensively presented. Concerning the characterization, on the one hand the chemical and thermal analysis of the cured resins was carried out. On the other hand, the effect of the coating on wood was assessed regarding several aspects namely combustibility, fire resistance and flame retardancy and thermal conductivity. The main strengths and weaknesses of the coatings in respect to the previous parameters were evaluated to confirm their suitability a performance.

4.1 Motivation and background

Wood was one of the first construction materials with species that can keep its original state and performance appropriately for long periods. Its role in the field of materials has changed along years from irreplaceable at the most early times, where no other materials were available, to replaceable from 1850-2000, period in which other materials substituted wood[324]. In the last years, it is competing with other materials such as plastics, aluminum, steel, concrete, gypsum and brick[325]. Nonetheless, it has switched its use to decreasingly replaceable, since it is gaining again importance owing to its versatility and environmentally friendly features[326]. In this respect, among the main positive environmental attributes of wood are its low intrinsic energy, low carbon impact and sustainability[327].

The former characteristic is referred to the energy consumed in all the process involved for the production of wood as a product until its point of use ("grey energy"). In comparison to other materials, this energy requirement is low[328]. Concerning the low carbon impact, wood as a prominent part of forests, helps positively by removing carbon from the atmosphere. Besides, carbon in wood remain unreleased until it is decayed[329]. The last property is related to the renewable nature of wood. This is an advantage over the majority of the materials employed in the industry, which are derived from fossil fuels. Apart from its convenient environmental features, wood is widely employed in construction owing to its mechanical and structural properties such as for instance its excellent ratio strength to weight[330]. Consequently, wood and wood composites nowadays are known for playing a major role in buildings and interior fittings[331]. Nevertheless, wood as a material displays also disadvantages such as its hygroscopicity and vulnerability against several decay agents. These agents can be classified in two types namely biotic and abiotic[332]. The former group is referred to the wood decay by the action of bacteria, fungi, insects or marine borers. The second type is related to the degrading action of moisture (rain, humidity and snow), ultraviolet radiation (sunlight), wind and fire. In this context, the degradation of wood and derived products upon fire exposure is of significant importance, owing not only to environmental but also to safety and health reasons.

4.1.1 Flame-retardant compounds and mechanisms

Along the years, different fireproofing compounds have been studied and tested for wood. The aim was retarding the fire ignition and/or reduce the expansion of the flames to avoid the fire-derived risks on wood and the loss of life and good[333]. Concerning the compounds employed as flame-retardants, there have been an evolution among the last decades. In the past, the most common flame-retardants employed were halogenated compounds (F, Br, I and Br). They could display a chemical structure based on aliphatic or aromatic carbon substrates in which the atoms of hydrogen were substituted by halogen atoms[334].

The other possibility was their inorganic form. Nevertheless, the former structure was mostly preferred, due to its major flame-retardant character[335]. The most typical flame-retardants of this type were those derived from chlorine and bromine, as they provided the lowest cost in achieving the flammability criteria. Within these two, bromine compounds were preferred due to the linkage C-Br. This bond is steady enough under exposure to environment, but also easily broken with heat upon fire exposure[336]. However, the major problem with this kind of compounds was the broad range of adverse consequences to humans such as inmunotoxicity, reproductive toxicity and carcinogenic effects[337]. For these reason they have been gradually substituted by other performing and non-toxic compounds. Boron wood preservatives have been reported as good flame-retardant. Besides, they display various advantages such as minimal toxicity to mammals and its cost effectiveness[338]. As flame-retardants they are usually employed in the form of borates e.g. borax. During their decomposition (290-450ºC) water, boric acid and boron oxide are released, leading to the formation of a vitreous layer, which can protect the surface of wood[339]. Nevertheless, the main disadvantage regarding boron compounds is that they are easily leached, owing to their high solubility in water[340]. Another compounds employed are the metal hydroxides, especially those of $Al(OH)_3$ and $Mg(OH)_2$. These compounds tend to decompose endothermically under fire exposure releasing H_2O, CO_2 and ceramic-like residues (e.g. Al_2O_3.). However, they also display some drawbacks such as the fact that high loading levels may be needed and the lower performance at harsh temperatures[341]. Phosphorous compounds are other of the most traditional alternatives to halogenated flame-retardants. They can be used in their organic or inorganic form. Nevertheless, the former form is preferred and the major part of the phosphorous flame-retardants are based on the assembly of any organic group to the phosphorous-oxygen bonds[334]. Thereby, the most typical examples are the phosphates (PO_4^{3-}), phosphonates (R_3PO_4), phosphinates (R_3PO_2) and their oxides.

During thermal degradation, these compounds are known for acting as catalysts of the dehydration reaction thus producing a char protecting layer. This type of flame-retardants are sometimes used in combination with other compounds such as nitrogen-derived molecules. Some examples reported in the literature are mono- and di-ammonium phosphate, which are able to produce a synergic effect enhancing the char formation[342,343]. Phosphorous flame-retardants can be used in condensed or vapor phase. Nonetheless, they also display some drawbacks such as the generation of a considerable amount of smoke and CO. Besides the compounds mentioned previously, there has been an increase interest on the utilization of silicon-based flame-retardants in the last years. Several type of silicon compounds have been tested as flame-retardants as displayed in table 45.

Table 45. Different types of silicon based compounds used as flame-retardants.

Types	Description
Silicones	-Structure based on a polymeric organosiloxane ($[R_2SiO]_n$). -e.g. polydimethil siloxane (PDMS)
Silica	-Inorganic structure (SiO_2) -Mainly used as filler
Silicates	-Standard structure (SiO_4^{4-}) -They display a variety of different structures
Layered materials	-They are refer to clays/nanoclays -They are composed of silicate layer with different dispersion morphology (intercalated, delaminated). -e.g. montmorillonite (MMT)
Silsesquioxanes	-They are based on silicate-caged structures ($[RSiO_{1.5}]_8$) -Characterized by nanometric dimensions -e.g. polyhedral oligomeric silsesquioxanes (POSS)

All these compounds have been reported to improve considerably the flame retardancy as either fillers, polymers or copolymers[341]. As described for other flame-retardants, silicon based compounds help to the formation of a protective barrier on the surface during combustion, which hinders the heat transfer into the material[344]. Furthermore, they lead to the reduction of the heat release upon combustion[345]. The main advantage of these type of flame-retardants is the low amount needed to ameliorate the fireproofing character, owing to their large surface area, especially in the cases of the compounds in the nano-scale.

The flame-retardancy of the compounds described above, is usually achieved by means of different mechanisms as it was already presented. These mechanisms can be summarized in three major types namely gas phase action, endothermic action and char forming action[334]. The former is based on the reduction of the heat released during combustion in the gas phase. The second type is related to the release of non-flammable gases (H_2O and CO_2), which can reduce the temperature during combustion leading to an endothermic decomposition. The latter mechanism is associated with the formation of a protective layer on the material surface. In the next table the flame-retardants compounds presented before are listed with their typical corresponding mechanism against fire degradation.

Table 46. Different types of flame-retardants and their action mechanism against fire.

Flame-retardant types	Mechanism		
	Gas phase action	**Endothermic action**	**Char forming action**
Halogenated	X		
Boron compounds			X
Metal hydroxides		X	
Phosphorous compounds	X		X
Silicon based compounds			X

4.1.2 Fire proofing methods for wood

As it was commented at the beginning of this chapter, wood is a combustible material whose structural and mechanical properties are compromised upon fire exposure. For this reason, another important parameter to consider is the treatment employed in protecting the combustible structure of wood. In this regard, several methods have been explored and tested over the years. Among them three major approaches have been considered in several sectors such as building and construction and transportation[346].

- Inclusion of the flame retardant compounds into the bulk structure. This treatment is associated to the introduction of the flame-retardant additives directly into the cell wall of wood. Some examples of this type of treatment are injection or impregnation[347]. The main disadvantage of this treatment is that high loadings are required, which affects the strength and elastic modulus of the material[348].

- Chemical bond of flame-retardant with compatible functional groups. This treatment is related to the reaction of the flame-retardant additives with the chemical groups of wood[349]. Thereby they can become an intrinsic part of the wood polymeric chains providing a longer durability and fireproofing effect. The major difficulty of this treatment is the selection of flame retardant compounds of suitable size and compatible functional groups to be incorporated into the wood polymeric chains.

- Surface modification of wood by means of flame-retardant compounds. This method is broadly used in various commercial applications. The major example is the utilization of fireproofing coatings, which is the most convenient, economical and efficient way to protect substrates against fire[350]. Its major advantage is the concentration of the fireproofing properties of the flame-retardant at the surface, which allows the protection of the bulk of the material[351].

Traditionally fire proofing coatings were based on *"cementious"* compounds e.g. oxychloride cement, vermiculite, gypsum and other minerals[352]. They were cost efficient and provide an easy application and resistance to weather. On the contrary, they displayed several weak points such as their considerable weight and thickness. Consequently, there has been an evolution over the years regarding the types of coatings towards more state of the art systems. In the last years, the utilization of intumescent coating systems has become a widely implemented alternative in the protection of wood against fire[353,354]. This coating system is composed of three main elements namely acid catalyst, char-forming compound and a blowing agent[354]. The process of intumescence has been described by Kozlowski et al., 2007 [355] and it is showed in figure 45.

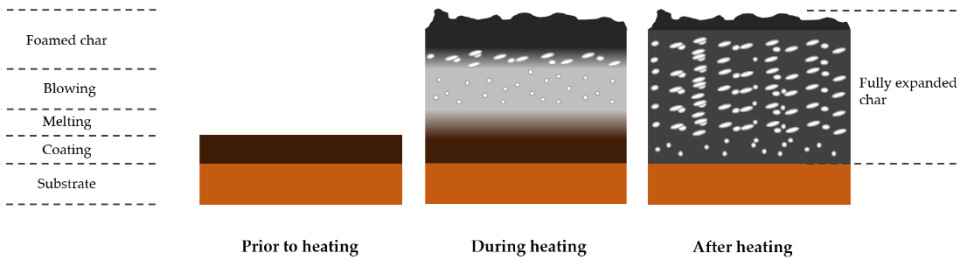

Figure 45. Representation of the stages of the intumescent process.

Their mechanism of action is characterized by the following stages:

- Softening and melting of the organic compounds (char-forming agent) by direct contact with the fire.
- Release and formation of the inorganic acids (catalyst).
- Carbonization of the char-forming agent.
- Liberation of the gaseous products by the blowing agent and formation of a thick porous foam layer on the surface.
- Crosslinking and solidification of the char foam layer, insulating the combustible material and avoiding the access of heat and oxygen.

Considering all the above-mentioned information, in this work it the resins synthetized in the previous chapter were used for the protection of wood against fire and the method selected was the surface modification of wood via flame-retardant (coating). The flame retardant compounds selected were a nanoclay and a type of silsesquioxanes, which were introduced in one of the different formulations of the resins as presented in the sections A.3.3.2 and B.3.2. of chapter 3. The aim was the wood protection by the means of an isolating char layer and the intumescent action of the nanoclay and the silsesquioxanes.

4.2 Experimental procedure

In the following subsections the main materials used, the process followed in the application of the resins as coatings and the techniques employed for the characterization of the coatings and their performance are described.

4.2.1 Basic elements for testing: flame-retardants and substrates

The flame-retardant compounds employed for the protection of wood against fire were formulation of the biosourced phenolic resins presented in the previous chapter (section B.3.2) *Reference*, R_A and R_B. They were based on the same polymeric matrix but they differ in the inorganic phase, which was majorly responsible for the flame-retardant action. In the former formulation no inorganic phase was added, whereas Delitte 43B (OMMT) and SO1458 (POSS) were present.

Concerning the wood substrate in which the fireproofing action was tested, two different species were selected namely maritime pine (*Pinus pinaster*) and beech (*Fagus sylvatica*). These two species were chosen as examples of a softwood and hardwood species. Thereby, it can be assessed the influence of the different wood structure of each species over the coating application and performance.

4.2.2 Process of coating application on the substrate

The process of application of the biosourced phenolic resins as coating for the protection of the wood substrates was subdivided in several stages: preparation of the substrates, deposition of the coating on the surface of the substrate and curing plus drying process.

The substrates preparation was carried out as follows, first the wood samples were conditioned during 7 days at specific conditions of temperature and relative humidity (25 ºC and 65%). Then, the surface of the wood samples was refreshed by means of sandpaper to open the pores and thus ease the contact and penetration of the resins during the deposition of the coatings afterwards. Three-grain size papers (80,100 and 120) were applied during the process of sanding of wood from the bigger to smaller one. This way a homogenous, flat, smooth surface was achieved for all the wood samples before coating application.

Concerning the deposition of the resins over the wood surface, two important features were considered namely mass of resin applied and method of application. The selection of the former parameter was based on the weight percent gain (WPG). The WPG is defined as the mass increment experimented by a substrate after treatment[356]. Thereby, different amount of resins were applied onto the wood surface, then submitted to the process of curing + drying and finally the WPG was calculated as showed in equation 7.

$$WPG\ (\%) = [(m_{coating} - m_{wood})/m_{wood}] \cdot 100 \qquad (7)$$

where $m_{coating}$: mass of the substrate after the application of the coating
m_{wood}: mass of the substrate before the application of the coating

The evaluation of the WPG, as the amount of the resin added onto the surface of the substrate, is displayed in figure 46. This previous test was performed on a glass plate of specific dimension.

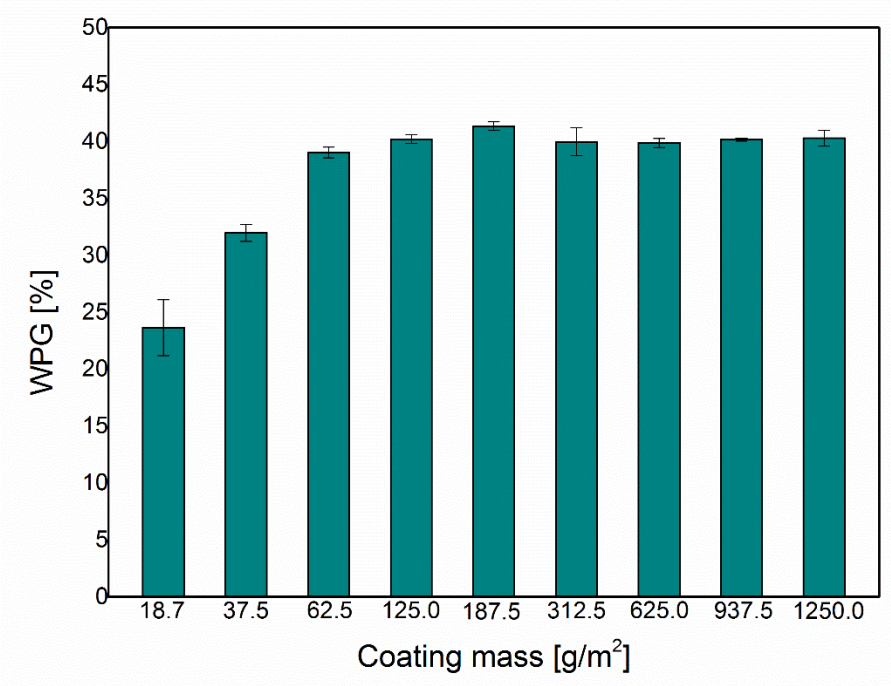

Figure 46. Evolution of the weight percent gain (WPG) of coated samples as the amount of resin added was increased.

The aim of this test was to determine the point of saturation of the coatings over an inert substrate, in which they remain as thin layer. From the previous figure it was seen that when the mass of the resin added to the wood samples was high, the WPG values remained constant (saturation point). Nevertheless, when this amount was decreased, there was a point at which the WPG started to decrease. The mass of resin added just before that point was selected as the amount of coating to be applied onto the wood samples (62,5 g/m^2).

Considering the method of application, different treatments were assessed for spreading the resins onto the wood samples such as glass rod, a brush and a paint roller. Based on the small size of the samples and small amount of the resins the treatment achieving the best results was the brush (more homogenous coating layer and higher amount of resin on the wood surface rather than in the application instrument). Accordingly, this was the method selected for resin deposition.

The last step of the coating application was the curing and drying of the resin layer onto the surface. In this respect, low temperatures were preferred to avoid the thermal modification of wood and therefore possible interferences on the real performance of the coatings on wood. It is known that thermal modification of wood at higher temperatures results in the modification of the pristine structure of wood and that can lead to an enhanced thermal performance[357]. Consequently, at temperature of 60ºC was selected for carrying out the process of curing and drying of the coatings on the surface of wood. A prior experiment on the liquid resins at this temperature was implemented with to see whether it was possible to cure them at this temperature and time needed for this operation. This was assessed with Rheolaser by measuring the elasticity index (EI) of the resin during heating (Figure 47). The procedure followed for this experiment was described in Annex V.5.

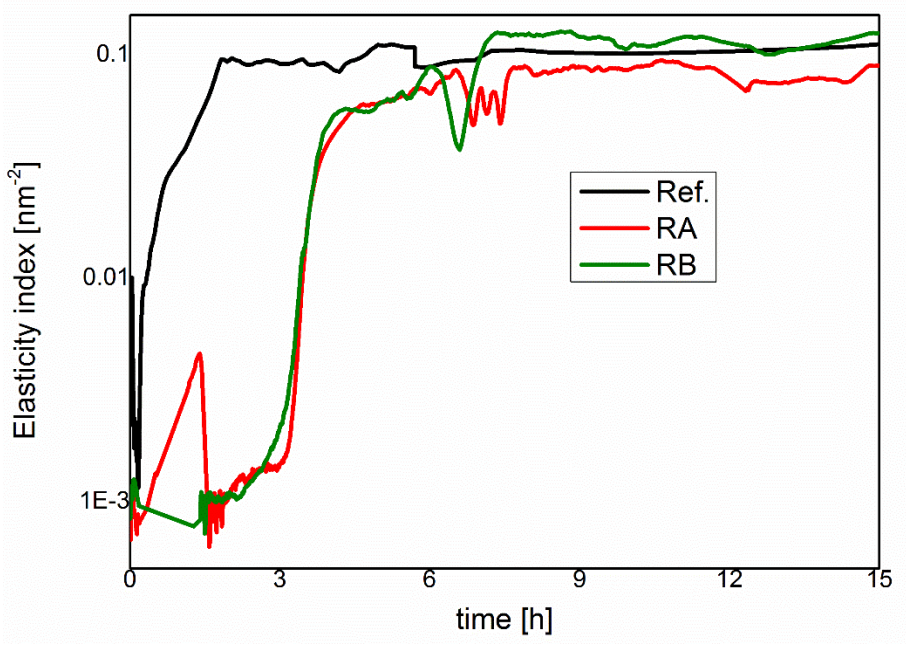

Figure 47. Evolution of the elasticity index (EI) of the resins at a fixed temperature with time.

It was observed in the previous figure that the EI was increasing as the time passed by. This was due to fact that as the heating time was increasing, the reticulation of the resins was promoted and therefore they started to switch from a viscous liquid to an elastic solid (curing process). There was a point at which the EI reached a constant value and at that point it could be concluded that the resins were already reticulated and the curing have arrived to the end (above 10h). Thus, to assure the proper curing and drying of the resins on the wood samples they were cured + dried at 60ºC during 15h. This process was carried out by introducing the coated wood samples directly after coating application into an oven with the defined parameters.

4.2.3. Characterization methods

The main techniques used for the characterization of the coatings and their performance on the substrate are displayed in Table 47.

Table 47. Characterization methods used for the assessment of the main characteristics and performance of the synthetized resins.

Component	Analysis	Technique	Annex	Section
Coatings	Thermal resistance	TGA[A]	Annex III	III.5
	Chemical structure	FTIR[B]		III.6.1
	Combustibility	Calorimetry pump analysis	Annex VI	VI.1
	Fire resistance	UNE-EN 60695-11-10:2014[C]		VI.2
	Conductivity	Hot disk analysis		VI.3

[A]TGA: Thermogravimetric analysis, [B]FTIR: Fourier transformed infrared spectroscopy analysis, [C] UNE-EN 60695-11-10:2014: Standardized method for the evaluation of the combustion of materials.

4.3 Results and discussion

Within this part, the results obtained from the previous experiments for the characterization of the coating and its performance for wood protection against fire are presented.

4.3.1 Characterization of the coating

The characterization of the coating was carried out concerning its chemical structure and thermal resistance. Prior to those analyses, a liquid sample of the different formulation of the resins (*Reference*, R_A and R_B) was cured at the defined conditions (60ºC and 15h) over an aluminum plate. The cured resin samples were then crushed in a mortar and the powder was ready to use for the characterization analysis.

4.3.1.1 Fourier Transformed spectroscopy analysis (FTIR)

By this technique, the chemical structure of the coatings was analyzed. Besides, the main linkages between the different components and the major functional groups were elucidated. In figure 48, the spectra of the individual components namely glyoxalated lignin and tannin, and that of the resins formulations are showed. It was clear from the previous figure that the spectra of the cured resins (coatings) was greatly influenced by their components. Thus, the signals from the main functional groups of both the glyoxalated lignin and mimosa tannin were found in the cured resin spectra. The main signal was the one detected in the range 3500-3300 cm^{-1} (broad and strong) associated with the hydroxyl groups. This was expected since the polyphenolic resins synthetized displayed an abundance of hydroxyl groups, as shown by the hydroxyl value in the previous chapter (section B.4.2.1).

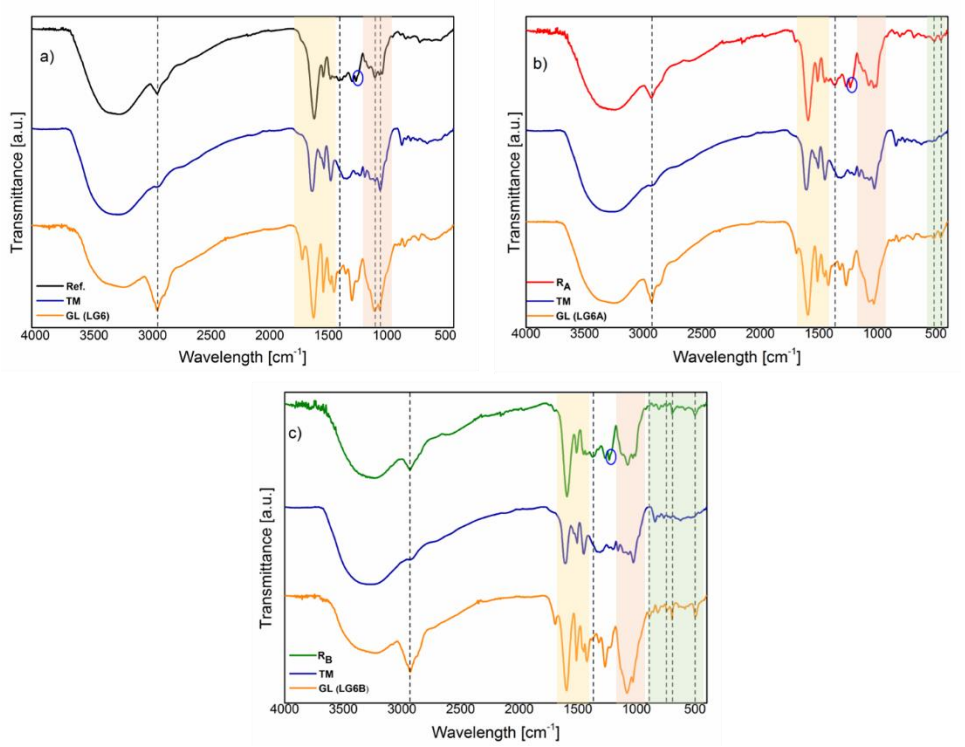

Figure 48. Infrared spectra of the components (GL: glyoxalated lignin, TM: mimosa tannin) and different resins formulations: a) formulation *Reference*, b) formulation R_A and c) formulation R_B.

Between 3000-2900 cm^{-1}, a medium-sharp band was seen related to the methyl and methylene groups. The mentioned signal is more prominent in the spectra the glyoxalated lignin than in the mimosa tannin, since these units are more abundant within its structure. Consequently, it might be attributed to the lignin-derived fractions present within the resin structure. Nevertheless, it could be also due to the reaction between lignin and tannin by means of methylene groups (-CH_2 and –CH-) as proposed by Pizzi, 2016[358]. He reported a mechanism for the reaction between tannins and glyoxalated lignin cured by hexamine (Figure 49). The mentioned mechanism consisted in the faster reaction between tannins and hexamine, which were connected via C-N bonds.

Then, glyoxalated lignin units were connected with the reacted tannins-hexamine moieties by means intermediate methylene groups. Thus, in this case the presence of a significant signal in the resins, would confirm the reaction between both components (lignin and tannins).

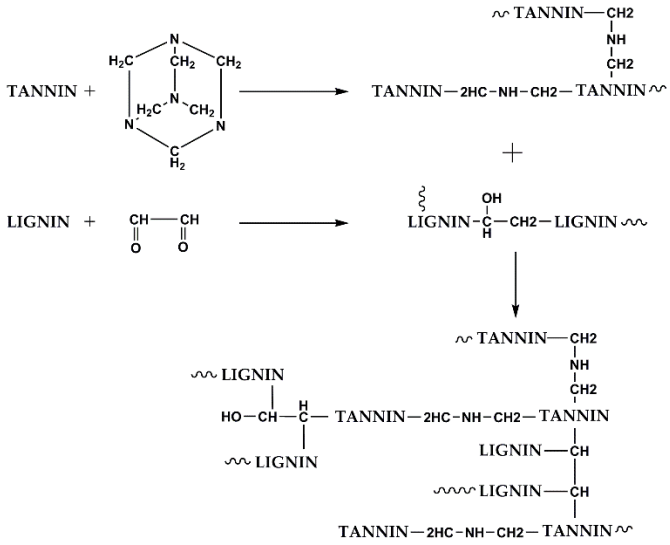

Figure 49. Proposed mechanism of reaction between tannins and lignin in the resins formulations, as described in Pizzi, 2016 [358].

The peak attributed to carbonyls groups at 1700 cm^{-1}, which was present in the spectra of the glyoxalated lignin, disappeared or became a small shoulder in the spectra of the resins. This may be due to the reaction between the tannin and lignins moieties through this functional group. In the next range (1600-1400 cm^{-1}), several peaks were detected characteristic from conjugated linkages from the aromatic rings. These peaks observed in the resins, were associated with the multiple aromatic rings present within the structure of both the lignin and tannin, which were already described in the characterization of both components in the previous chapters. At 1370 cm^{-1} a medium-weak and broad signal was seen in the resins spectra, related to the deformation of the O-H linkage. This was derived from the tannin fractions, which contain various phenolic groups attached to the flavan-3-ol moieties. In fact, a similar medium and broad signal was observed in the spectra of the mimosa tannin.

An important signal was detected at 1235 cm^{-1} attributed to the bond C-N from amine (blue circle), as described in the above-mentioned reaction mechanism. Besides, this assignment was in agreement with the work of Sumathirathne and Karunanayake, 2017 on the synthesis of tannin-phenol resins cured with hexamine[359]. They related the presence of a peak at 1239 cm^{-1} to the stretching of the C-N bond coupled with the stretching of other adjacent bonds in other molecules. This signal confirmed the curing reaction between the tannin fractions and hexamine[304]. Another significant band was observed in the range 1150-900 cm^{-1} for the resins spectra. In this interval different signal related to the C-O linkage were determined. The most significant contribution was that of C-O bonds derived from the primary and secondary alcohols present within the glyoxalated lignins structures. On the other hand, another contribution to the C-O band was that of the furan heterocycles of the flavan-3-ol units from the tannin fraction. Besides these contributions, in the mentioned interval there was also the signal of Si-O-Si stretching derived from the structure of the glyoxalated lignins (LG6A and LG6B), which was overlapped by the C-O band as explain in the previous chapter in the section A.4.1. Between 900-400 cm^{-1}, the signals detected corresponded only to the linkages and functional group of the inorganic nanoparticles added during the synthesis of the resins (POSS and OMMT).

The assignments for the above-mentioned signals detected in the different formulations of the resins are summarized and listed in table 48. Considering these assignments, it was observed that the main differences between the resins formulation regarding their structure and functional groups were observed in last part of the spectra. Thereby, significant differences were seen in the range 1200-1000 cm^{-1} (orange section in figure 48), related to C-O band and the overlapped signal of Si-O-Si.

Table 48. List of assignments of the main signals detected in the spectra of the resins and their components.

Wavelength (cm^{-1})	Assignments	Identified bands (cm^{-1})		
		GL	TM	Resin
3300	O-H stretching	X	X	X
2900	C-H stretching	X	X	X
1700	C=O stretching	X		
1600	C=C-C aromatic stretching vibrations	X	X	X
1510		X	X	X
1460		X	X	X
1360-1370	O-H deformation phenolic substituents			X
1314	O-H stretching of phenol		X	
1270	C-O stretching in guaiacol ring	X		X
1235	C-N vibrations of amines			X
1160-1025	C-O-C stretching of flavonoid pyran ring		X	X
1100-1000	Si-O-Si symmetric stretching	X(A,B)		X(A',B')
1075-1030	C-O stretching and deformation of primary alcohol	X		X
890	Si-OH bending vibrations	X(B)		X(B')
745	C-H deformation of aromatic ring (POSS)	X(B)		X(B')
695	Si-C stretching vibration (POSS)	X(B)		X(B')
520	Si-O-Si bending (OMMT)	X(A)		X(A')
499	Si-O bending vibration (POSS)	X(B)		X(B')
460	Si-O-Si deformation vibration (OMMT)	X(A)		X(A')

GL: glyoxalated lignin, TM: tannin mimosa, A: formulation GL(LG6A), B: formulation GL (LG6B), A': formulation resin R_A, B': formulation resin R_B

In this respect, the mentioned band was considerably more intense in the formulations R_A and R_B, owing to the presence of more aliphatic hydroxyls and the presence of Si-O-Si bonds from POSS and OMMT. The other interval displaying significant divergences between the resins formulations was the range 900-400 cm^{-1} (green section in figure 48).

No signals were detected here for the formulation *Reference*. On the other hand, the formulation R_A displayed two signals and the formulation R_B presented four signals (table 48). This was due to the fact that these last formulations were based on glyoxalated and hybridized lignins (presence of inorganic nanoparticles). Finally, based on the previous results it could be concluded that during the curing of the resins a reaction between the lignin and tannin occurred, since the typical bands detected in the spectra of both individual components were observed in the spectra of the final resin afterwards.

4.3.1.2 Thermogravimetric analysis (TGA)

This method was used as an approximate indicator of the actual thermal resistance of the cured resins. This could provide a previous idea of the fireproofing performance of the coatings on the wood samples afterwards. In figure 50, the thermogravimetric and derivative thermogravimetric curves for the different cured resins formulations are displayed.

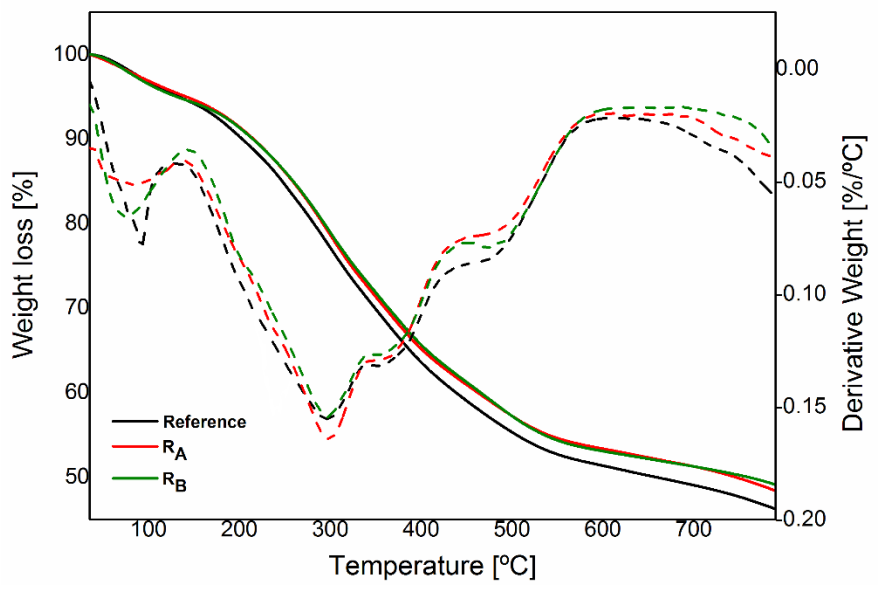

Figure 50. Curves of the thermal analysis of the different resin formulations cured (coatings).

The degradation of the cured resins occurred through several steps. The first one (80-110ºC) was attributed to vaporization of the moisture in the powder-state coatings. Then main stage of degradation was located in the range 295-300ºC and represented the 20% of the mass loss of the cured resins. Following to this stage, two other degradation steps (≈10% weight loss) were detected between 350-370ºC and 475-485ºC respectively. The previous degradation stages occurred at temperatures similar to those reported in the previous chapter for the hybridized-glyoxalated lignins (section A.4.5). Nevertheless, in this case of the cured resins the loss of weight was considerably reduced compared to the modified lignins alone. This means that the polymeric structure formed during the curing of the resins, presents a greater thermal resistance than that of one its components. Thereby, it would be confirmed the reaction of the lignin with the tannin and the curing agent leading to a more branched and resistant polymeric structure. In table 49, the main parameters determined from the analysis are presented.

Table 49. Thermogravimetric parameters determined for the different formulation of the cured resins

	$T_{10\%}$ (ºC)	$T_{50\%}$ (ºC)	Residue (wt.%)	Degradation stages (ºC)			
Reference	202.75	657.51	45.96	99.56	296.23	358.92	475.11
R_A	215.19	745.07	48.13	77.07	299.62	361.02	480.75
R_B	214.46	759.13	48.55	81.10	301.71	367.30	482.85

In regards to the previous results, it was seen that the stages of degradation occurred within a narrow range of temperature in the different formulations of the coatings. However, the mass loss had a different development among the different cured resins. It was seen in table 49 and figure 50 that the loss of mass started to diverge between the resins, especially for R_A and R_B, as the temperature incremented.

Consequently, slight difference were regarded concerning the $T_{10\%}$, whereas considerable differences were encountered in the temperature at which the resins had lost the half of their mass ($T_{50\%}$). Besides, the residue remaining after thermal degradation was slightly higher in those formulations as well. All these results were attributed to the fact that formulations R_A and R_B had OMMT and POSS respectively within their structure. These inorganic compounds are widely reported to provide a synergic effect regarding the flame-retardancy and thermal resistance [360,361]. Based on these results, it was decided to select only the coatings formulations R_A and R_B, since they will provide an improved thermal performance compared to the *Reference*.

4.3.2 Evaluation of the coating performance

Within this part, different experiments, which were carried out directly on the coated-wood samples, are displayed to assess the efficiency of coatings against fire exposure and derived thermal properties.

4.3.2.1 Calorimetry Pump analysis

This technique was carried to evaluate the influence of the coating formulations over the heat release during the combustion of the wood samples. The methodology followed is described in Annex VI.1. The machine employed for this analysis provided the higher heating values (HHV) of the samples introduced. This parameter is defined as "*the amount of heat released by the unit mass or volume of fuel (initially at 25 °C) once it is combusted and the products have returned to a temperature of 25 °C, including the latent heat of vaporization of water*"[362]. Thus, the samples were put into the calorimetry pump without coating (control samples) and with coating (R_A and R_B formulations) to elucidate the changes in the parameter measured due to the application of the coating on wood (Figure 51).

Figure 51. Calorimeter employed for the determination of the combustibility of the samples: a) Whole machine with the screen for the results and oval vessel with water in which the calorimetry pump is introduced, b) Calorimetry pump with pressurized sealing and releasing valves, c) Pan for the sample in contact with the wire, which created the spark for the combustion.

The results concerning the heat produced during the combustion of the wood samples (control and coated samples) are presented in figure 52.

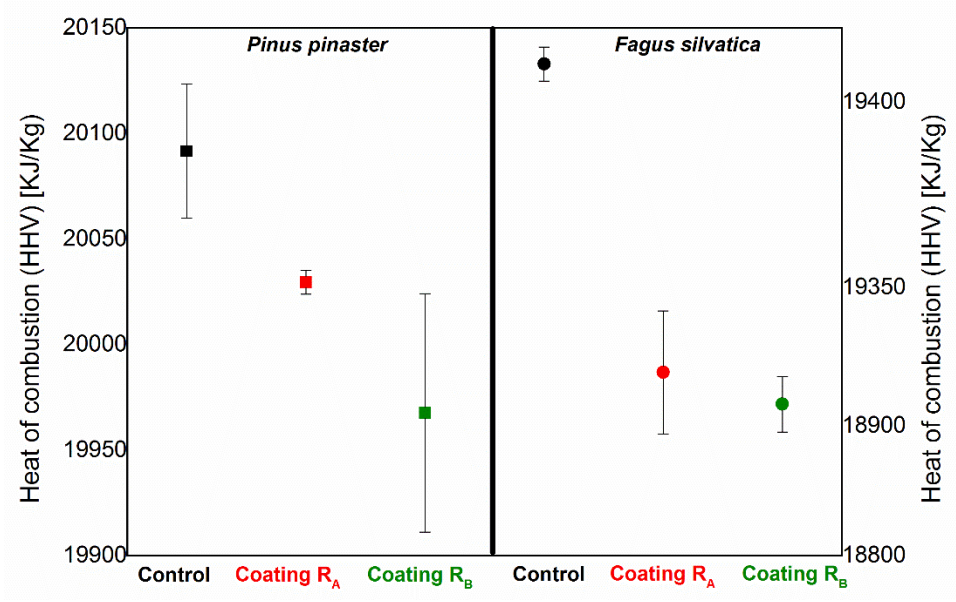

Figure 52. Heat of combustion of the wood samples before and after the application of the coatings.

The heat of combustion determined, showed higher values in the samples of *Pinus pinaster* compared to those of *Fagus sylvatica*. This is normally associated with the higher lignin content of conifers compared to hardwood species[363]. Moreover, it is also due to the presence of a greater amount of resin, oil and wax in softwood species. These compounds, which take part typically of the extractives, are reported to increase the heat of combustion of wood species[364]. The calorific values of the control samples determined, expressed as HHV, were within the typical ranges of *Pinus pinaster* (19.55-20.99 MJ/Kg) and *Fagus sylvatica* (19.33-19.21 MJ/Kg) as reported in the literature[363,365–367]. However, after the application of the coating the caloric values of the samples were reduced. This means that the heat release from wood during combustion was lower and therefore the combustibility of the samples was decreased. This tendency was more marked in the *Fagus sylvatica* coated samples than in the *Pinus Pinaster* ones. This could be attributed to the significant presence of resins in the wood of *Pinus pinaster*[368]. The mentioned resins would hinder the interaction between the functional groups of the wood surface and those of the coatings. Moreover, during combustion the resins would be exudated and release through the wood pores. This may induce small cracking in the protective surface layer of the coating. Based on the results described previously and the data of the masses of the wood samples and the coatings applied, it was calculated the reduction of the combustibility achieved related to the mass of coating used (Table 50).

Table 50. Capacity of the coatings for reducing the combustibility of the wood samples.

Wood species	Sample mass (g)	Coating formulation	Coating mass (g)	Reduction of HHV	
				KJ/g_{sample}	$KJ/g_{coating}$
Pine	0.63±0.04	R_A	0.053±0.001	0.057±0.001	0.723±0.027
	0.50±0.02	R_B	0.054±0.002	0.073±0.005	0.693±0.001
Beech	0.87±0.03	R_A	0.050±0.001	0.521±0.062	7.901±2.632
	0.76±0.03	R_B	0.055±0.001	0.469±0.047	6.607±0.302

In regards to the previous results, it was seen that even with a small amount of coating the reduction of the heat release during combustion was significant (≈8 KJ/g or 8 MJ/Kg at maximum). The mentioned parameter achieved by the coatings was related to the presence of the inorganic heat resistant components (OMMT, POSS). Moreover, these components compensated the action of lignin, which is known by its considerable calorific value[369]. Consequently, these components were proved to improve the thermal performance on the coating in this case regarding the heat release during combustion.

4.3.2.2 Assay for assessing the flammability and fire-resistance of the coatings

This analysis was based on the standard UNE-EN 60695-11-10:2014 and it was carried out for the horizontal combustion with a contact angle between the wood samples and the flame of 45 º. The samples were prepared with dimensions 125x13x3 mm according to the standard. Once the samples were prepared and the coating was applied, the weight percentage gain of the coated samples was determined to elucidate the degree of retention of the coatings in each wood species (Figure 53).

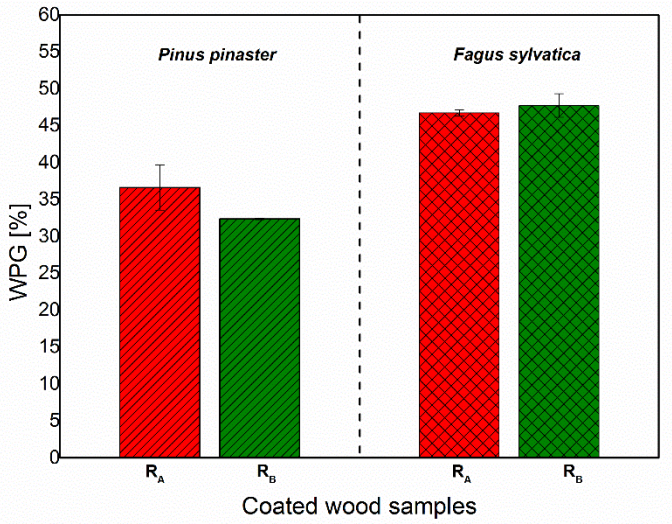

Figure 53. Weight percentage gain of the wood samples after the application of the coating.

As showed in the previous figure, the coated wood samples of *Fagus sylvatica* displayed a higher weight percentage gain (WPG) than the *Pinus pinaster* ones. This means that a greater degree of retention of the coating was achieved on the former wood species. These was related to a better interaction of the surface of the *Fagus sylvatica* wood with the coating, compared to that of the *Pinus pinaster*. After preparation of the samples, they were exposed to fire as described in the protocol of the assay in Annex VI.2. During the exposure of the samples to flames, significant divergences were seen between the control samples (without coating) and the coated ones. On the one hand, in the control samples a fast ignition, combustion and spread of the flames was observed. In these samples, black fumes were also exhausted and an intense glowing was observed during combustion. Besides in some of the samples (*Pinus pinaster*), exudation and dripping was seen during fire exposure. These events were attributed to the higher extractive content of *Pinus pinaster* wood compared to *Fagus sylvatica* wood[370]. On the other hand, in the coated wood samples the phenomena described previously were induced a different development. Thereby, the combustion of the samples display a lower impact over the integrity of the wood samples. It seemed that the combustion was occurring directly onto the coating layer but around the wood bulk. Another important facts were that not black fumes were exhausted and without intense glowing. Moreover, the propagation of the flames along the wood was slowed down. These differences between the control and coated wood samples are presented in figure 54.

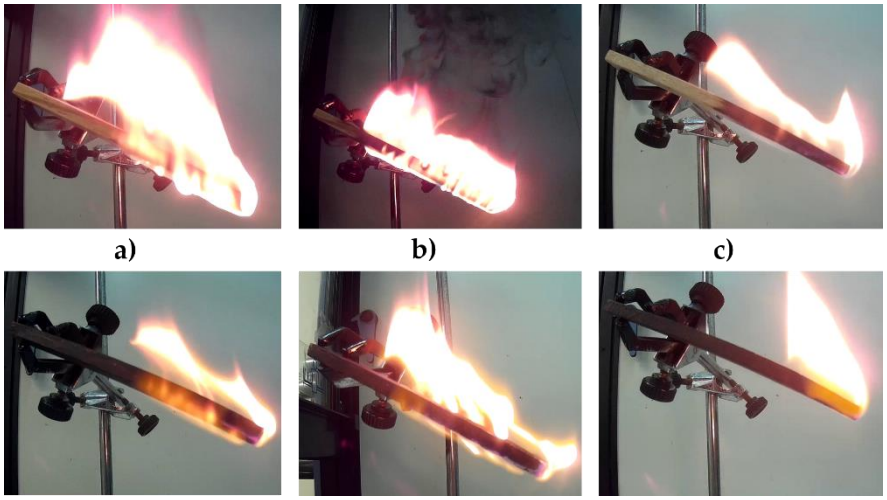

Figure 54. Differences observed between the uncoated wood (upside images) and coated wood (downside images) samples concerning several phenomena occurring during fire exposure: a) fire attack and glowing during combustion, b) fumes exhaustion during combustion, c) flame propagation just after 30s flame exposure.

One of the parameters measured with this analysis was the performance of the coating over the fire resistance of the wood samples. Thereby it was determined the mass degradation of the wood samples after combustion as described as the percentage of wood remaining after fire exposure. The results are displayed in table 51.

Table 51. Resistance of the wood samples (control and coated) to fire exposure.

Samples		Wood dry (g)	Residue remaining (g)	Residue remaining (%)
Pinus pinaster	Control	6.49±0.65	0.66±0.23	10.14±2.96
	R_A	6.51±0.15	1.94±0.15	29.88±1.69
	R_B	6.04±0.29	1.58±0.02	26.19±0.92
Fagus sylvatica	Control	5.76±0.41	0.84±0.11	14.64±2.01
	R_A	6.11±0.12	3.27±0.58	53.54±5.65
	R_B	6.25±0.22	3.63±0.42	58.17±4.62

In regards to the previous results, it was clear that the coatings achieved an enhanced thermal resistance of wood. Moreover, the coating application aided to maintain wood integrity during combustion. This was evidenced by the increment of the residue of wood remaining after combustion, which was between 15-20% and 40-45% for the *Pinus pinaster* and *Fagus Sylvatica* samples respectively (Figure 55). In both control and coated samples, it was observed that *Pinus pinaster* wood samples were burnt easier than those of *Fagus Sylvatica*.

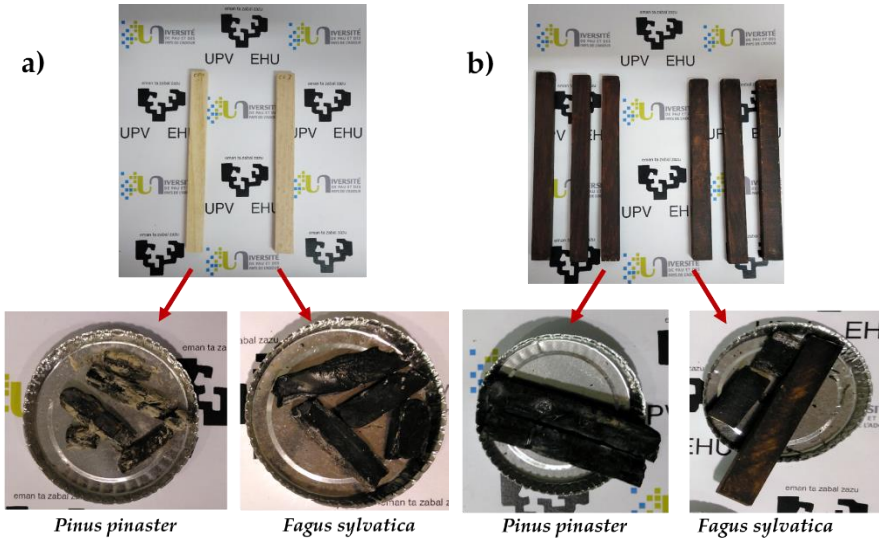

Figure 55. Wood samples of *Pinus pinaster* and *Fagus sylvatica* before (a) and after fire exposure (b).

The other important parameter elucidated by this analysis, was the influence of the coating on the flame propagation along the wood. The results (table 51) showed a significant influence of the coatings on the flame propagation. Thereby in control samples, the flames spread rapidly, whereas in the coated wood samples the advancement was slowed down. This was readily observed from the linear combustion speed (LCS), which was calculated as depicted in equation 8.

$$LCS=[L/t]\cdot[60s/min] \quad (8)$$

Where L: length of the wood sample damaged
t: time elapsed during sample damage

Thus, it was seen that the coating reduce the linear combustion speed by a 50% in *Pinus pinaster* wood samples and by 70-80% in *Fagus silvatica* wood samples approximately. Another positive impact of the coating was that it avoided the flames to reach from the point of initial contact to the opposite end, in the *Fagus sylvatica* wood samples. This means that in those samples the coating provided a self-extinguishing effect for the flames. Considering the previous results and based on the standard method used (UNE-EN 60695-11-10:2014) the coatings were categorized regarding horizontal burning as showed in table 52. In this respect, it was seen that the performance of the coatings in the *Fagus Sylvatica* was better than in *Pinus pinaster* wood samples, since it presented a higher category regarding the flammability of the samples. Thus, the former wood samples were classified as HB (self-extinguishing), meaning that the linear combustion speed was below 40mm/min. On the other side, the latter wood samples were classified as H75, meaning that their linear combustion speed was above 40mm/min but below 75mm/min. Accordingly, the coatings could appropriate (in the case of the hardwood species) for the surface protection of wood structural elements and interior fittings.

Table 52. Flame propagation along the wood samples (control and coated) and related parameters.

Samples		Length (mm)		LCS[C] (mm/min)	Category
		D[A]	R[B]		
Pinus pinaster	Control	125	0	116.07±10.73	---
	R_A	125	0	53.08±11.17	HB75
	R_B	125	0	65.66±13.90	HB75
Fagus sylvatica	Control	125	0	94.95±1.70	---
	R_A	72.33±2.48	52.67±2.48	26.07±1.51	HB
	R_B	70.33±1.33	54.67±1.33	21.07±1.29	HB

[A]D: length damaged from the wood samples, [B]R: length remaining undamaged from the wood samples, [C]LCS: linear combustion speed.

From this assay it was seen both for the thermal resistance of the samples and the flame propagation, that the coatings displayed a better performance on *Fagus sylvatica* than in *Pinus pinaster* wood. This was attributed to lower content of extracts of the former species that it is reported to have a minor influence over coating properties such as penetration and retention on the wood[371]. Then, since a higher amount of coating was retained in the *Fagus sylvatica wood* samples, they showed and improved effect over the studied parameters compared to the *Pinus pinaster* wood samples.

4.3.2.3 Assay for assessing the heat transfer of the coatings

This analysis was performed to determine the influence of the coating over the transfer of heat along the wood samples. With this purpose, wood samples (control and coated) of *Pinus pinaster* and *Fagus sylvatica* of size 50x24x10 mm were selected. The methodology employed is described in Annex VI.3. The heat transfer was measured in the transverse direction with a "*Hot Disk TPS 1500*" as showed in figure 56.

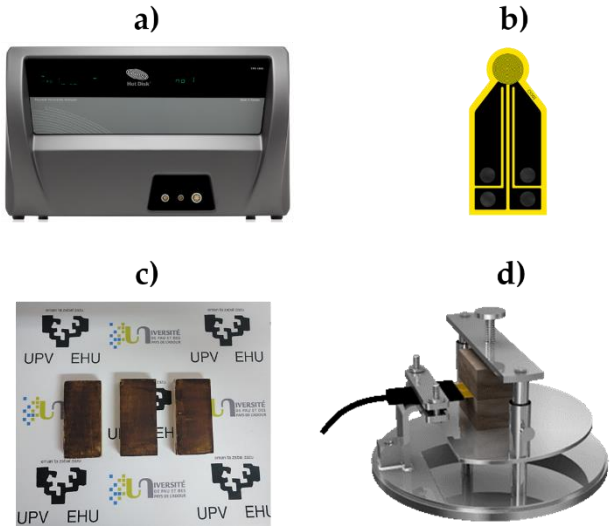

Figure 56. Elements and setting for the performing the analysis of the heat transfer: a) machine Hot Disk TPS 1500, b) Probe measuring the heat change, c) wood samples for analysis, d) setup with the probe and samples ready to perform the measures.

By means of this technique of analysis, several parameters related to the heat transfer were elucidated namely thermal conductivity, thermal diffusivity and volumetric heat capacity. The former is defined by the ability of a material to conduct heat by means of the transfer of the vibrational energy between two adjacent molecules[372]. The second parameter describes the rate at which the temperature can be spread through a material, from the hot to the cold point[373]. The latter could be defined as based on its units, as the amount of energy (heat) necessary to add to one unit of volume to increase its temperature in one degree. These three parameters are interrelated as it can be seen from equation 9.

$$\alpha=[\lambda/(\rho\cdot C_P)] \quad (9)$$

Where α: thermal diffusivity (m^2/s)
λ: thermal conductivity (W/mK)
ρ: density (Kg/m^3) and C_P: specific heat ($J/K\cdot g$)
VHC: volumetric heat capacity VHC= $\rho\cdot C_P$

The results obtained for these parameters are showed in figure 57. Concerning the thermal conductivity of the wood samples, it was only detected a small decreased in the values of the conductivity after the application of the coatings in the samples of *Fagus sylvatica*. Nevertheless, in general no big differences were observed between the control wood samples and those with the coating applied. This showed that the thin layer of the coating applied onto the wood sample did not provide a significant isolating power against heat. The variation of the thermal diffusivity between the uncoated and coated wood samples was more noticeable than in the previous case. Thereby, it was seen in both *Pinus pinaster* and *Fagus silvatica* wood samples that the parameters was reduced after the application of the coatings. This means that the speed of propagation of the temperature through the wood was diminished by the coating layer. This was concurrent with the lower fame propagation observed in the coated samples in the previous section. Finally, regarding the heat capacity, the results showed an increment in the values of this parameter in the coated samples compared to the control ones.

This was because after the application of the coatings the wood samples needed a greater amount of heat to increase their temperature. Thus, it could be said that the coatings provide a protective effect.

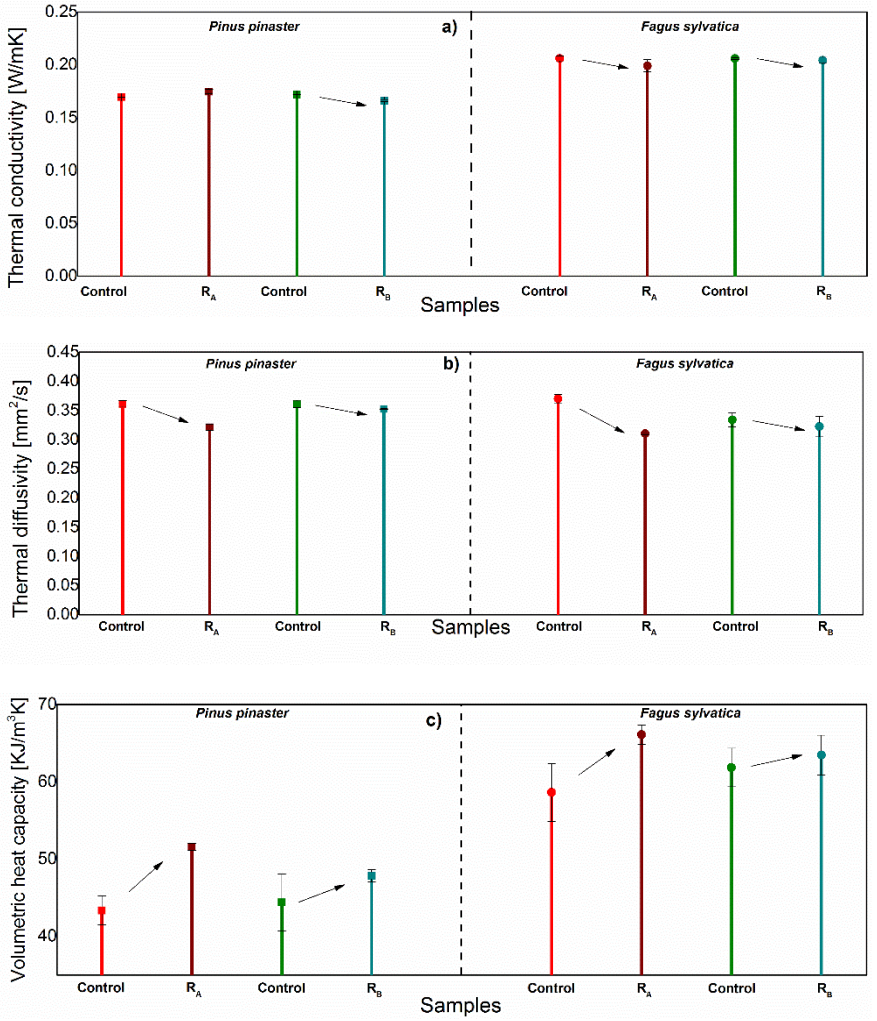

Figure 57. Evolution of different parameters related to heat transfer before (control) and after the application of the coatings (R_A and R_B): a) thermal conductivity, b) thermal diffusivity, c) volumetric heat capacity.

4.4 Conclusions

Along this chapter, several aspects related to the chemistry and thermal performance of the coatings were evaluated. Taking into consideration the results displayed and the corresponding discussion the following conclusions were reached:

- The evaluation of the structure of the coating after the curing confirmed that the different components present namely lignin and tannins reacted between each other and with the curing agent (hexamine), since new bands were detected in their infrared spectra associated with those linkages.
- The thermal analysis of the coating in powder state proved the higher performance of the formulations containing inorganic nanoparticles (R_A and R_B) compared to the one without them (Reference). Therefore, these formulations were selected for their evaluation as flame retardant.
- The analysis of the combustibility proved that the coatings reduced the heat liberated by the wood samples during combustion.
- The assay of the fire resistance confirmed that the coatings provided a protective effect on the integrity of the wood bulk (higher residue remaining after combustion) and that they reduced the flame propagation along the wood samples. These effects were improved in the *Fagus silvatica* wood samples compared to the *Pinus pinaster* ones.
- The analyses of the transfer of heat showed that the thin layer of the coating did not provide a significant effect as thermal insulator. However, it decrease the progress of the temperature across the wood structure.

5. Final conclusions, future works and scientific production

5.1 Final conclusions

The present work was focused on the production of phenolic resins from renewable raw materials, aiming their utilization as coatings in the protection of wood against fire. For this purpose, two phenolic compounds namely lignin and tannins were assessed and they were successfully employed.

First, it was seen that two different sources lignocellulosic biomass namely almond shells and maritime pine residues could be valorised as source of lignin, owing to the significant content of this compound (≈30%) and their local availability. Concerning the extraction process, after evaluation of different possibilities it was proved that the implementation of a single-stage organosolv extraction was the most convenient process. Through the mentioned process a considerable extraction yield was achieved (≈80%) and the lignins obtained presented high purity. The type of lignocellulosic biomass considerably influenced the properties and structure of the lignins extracted. Differences were encountered between them concerning the molecular weight. In addition, it was confirmed by different chemical analysis, the predominance of guaiacyl units in the lignin from maritime pine residues and of syringyl moieties in that extracted from almond shells. These pristine lignins were not suitable for the utilization in the synthesis of the resins and therefore it was concluded that a process of modification was necessary. Consequently, they were subjected to a process of functionalization in two stages: glyoxalation and hybridization with inorganic nanoparticles. The glyoxalation attained an increment in the content of hydroxyl groups as proved by the analyses performed. This was convenient for the utilization of the lignins in further synthesis, since it improves their reactivity. On the other hand, after the hybridization it was confirmed that the inorganic nanoparticles added were substituted within the lignins structure, leading to improved thermal properties.

During the process of functionalization, divergences were detected as well between the two lignins extracted, highlighting the influence of their origin. It was observed that the process of functionalization obtained better results in the case of the lignin extracted from maritime pine residues. Thus, this lignin reached a higher degree of glyoxalation and of substitution of inorganic nanoparticles within its structure. Accordingly, this modified lignin was selected for the synthesis of the phenolic resins.
Concerning the tannins, the commercial mimosa extract selected, which displayed more advantages compared to other extracts obtained at the laboratory scale and to other species, provided a suitable structure and reactivity for its utilization in the synthesis of phenolic resins. Three resins formulations based on lignin, tannins and inorganic nanoparticles (POSS and OMMT) were successfully synthetized. From the chemical characterization, it was seen that the low values of the non-volatile content and viscosity would ease the application of the resins onto the wood surface. Moreover, the considerable hydroxyl values obtained, especially in the formulations R_A and R_B, proved their high reactivity. These features would be beneficial for their application as wood coating. Concerning the thermal analysis of the resins, it was observed that the inclusion of inorganic nanoparticles into the resins formulation had a significant influence over the curing and degradation processes, by delaying both to higher temperatures. This lead to an improvement of the thermal resistance of the resins and therefore allowed the utilization of these resins to protect wood against fire.

The phenolic resins synthetized, based on modified lignin and tannins, were satisfactory applied onto the wood surface as coatings. The main parameters for the implementation of the coatings were assessed and elucidated. Thus, it was determined that 62.5g/m^2 of resins should be cured onto wood surface (previously prepared) during 15h at 60ºC. Then the coating was characterized and it was observed that the main components of the resins, namely lignin and tannins, reacted between each other and with the reticulation agent during the curing of the coating.

Moreover, it was detected that the formulations of the coatings with inorganic nanoparticles incorporated (R_A and R_B) were significantly more resistant to thermal degradation. Accordingly, the other formulation of the resin (Reference) was not selected as coating for wood protection. The coatings displayed a significant influence over the performance of wood against fire exposure in different aspects. First, it was determined that the heat release during the combustion of the wood samples was decreased after the application of the coatings. The coating also achieved a protective effect of the wood integrity and a delay of the flames propagation during fire exposure. These features proved that the coating was suitable as flame-retardant for wood. Nevertheless, concerning the transfer of heat no significant effect was achieved by the thin layer of the coating as thermal insulator.

To sum up, in this work it was achieved a small scale process, promoting the concept of circular economy in which wood residues were used as raw materials to synthetize a biosourced product (resins) for protecting wood against fire.

5.2 Future works

To keep on with the topic of this research, the following points would be proposed:

- Optimization of the process of synthesis of the resins: variation of the ratio lignin:tannins, addition of a higher amount of inorganic nanoparticles, enhancement of the process of introduction of inorganic nanoparticles.
- Comprehensive study of the curing reaction of the resins to determine parameters such as the point of gel, degree of reticulation etc. and to optimize the curing conditions of the coatings.

- Scale up the process of synthesis of the resins and production of the coatings, to attract the potential interest of the industry.
- Evaluate the performance of the resins in the protection of wood against fire by an impregnation treatment instead of the coating deposition.
- Assess the performance of the coatings against other decay agents of wood such as water, sunlight, bacteria and fungi. Carry out the corresponding modification on the resins to achieve protection against those agents.

5.3 Scientific production

In this section are listed the works published (articles and book chapters), the participations in conferences and prices and awards derived from those works.

5.3.1 Published works

During the development of this doctoral thesis, the following articles have been written and published in scientific journals, related to the topic of the thesis:

I. **Authors:** **de Hoyos-Martínez, PL.**, Erdocia X., Charrier-El Bouhtoury F., Prado R., Labidi, J.

   Title: Multistage treatment of almonds waste biomass: Characterization and assessment of the potential applications of raw material and products

   Journal: Waste Management

   Year: 2018

   Impact factor: 5.431 (published)

   JC and JR: Environmental Engineering (9/52) Q1

II. **Authors:** **de Hoyos-Martinez PL.**, Merle J., Labidi J., Charrier–El Bouhtoury, F.

Title: Tannins extraction: A key point for their valorization and cleaner production

Journal: Journal of Cleaner Production

Year: 2018

Impact factor: 6.395 (published)

JC and JR: Green sustainable science and technology (6/35) Q1

III. **Authors:** **de Hoyos Martinez PL.**, Robles E., Khoukh A., Charrier-El Bouhtoury F., Labidi, J.

Title: Formulation of multifunctional materials based on the reaction of glyoxalated lignins and a nanoclay/nanosilicate

Journal: Biomacromolecules

Year: 2019

Impact factor: 5.667 (current)

JC and JR: Polymer science (7/87) Q1

IV. **Authors:** **de Hoyos Martinez, P.L.**, Issaoui H., Herrera R., Labidi, J., Charrier-El Bouhtoury, F.

Title: Coatings based on biosourced phenolic resins for protection of wood against fire

Journal:

Year: 2019

Impact factor: (current)

JC and JR:
(submission state)

Other articles non-related to the topic of thesis have been published as well as part of collaborations:

I. **Authors:** Fernández-Rodríguez J., Erdocia X., **De-Hoyos PL.**, Alriols MG., Labidi J.

Title: Small Phenolic Compounds Production from Kraft Black Liquor by Lignin Depolimerisation with Different Catalytic Agents

Journal: Chemical Engineering Transactions

Year: 2017

SJR indicator: 0.293 (published)

JC and JR: Chemical Engineering (293/688)

II. **Authors:** Herrera R., Arrese A., **de Hoyos-Martinez P.L.**, Labidi J., Llano-Ponte R.

Title: Evolution of thermally modified wood properties exposed to natural and artificial weathering and its potential as an element for façades systems

Journal: Construction and Building Materials

Year: 2018

Impact factor: 4.046 (published)

JC and JR: Materials science, multidisciplinary (70/293) Q1

III. **Authors:** Tahari N., **de Hoyos-Martinez P.L.**, Abderrabba M., Ayadi S., Labidi J.

Title: Hydrogel based on lignin and montmorillonite for toluene removal

Journal: Reactive and functional polymers

Year: 2018

Impact factor: 3.074 (current)

JC and JR: Polymer science (18/87) Q1
(under revision)

Besides the mentioned articles, during the development of the doctoral thesis the following chapters of book have been published:

I. **Authors:** Fernández-Rodríguez J., Erdocia X., **de Hoyos P. L.**, Sequeiros A., Labidi J.

Title: Catalytic Cascade Transformations of Biomass into Polyols

Book: Production of Biofuels and Chemicals with Bifunctional Catalysts

Chapter: 6

Year: 2017

Publisher: Springer

II. **Authors:** Saad H., **de Hoyos P. L.**, Srasra E., Charrier-El Bouhtoury, F.

Title: Advances in Bio-Nanohybrid Materials

Book: Green and Sustainable Advanced Materials: Processing and Characterization, Volume 1

Chapter: 11

Year: 2018

Publisher: Wiley

5.3.2 Contributions in scientific conferences

In this part are presented all the works presented in scientific conferences during the development of the doctoral thesis:

I. **Authors:** **Pedro Luis de Hoyos Martínez**, Xabier Erdocia, Fatima Charrier-El Bouhtoury, Jalel Labidi

Title: "Almond shell lignin extraction via consecutive organosolv delignification treatments and its characterization"

Congress: FP1306 COST Action, Second Workshop and Third MC Meeting: Valorization of lignocellulosic biomass side streams for sustainable production of chemicals, materials & fuels using low environmental impact technologies.

Particpation: Poster

Date: 4th-6th April, 2016

Place: Dubrovnik (Croatia)

II. **Authors:** Itziar Egüés, Arantxa Olasagasti, Xabier Erdocia, **Pedro Luis de Hoyos Martinez**, Silvia H. Fuentes, Jalel Labidi

Title: "Lignin-based resol resins: effect Lignin-of lignin fractionation"

Congress: 14th European Workshop on Lignocellulosics and Pulp (EWLP).

Particpation: Poster

Date: 28th-30th June, 2016

Place: Autrans (France)

III. **Authors: Pedro Luis de Hoyos Martinez**, Xabier Erdocia Iriarte, Fatima Charrier El- Bouhtoury, Jalel Labidi

Title: "Extraction of almond shells lignin by means of sequential organosolv treatments and its latter characterization"

Congress: XXIII TECNICELPA - International Forest, Pulp and Paper Conference

Particpation: Poster

Date: 12th-14th October, 2016

Place: Porto (Portugal)

IV. **Authors: Pedro Luis de Hoyos Martinez**, Jalel Labidi, Fatima Charrier El- Bouhtoury

Title: "Tannins general classification, characterization techniques and potential applications"

Congress: International Conference on Materials and Energy (ICOME)

Particpation: Poster presentation

Date: 6th-9th July, 2017

Place: Tianjin (China)

V. **Authors: Pedro Luis de Hoyos Martinez**, Jalel Labidi, Fatima Charrier El- Bouhtoury

Title: "Biobased phenolic resins for wood protection against fire"

Congress: FP1407 COST Action, 3rd meeting: "Wood modification, research and applications".

Particpation: Poster presentation

Date: 14th-15th September, 2017

Place: Kuchl (Austria)

VI. **Authors:** **Pedro Luis de Hoyos Martinez**, Jalel Labidi, Fatima Charrier El- Bouhtoury

Title: "Formulation of a hybrid organic-inorganic matrix coating for the protection of wood"

Congress: 10th World Congress of Chemical Engineering (WCCE)

Particpation: Poster

Date: 1st-5th October, 2017

Place: Barcelona (Spain)

VII. **Authors:** **Pedro Luis de Hoyos Martinez**, Jalel Labidi, Fatima Charrier El- Bouhtoury

Title: "Bio-sourced hybrid phenolic fireproofing resins for novel applications"

Congress: International Conference on Materials and Energy (ICOME).

Particpation: Poster presentation

Date: 30th-4th April/May, 2018

Place: San Sebastian (Spain)

VIII. **Authors:** **Pedro Luis de Hoyos Martinez**, Jalel Labidi, Fatima Charrier El- Bouhtoury

Title: "Chemical characterization and curing behaviour of hybrid biosourced phenolic resins."

Congress: 4th Iberoamerican Congress on Biorefineries (4-CIAB).

Particpation: Poster

Date: 24th-26th October, 2018

Place: Spain (Spain)

IX. **Authors:** **Pedro Luis de Hoyos Martinez**, René Herrera, Jalel Labidi, Fatima Charrier El- Bouhtoury

Title: "Preliminary analysis of bio-sourced hybrid resins as coatings for wood protection."

Congress: FP 1407 COST Action: "Living with modified wood".

Particpation: Poster presentation

Date: 12th-13th December, 2018

Place: Belgrade (Serbia)

X. **Authors:** René Herrera Díaz, Oihana Gordobil, **Pedro L. de Hoyos-Martínez**, Jalel Labidi, Rodrigo Llano-Ponte

Title: "Improving hydrophobicity and thermal stability of wood through esterification with fatty acids."

Congress: FP 1407 COST Action: "Living with modified wood".

Particpation: Poster presentation

Date: 12th-13th December, 2018

Place: Belgrade (Serbia)

XI. **Authors:** **Pedro Luis de Hoyos Martinez**, René Herrera, Jalel Labidi, Fatima Charrier El- Bouhtoury

Title: "Biosourced phenolic resins as coatings for the protection of wood and wood composites against fire."

Congress: International Research Group on Wood Protection 50th Conference (IRG-WP50).

Particpation: Oral presentation

Date: 12th-16th May, 2019

Place: Quebec (Canada)

5.3.3 Recognitions and awards

During the development of the doctoral thesis, the following awards were won, thanks to thesis-related activities and works:

I. **Event:** "Journées de l'Ecole Doctorale des Sciences Exactes et leurs Applications (ED211)"-University of Pau and Pays de l'Adour

Award: Best poster presentation award

Date: 21st-22nd June, 2017

Place: Pau (France)

II. **Event:** International Conference on Materials and Energy (ICOME)

Award: Best poster award

Date: 30th-4th April/May, 2018

Place: San Sebastian (Spain)

III. **Event:** "13th Journées des Thèses des Bois"-Xylofutur

Award: "GDR Bois award" to oral presentation

Date: 13th September, 2018

Place: Limoges (France)

IV. **Event:** FP 1407 COST Action, final conference: "Living with modified wood".

Award: Best poster presentation award

Date: 12th-13th December, 2018

Place: Belgrade (Serbia)

V. **Event:** "Ma thèse en 180s".

Award: 4th Price and classification for Regional Final

Date: 19th March, 2019

Place: Pau (France)

VI. **Place:** Belgrade (Serbia)**Event:** International Research Group on Wood Protection 50th Conference (IRG-WP50).

Award: "Ron Cockcroft Award (RCA)"

Date: 12th-16th May, 2019

Place: Quebec (Canada)

VII. **Event:** International Research Group on Wood Protection 50th Conference (IRG-WP50).

Award: "Viance Innovation Award" to most innovative oral presentation

Date: 12th-16th May, 2019

Place: Quebec (Canada)

6. References

(1) United Nations. World Population Prospects: The 2019 Revision. United Nations Population Division: New York 2019.

(2) European Comission. *Europe 2020: A Strategy for Smart, Sustainable and Inclusive Growth*; Brussels, 2010.

(3) European Comission. What is Horizon 2020? https://ec.europa.eu/eurostat/web/sdi/overview (accessed Jun 17, 2019).

(4) European Environmental Agency (EEA). Greenhouse Gas Emissions Statistics from the 28 European Countries (Database). 2017.

(5) Secretariat U. N. F. C. C. C. *Report of the Conference of the Parties on Its Twenty-First Session, Held in Paris from 30 November to 13 December 2015. In Addendum. Part Two: Action Taken by the Conference of the Parties at Its Twenty-First Session.*; Paris, 2015.

(6) Ren, J.; Manzardo, A.; Toniolo, S.; Scipioni, A. Sustainability of Hydrogen Supply Chain. Part I: Identification of Critical Criteria and Cause–effect Analysis for Enhancing the Sustainability Using DEMATEL. *Int. J. Hydrogen Energy* **2013**, *38* (33), 14159–14171.

(7) Brennan, G.; Tennant, M.; Blomsa, F. Business and Production Solutions: Closing Loops and the Circular Economy. In *Sustainability: Key Issues*; Kopnina, H., Shoreman-Ouimet, E., Eds.; Earthscan Routledge: 219-239, 2015; p 393.

(8) Geissdoerfer, M.; Savaget, P.; Bocken, N. M. P.; Hultink, E. J. The Circular Economy – A New Sustainability Paradigm? *J. Clean. Prod.* **2017**, *143*, 757–768.

(9) Ellen MacArthur Foundation. *Growth within: A Circular Economy Vision for a Competitive Europe*; 2015.

(10) Webster, K. The Circular Economy: A Wealth of Flows. *Ellen MacArthur Found. Publ.* **2017**.

(11) Lett, L. A. Las Amenazas Globales, El Reciclaje de Residuos Y El Concepto de Economía Circular. *Rev. Argent. Microbiol.* **2014**, *46* (1), 1–2.

(12) Ghisellini, P.; Cialani, C.; Ulgiati, S. A Review on Circular Economy: The Expected Transition to a Balanced Interplay of Environmental and Economic Systems. *J. Clean. Prod.* **2016**, *114*, 11–32.

(13) Su, B.; Heshmati, A.; Geng, Y.; Yu, X. A Review of the Circular Economy in China: Moving from Rhetoric to Implementation. *J. Clean. Prod.* **2013**, *42*, 215–227.

(14) EU. Directive 2008/98/EC of the European Parliament and of the Council of 19 November 2008 on Waste and Repealing Certain Directives. *Off. J. EU, L 312, 19.11.2008* **2008**.

(15) European Parliament. Directive 2009/28/EC of the European Parliament and of the Council of 23 April 2009. *Off. J. Eur. Union* **2009**, *140* (16), 16–62.

(16) Stahel, W. R. Reuse Is the Key to the Circular Economy. **2014**.

(17) Zabaniotou, A.; Kamaterou, P. Food Waste Valorization Advocating Circular Bioeconomy - A Critical Review of Potentialities and Perspectives of Spent Coffee Grounds Biorefinery. *J. Clean. Prod.* **2019**, *211*, 1553–1566.

(18) Nizami, A. S.; Rehan, M.; Waqas, M.; Naqvi, M.; Ouda, O. K. .; Shahzad, K.; Miandad, R.; Khan, M. Z.; Syamsiro, M.; Ismail, I. M. I.; et al. Waste Biorefineries: Enabling Circular Economies in Developing Countries. *Bioresour. Technol.* **2017**, *241*, 1101–1117.

(19) de Jong, E.; Jungmeier, G. Biorefinery Concepts in Comparison to Petrochemical Refineries. In *Industrial Biorefineries & White Biotechnology*; Elsevier, 2015; pp 3–33.

(20) Berntsson, T.; Sandén, B.; Olsson, L.; Åsblad, A. What Is a Biorefinery? In *Systems Perspectives on Biorefineries*; 2012; pp 16–25.

(21) Cherubini, F. The Biorefinery Concept: Using Biomass instead of Oil for Producing Energy and Chemicals. *Energy Convers. Manag.* **2010**, *51* (7), 1412–1421.

(22) Cherubini, F.; Jungmeier, G.; Wellisch, M.; Willke, T.; Skiadas, I.; Van Ree, R.; de Jong, E. Toward a Common Classification Approach for Biorefinery Systems. *Biofuels, Bioprod. Biorefining* **2009**, *3* (5), 534–546.

(23) Gnansounou, E.; Pandey, A. Classification of Biorefineries Taking into Account Sustainability Potentials and Flexibility. In *Life-Cycle Assessment of Biorefineries*; Elsevier, 2017; pp 1–39.

(24) Hingsamer, M.; Jungmeier, G. Biorefineries. In *The Role of Bioenergy in the Bioeconomy*; Academic Press, 2019; pp 179–222.

(25) Bilgili, F.; Ozturk, I. Biomass Energy and Economic Growth Nexus in G7 Countries: Evidence from Dynamic Panel Data. *Renew. Sustain. Energy Rev.* **2015**, *49*, 132–138.

(26) Lewandowski, I.; Gaudet, N.; Lask, J.; Maier, J.; Tchouga, B.; Vargas-Carpintero, R. Bioeconomy. In *Shaping the Transition to a Sustainable Biobased Economy*; Lewandowski, I., Ed.; Springer International Publishing: Cham, 2018.

(27) European Comission. Innovating for Sustainable Growth: A Bioeconomy for Europe. *Off. J. Eur. Union* **2012**, *8* (2), 60.

(28) Sánchez, J.; Curt, M. D.; Robert, N.; Fernández, J. Biomass Resources. In *The Role of Bioenergy in the Bioeconomy*; Academic Press, 2019; pp 25–111.

(29) Institut National de l'Information Géographique et Forestière. *Data Sheet: Caractéristiques Des Forêts de Production Hors Peupleraies (Campagnes 2012 À 2016)*; 2018.

(30) FCBA Institute Technologique. *Memento 2018*; 2018.

(31) Abad Viñas, R.; Caudullo, G.; Oliveira, S.; de Rigo, D. Pinus Pinaster in Europe: Distribution, Habitat, Usage and Threats. In *European Atlas of Forest Tree Species*; San-Miguel-Ayanz, J., de Rigo, D., Caudullo, G., Houston Durrant, T., Mauri, A., Eds.; Official EU, 2016.

(32) Ebringerová, A.; Hromádková, Z.; Košťálová, Z.; Sasinková, V. Chemical Valorization of Agricultural by-Products: Isolation and Characterization of Xyland-Based Antioxidants from Almond Shell Biomass. *BioResources* **2007**, *3* (1), 60–70.

(33) Chen, K.; Escott, C.; Loira, I.; del Fresno, J.; Morata, A.; Tesfaye, W.; Calderon, F.; Benito, S.; Suárez-Lepe, J. The Effects of Pre-Fermentative Addition of Oenological Tannins on Wine Components and Sensorial Qualities of Red Wine. *Molecules* **2016**, *21* (12), 1445.

(34) Çöpür, Y.; Güler, C.; Akgül, M.; Taşçıoğlu, C. Some Chemical Properties of Hazelnut Husk and Its Suitability for Particleboard Production. *Build. Environ.* **2007**, *42* (7), 2568–2572.

(35) Zhang, Y.-H. P. Reviving the Carbohydrate Economy via Multi-Product Lignocellulose Biorefineries. *J. Ind. Microbiol. Biotechnol.* **2008**, *35* (5), 367–375.

(36) Agbor, V.; Carere, C.; Cicek, N.; Sparling, R.; Levin, D. Biomass Pretreatment for Consolidated Bioprocessing (CBP). In *Advances in Biorefineries*; Woodhead Publishing, 2014; pp 234–258.

(37) Qian, E. W. Pretreatment and Saccharification of Lignocellulosic Biomass. In *Research Approaches to Sustainable Biomass Systems*; Academic Press, 2014; pp 181–204.

(38) Binod, P.; Pandey, A. Introduction. In *Pretreatment of Biomass*; Elsevier, 2015; pp 3–6.

(39) Bajpai, P. Structure of Lignocellulosic Biomass. In *Pretreatment of Lignocellulosic Biomass for Biofuel Production*; Springer, Singapore, 2016; pp 7–12.

(40) Hörhammer, H.; Dou, C.; Gustafson, R.; Suko, A.; Bura, R. Removal of Non-Structural Components from Poplar Whole-Tree Chips to Enhance Hydrolysis and Fermentation Performance. *Biotechnol. Biofuels* **2018**, *11* (1), 222.

(41) Saini, J. K.; Saini, R.; Tewari, L. Lignocellulosic Agriculture Wastes as Biomass Feedstocks for Second-Generation Bioethanol Production: Concepts and Recent Developments. *3 Biotech* **2015**, *5* (4), 337–353.

(42) de Jong, E.; Gosselink, R. J. A. Lignocellulose-Based Chemical Products. In *Bioenergy Research: Advances and Applications*; Elsevier, 2014; pp 277–313.

(43) Mena, P.; Calani, L.; Bruni, R. Bioactivation of High-Molecular-Weight Polyphenols by the Gut Microbiome. In *Diet-Microbe Interactions in the Gut*; Academic Press, 2015; pp 73–101.

(44) Mahmood, N.; Yuan, Z.; Schmidt, J.; Xu, C. (Charles). Depolymerization of Lignins and Their Applications for the Preparation of Polyols and Rigid Polyurethane Foams: A Review. *Renew. Sustain. Energy Rev.* **2016**, *60*, 317–329.

(45) Ponnusamy, V. K.; Nguyen, D. D.; Dharmaraja, J.; Shobana, S.; Banu, J. R.; Saratale, R. G.; Chang, S. W.; Kumar, G. A Review on Lignin Structure, Pretreatments, Fermentation Reactions and Biorefinery Potential. *Bioresour. Technol.* **2019**, *271*, 462–472.

(46) Figueiredo, P.; Lintinen, K.; Hirvonen, J. T.; Kostiainen, M. A.; Santos, H. A. Properties and Chemical Modifications of Lignin: Towards Lignin-Based Nanomaterials for Biomedical Applications. *Prog. Mater. Sci.* **2018**, *93*, 233–269.

(47) Lourenço, A.; Pereira, H. Compositional Variability of Lignin in Biomass. In *Lignin - Trends and Applications*; InTech, 2018; pp 65–98.

(48) Hu, L.; Pan, H.; Zhou, Y.; Hse, C.-Y.; Liu, C.; Zhang, B.; Xu, B. Chemical Groups and Structural Characterization of Lignin via Thiol-Mediated Demethylation. *J. Wood Chem. Technol.* **2014**, *34* (2), 122–134.

(49) Brunner, G. Processing of Biomass with Hydrothermal and Supercritical Water. In *Supercritical Fluid Science and Technology*; Elsevier, 2014; Vol. 5, pp 395–509.

(50) Tobimatsu, Y.; Schuetz, M. Lignin Polymerization: How Do Plants Manage the Chemistry so Well? *Curr. Opin. Biotechnol.* **2019**, *56*, 75–81.

(51) Wang, Y.; Chantreau, M.; Sibout, R.; Hawkins, S. Plant Cell Wall Lignification and Monolignol Metabolism. *Front. Plant Sci.* **2013**, *4*, 220.

(52) del Río, J. C.; Rencoret, J.; Gutiérrez, A.; Lan, W.; Kim, H.; Ralph, J. Lignin Monomers from Outside the Canonical Monolignol Biosynthetic Pathway. In *19th International Symposium on Wood, Fiber and Pulping Chemistry*; 2017; p Porto Seguro.

(53) Meents, M. J.; Watanabe, Y.; Samuels, A. L. The Cell Biology of Secondary Cell Wall Biosynthesis. *Ann. Bot.* **2018**, *121* (6), 1107–1125.

(54) Dixon, R. A.; Chen, F.; Guo, D.; Parvathi, K. The Biosynthesis of Monolignols: A "metabolic Grid", or Independent Pathways to Guaiacyl and Syringyl Units? *Phytochemistry* **2001**, *57* (7), 1069–1084.

(55) Naseem, A.; Tabasum, S.; Zia, K. M.; Zuber, M.; Ali, M.; Noreen, A. Lignin-Derivatives Based Polymers, Blends and Composites: A Review. *Int. J. Biol. Macromol.* **2016**, *93*, 296–313.

(56) Paliwal, R.; Giri, K.; Rai, J. P. . Microbial Ligninolysis: Avenue for Natural Ecosystem Management. In *Handbook of Research on Uncovering New Methods for Ecosystem Management through Bioremediation*; Singh, S., Srivastava, K., Eds.; IGI Global, 2015; pp 120–145.

(57) Santos, R. B.; Hart, P.; Jameel, H.; Chang, H. Wood Based Lignin Reactions Important to the Biorefinery and Pulp and Paper Industries. *BioResources* **2013**, *8* (1), 1456–1477.

(58) Cao, L.; Yu, I. K. M.; Liu, Y.; Ruan, X.; Tsang, D. C. W.; Hunt, A. J.; Ok, Y. S.; Song, H.; Zhang, S. Lignin Valorization for the Production of Renewable Chemicals: State-of-the-Art Review and Future Prospects. *Bioresour. Technol.* **2018**, *269*, 465–475.

(59) Ragauskas, A. J.; Beckham, G. T.; Biddy, M. J.; Chandra, R.; Chen, F.; Davis, M. F.; Davison, B. H.; Dixon, R. A.; Gilna, P.; Keller, M.; et al. Lignin Valorization: Improving Lignin Processing in the Biorefinery. *Science (80-.).* **2014**, *344* (6185), 1246843–1246843.

(60) Zheng, T.; Zheng, D.; Qiu, X.; Yang, D.; Fan, L.; Zheng, J. A Novel Branched Claw-Shape Lignin-Based Polycarboxylate Superplasticizer: Preparation, Performance and Mechanism. *Cem. Concr. Res.* **2019**, *119*, 89–101.

(61) Wang, C.; Kelley, S. S.; Venditti, R. A. Lignin-Based Thermoplastic Materials. *ChemSusChem* **2016**, *9* (8), 770–783.

(62) Stanzione, J. F.; Giangiulio, P. A.; Sadler, J. M.; La Scala, J. J.; Wool, R. P. Lignin-Based Bio-Oil Mimic as Biobased Resin for Composite Applications. *ACS Sustain. Chem. Eng.* **2013**, *1* (4), 419–426.

(63) Xiao, S.; Feng, J.; Zhu, J.; Wang, X.; Yi, C.; Su, S. Preparation and Characterization of Lignin-Layered Double Hydroxide/styrene-Butadiene Rubber Composites. *J. Appl. Polym. Sci.* **2013**, *130* (2), 1308–1312.

(64) Xing, Q.; Buono, P.; Ruch, D.; Dubois, P.; Wu, L.; Wang, W.-J. Biodegradable UV-Blocking Films through Core–Shell Lignin–Melanin Nanoparticles in Poly(butylene Adipate-Co-Terephthalate). *ACS Sustain. Chem. Eng.* **2019**, *7* (4), 4147–4157.

(65) Yang, D.; Wang, S.; Zhong, R.; Liu, W.; Qiu, X. Preparation of lignin/TiO2 Nanocomposites and Their Application in Aqueous Polyurethane Coatings. *Front. Chem. Sci. Eng.* **2019**, *13* (1), 59–69.

(66) Azadi, P.; Inderwildi, O. R.; Farnood, R.; King, D. A. Liquid Fuels, Hydrogen and Chemicals from Lignin: A Critical Review. *Renew. Sustain. Energy Rev.* **2013**, *21*, 506–523.

(67) Stojanovska, E.; Pampal, E. S.; Kilic, A.; Quddus, M.; Candan, Z. Developing and Characterization of Lignin-Based Fibrous Nanocarbon Electrodes for Energy Storage Devices. *Compos. Part B Eng.* **2019**, *158*, 239–248.

(68) El Mansouri, N. E.; Yuan, Q.; Huang, F. Preparation and Characterization of Phenol-Formaldehyde Resins Modified with Alkaline Rice Straw Lignin. *BioResources* **2018**, *13* (4), 8061–8075.

(69) Nagatani, M.; Tsurumaki, A.; Takamatsu, K.; Saito, H.; Nakamura, N.; Ohno, H. Preparation of Epoxy Resins Derived from Lignin Solubilized in Tetrabutylphosphonium Hydroxide Aqueous Solutions. *Int. J. Biol. Macromol.* **2019**, *132*, 585–591.

(70) Zhu, S.; Chen, K.; Xu, J.; Li, J.; Mo, L. Bio-Based Polyurethane Foam Preparation Employing Lignin from Corn Stalk Enzymatic Hydrolysis Residues. *RSC Adv.* **2018**, *8* (28), 15754–15761.

(71) Technical Research Centre of Finland (VTT). Wood Components to Boost Quality of Food Products. *ScienceDaily* **2016**, *1*.

(72) Ge, Y.; Li, Z. Application of Lignin and Its Derivatives in Adsorption of Heavy Metal Ions in Water: A Review. *ACS Sustain. Chem. Eng.* **2018**, *6* (5), 7181–7192.

(73) Witzler, M.; Alzagameem, A.; Bergs, M.; Khaldi-Hansen, B. El; Klein, S. E.; Hielscher, D.; Kamm, B.; Kreyenschmidt, J.; Tobiasch, E.; Schulze, M. Lignin-Derived Biomaterials for Drug Release and Tissue Engineering. *Molecules* **2018**, *23* (8).

(74) Gordobil, O.; Herrera, R.; Yahyaoui, M.; İlk, S.; Kaya, M.; Labidi, J. Potential Use of Kraft and Organosolv Lignins as a Natural Additive for Healthcare Products. *RSC Adv.* **2018**, *8* (43), 24525–24533.

(75) Thakur, V. K.; Thakur, M. K.; Raghavan, P.; Kessler, M. R. Progress in Green Polymer Composites from Lignin for Multifunctional Applications: A Review. *ACS Sustain. Chem. Eng.* **2014**, *2* (5), 1072–1092.

(76) Arbenz, A.; Avérous, L. Tannins: A Resource to Elaborate Aromatic and Biobased Polymers. In *Biodegradable and Biobased Polymers for Environmental and Biomedical Applications*; John Wiley & Sons, Inc.: Hoboken, NJ, USA, 2016; pp 97–148.

(77) Laurichesse, S.; Avérous, L. Chemical Modification of Lignins: Towards Biobased Polymers. *Prog. Polym. Sci.* **2014**, *39* (7), 1266–1290.

(78) Arapitsas, P. Hydrolyzable Tannin Analysis in Food. *Food Chem.* **2012**, *135* (3), 1708–1717.

(79) A. Bele, A.; M. Jadhav, V.; Kadam, V. J. Potential of Tannnins: A Review. *Asian J. Plant Sci.* **2010**, *9* (4), 209–214.

(80) Bate-Smith, E. C.; Swain, T. Flavonoid Compound. In *Comparative biochemistry*; Mason, H. S., Florkin, A. M., Eds.; Academic Press: New York, 1962; pp 755–809.

(81) Sathish P; Jaswanth G; Gopinath, G. K. B.; Gayathri P K; Yuvaraj D. Phytochemical Investigation and Antibacterial Activity of Salt Marsh Plant Extracts. *J. Chem. Pharm. Sci.* **2016**, *9* (1), 292–294.

(82) Maie, N.; Pisani, O.; JaffÉ, R. Mangrove Tannins in Aquatic Ecosystems: Their Fate and Possible Influence on Dissolved Organic Carbon and Nitrogen Cycling. *Limnol. Oceanogr.* **2008**, *53* (1), 160–171.

(83) Geoffroy, T. R.; Fortin, Y.; Stevanovic, T. Hot-Water Extraction Optimization of Sugar Maple (Acer Saccharum Marsh.) and Red Maple (Acer Rubrum L.) Bark Applying Principal Component Analysis. *J. Wood Chem. Technol.* **2017**, *37* (4), 261–272.

(84) Tabaraki, R.; Safari, A.; Yeganeh, F. A. Ultrasonic-Assisted Extraction of Condensed Tannin from Acron, Gland, Leaf and Gall of Oak Using Response Surface Methodology. *J. Appl. Chem. Res.* **2013**, *7* (3), 67–77.

(85) Cheng, V. J.; Bekhit, A. E.-D. A.; McConnell, M.; Mros, S.; Zhao, J. Effect of Extraction Solvent, Waste Fraction and Grape Variety on the Antimicrobial and Antioxidant Activities of Extracts from Wine Residue from Cool Climate. *Food Chem.* **2012**, *134* (1), 474–482.

(86) Frutos, P.; Hervás, G.; Giráldez, F. J.; Mantecón, A. R. Review. Tannins and Ruminant Nutrition. *Spanish J. Agric. Res.* **2004**, *2* (2), 191.

(87) Guglielmelli, A.; Calabro`, S.; Primi, R.; Carone, F.; Cutrignelli, M. I.; Tudisco, R.; Piccolo, G.; Ronchi, B.; Danieli, P. P. In Vitro Fermentation Patterns and Methane Production of Sainfoin (Onobrychis Viciifolia Scop.) Hay with Different Condensed Tannin Contents. *Grass Forage Sci.* **2011**, *66* (4), 488–500.

(88) Hassanpour, S.; MaheriSis, N.; Eshratkhah, B.; mehmandar, F. B. Plants and Secondary Metabolites (Tannins): A Review. *Int. J. For. Soil Eros.* **2011**, *1* (1), 47–53.

(89) Salminen, J.-P.; Karonen, M. Chemical Ecology of Tannins and Other Phenolics: We Need a Change in Approach. *Funct. Ecol.* **2011**, *25* (2), 325–338.

(90) Hagerman, A. E. *Tannin Chemistry*; Miami University, Ed.; Oxford, 2002.

(91) Haslam, E. Vegetable Tannins – Lessons of a Phytochemical Lifetime. *Phytochemistry* **2007**, *68* (22–24), 2713–2721.

(92) Bennick, A. Interaction of Plant Polyphenols with Salivary Proteins. *Crit. Rev. Oral Biol. Med.* **2002**, *13* (2), 184–196.

(93) Dai, J.; Mumper, R. J. Plant Phenolics: Extraction, Analysis and Their Antioxidant and Anticancer Properties. *Molecules* **2010**, *15* (12), 7313–7352.

(94) Tahir, P. M.; Halip, J. A.; Lee, S. H. Tannin-Based Bioresin as Adhesives. In *Lignocellulose for future bioeconomy*; Elsevier, 2019; pp 109–133.

(95) Smeriglio, A.; Barreca, D.; Bellocco, E.; Trombetta, D. Proanthocyanidins and Hydrolysable Tannins: Occurrence, Dietary Intake and Pharmacological Effects LINKED ARTICLES. *Br. J. Pharmacol.* **2017**, *174*, 1244–1262.

(96) Landete, J. M. Ellagitannins, Ellagic Acid and Their Derived Metabolites: A Review about Source, Metabolism, Functions and Health. *Food Res. Int.* **2011**, *44* (5), 1150–1160.

(97) Kofi Busia. Tannins. In *Fundamentals of Herbal Medicine : History, Phytopharmacology and Phytotherapeutics Vol 1*; 2016; p 734.

(98) Jan, S.; Abbas, N.; Jan, S.; Abbas, N. Chemistry of Himalayan Phytochemicals. In *Himalayan Phytochemicals*; Elsevier, 2018; pp 121–166.

(99) Glombitza, K.-W.; Pauli, K. Fucols and Phlorethols from the Brown Alga Scytothamnus Australis Hook. et Harv. (Chnoosporaceae). *Bot. Mar.* **2003**, *46* (3), 315–320.

(100) Lopes, G.; Sousa, C.; Silva, L. R.; Pinto, E.; Andrade, P. B.; Bernardo, J.; Mouga, T.; Valentão, P. Can Phlorotannins Purified Extracts Constitute a Novel Pharmacological Alternative for Microbial Infections with Associated Inflammatory Conditions? *PLoS One* **2012**, *7* (2), e31145.

(101) Sathya, R.; Kanaga, N.; Sankar, P.; Jeeva, S. Antioxidant Properties of Phlorotannins from Brown Seaweed Cystoseira Trinodis (Forsskål) C. Agardh. *Arab. J. Chem.* **2017**, *10*, S2608–S2614.

(102) Koivikko, R.; Eränen, J. K.; Loponen, J.; Jormalainen, V. Variation of Phlorotannins Among Three Populations of Fucus Vesiculosus as Revealed by HPLC and Colorimetric Quantification. *J. Chem. Ecol.* **2008**, *34* (1), 57–64.

(103) Vivas, N.; Vivas de Gaulejac, N.; Vitry, C.; Mouche, C.; Kahn, N.; Nonier-Bourden, M. F.; Absalon, C. Impact of Ethanol Content on the Scavenging Activities of Oak Wood C-Glycosidic Ellagitannins. Application to the Evaluation of the Nutritional Status of Spirits. *J. Inst. Brew.* **2013**, *119* (3), n/a-n/a.

(104) Nicolle, P.; Marcotte, C.; Angers, P.; Pedneault, K. Co-Fermentation of Red Grapes and White Pomace: A Natural and Economical Process to Modulate Hybrid Wine Composition. *Food Chem.* **2018**, *242*, 481–490.

(105) Dong, G.; Liu, H.; Yu, X.; Zhang, X.; Lu, H.; Zhou, T.; Cao, J. Antimicrobial and Anti-Biofilm Activity of Tannic Acid against Staphylococcus Aureus. *Nat. Prod. Res.* **2018**, *32* (18), 2225–2228.

(106) Vu, T. T.; Kim, H.; Tran, V. K.; Vu, H. D.; Hoang, T. X.; Han, J. W.; Choi, Y. H.; Jang, K. S.; Choi, G. J.; Kim, J.-C. Antibacterial Activity of Tannins Isolated from Sapium Baccatum Extract and Use for Control of Tomato Bacterial Wilt. *PLoS One* **2017**, *12* (7), e0181499.

(107) Xiao, X.; He, L.; Chen, Y.; Wu, L.; Wang, L.; Liu, Z. Anti-Inflammatory and Antioxidative Effects of Camellia Oleifera Abel Components. *Future Med. Chem.* **2017**, *9* (17), 2069–2079.

(108) Fujiki, H.; Sueoka, E.; Rawangkan, A.; Suganuma, M. Human Cancer Stem Cells Are a Target for Cancer Prevention Using (−)-Epigallocatechin Gallate. *J. Cancer Res. Clin. Oncol.* **2017**, *143* (12), 2401–2412.

(109) Sabino, A. P. L.; Eustáquio, L. M. S.; Miranda, A. C. F.; Biojone, C.; Mariosa, T. N.; Gouvêa, C. M. C. P. Stryphnodendron Adstringens ("Barbatimão") Leaf Fraction: Chemical Characterization, Antioxidant Activity, and Cytotoxicity Towards Human Breast Cancer Cell Lines. *Appl. Biochem. Biotechnol.* **2018**, *184* (4), 1375–1389.

(110) Miyamoto, K.; Grigsby, W.; Tohmura, S.-I. Using Renewables in Panelboard Resins to Influence Volatile Organic Compound Emissions from Panels. *J. Wood Chem. Technol.* **2019**, *39* (3), 166–177.

(111) Merle, J.; Birot, M.; Deleuze, H.; Mitterer, C.; Carré, H.; Bouhtoury, F. C.-E. New Biobased Foams from Wood Byproducts. *Mater. Des.* **2016**, *91*, 186–192.

(112) Zhu, J.; Njuguna, J.; Abhyankar, H.; Zhu, H.; Perreux, D.; Thiebaud, F.; Chapelle, D.; Pizzi, A.; Sauget, A.; de Larminat, A.; et al. Effect of Fibre Configurations on Mechanical Properties of Flax/tannin Composites. *Ind. Crops Prod.* **2013**, *50*, 68–76.

(113) Wise, L. E.; Maxine, M.; D'Addieco, A. A. Chlorite Holocellulose, Its Fractionation and Bearing on Summative Wood Analysis and on Studies on the Hemicelluloses. *Tech. Assoc. Pulp Pap. Ind.* **1946**, *29*, 210–218.

(114) Rowell, R. *The Chemistry of Solid Wood*; American Chemical Society, Ed.; 1984.

(115) Nabarlatz, D.; Ebringerová, A.; Montané, D. Autohydrolysis of Agricultural by-Products for the Production of Xylo-Oligosaccharides. *Carbohydr. Polym.* **2007**, *69* (1), 20–28.

(116) Sequeiros, A.; Gatto, D. A.; Labidi, J.; Serrano, L. Different Extraction Methods to Obtain Lignin from Almond Shell. *J. Biobased Mater. Bioenergy* **2014**, *8* (3), 370–376.

(117) González-Muñoz, M. J.; Alvarez, R.; Santos, V.; Parajó, J. C. Production of Hemicellulosic Sugars from Pinus Pinaster Wood by Sequential Steps of Aqueous Extraction and Acid Hydrolysis. *Wood Sci. Technol.* **2012**, *46* (1–3), 271–285.

(118) Vila, C.; Santos, V.; Saake, B.; Parajó, J. C. Manufacture, Characterization, and Properties of Poly-(Lactic Acid) and Its Blends with Esterified Pine Lignin. *BioResources* **2016**, *11* (2), 5322–5332.

(119) Fernández-Rodríguez, J.; Gordobil, O.; Robles, E.; González-Alriols, M.; Labidi, J. Lignin Valorization from Side-Streams Produced during Agricultural Waste Pulping and Total Chlorine Free Bleaching. *J. Clean. Prod.* **2017**, *142*, 2609–2617.

(120) Vishtal, A. G.; Kraslawski, A. Challenges in Industrial Applications of Technical Lignins. *BioResources* **2011**, *6* (3), 3547–3568.

(121) Sjöström, E. Wood-Based Chemicals and Pulping by-Products. In *Wood Chemistry*; Academic Press, 1993; pp 225–248.

(122) Sen, S.; Patil, S.; Argyropoulos, D. S. Thermal Properties of Lignin in Copolymers, Blends, and Composites: A Review. *Green Chem.* **2015**, *17* (11), 4862–4887.

(123) Fernández-Rodríguez, J.; Erdocia, X.; Hernández-Ramos, F.; Alriols, M. G.; Labidi, J. Lignin Separation and Fractionation by Ultrafiltration. In *Separation of Functional Molecules in Food by Membrane Technology*; Academic Press, 2019; pp 229–265.

(124) Gillet, S.; Aguedo, M.; Petitjean, L.; Morais, A. R. C.; da Costa Lopes, A. M.; Łukasik, R. M.; Anastas, P. T. Lignin Transformations for High Value Applications: Towards Targeted Modifications Using Green Chemistry. *Green Chem.* **2017**, *19* (18), 4200–4233.

(125) Galkin, M. V.; Samec, J. S. M. Lignin Valorization through Catalytic Lignocellulose Fractionation: A Fundamental Platform for the Future Biorefinery. *ChemSusChem* **2016**, *9* (13), 1544–1558.

(126) Glasser, W. G. Lignin-Based Polymers. *Encycl. Mater. Sci. Technol.* **2001**, 1–4.

(127) Aro, T.; Fatehi, P. Production and Application of Lignosulfonates and Sulfonated Lignin. *ChemSusChem* **2017**, *10* (9), 1861–1877.

(128) Houtman, C. Lessons Learned from 150 Years of Pulping Wood. In *Lignin valorization : emerging approaches*; Beckham, G. T., Ed.; Royal Society of Chemistry, 2018; pp 62–73.

(129) Fan, J.; Zhan, H. Optimization of Synthesis of Spherical Lignosulphonate Resin and Its Structure Characterization. *Chinese J. Chem. Eng.* **2008**, *16* (3), 407–410.

(130) Calvo-Flores, F. G.; Dobado, J. A.; García, J. I.; Martin-Martinez, F. J. *Lignin and Lignans as Renewable Raw Materials : Chemistry, Technology and Applications.*; Wiley, 2015.

(131) Elumalai, S.; Pan, X. J. Chemistry and Reactions of Forest Biomass in Biorefining. In *Sustainable Production of Fuels, Chemicals, and Fibers from Forest Biomass*; 2011; pp 109–144.

(132) Matsushita, Y. Conversion of Technical Lignins to Functional Materials with Retained Polymeric Properties. *J. Wood Sci.* **2015**, *61* (3), 230–250.

(133) Restolho, J. A.; Prates, A.; de Pinho, M. N.; Afonso, M. D. Sugars and Lignosulphonates Recovery from Eucalyptus Spent Sulphite Liquor by Membrane Processes. *Biomass and Bioenergy* **2009**, *33* (11), 1558–1566.

(134) Lora, J. Industrial Commercial Lignins: Sources, Properties and Applications. In *Monomers, Polymers and Composites from Renewable Resources*; Elsevier, 2008; pp 225–241.

(135) Chung, H.; Washburn, N. R. Chemistry of Lignin-Based Materials. *Green Mater.* **2013**, *1* (3), 137–160.

(136) Gierer, J. Chemical Aspects of Kraft Pulping. *Wood Sci. Technol.* **1980**, *14* (4), 241–266.

(137) Kim, T. H. Pretreatment of Lignocellulosic Biomass. In *Bioprocessing technologies in biorefinery for sustainable production of fuels, chemicals, and polymers*; Yang, S.-T., El Enshasy, H., Thongchul, N., Eds.; Wiley, 2013; pp 91–110.

(138) Agbor, V. B.; Cicek, N.; Sparling, R.; Berlin, A.; Levin, D. B. Biomass Pretreatment: Fundamentals toward Application. *Biotechnol. Adv.* **2011**, *29* (6), 675–685.

(139) Kim, J. S.; Lee, Y. Y.; Kim, T. H. A Review on Alkaline Pretreatment Technology for Bioconversion of Lignocellulosic Biomass. *Bioresour. Technol.* **2016**, *199*, 42–48.

(140) Behera, S.; Arora, R.; Nandhagopal, N.; Kumar, S. Importance of Chemical Pretreatment for Bioconversion of Lignocellulosic Biomass. *Renew. Sustain. Energy Rev.* **2014**, *36*, 91–106.

(141) Moulthrop, J. S.; Swatloski, R. P.; Moyna, G.; Rogers, R. D. High-Resolution 13C NMR Studies of Cellulose and Cellulose Oligomers in Ionic Liquid Solutions. *Chem. Commun.* **2005**, No. 12, 1557.

(142) Prado, R.; Erdocia, X.; Labidi, J. Lignin Extraction and Purification with Ionic Liquids. *J. Chem. Technol. Biotechnol.* **2013**, *88* (7), 1248–1257.

(143) Kumar, A. K.; Sharma, S. Recent Updates on Different Methods of Pretreatment of Lignocellulosic Feedstocks: A Review. *Bioresour. Bioprocess.* **2017**, *4* (1), 7.

(144) Wild, P. J. de; Huijgen, W. J. J.; Linden, R.; Uil, H. den; Snelders, J.; Benjelloun-Mlayah, B. Organosolv Fractionation of Lignocellulosic Biomass for an Integrated Biorefinery. *NPT Procestechnol.* **2015**, *1*, 10–11.

(145) Sannigrahi, P.; Ragauskas, A. J. Fundamentals of Biomass Pretreatment by Fractionation. In *Aqueous Pretreatment of Plant Biomass for Biological and Chemical Conversion to Fuels and Chemicals*; John Wiley & Sons, Ltd: Chichester, UK, 2013; pp 201–222.

(146) McDonough, T. The Chemistry of Organosolv Delignification. *TAPPI J.* **1993**, *76* (8), 186–193.

(147) Chaturvedi, V.; Verma, P. An Overview of Key Pretreatment Processes Employed for Bioconversion of Lignocellulosic Biomass into Biofuels and Value Added Products. *3 Biotech* **2013**, *3* (5), 415–431.

(148) Lora, J. H.; Glasser, W. G. Recent Industrial Applications of Lignin: A Sustainable Alternative to Nonrenewable Materials. *J. Polym. Environ.* **2002**, *10* (1/2), 39–48.

(149) Pandey, M. P.; Kim, C. S. Lignin Depolymerization and Conversion: A Review of Thermochemical Methods. *Chem. Eng. Technol.* **2011**, *34* (1), 29–41.

(150) Huijgen, W. J. J.; Telysheva, G.; Arshanitsa, A.; Gosselink, R. J. A.; de Wild, P. J. Characteristics of Wheat Straw Lignins from Ethanol-Based Organosolv Treatment. *Ind. Crops Prod.* **2014**, *59*, 85–95.

(151) You, T.-T.; Zhang, L.-M.; Zhou, S.-K.; Xu, F. Structural Elucidation of Lignin–carbohydrate Complex (LCC) Preparations and Lignin from Arundo Donax Linn. *Ind. Crops Prod.* **2015**, *71*, 65–74.

(152) Gordobil, O.; Egüés, I.; Llano-Ponte, R.; Labidi, J. Physicochemical Properties of PLA Lignin Blends. *Polym. Degrad. Stab.* **2014**, *108*, 330–338.

(153) Goldmann, W. M.; Ahola, J.; Mankinen, O.; Kantola, A. M.; Komulainen, S.; Telkki, V.-V.; Tanskanen, J. Determination of Phenolic Hydroxyl Groups in Technical Lignins by Ionization Difference Ultraviolet Spectrophotometry (Δε-IDUS Method). *Period. Polytech. Chem. Eng.* **2016**, *61* (2), 93–101.

(154) Erdocia, X.; Prado, R.; Corcuera, M. Ã.; Labidi, J. Influence of Reaction Conditions on Lignin Hydrothermal Treatment. *Front. Energy Res.* **2014**, *2*, 13.

(155) dos Santos, P. S. B.; de Cademartori, P. H. G.; Prado, R.; Gatto, D. A.; Labidi, J. Composition and Structure of Organosolv Lignins from Four Eucalypt Species. *Wood Sci. Technol.* **2014**, *48* (4), 873–885.

(156) Chen, L.; Wang, X.; Yang, H.; Lu, Q.; Li, D.; Yang, Q.; Chen, H. Study on Pyrolysis Behaviors of Non-Woody Lignins with TG-FTIR and Py-GC/MS. *J. Anal. Appl. Pyrolysis* **2015**, *113*, 499–507.

(157) Asmadi, M.; Kawamoto, H.; Saka, S. Thermal Reactions of Guaiacol and Syringol as Lignin Model Aromatic Nuclei. *J. Anal. Appl. Pyrolysis* **2011**, *92* (1), 88–98.

(158) Constant, S.; Wienk, H. L. J.; Frissen, A. E.; Peinder, P. de; Boelens, R.; van Es, D. S.; Grisel, R. J. H.; Weckhuysen, B. M.; Huijgen, W. J. J.; Gosselink, R. J. A.; et al. New Insights into the Structure and Composition of Technical Lignins: A Comparative Characterisation Study. *Green Chem.* **2016**, *18* (9), 2651–2665.

(159) Lourenço, A.; Gominho, J.; Marques, A. V.; Pereira, H. Reactivity of Syringyl and Guaiacyl Lignin Units and Delignification Kinetics in the Kraft Pulping of Eucalyptus Globulus Wood Using Py-GC–MS/FID. *Bioresour. Technol.* **2012**, *123*, 296–302.

(160) Chiang, V. L. Understanding Gene Function and Control in Lignin Formation in Wood. *Agric. Biotechnol.* **2005**, *17*, 139–144.

(161) Sun, Q.; Khunsupat, R.; Akato, K.; Tao, J.; Labbé, N.; Gallego, N. C.; Bozell, J. J.; Rials, T. G.; Tuskan, G. A.; Tschaplinski, T. J.; et al. A Study of Poplar Organosolv Lignin after Melt Rheology Treatment as Carbon Fiber Precursors. *Green Chem.* **2016**, *18* (18), 5015–5024.

(162) Schorr, D.; Diouf, P. N.; Stevanovic, T. Evaluation of Industrial Lignins for Biocomposites Production. *Ind. Crops Prod.* **2014**, *52*, 65–73.

(163) Brebu, M.; Vasile, C. Thermal Degradation of Lignin—a Review. *Cellul. Chem. Technol.* **2010**, *44* (9), 353.

(164) Gordobil, O.; Moriana, R.; Zhang, L.; Labidi, J.; Sevastyanova, O. Assesment of Technical Lignins for Uses in Biofuels and Biomaterials: Structure-Related Properties, Proximate Analysis and Chemical Modification. *Ind. Crops Prod.* **2016**, *83*, 155–165.

(165) Bertini, F.; Canetti, M.; Cacciamani, A.; Elegir, G.; Orlandi, M.; Zoia, L. Effect of Ligno-Derivatives on Thermal Properties and Degradation Behavior of poly(3-Hydroxybutyrate)-Based Biocomposites. *Polym. Degrad. Stab.* **2012**, *97* (10), 1979–1987.

(166) Laurichesse, S.; Avérous, L. Chemical Modification of Lignins: Towards Biobased Polymers. *Prog. Polym. Sci.* **2014**, *39* (7), 1266–1290.

(167) Domínguez-Robles, J.; Tamminen, T.; Liitiä, T.; Peresin, M. S.; Rodríguez, A.; Jääskeläinen, A.-S. Aqueous Acetone Fractionation of Kraft, Organosolv and Soda Lignins. *Int. J. Biol. Macromol.* **2018**, *106*, 979–987.

(168) Lê, H. Q.; Zaitseva, A.; Pokki, J.-P.; Ståhl, M.; Alopaeus, V.; Sixta, H. Solubility of Organosolv Lignin in γ-Valerolactone/Water Binary Mixtures. *ChemSusChem* **2016**, *9* (20), 2939–2947.

(169) Wagner, A.; Tobimatsu, Y.; Phillips, L.; Flint, H.; Geddes, B.; Lu, F.; Ralph, J. Syringyl Lignin Production in Conifers: Proof of Concept in a Pine Tracheary Element System. *Proc. Natl. Acad. Sci. U. S. A.* **2015**, *112* (19), 6218–6223.

(170) Costes, L.; Laoutid, F.; Aguedo, M.; Richel, A.; Brohez, S.; Delvosalle, C.; Dubois, P. Phosphorus and Nitrogen Derivatization as Efficient Route for Improvement of Lignin Flame Retardant Action in PLA. *Eur. Polym. J.* **2016**, *84*, 652–667.

(171) Oliveira, L.; Evtuguin, D.; Cordeiro, N.; Silvestre, A. J. D. Structural Characterization of Stalk Lignin from Banana Plant. *Ind. Crops Prod.* **2009**, *29* (1), 86–95.

(172) Hu, J.; Xiao, R.; Shen, D.; Zhang, H. Structural Analysis of Lignin Residue from Black Liquor and Its Thermal Performance in Thermogravimetric-Fourier Transform Infrared Spectroscopy. *Bioresour. Technol.* **2013**, *128*, 633–639.

(173) An, L.; Wang, G.; Jia, H.; Liu, C.; Sui, W.; Si, C. Fractionation of Enzymatic Hydrolysis Lignin by Sequential Extraction for Enhancing Antioxidant Performance. *Int. J. Biol. Macromol.* **2017**, *99*, 674–681.

(174) Chirila, O.; Totolin, M.; Cazacu, G.; Dobromir, M.; Vasile, C. Lignin Modification with Carboxylic Acids and Butyrolactone under Cold Plasma Conditions. *Ind. Eng. Chem. Res.* **2013**, *52* (37), 13264–13271.

(175) Hashim, S. N. A. S.; Zakaria, S.; Chia, C. H.; Jaafar, S. N. S. Enhanced Thermal Stability of Esterified Lignin in Different Solvent Mediums. *Polym. from Renew. Resour.* **2018**, *9* (1), 39–49.

(176) Gordobil, O.; Delucis, R.; Egüés, I.; Labidi, J. Kraft Lignin as Filler in PLA to Improve Ductility and Thermal Properties. *Ind. Crops Prod.* **2015**, *72*, 46–53.

(177) Jiang, J.; Li, J.; Gao, Q. Effect of Flame Retardant Treatment on Dimensional Stability and Thermal Degradation of Wood. *Constr. Build. Mater.* **2015**, *75*, 74–81.

(178) Poletto, M. Assessment of the Thermal Behavior of Lignins from Softwood and Hardwood Species. *Maderas. Cienc. y Tecnol.* **2017**, *19* (1), 63–74.

(179) Zhao, J.; Xiuwen, W.; Hu, J.; Liu, Q.; Shen, D.; Xiao, R. Thermal Degradation of Softwood Lignin and Hardwood Lignin by TG-FTIR and Py-GC/MS. *Polym. Degrad. Stab.* **2014**, *108*, 133–138.

(180) Hagerman, A. E. Extraction of Tannin from Fresh and Preserved Leaves. *J. Chem. Ecol.* **1988**, *14* (2), 453–461.

(181) Bacelo, H. A. M.; Santos, S. C. R.; Botelho, C. M. S. Tannin-Based Biosorbents for Environmental Applications – A Review. *Chem. Eng. J.* **2016**, *303*, 575–587.

(182) Mailoa, M. N.; Mahendradatta, M.; Laga, A.; Djide, N. Tannin Extract of Guava Leaves (Psidium Guajava L) Variation with Concentration Organic Solvents. *Int. J. Sci. Technol. Res.* **2013**, *2* (9), 106–110.

(183) Jensen, W. B. The Origin of the Soxhlet Extractor. *J. Chem. Educ.* **2007**, *84* (12), 1913.

(184) Luque de Castro, M. D.; Priego-Capote, F. Soxhlet Extraction: Past and Present Panacea. *J. Chromatogr. A* **2010**, *1217* (16), 2383–2389.

(185) Markom, M.; Hasan, M.; Daud, W. R. W.; Singh, H.; Jahim, J. M. Extraction of Hydrolysable Tannins from Phyllanthus Niruri Linn.: Effects of Solvents and Extraction Methods. *Sep. Purif. Technol.* **2007**, *52* (3), 487–496.

(186) Widyawati, P. S.; Dwi, T.; Budianta, W.; Kusuma, F. A.; Wijaya, E. L. Difference of Solvent Polarity To Phytochemical Content and Antioxidant Activity of Pluchea Indicia Less Leaves Extracts. *Int. J. Pharmacogn. Phytochem. Res.* **2014**, *6* (4), 850–855.

(187) Chupin, L.; Motillon, C.; Charrier-El Bouhtoury, F.; Pizzi, A.; Charrier, B. Characterisation of Maritime Pine (Pinus Pinaster) Bark Tannins Extracted under Different Conditions by Spectroscopic Methods, FTIR and HPLC. *Ind. Crops Prod.* **2013**, *49*, 897–903.

(188) Lochab, B.; Shukla, S.; Varma, I. K. Naturally Occurring Phenolic Sources: Monomers and Polymers. *RSC Adv.* **2014**, *4* (42), 21712–21752.

(189) Ajila, C. M.; Brar, S. K.; Verma, M.; Tyagi, R. D.; Godbout, S.; Valéro, J. R. Extraction and Analysis of Polyphenols: Recent Trends. *Crit. Rev. Biotechnol.* **2011**, *31* (3), 227–249.

(190) Azmir, J.; Zaidul, I. S. M.; Rahman, M. M.; Sharif, K. M.; Mohamed, A.; Sahena, F.; Jahurul, M. H. A.; Ghafoor, K.; Norulaini, N. A. N.; Omar, A. K. M. Techniques for Extraction of Bioactive Compounds from Plant Materials: A Review. *J. Food Eng.* **2013**, *117* (4), 426–436.

(191) Talmaciu, A. I.; Ravber, M.; Volf, I.; Knez, Ž.; Popa, V. I. Isolation of Bioactive Compounds from Spruce Bark Waste Using Sub- and Supercritical Fluids. *J. Supercrit. Fluids* **2016**, *117*, 243–251.

(192) Liang, X.; Fan, Q. Application of Sub-Critical Water Extraction in Pharmaceutical Industry. *J. Mater. Sci. Chem. Eng.* **2013**, *1* (5), 1–6.

(193) Vergara-Salinas, J. R.; Bulnes, P.; Zúñiga, M. C.; Pérez-Jiménez, J.; Torres, J. L.; Mateos-Martín, M. L.; Agosin, E.; Pérez-Correa, J. R. Effect of Pressurized Hot Water Extraction on Antioxidants from Grape Pomace before and after Enological Fermentation. *J. Agric. Food Chem.* **2013**, *61* (28), 6929–6936.

(194) Sousa, A. D.; Maia, A. I. V.; Rodrigues, T. H. S.; Canuto, K. M.; Ribeiro, P. R. V.; de Cassia Alves Pereira, R.; Vieira, R. F.; de Brito, E. S. Ultrasound-Assisted and Pressurized Liquid Extraction of Phenolic Compounds from Phyllanthus Amarus and Its Composition Evaluation by UPLC-QTOF. *Ind. Crops Prod.* **2016**, *79*, 91–103.

(195) Routray, W.; Orsat, V. Microwave-Assisted Extraction of Flavonoids: A Review. *Food Bioprocess Technol.* **2012**, *5* (2), 409–424.

(196) Naima, R.; Oumam, M.; Hannache, H.; Sesbou, A.; Charrier, B.; Pizzi, A.; Charrier – El Bouhtoury, F. Comparison of the Impact of Different Extraction Methods on Polyphenols Yields and Tannins Extracted from Moroccan Acacia Mollissima Barks. *Ind. Crops Prod.* **2015**, *70*, 245–252.

(197) Chemat, F.; Zill-e-Huma; Khan, M. K. Applications of Ultrasound in Food Technology: Processing, Preservation and Extraction. *Ultrason. Sonochem.* **2011**, *18* (4), 813–835.

(198) Ali, A.; Lim, X. Y.; Chong, C. H.; Mah, S. H.; Chua, B. L. Optimization of Ultrasound-Assisted Extraction of Natural Antioxidants from Piper Betle Using Response Surface Methodology. *LWT* **2018**, *89*, 681–688.

(199) Reátegui, J. L. P.; Machado, A. P. da F.; Barbero, G. F.; Rezende, C. A.; Martínez, J. Extraction of Antioxidant Compounds from Blackberry (Rubus Sp.) Bagasse Using Supercritical CO2 Assisted by Ultrasound. *J. Supercrit. Fluids* **2014**, *94*, 223–233.

(200) Deng, Y.; Zhao, Y.; Padilla-Zakour, O.; Yang, G. Polyphenols, Antioxidant and Antimicrobial Activities of Leaf and Bark Extracts of Solidago Canadensis L. *Ind. Crops Prod.* **2015**, *74*, 803–809.

(201) Belwal, T.; Giri, L.; Bhatt, I. D.; Rawal, R. S.; Pande, V. An Improved Method for Extraction of Nutraceutically Important Polyphenolics from Berberis Jaeschkeana C.K. Schneid. Fruits. *Food Chem.* **2017**, *230*, 657–666.

(202) Bouaoudia-Madi, N.; Boulekbache-Makhlouf, L.; Kadri, N.; Dahmoune, F.; Remini, H.; Dairi, S.; Oukhmanou-Bensidhoum, S.; Madani, K. Phytochemical Analysis of Myrtus Communis Plant: Conventional versus Microwave Assisted-Extraction Procedures. *J. Complement. Integr. Med.* **2017**, *14* (4).

(203) Kemppainen, K.; Siika-aho, M.; Pattathil, S.; Giovando, S.; Kruus, K. Spruce Bark as an Industrial Source of Condensed Tannins and Non-Cellulosic Sugars. *Ind. Crops Prod.* **2014**, *52*, 158–168.

(204) Aspé, E.; Fernández, K. The Effect of Different Extraction Techniques on Extraction Yield, Total Phenolic, and Anti-Radical Capacity of Extracts from Pinus Radiata Bark. *Ind. Crops Prod.* **2011**, *34* (1), 838–844.

(205) Vieira, M. C.; Lelis, R. C. C.; Couto Da Silva, B.; De, G.; Oliveira, L.; De Pesquisa, A. Tannin Extraction from the Bark of Pinus Oocarpa Var. Oocarpa with Sodium Carbonate and Sodium Bisulfite. *Floresta e Ambient.* **2011**, *18* (181), 1–81.

(206) Çam, M.; Hışıl, Y. Pressurised Water Extraction of Polyphenols from Pomegranate Peels. *Food Chem.* **2010**, *123* (3), 878–885.

(207) Bianchi, S.; Kroslakova, I.; Janzon, R.; Mayer, I.; Saake, B.; Pichelin, F. Characterization of Condensed Tannins and Carbohydrates in Hot Water Bark Extracts of European Softwood Species. *Phytochemistry* **2015**, *120*, 53–61.

(208) Erşan, S.; Güçlü Üstündağ, Ö.; Carle, R.; Schweiggert, R. M. Subcritical Water Extraction of Phenolic and Antioxidant Constituents from Pistachio (Pistacia Vera L.) Hulls. *Food Chem.* **2018**, *253*, 46–54.

(209) Antwi-Boasiako, C.; Animapauh, S. O. Tannin Extraction from the Barks of Three Tropical Hardwoods for the Production of Adhesives. *J. Appl. Sci. Res.* **2012**, *8* (6), 2959–2965.

(210) Aires, A.; Carvalho, R.; Saavedra, M. J. Valorization of Solid Wastes from Chestnut Industry Processing: Extraction and Optimization of Polyphenols, Tannins and Ellagitannins and Its Potential for Adhesives, Cosmetic and Pharmaceutical Industry. *Waste Manag.* **2016**, *48*, 457–464.

(211) Arbenz, A.; Avérous, L. Tannins: A Resource to Elaborate Aromatic and Biobased Polymers. In *Biodegradable and Biobased Polymers for Environmental and Biomedical Applications*; John Wiley & Sons, Inc.: Hoboken, NJ, USA, 2016; pp 97–148.

(212) Szczurek, A.; Fierro, V.; Pizzi, A.; Stauber, M.; Celzard, A. A New Method for Preparing Tannin-Based Foams. *Ind. Crops Prod.* **2014**, *54*, 40–53.

(213) Gujrathi, A. M.; Babu, B. V. Environment Friendly Products from Black Wattle. *Energy Educ. Sci. Technol.* **2007**, *19* (1), 37–44.

(214) Pizzi, A. Tannin Autocondensation and Polycondensation for Zero Emission Tannin Wood Adhesives. In *Plant Polyphenols 2*; Springer US: Boston, MA, 1999; pp 805–821.

(215) Xiong, J.; Grace, M. H.; Esposito, D.; Wang, F.; Lila, M. A. Phytochemical Characterization and Anti-Inflammatory Properties of Acacia Mearnsii Leaves. *Nat. Prod. Commun.* **2016**, *11* (5), 1934578X1601100.

(216) Pansera, M. R.; Iob, G. A.; Atti-Santos, A. C.; Rossato, M.; Atti-Serafini, L.; Cassel, E. Extraction of Tannin by Acacia Mearnsii with Supercritical Fluids. *Brazilian Arch. Biol. Technol.* **2004**, *47* (6), 995–998.

(217) Olajuyigbe, O. O.; Afolayan, A. J. Phytochemical Assessment and Antioxidant Activities of Alcoholic and Aqueous Extracts of Acacia Mearnsii De Wild. *Int. J. Pharmacol.* **2011**, *7* (8), 856–861.

(218) Mahdi, H.; Palmina, K.; Glavtch, I. CHARACTERIZATION OF ACACIA NILOTICA AS AN INDIGENOUS TANNING MATERIAL OF SUDAN. *Journal of Tropical Forest Science*. Forest Research Institute Malaysia 2006, pp 181–187.

(219) Medeiros, J. X.; Calegari, L.; Silva, G. H.; Tanajura, J. A.; Braz, R. L. Bark and Fruit Extracts Anadenanthera Colubrina (Vell.), Mimosa Tenuiflora (Willd.) and Acacia Mearnsii (Wild.) Species. *J. Exp. Agric. Int.* **2019**, *30* (1), 1–7.

(220) Rosales, M.; Galindo, A.; González, R. F. Taninos Condensados En La Corteza de Pinus Chihuahuana Y Pinus Durangensis. Información Tecnológica. *Inf. Tecnológica* **2002**, *13* (1), 39–42.

(221) Frazier, R. A.; Deaville, E. R.; Green, R. J.; Stringano, E.; Willoughby, I.; Plant, J.; Mueller-Harvey, I. Interactions of Tea Tannins and Condensed Tannins with Proteins. *J. Pharm. Biomed. Anal.* **2010**, *51* (2), 490–495.

(222) Pasch, H.; Pizzi, A.; Rode, K. MALDI–TOF Mass Spectrometry of Polyflavonoid Tannins. *Polymer (Guildf).* **2001**, *42* (18), 7531–7539.

(223) Chen, X.; Xiong, J.; Huang, S.; Li, X.; Zhang, Y.; Zhang, L.; Wang, F. Analytical Profiling of Proanthocyanidins from Acacia Mearnsii Bark and In Vitro Assessment of Antioxidant and Antidiabetic Potential. *Molecules* **2018**, *23* (11), 2891.

(224) Venter, P. B.; Senekal, N. D.; Kemp, G.; Amra-Jordaan, M.; Khan, P.; Bonnet, S. L.; van der Westhuizen, J. H. Analysis of Commercial Proanthocyanidins. Part 3: The Chemical Composition of Wattle (Acacia Mearnsii) Bark Extract. *Phytochemistry* **2012**, *83*, 153–167.

(225) Belgacem, M. N.; Gandini, A. The State of the Art. In *Monomers, Polymers and Composites from Renewable Resources*; Belgacem, M. N., Gandini, A., Eds.; Elsevier, 2008; pp 1–17.

(226) Missio, A. L.; Tischer, B.; dos Santos, P. S. B.; Codevilla, C.; de Menezes, C. R.; Barin, J. S.; Haselein, C. R.; Labidi, J.; Gatto, D. A.; Petutschnigg, A.; et al. Analytical Characterization of Purified Mimosa (Acacia Mearnsii) Industrial Tannin Extract: Single and Sequential Fractionation. *Sep. Purif. Technol.* **2017**, *186*, 218–225.

(227) Frollini, E.; Silva, C. G.; Ramires, E. C. Phenolic Resins as a Matrix Material in Advanced Fiber-Reinforced Polymer (FRP) Composites. In *Advanced Fibre-Reinforced Polymer (FRP) Composites for Structural Applications*; Woodhead Publishing, 2013; pp 7–43.

(228) dos Santos Grasel, F.; Ferrão, M. F.; Wolf, C. R.; Ligabue, R. A. Characterization of Natural Tanning Extracts by FTIR and Multivariate Analysis. In *XXXIII IULTCS Congress*; Hamburg, 2015; pp 67–77.

(229) Lisperguer, J.; Saravia, Y.; Vergara, E. Structure and Thermal Behavior of Tannins from Acacia Dealbata Bark and Their Reactivity toward Formaldehyde. *J. Chil. Chem. Soc.* **2016**, *61* (4), 3188–3190.

(230) Thébault, M.; Pizzi, A.; Santiago-Medina, F. J.; Al-Marzouki, F. M.; Abdalla, S. Isocyanate-Free Polyurethanes by Coreaction of Condensed Tannins with Aminated Tannins. *J. Renew. Mater.* **2017**, *5* (1), 21–29.

(231) Pantoja-Castro, M. A.; González-Rodríguez, H. Revista Latinoamericana de Química. *Rev. Latinoam. química* **2011**, *39* (3), 107–112.

(232) Jiang, X.; Liu, J.; Du, X.; Hu, Z.; Chang, H.; Jameel, H. Phenolation to Improve Lignin Reactivity toward Thermosets Application. *ACS Sustain. Chem. Eng.* **2018**, *6* (4), 5504–5512.

(233) Fernández-Rodríguez, J.; Erdocia, X.; de Hoyos, P. L.; Sequeiros, A.; Labidi, J. Catalytic Cascade Transformations of Biomass into Polyols. In *Production of Biofuels and Chemicals with Bifunctional Catalysts*; Springer, Singapore, 2017; pp 187–219.

(234) Sawamura, K.; Tobimatsu, Y.; Kamitakahara, H.; Takano, T. Lignin Functionalization through Chemical Demethylation: Preparation and Tannin-Like Properties of Demethylated Guaiacyl-Type Synthetic Lignins. *ACS Sustain. Chem. Eng.* **2017**, *5* (6), 5424–5431.

(235) Wang, G.; Chen, H. Carbohydrate Elimination of Alkaline-Extracted Lignin Liquor by Steam Explosion and Its Methylolation for Substitution of Phenolic Adhesive. *Ind. Crops Prod.* **2014**, *53*, 93–101.

(236) Pan, H.; Sun, G.; Zhao, T. Synthesis and Characterization of Aminated Lignin. *Int. J. Biol. Macromol.* **2013**, *59*, 221–226.

(237) Du, X.; Li, J.; Lindström, M. E. Modification of Industrial Softwood Kraft Lignin Using Mannich Reaction with and without Phenolation Pretreatment. *Ind. Crops Prod.* **2014**, *52*, 729–735.

(238) Mu, Y.; Wang, C.; Zhao, L.; Chu, F. Study on Composite Adhesive of Hydroxymethylated Lignosulfonate/phenol-Formaldehyde Resin with Low Free Formaldehyde. *Chem. Ind. For. Prod.* **2009**, *29* (3), 38–42.

(239) Mankar, S.; Chaudhari, A.; of, I. S.-I. J.; 2012, undefined. Lignin in Phenol-Formaldehyde Adhesives. *Int. J. Knowl. Eng.* **2012**, *3* (1), 116–118.

(240) Ramires, E. C.; Megiatto, J. D.; Gardrat, C.; Castellan, A.; Frollini, E. Biobased Composites from Glyoxal–phenolic Resins and Sisal Fibers. *Bioresour. Technol.* **2010**, *101* (6), 1998–2006.

(241) Lan-Ping, F.; Gambier, F.; Pizzi, A.; Zhou-Ding, G.; Brosse, N. Wood Adhesives from Agricultural by-Products: Lignins and Tannins for the Elaboration of Particleboards. *Cellul. Chem Techn.* **2012**, *46* (7–8), 457–462.

(242) Younesi-Kordkheili, H.; Kazemi-Najafi, S.; Eshkiki, R. B.; Pizzi, A. Improving Urea Formaldehyde Resin Properties by Glyoxalated Soda Bagasse Lignin. *Eur. J. Wood Wood Prod.* **2015**, *73* (1), 77–85.

(243) Koumba-Yoya, G.; Stevanovic, T. Study of Organosolv Lignins as Adhesives in Wood Panel Production. *Polymers (Basel).* **2017**, *9* (12), 46.

(244) Guigo, N.; Vincent, L.; Mija, A.; Naegele, H.; Sbirrazzuoli, N. Innovative Green Nanocomposites Based on Silicate Clays/lignin/natural Fibres. *Compos. Sci. Technol.* **2009**, *69* (11–12), 1979–1984.

(245) Alemán, J. V.; Chadwick, A. V.; He, J.; Hess, M.; Horie, K.; Jones, R. G.; Kratochvíl, P.; Meisel, I.; Mita, I.; Moad, G.; et al. Definitions of Terms Relating to the Structure and Processing of Sols, Gels, Networks, and Inorganic-Organic Hybrid Materials (IUPAC Recommendations 2007). *Pure Appl. Chem.* **2007**, *79* (10), 1801–1829.

(246) Saad, H.; de Hoyos-Martinez, P. L.; Ezzeddine, S.; Charrier-El Bouhtoury, F. Advances in Bio-Nanohybrid Materials. In *Green and Sustainable Advanced Materials, Volume 1*; Shakel Ahmed and Chaudhery Mustansar Hussain, Ed.; Scrivener Publishing LLC, 2018; pp 289–332.

(247) Sevastyanova, O.; Qin, W.; Kadla, J. F. Effect of Nanofillers as Reinforcement Agents for Lignin Composite Fibers. *J. Appl. Polym. Sci.* **2010**, *117* (5), 2877–2881.

(248) Leszczyńska, A.; Njuguna, J.; Pielichowski, K.; Banerjee, J. R. Polymer/montmorillonite Nanocomposites with Improved Thermal Properties: Part I. Factors Influencing Thermal Stability and Mechanisms of Thermal Stability Improvement. *Thermochim. Acta* **2007**, *453* (2), 75–96.

(249) López, M.; Blanco, M.; Ramos, J. A.; Vazquez, A.; Gabilondo, N.; del Val, J. J.; Echeverría, J. M.; Mondragon, I. Synthesis and Characterization of Resol-Layered Silicate Nanocomposites. *J. Appl. Polym. Sci.* **2007**, *106* (4), 2800–2807.

(250) Nazir, M. S.; Mohamad Kassim, M. H.; Mohapatra, L.; Gilani, M. A.; Raza, M. R.; Majeed, K. Characteristic Properties of Nanoclays and Characterization of Nanoparticulates and Nanocomposites. In *Nanoclay Reinforced Polymer Composites*; Springer, Singapore, 2016; pp 35–55.

(251) El-Sheikhy, R.; Al-Shamrani, M. On the Processing and Properties of Clay/Polymer Nanocomposites CPNC. *Lat. Am. J. Solids Struct.* **2015**, *12* (2), 385–419.

(252) Bitinis, N.; Hernandez, M.; Verdejo, R.; Kenny, J. M.; Lopez-Manchado, M. A. Recent Advances in Clay/Polymer Nanocomposites. *Adv. Mater.* **2011**, *23* (44), 5229–5236.

(253) Roy, S.; Lee, B. J.; Kakish, Z. M.; Jana, S. C. Exploiting POSS–Sorbitol Interactions: Issues of Reinforcement of Isotactic Polypropylene Spun Fibers. *Macromolecules* **2012**, *45* (5), 2420–2433.

(254) Zhang, W.; Camino, G.; Yang, R. Polymer/polyhedral Oligomeric Silsesquioxane (POSS) Nanocomposites: An Overview of Fire Retardance. *Prog. Polym. Sci.* **2017**, *67*, 77–125.

(255) Ayandele, E.; Sarkar, B.; Alexandridis, P. Polyhedral Oligomeric Silsesquioxane (POSS)-Containing Polymer Nanocomposites. *Nanomater. (Basel, Switzerland)* **2012**, *2* (4), 445–475.

(256) Kuo, S.-W.; Chang, F.-C. POSS Related Polymer Nanocomposites. *Prog. Polym. Sci.* **2011**, *36* (12), 1649–1696.

(257) Mansouri, N.-E. El; Yuan, Q.; Huang, F. Study of Chemical Modification of Alkaline Lignin by the Glyoxalation Reaction. *BioResources* **2011**, *6* (4), 4523–4536.

(258) Malutan, T.; Nicu, R.; Popa, V. I. Contribution to the Study of Hydroxymethylation Reaction of Alkali Lignin. *BioResources* **2007**, *3* (1), 13–20.

(259) Younesi-Kordkheili, H.; Pizzi, A. A Comparison between Lignin Modified by Ionic Liquids and Glyoxalated Lignin as Modifiers of Urea-Formaldehyde Resin. *J. Adhes.* **2017**, *93* (14), 1120–1130.

(260) Hazwan Hussin, M.; Aziz, A. A.; Iqbal, A.; Ibrahim, M. N. M.; Latif, N. H. A. Development and Characterization Novel Bio-Adhesive for Wood Using Kenaf Core (Hibiscus Cannabinus) Lignin and Glyoxal. *Int. J. Biol. Macromol.* **2019**, *122*, 713–722.

(261) Telysheva, G.; Dizhbite, T.; Evtuguin, D.; Mironova-Ulmane, N.; Lebedeva, G.; Andersone, A.; Bikovens, O.; Chirkova, J.; Belkova, L. Design of Siliceous Lignins – Novel Organic/inorganic Hybrid Sorbent Materials. *Scr. Mater.* **2009**, *60* (8), 687–690.

(262) Holtzer, M.; Bobrowski, A.; Metalurgija, B. G.-; 2011, undefined. Montmorillonite: A Comparison of Methods for Its Determination in Foundry Bentonites. *Metalurgija* **2011**, *50* (2), 119–122.

(263) Klapiszewski, L.; Szalaty, T. J.; Zdarta, J.; Jesionowski, T. Activated Lignin and Aminosilane-Grafted Silica as Precursors in Hybrid Material Production. *Physicochem. Probl. Miner. Process.* **2016**, *52*.

(264) Yu, B.; Tao, Y.; Liu, L.; Shi, Y.; Yang, H.; Jie, G.; Lo, S.; Tai, Q.; Song, L.; Hu, Y. Thermal and Flame Retardant Properties of Transparent UV-Curing Epoxy Acrylate Coatings with POSS-Based Phosphonate Acrylate. *RSC Adv.* **2015**, *5* (92), 75254–75262.

(265) Jerman, I.; Koželj, M.; Orel, B. The Effect of Polyhedral Oligomeric Silsesquioxane Dispersant and Low Surface Energy Additives on Spectrally Selective Paint Coatings with Self-Cleaning Properties. *Sol. Energy Mater. Sol. Cells* **2010**, *94* (2), 232–245.

(266) Gao, X.; Liu, H.; Wei, H.; Zheng, J.; Huang, G. Effect of Incompletely Condensed Tri-Silanol-Phenyl-POSS on the Thermal Stability of Silicone Rubber. *Polym. Bull.* **2018**, 1–16.

(267) Zhang, W.; Ma, Y.; Wang, C.; Li, S.; Zhang, M.; Chu, F. Preparation and Properties of Lignin–phenol–formaldehyde Resins Based on Different Biorefinery Residues of Agricultural Biomass. *Ind. Crops Prod.* **2013**, *43*, 326–333.

(268) Krukowski, E. G.; Goodman, A.; Rother, G.; Ilton, E. S.; Guthrie, G.; Bodnar, R. J. FT-IR Study of CO2 Interaction with Na+ Exchanged Montmorillonite. *Appl. Clay Sci.* **2015**, *114*, 61–68.

(269) An, Y.; Zhang, X.; Wang, X.; Chen, Z.; Wu, X. Nano@lignocellulose Intercalated Montmorillonite as Adsorbent for Effective Mn(II) Removal from Aqueous Solution. *Sci. Reports* | **2018**, *8*, 10863.

(270) Navarrete, P.; Pizzi, A.; Pasch, A.; Delmotte, L. Study on Lignin–Glyoxal Reaction by MALDI-TOF and CP-MAS 13C-NMR. *J. Adhes. Sci. Technol.* **2012**, *26* (8–9), 1069–1082.

(271) Căpraru, A.-M.; Ungureanu, E.; Trincă, L. C.; Măluţan, T.; Popa, V. I. Chemical and Spectral Characteristics of Annual Plant Lignins Modified by Hydroxymethylation Reaction. *Cellul. Chem. Technol.* **2012**, *46* (9), 589–597.

(272) Hu, J.; Shen, D.; Xiao, R.; Wu, S.; Zhang, H. Free-Radical Analysis on Thermochemical Transformation of Lignin to Phenolic Compounds. *Energy & Fuels* **2013**, *27* (1), 285–293.

(273) Esposito Corcione, C.; Mensitieri, G.; Maffezzoli, A. Analysis of the Structure and Mass Transport Properties of Nanocomposite Polyurethane. *Polym. Eng. Sci.* **2009**, *49* (9), 1708–1718.

(274) Rahnama, M. R.; Barikani, M.; Barmar, M.; Honarkar, H. An Investigation into the Effects of Different Nanoclays on Polyurethane Nanocomposites Properties. *Polym. Plast. Technol. Eng.* **2014**, *53* (8), 801–810.

(275) Gournis, D.; Lappas, A.; Karakassides, M. A.; Többens, D.; Moukarika, A. A Neutron Diffraction Study of Alkali Cation Migration in Montmorillonites. *Phys. Chem. Miner.* **2008**, *35* (1), 49–58.

(276) Galimberti, M.; Martino, M.; Guenzi, M.; Leonardi, G.; Citterio, A. Thermal Stability of Ammonium Salts as Compatibilizers in Polymer/layered Silicate Nanocomposites. *e-Polymers* **2009**, *9* (1).

(277) Esposito Corcione, C.; Striani, R.; Montagna, F.; Cannoletta, D. Organically Modified Montmorillonite Polymer Nanocomposites for Stereolithography Building Process. *Polym. Adv. Technol.* **2015**, *26* (1), 92–98.

(278) Barry, A. J.; Daudt, W. H.; Domicone, J. J.; Gilkey, J. W. Crystalline Organosilsesquioxanes. *J. Am. Chem. Soc.* **1955**, *77* (16), 4248–4252.

(279) Fu, B. .; Hsiao, B. .; Pagola, S.; Stephens, P.; White, H.; Rafailovich, M.; Sokolov, J.; Mather, P. .; Jeon, H. .; Phillips, S.; et al. Structural Development during Deformation of Polyurethane Containing Polyhedral Oligomeric Silsesquioxanes (POSS) Molecules. *Polymer (Guildf).* **2001**, *42* (2), 599–611.

(280) Ang, A.; Ashaari, Z.; Bakar, E. S.; Ibrahim, N. A. Characterization and Optimization of the Glyoxalation of a Methanol-Fractionated Alkali Lignin Using Response Surface Methodology. *BioResources* **2015**, *10* (3), 4795–4810.

(281) Yang, H.; Xu, S.; Jiang, L.; Dan, Y. Thermal Decomposition Behavior of Poly (Vinyl Alcohol) with Different Hydroxyl Content. *J. Macromol. Sci. Part B* **2012**, *51* (3), 464–480.

(282) Hesse, W. Phenolic Resins. In *Ullmann's Encyclopedia of Industrial Chemistry*; 2005; pp 1–16.

(283) Pilato, L. Phenolic Resins: 100 Years and Still Going Strong. *React. Funct. Polym.* **2013**, *73* (2), 270–277.

(284) Asim, M.; Saba, N.; Jawaid, M.; Nasir, M.; Pervaiz, M.; Alothman, O. Y. A Review on Phenolic Resin and Its Composites. *Curr. Anal. Chem.* **2018**, *14* (3), 185–197.

(285) Pizzi, A. Phenolic Resin Adhesives. In *Handbook of Adhesive Technology, Third Edition*; Pizzi, A., Mittal, K. L., Eds.; CRC Press, 2017.

(286) Benk, A.; Talu, M.; Coban, A. Phenolic Resin Binder for the Production of Metallurgical Quality Briquettes from Coke Breeze: Part I. *Fuel Process. Technol.* **2008**, *89* (1), 28–37.

(287) Hatchard, T. D.; Bissonnette, P.; Obrovac, M. N. Phenolic Resin as an Inexpensive High Performance Binder for Li-Ion Battery Alloy Negative Electrodes. *J. Electrochem. Soc.* **2016**, *163* (9), A2035–A2039.

(288) Knop, A.; Pilato, L. A. Heat and Sound Insulation Materials. In *Phenolic Resins*; Springer Berlin Heidelberg: Berlin, Heidelberg, 1985; pp 213–229.

(289) Taverna, M. E.; Ollearo, R.; Morán, J.; Nicolau, V.; Estenoz, D.; Frontini, P. Bioresources. *BioResources* **2015**, *10* (4), 8325–8338.

(290) Kimura, H.; Ohtsuka, K.; Matsumoto, A. New Thermosetting Resin from Benzoxazine and Cyanate Ester Resin. *Adv. Polym. Technol.* **2013**, *32* (S1), E651–E659.

(291) Pizzi, A. Biosourced Thermosets for Lignocellulosic Composites. In *Thermoset Composites*; Khan, A., Bhawani, S. A., Asiri, A. M., Khan, I., Eds.; Materials Research Foundation, 2018; pp 81–111.

(292) Biron, M. Biobricks: The Breakthrough of Drop-In Solutions. In *Industrial Applications of Renewable Plastics*; William Andrew Publishing, 2017; pp 155–369.

(293) Li, X.; Pizzi, A.; Zhou, X.; Fierro, V.; Celzard, A. Formaldehyde-Free Prorobitenidin/Profi Setinidin Tannin/Furanic Foams Based on Alternative Aldehydes: Glyoxal and Glutaraldehyde. *J. Renew. Mater.* **2015**, *3* (2), 142–150.

(294) Lacoste, C.; Basso, M. C.; Pizzi, A.; Laborie, M.-P.; Garcia, D.; Celzard, A. Bioresourced Pine Tannin/furanic Foams with Glyoxal and Glutaraldehyde. *Ind. Crops Prod.* **2013**, *45*, 401–405.

(295) Solt, P.; Konnerth, J.; Gindl-Altmutter, W.; Kantner, W.; Moser, J.; Mitter, R.; van Herwijnen, H. W. G. Technological Performance of Formaldehyde-Free Adhesive Alternatives for Particleboard Industry. *Int. J. Adhes. Adhes.* **2019**, *94*, 99–131.

(296) Yang, C. Q.; Weishu Wei, W.; McIlwaine, D. B. Evaluating Glutaraldehyde as a Nonformaldehyde Durable Press Finishing Agent for Cotton Fabrics. *Text. Res. J.* **2000**, *70* (3), 230–236.

(297) Migneault, I.; Dartiguenave, C.; Bertrand, M. J.; Waldron, K. C. Glutaraldehyde: Behavior in Aqueous Solution, Reaction with Proteins, and Application to Enzyme Crosslinking. *Biotechniques* **2004**, *37* (5), 790–802.

(298) Pizzi, A. Natural Phenolic Adhesives I: Tannin. In *Handbook of Adhesive Technology, Revised and Expanded*; Pizzi, A., Mittal, K. L., Eds.; CRC Press, 2003; pp 567–581.

(299) Faris, A. H.; Rahim, A. A.; Ibrahim, M. N. M.; Alkurdi, A. M.; Shah, I. Combination of Lignin Polyol-Tannin Adhesives and Polyethylenimine for the Preparation of Green Water-Resistant Adhesives. *J. Appl. Polym. Sci.* **2016**, *133* (20), n/a-n/a.

(300) Wang, M.; Leitch, M.; (Charles) Xu, C. Synthesis of Phenol–formaldehyde Resol Resins Using Organosolv Pine Lignins. *Eur. Polym. J.* **2009**, *45* (12), 3380–3388.

(301) Çetin, N. S.; Özmen, N. Use of Organosolv Lignin in Phenol–formaldehyde Resins for Particleboard Production: I. Organosolv Lignin Modified Resins. *Int. J. Adhes. Adhes.* **2002**, *22* (6), 477–480.

(302) Rakotovelo, A.; Peruch, F.; Grelier, S. Lignine : Structure, Production et Valorisation Chimique. *Meteriaux bois Pap.* **2019**.

(303) Lei, H.; Pizzi, A.; Du, G. Environmentally Friendly Mixed Tannin/lignin Wood Resins. *J. Appl. Polym. Sci.* **2008**, *107* (1), 203–209.

(304) Mansouri, H. R.; Navarrete, P.; Pizzi, A.; Tapin-Lingua, S.; Benjelloun-Mlayah, B.; Pasch, H.; Rigolet, S. Synthetic-Resin-Free Wood Panel Adhesives from Mixed Low Molecular Mass Lignin and Tannin. *Eur. J. Wood Wood Prod.* **2011**, *69* (2), 221–229.

(305) Chupin, L.; Charrier, B.; Pizzi, A.; Perdomo, A.; Charrier-El Bouhtoury, F. Study of Thermal Durability Properties of Tannin–lignosulfonate Adhesives. *J. Therm. Anal. Calorim.* **2015**, *119* (3), 1577–1585.

(306) Brosse, N.; Pizzi, A. Tannins for Wood Adhesives, Foams and Composites. In *Bio-based wood adhesives : preparation, characterization, and testing*; He, Z., Ed.; CRC Press, 2017; pp 197–220.

(307) Tondi, G. Tannin-Based Copolymer Resins: Synthesis and Characterization by Solid State 13C NMR and FT-IR Spectroscopy. *Polymers (Basel).* **2017**, *9* (12), 223.

(308) Navarrete Fuentes, P. J. Adhesifs Naturels a Base de Tanins, Tanin/lignine et Tanin/gluten Pour La Fabrication de Panneaux de Bois, Université Henry Poincaré, 2011.

(309) Shahid, S. A.; Ali, M.; Zafar, Z. I. Characterization of Phenol-Formaldehyde Resins Modified with Crude Bio-Oil Prepared from Ziziphus Mauritiana Endocarps. *BioResources* **2014**, *9* (3), 5362–5384.

(310) Çetin, N. S.; Özmen, N. Studies on Lignin-Based Adhesives for Particleboard Panels. *Turkish J. Agric. Technol.* **2003**, *27*, 183–189.

(311) Younesi-Kordkheili, H. Ionic Liquid Modified Lignin-Phenol-Glyoxal Resin: A Green Alternative Resin for Production of Particleboards. *J. Adhes.* **2018**, 1–13.

(312) Lin, R.; Sun, J.; Yue, C.; Wang, X.; Tu, D.; Gao, Z. Study on Preparation and Properties of Phenol-Formaldehyde-Chinese Fir Liquefaction Copolymer Resin. *Maderas. Cienc. y Tecnol.* **2014**, *16* (2), 159–174.

(313) Chaouch, M.; Diouf, P. N.; Laghdir, A.; Yin, S. Bio-Oil from Whole-Tree Feedstock in Resol-Type Phenolic Resins. *J. Appl. Polym. Sci.* **2014**, *131* (6), n/a-n/a.

(314) Siddiqui, H.; Mahmood, N.; Yuan, Z.; Crapulli, F.; Dessbesell, L.; Rizkalla, A.; Ray, A.; Xu, C. (Charles). Sustainable Bio-Based Phenol-Formaldehyde Resoles Using Hydrolytically Depolymerized Kraft Lignin. *Molecules* **2017**, *22* (11), 1850.

(315) Ammar, M.; Khiari, R.; Belgacem, M. N.; Elaloui, E. *Mediterranean Journal of Chemistry.*; 2014; Vol. 2.

(316) Pizzi, A.; Meikleham, N.; Dombo, B.; Roll, W. Autocondensation-Based, Zero-Emission, Tannin Adhesives for Particleboard. *Holz als Roh- und Werkst.* **1995**, *53* (1), 201–204.

(317) Dunky, M. Adhesives in the Wood Industry. In *Handbook of Adhesive Technology*; Pizzi, A., Mittal, K. L., Eds.; CRC Press: Boca Raton, FL, USA, 2003; p 64.

(318) Moubarik, A.; Charrier, B.; Allal, A.; Charrier, F.; Pizzi, A. Development and Optimization of a New Formaldehyde-Free Cornstarch and Tannin Wood Adhesive. *Eur. J. Wood Wood Prod.* **2010**, *68* (2), 167–177.

(319) Solomon, D. H.; Hopwood, J. J. Reactivity of Functional Groups in Surface Coating Polymers. Part I. Hydroxyl Groups in Alkyd Resins. *J. Appl. Polym. Sci.* **1966**, *10* (7), 981–991.

(320) Marengo, E.; Bobba, M.; Robotti, E.; Lenti, M. Hydroxyl and Acid Number Prediction in Polyester Resins by near Infrared Spectroscopy and Artificial Neural Networks. *Anal. Chim. Acta* **2004**, *511* (2), 313–322.

(321) Sunitha, K.; Santhosh Kumar, K. S.; Mathew, D.; Reghunadhan Nair, C. P. Shape Memory Polymers (SMPs) Derived from Phenolic Cross-Linked Epoxy Resin via Click Chemistry. *Mater. Lett.* **2013**, *99*, 101–104.

(322) Uttaravalli, A. N.; Dinda, S. Hydroxyl-Functionalized Resin: Preparation, Characterization, Parameter Optimization and Property Prediction. *Pigment Resin Technol.* **2018**, *47* (3), 236–245.

(323) Corcione, C.; Frigione, M. Characterization of Nanocomposites by Thermal Analysis. *Materials (Basel).* **2012**, *5* (12), 2960–2980.

(324) Schulz, H. The Development of Wood Utilization in the 19th, 20th and 21st Centuries. *Eur. J. Wood Wood Prod.* **1993**, *51*, 75–82.

(325) Gustavsson, L.; Madlener, R.; Hoen, H.-F.; Jungmeier, G.; Karjalainen, T.; KlÖhn, S.; Mahapatra, K.; Pohjola, J.; Solberg, B.; Spelter, H. The Role of Wood Material for Greenhouse Gas Mitigation. *Mitig. Adapt. Strateg. Glob. Chang.* **2006**, *11* (5–6), 1097–1127.

(326) Woodard, A. C.; Milner, H. R. Sustainability of Timber and Wood in Construction. In *Sustainability of Construction Materials*; Woodhead Publishing, 2016; pp 129–157.

(327) Falk, R. H. Wood as a Sustainable Building Material. *For. Prod. J.* **2009**, *59* (9), 6–12.

(328) Cabeza, L. F.; Barreneche, C.; Miró, L.; Morera, J. M.; Bartolí, E.; Inés Fernández, A. Low Carbon and Low Embodied Energy Materials in Buildings: A Review. *Renew. Sustain. Energy Rev.* **2013**, *23*, 536–542.

(329) Buchanan, A. H.; Levine, S. B. Wood-Based Building Materials and Atmospheric Carbon Emissions. *Environ. Sci. Policy* **1999**, *2* (6), 427–437.

(330) de la Roche, I.; Dangerfield, J. A.; Karacabeyli, E. Wood Products And Sustainable Construction. *New Zel. Timber Des. J.* **2003**, *12* (1), 9–13.

(331) Kim, J. I.; Park, J. Y.; Kong, Y. T.; Lee, B. H.; Kim, H. J.; Roh, J. K. Performance of Flame-Retardant Polyurethane Coatings for Wood and Wood-Based Materials. *J. Korean Wood Sci. Technol.* **2002**, *30* (2), 172–179.

(332) Asif, M. Sustainability of Timber, Wood and Bamboo in Construction. *Sustain. Constr. Mater.* **2009**, 31–54.

(333) Saxena, N. K.; Gupta, D. R. Development and Evaluation of Fire Retardant Coatings. *Fire Technol.* **1990**, *26* (4), 329–341.

(334) Morgan, A. B.; Gilman, J. W. An Overview of Flame Retardancy of Polymeric Materials: Application, Technology, and Future Directions. *Fire Mater.* **2013**, *37* (4), 259–279.

(335) Horrocks, A. R.; Kandola, B. K.; Davies, P. J.; Zhang, S.; Padbury, S. A. Developments in Flame Retardant Textiles – a Review. *Polym. Degrad. Stab.* **2005**, *88* (1), 3–12.

(336) van Krevelen, D. W.; Nijenhuis, K. . Properties of Polymers : Their Correlation with Chemical Structure ; Their Numerical Estimation and Prediction from Additive Group Contributions; Elsevier: New York, 2009; pp 247–294.

(337) Shaw, S. Halogenated Flame Retardants: Do the Fire Safety Benefits Justify the Risks? *Rev. Environ. Health* **2010**, *25* (4), 261–306.

(338) Kartal, S. N.; Yoshimura, T.; Imamura, Y. Decay and Termite Resistance of Boron-Treated and Chemically Modified Wood by in Situ Co-Polymerization of Allyl Glycidyl Ether (AGE) with Methyl Methacrylate (MMA). *Int. Biodeterior. Biodegradation* **2004**, *53* (2), 111–117.

(339) Temiz, A.; Gezer, E. D.; Yildiz, U. C.; Yildiz, S. Combustion Properties of Alder (Alnus Glutinosa L.) Gaertn. Subsp. Barbata (C.A. Mey) Yalt.) and Southern Pine (Pinus Sylvestris L.) Wood Treated with Boron Compounds. *Constr. Build. Mater.* **2008**, *22* (11), 2165–2169.

(340) Baysal, E.; Sonmez, A.; Colak, M.; Toker, H. Amount of Leachant and Water Absorption Levels of Wood Treated with Borates and Water Repellents. *Bioresour. Technol.* **2006**, *97* (18), 2271–2279.

(341) Laoutid, F.; Bonnaud, L.; Alexandre, M.; Lopez-Cuesta, J.-M.; Dubois, P. New Prospects in Flame Retardant Polymer Materials: From Fundamentals to Nanocomposites. *Mater. Sci. Eng. R Reports* **2009**, *63* (3), 100–125.

(342) Di Blasi, C.; Branca, C.; Galgano, A. Thermal and Catalytic Decomposition of Wood Impregnated with Sulfur- and Phosphorus-Containing Ammonium Salts. *Polym. Degrad. Stab.* **2008**, *93* (2), 335–346.

(343) George. Treatment of Wood with Glucose-Diammonium Phosphate for Fire and Fungal Decay Protection. In *"6th pacific rim bio-based composites symposium & workshop on the chemical modification of 72 cellulosics";* Volume 2, Corvallis: Oregon (USA), 2002.

(344) Song, R.; Wang, Z.; Meng, X.; Zhang, B.; Tang, T. Influences of Catalysis and Dispersion of Organically Modified Montmorillonite on Flame Retardancy of Polypropylene Nanocomposites. *J. Appl. Polym. Sci.* **2007**, *106* (5), 3488–3494.

(345) Kashiwagi, T.; Gilman, J. Silicon Based Flame Retardants. In *Fire retardancy of polymeric materials*; Marcel Dekker Inc.: New York, 2000; pp 353–389.

(346) Lu, S.-Y.; Hamerton, I. Recent Developments in the Chemistry of Halogen-Free Flame Retardant Polymers. *Prog. Polym. Sci.* **2002**, *27* (8), 1661–1712.

(347) Fu, Q.; Medina, L.; Li, Y.; Carosio, F.; Hajian, A.; Berglund, L. A. Nanostructured Wood Hybrids for Fire-Retardancy Prepared by Clay Impregnation into the Cell Wall. *ACS Appl. Mater. Interfaces* **2017**, *9* (41), 36154–36163.

(348) Du, L.; Xu, G.; Zhang, Y.; Qian, J.; Chen, J. Synthesis and Properties of a Novel Intumescent Flame Retardant (IFR) and Its Application in Halogen-Free Flame Retardant Ethylene Propylene Diene Terpolymer (EPDM). *Polym. Plast. Technol. Eng.* **2011**, *50* (4), 372–378.

(349) Liang, S.; Neisius, N. M.; Gaan, S. Recent Developments in Flame Retardant Polymeric Coatings. *Prog. Org. Coatings* **2013**, *76* (11), 1642–1665.

(350) Beh, J. H.; Yew, M. C.; Yew, M. K.; Saw, L. H. Fire Protection Performance and Thermal Behavior of Thin Film Intumescent Coating. *Coatings* **2019**, *9* (8), 483.

(351) Qu, H.; Wu, W.; Zheng, Y.; Xie, J.; Xu, J. Synergistic Effects of Inorganic Tin Compounds and Sb2O3 on Thermal Properties and Flame Retardancy of Flexible Poly(vinyl Chloride). *Fire Saf. J.* **2011**, *46* (7), 462–467.

(352) Weil, E. D. Fire-Protective and Flame-Retardant Coatings - A State-of-the-Art Review. *J. Fire Sci.* **2011**, *29* (3), 259–296.

(353) Xiao, Z.; Liu, S.; Zhang, Z.; Mai, C.; Xie, Y.; Wang, Q. Fire Retardancy of an Aqueous, Intumescent, and Translucent Wood Varnish Based on Guanylurea Phosphate and Melamine-Urea-Formaldehyde Resin. *Prog. Org. Coatings* **2018**, *121*, 64–72.

(354) Puri, R. G.; Khanna, A. S. Intumescent Coatings: A Review on Recent Progress. *J. Coatings Technol. Res.* **2017**, *14* (1), 1–20.

(355) Kozlowski, R.; Wesolek, D.; Wladyka-Przybylak, M.; Duquesne, S.; Vannier, A.; Bourbigot, S.; Delobel, R. Intumescent Flame-Retardant Treatments for Flexible Barriers. In *Multifunctional Barriers for Flexible Structure*; Springer Berlin Heidelberg: Berlin, Heidelberg, 2007; pp 39–61.

(356) Hill, C. A. S. Thermal Modification of Wood. In *Wood modification : chemical, thermal and other processes*; John Wiley & Sons, 2006; pp 99–127.

(357) Herrera, R.; Arrese, A.; de Hoyos-Martinez, P. L.; Labidi, J.; Llano-Ponte, R. Evolution of Thermally Modified Wood Properties Exposed to Natural and Artificial Weathering and Its Potential as an Element for Façades Systems. *Constr. Build. Mater.* **2018**, *172*, 233–242.

(358) Pizzi, A. Wood Products and Green Chemistry. *Ann. For. Sci. Springer Verlag* **2016**, *73* (1), 185–23.

(359) Karunanayake, L.; Sumathirathne, L. Synthesis of Novel Porous Tannin-Phenol-Formaldehyde Cation Exchange Resin from Terminalia Arjuna (Kumbuk). *J. Natl. Sci. Found. Sri Lanka* **2017**, *45* (3), 219.

(360) Liu, Y.; Wang, J.-S.; Deng, C.-L.; Wang, D.-Y.; Song, Y.-P.; Wang, Y.-Z. The Synergistic Flame-Retardant Effect of O-MMT on the Intumescent Flame-Retardant PP/CA/APP Systems. *Polym. Adv. Technol.* **2010**, *21* (11), 789–796.

(361) Rezakazemi, M.; Vatani, A.; Mohammadi, T. Synergistic Interactions between POSS and Fumed Silica and Their Effect on the Properties of Crosslinked PDMS Nanocomposite Membranes. *RSC Adv.* **2015**, *5* (100), 82460–82470.

(362) Basu, P.; Basu, P. Biomass Characteristics. *Biomass Gasif. Pyrolysis* **2010**, 27–63.

(363) dos Santos Viana, H. F.; Rodrigues, A. M.; Godina, R.; Matias, J. C. de O.; Nunes, L. J. R. Evaluation of the Physical, Chemical and Thermal Properties of Portuguese Maritime Pine Biomass. *Sustainability* **2018**, *10* (8), 1–15.

(364) White, R. H. Effect of the Lignin Content and Extractives on the Higher Heating Value of Wood. *Wood Fiber Sci.* **1983**, *19* (4), 446–452.

(365) Demirbas, A. Relationships Between Heating Value and Lignin, Moisture, Ash and Extractive Contents of Biomass Fuels. *Energy Exploration & Exploitation*. Sage Publications, Ltd. 2002, pp 105–111.

(366) Griu, T.; Lunguleasa, A. The Use of the White Poplar (Populus Alba L.) Biomass as Fuel. *J. For. Res.* **2016**, *27* (3), 719–725.

(367) Álvarez-Álvarez, P.; Pizarro, C.; Barrio-Anta, M.; Cámara-Obregón, A.; Bueno, J.; Álvarez, A.; Gutiérrez, I.; Burslem, D. Evaluation of Tree Species for Biomass Energy Production in Northwest Spain. *Forests* **2018**, *9* (4), 160.

(368) Rodríguez-García, A.; Martín, J. A.; López, R.; Sanz, A.; Gil, L. Effect of Four Tapping Methods on Anatomical Traits and Resin Yield in Maritime Pine (Pinus Pinaster Ait.). *Ind. Crops Prod.* **2016**, *86*, 143–154.

(369) Demirbas, A. Higher Heating Values of Lignin Types from Wood and Non-Wood Lignocellulosic Biomasses. *Energy Sources, Part A Recover. Util. Environ. Eff.* **2017**, *39* (6), 592–598.

(370) Telmo, C.; Lousada, J. The Explained Variation by Lignin and Extractive Contents on Higher Heating Value of Wood. *Biomass and Bioenergy* **2011**, *35* (5), 1663–1667.

(371) De Meijer, M. A Review of Interfacial Aspects in Wood Coatings: Wetting, Surface Energy, Substrate Penetration and Adhesion. In *COST E18 Final Seminar: High performance wood coatings*; 2005; p 16.

(372) Burger, N.; Laachachi, A.; Ferriol, M.; Lutz, M.; Toniazzo, V.; Ruch, D. Review of Thermal Conductivity in Composites: Mechanisms, Parameters and Theory. *Prog. Polym. Sci.* **2016**, *61*, 1–28.

(373) Mishra, R.; Militky, J.; Mishra, R.; Militky, J.; Venkataraman, M. Nanoporous Materials. In *Nanotechnology in Textiles*; Woodhead Publishing, 2019; pp 311–353.

(374) Hedge, J. E.; Hofreiter, B. T. Methodology for Carbohydrates: Determination of Total Carbohydrates by Anthrone Method. In *Carbohydrate Chemistry*; Whistler R L, Be Miller, J. N., Eds.; Academic Press: New York, 1962.

(375) Chandra, S.; Khan, S.; Avula, B.; Lata, H.; Yang, M. H.; Elsohly, M. A.; Khan, I. A. Assessment of Total Phenolic and Flavonoid Content, Antioxidant Properties, and Yield of Aeroponically and Conventionally Grown Leafy Vegetables and Fruit Crops: A Comparative Study. *Evid. Based. Complement. Alternat. Med.* **2014**, *2014*, 253875.

(376) Scalbert, A.; Monties, B.; Janin, G. Tannins in Wood: Comparison of Different Estimation Methods. *J. Agric. Food Chem.* **1989**, *37* (5), 1324–1329.

(377) Yazaki, Y.; Hillis, W. E. Molecular Size Distribution of Radiate Pine Bark Extracts and Its Effect on Properties. *Holtzforschung* **1998**, *34*, 125–130.

Annexes

Annex I: Characterization of the lignocellulosic biomass

I.1 Moisture content

Procedure TAPPI T264-cm-97. Preparation of wood for chemical analysis.

I.2 Extractives content

Procedure TAPPI T204-cm-97. Solvent extractives of wood and pulp.

I.3 Ashes content

Procedure TAPPI T211 om-02. Ash in wood, pulp, paper and paperboard: combustion at 525 °C

I.4 Acid insoluble lignin content

Procedure TAPPI T222-om-98. Quantitative acid hydrolysis with 72% H_2SO_4.

I.5 Holocellulose content of biomass

Holocellulose comprises the water insoluble carbohydrates fraction of the lignocellulose, that is, the sum of hemicellulose and cellulose. The holocellulose content was determined according to the method proposed by Wise et al., 1946.

I.6 Cellulose content of biomass

The procedure to obtain the wood cellulose is referred as the ''Rowell method'' from the book: The Chemistry of Solid Wood, 1984, edited by Professor R. Rowell.

Annex II: Characterization of the liquor from organosolv extraction

II.1.1 Density

The density was calculated gravimetrically by measuring the weight of known volume of a volumetric flask filled with the liquid fraction.

II.1.2 pH

The pH of the liquid fraction was determined using a pH meter "CRISON basic 20".

II.2 Chemical composition of the liquor

The chemical composition of the liquor obtained from the organosolv extraction process was assessed based on the content of total dissolved solids, the organic content, inorganic content and the lignin content.

The percentage of total dissolved solids (TDS) was performed according to the ASTM D4426-96 standard.

The inorganic content (IC) was determined by the combustion of a liquor sample in a muffle. The crucible assembly-solid residue obtained in the previous experiment (total dry solids) is combusted in the oven at 525 ºC for 3 hours. Subsequently, after cooling to room temperature in desiccators, the crucible is weighed assembly (m_f).

$$IM\ (\%) = [(m_f - m_i)/m] \cdot 100 \qquad (10)$$

m_f: final weight of the crucible after combustion
m_i: weight of dried crucible with solid dry residue
m: weight of the liquid sample

The organic matter (OM) is determined by the difference between the percentage of total dissolved solids (TDS) and inorganic content (IM).

$$OM\ (\%) = TDS\ (\%) - IM\ (\%) \quad (11)$$

The lignin content in the liquor (LC) was calculated as the ratio between the lignin extracted and the volume of the liquor obtained from the organosolv process.

$$LC\ (\%) = [m_L/(V_L \cdot \rho_L)] \cdot 100 \quad (12)$$

m_L: mass of lignin extracted

V_L: volume of liquor obtained from the organosolv process

ρ_L: density of the liquor obtained from the organosolv process

Annex III: Characterization of the lignins

III.1.1 Klason lignin (acid-insoluble lignin)

3.75 mL of 72% of H_2SO_4 was added to 3.75 mg of lignin sample and was maintained for 1 h at 30 °C. Then, 36.25 mL of distilled water was added, and it was hydrolyzed at 120°C during 1.5 h. After cool down for 15 minutes, the solid residue was filtrated, oven dried and weighed as Klason lignin. The percentage of this parameter is calculated as follows:

$$\text{Klason lignin (\%)} = [A/W] \cdot 100 \quad (13)$$

A: weight of acid-insoluble lignin
W: weight of the initial sample

III.1.2 Acid-soluble lignin

The filtrated liquid fraction from the previous method was reserved for determination of acid soluble lignin fraction by spectrophotometry (UV absorption at 205 nm).

III.1.3 Ash content

The ash content of the lignins was determined by following the same procedure described in Annex I.3 of combustion at 525 ºC.

III.1.4 Carbohydrate content by means of high performance liquid chromatography (HPLC)

A part of the filtrated liquid fraction reserved from the acid-insoluble lignin was injected into a high performance liquid chromatography equipment to elucidate the main monosaccharides present in the lignin samples. This liquid phase was analyzed via High Performance Liquid Chromatography (HPLC) using a Jasco LC Net II/ADC chromatograph equipped with a refractive index detector and a diode array detector.

An aliquot of the liquid phase was used to quantify the main monosaccharides and degradation products employing a Phenomenex

Rezex ROA column. The mobile phase (0.005 N H_2SO_4) was eluted at a flow rate of 0.35 mL·min^{-1} at 40 ºC. Standards of high purity of D-(+)-glucose, D-(+)-xylose and D-(-)-arabinose (provided by Flucka) were employed as calibration. The carbohydrate content was determined as follows:

$$\text{Carbohydrate content (\%)} = [(A \cdot B)/(C \cdot 1000)] \cdot 100 \quad (14)$$

A: concentration obtained in the HPLC

B: total volume filtrated in the acid-insoluble lignin method

C: initial weight of lignin

III.2 Total hydroxyl groups content

The total hydroxyl group content of the lignin samples was determined by the Folin-Ciocalteu spectrophotometric method employing gallic acid as reference and dimethyl sulfoxide (DMSO) as solvent standard. The samples of lignin were prepared with a concentration 2 g·L^{-1} in dimethyl sulphoxide (DMSO). For the assay, aliquots of 0.5 mL lignin solution were mixed with 2.5 mL of Folin Ciocalteau reagent (Merck) and 5mL Na_2CO_3 and brought to a volume of 50 mL with distillate water. Following to that, the samples were covered to protect them against light and kept into a thermostatic bath at 40 ºC for 30 min. After this time, the absorbance of the samples at 750 nm was measured using a spectrophotometer Jasco V-630 UV with UV quartz cells and a 10mm light path. The calibration curve was done using solutions of gallic acid in DMSO in the range 100-1000 mg·L^{-1}. The results were presented either as concentration of gallic acid equivalents, as percentage of gallic acid equivalents and as percentage of hydroxyl groups:

$$C_{GAE}\,(\text{mg}\cdot\text{L}^{-1}) = A/K_{cal} \quad (15)$$

A: absorbance measured at 750 nm

K_{cal}: slope of the calibration curve obtained with gallic acid

$$GAE\ (\%) = C_{GAE} / C_{sample} \quad (16)$$

C_{GAE}: concentration of gallic acid equivalents

C_{sample}: initial concentration of the lignin samples

$$OH(\%) = C_{GAE}\ (1/M_{wGA}) \cdot n \cdot M_{wOH} \cdot (1/C_{sample}) \cdot 100 \quad (17)$$

C_{GAE}: concentration of gallic acid equivalents

M_{wGA}: molecular weight of gallic acid

n: number of hydroxyl groups

M_{wOH}: molecular weight of hydroxyl groups

C_{sample}: initial concentration of the lignin samples

III.3 Molecular weight determination by means of High performance size exclusion chromatography (HPSEC)

This analysis was performed with a chromatograph Jasco instrument equipped with an interface LC Net II/ADC, a reflex index detector RI-2031Plus and two PolarGel-M (300 mm × 7.5 mm) columns displayed in series. The analyses were carried out using dimetylformamide with 0.1% lithium bromide as mobile phase and a 0.7·mL min^{-1} flow at 40 °C. The equipment was calibrated using polystyrene standards from Sigma-Aldrich ranging between 70000 and 266 $g \cdot mol^{-1}$. All of the samples were analyzed in duplicate and if still considerable divergences were observed, a triplicate was carried out.

III.4 Pyrolysis-gas chromatography/mass spectroscopy analysis (Py-GC/MS)

The equipment used was a 5150 Pyroprobe pyrolyzer branched to a gas chromatograph (Agilent 6890), which was coupled to a mass spectrometer (Agilent 5973). The GC column size dimensions were 30 m × 0.25 mm × 0.25 μm.

The samples in the range of 400−800 μg, were pyrolyzed at 600 °C for 15 s using a heating rate of 20 $°C \cdot ms^{-1}$. Then, the pyrolyzates were purged from the pyrolysis interface into the GC injector under inert conditions (He).

The GC oven was programmed in the following intervals: start at 50 °C and hold for 2 min; temperature increases to 120 °C at 10 °C·min^{-1} holding it for 5 min; increment of temperature to 280 °C at 10 °C·min^{-1} hold during 8 min; and a final temperature raise to 300 °C at 10 °C·min^{-1} hold for another 10 min. The identification of the compounds was achieved by the gas chromatograph coupled to the mass spectrometer (GC–MS). This identification was carried out by comparing the obtained mass spectra to the National Institute of Standards Library (NIST) and the mass spectra of other compounds reported in the literature, especially through their m/z numbers.

III.5 Thermogravimetric analysis (TGA)

This analysiswas performed in a TA instrument thermogravimetric analysis (TGA) Q5000 IR equipment, under dynamic nitrogen flow with a flow rate of 40 mL min^{-1}. Samples in the range of 5−10 mg were placed in a platinum crucible and heated in a temperature range of 30−800 °C at a constant heating rate of 10 °C min^{-1} under a N_2 or O_2 atmosphere (airflow 60mL·min^{-1}). For the quantitative calculations, the response factors between the weight gain (thermogravimetric) and the mass loss rate (differential thermogravimetric) were determined.

III.6.1 Fourier Transformed Infrared Spectroscopy analysis (FTIR)

The Fourier transformed infrared (FTIR) analysis was performed on a Spectrum Two FTIR Spectrometer PerkinElmer (USA) with a L1050231 Universal Attenuated Total Reflectance accessory (ATR). First, a background spectrum was collected to subtract it from the spectrum of the sample.

Then, a few mg of the sample were analyzed, with a number of 64 scans accumulated in transmission mode and a resolution of 4 cm^{-1}. The spectrum was obtained in the range of 4000−400 cm^{-1}.

III.6.2 ^{1}H-Nuclear Magnetic Resonance spectroscopy analysis (^{1}H-NMR)

The ^{1}H NMR analysis was performed in a 400 MHz Bruker AVANCE spectrometer (equipped with a 5 mm BBFO probe) at ambient temperature by using dimethyl sulfoxide (DMSO) as solvent. The chemical shifts are quoted in ppm relative to tetramethylsilane (δH = 0.00 ppm). The experimental conditions consisted of a pulse width 8.1 ms (zg pulse program), an acquisition time of 1.9 s, a pre-scan delay of 6.5 μs, and a relaxation delay between scans of 5 s. The spectrum width was 16.0 ppm (6400 Hz) and 128 scans were accumulated.

III.6.2.1 Determination of hydroxyl groups by means of ^{1}H-Nuclear Magnetic Resonance spectroscopy analysis (^{1}H-NMR)

To confirm the presence of hydroxyl groups within the signals from the NMR spectra, the samples were added to trifluoroacetic acid (TFA) prior to the ^{1}H NMR analysis. TFA is known to react with alcohols through the hydroxyl groups, leading to the esterification of the polymer. By comparing the spectra of the samples without any TFA added and the spectra after addition of a small volume of TFA, the position of the peaks due to the hydroxyl groups can be determined. Thereby, it is seen that some peaks present in the spectra of the original samples, disappear after adding TFA. These signals can be undoubtedly defined as hydroxyl derived protons.

III.7 X-ray Diffraction analysis

X-ray powder diffraction was measured to evaluate the introduction and substitution of the inorganic nanoparticles in the modified lignin structure. Diffraction scatters were collected with a Panalytical Phillips X'Pert PRO multipurpose diffractometer (Almelo, the Netherlands) using monochromatic Cu Kα radiation (λ = 1.541874 Å) in the 2θ range from 3° to 70° with a step size of 0.026 at room temperature and a counting time of 148.92 s.

Annex IV: Characterization of the tannins

IV.1 Anthrone method (total carbohydrate content)

This method was based on the procedure described by Hedge and Hofreiter, 1962 [374]. A sample amount of 100 mg was taken into boiling tubes and hydrolyzed by keeping it in boiling water bath for 3 h with 5 mL of a solution of HCl 2.5 N. After that, the samples were cooled down to room temperature and they were diluted to a volume of 100 mL with distilled water. Then, they were centrifuged and the supernatant was taken for analysis. An aliquot of 0.5 mL of this supernatant was diluted to 1mL with distilled water and added 4mL of the anthrone reagent (200mg of athrone in 100 mL of sulfuric acid 95 %). Then, it was heated during 8 minutes in a boiling water bath and cooled rapidly to read the absorbance at 630 nm using a spectrophotometer Jasco V-630 UV with UV quartz cells and a 10 mm light path. The calibration curve was done using solutions of glucose in water in the range 0-100 $mg \cdot L^{-1}$. The results were presented either as concentration in mg/L or percentage of glucose:

$$C_{glucose}\ (mg \cdot L^{-1}) = A/K_{cal} \quad (18)$$

A: absorbance measured at 630 nm

K_{cal}: slope of the calibration curve obtained with glucose

$$Glucose\ (\%) = C_{glucose}/C_{sample} \quad (18)$$

$C_{glucose}$: concentration of glucose standard

C_{sample}: initial concentration of the extracts

IV.2 Total flavonoid content

This method was carried out based on the work by Chandra et al., 2014 [375]. Extracts of $1 mg \cdot mL^{-1}$ in ethanol were prepared and then diluted to 1 mL with methanol. Following to this, the samples were added 4 mL of distilled water and 0.3 mL of $NaNO_2$ (5%) and incubated during 5 minutes. After that, 0.3 mL $AlCl_3$ (10%) were added and the mixture was agitated by

means of a vortex and left stand during 6 minutes. Then, 2 mL of NaOH 1M and the samples were brought to a volume of 10 mL of distilled water. Finally it was left stand during 15 minutes and the absorbance was measured at 510 nm using a spectrophotometer Jasco V-630 UV with UV quartz cells and a 10mm light path. The calibration curve was done using solutions of quercetin in methanol in the range 0-120 $mg \cdot L^{-1}$. The results were presented either as concentration in mg/L or percentage of quercetin equivalents:

$$C_{QE}\,(mg \cdot L^{-1}) = A/K_{cal} \qquad (19)$$

A: absorbance measured at 510 nm

K_{cal}: slope of the calibration curve obtained with quercetin

$$QE\,(\%) = C_{QE}/C_{sample} \qquad (20)$$

$C_{quercetin}$: concentration of quercetin equivalents

C_{sample}: initial concentration of the extracts

IV.3 Total condensed tannin content

This method was carried out based on the work by Scalbert et al., 1989 [376]. An aliquot of 0.5 mL of aqueous extract (diluted 100 times) was added to 5 mL of an acidic ferrous solution (77 mg of FeSO4·7H2O in 500 mL of HCl/BuOH (2/3)). The tubes were covered and placed in a water bath at 95 C for 15 minutes.

Then, the absorbance was measured at 530 nm using a spectrophotometer Jasco V-630 UV with UV quartz cells and a 10 mm light path. The results were expressed as concentration in percentage of cyaniding equivalents. This content was calculated using the formula given below:

$$CyE\,(\%) = [(A \cdot V_T \cdot D \cdot M_{wCy})/(l \cdot \varepsilon \cdot \nu \cdot m_{sample})]*100 \qquad (20)$$

A: absorbance of the sample at 530nm

V_T: total volume of reaction

D: dilution factor

M_{wCy}: molecular weight cyanindin

l: path length

ε: molar extinction coefficient
ν: volume of aliquot of extract
m_{sample}: mass of dry extract sample

IV.4 Stiansy index (tannins reactivity)

The reactivity of extractives with regard to formaldehyde was determined by the Stiasny number measurement as described by Yazaki and Hills., 1998 [377]. A solution of extracts of 4 $g.L^{-1}$ was prepared. Then, 25 mL of this solution was poured in a round bottom flask and 5 mL of formaldehyde (37%) and 2.5 mL of HCl (10 M) were added. The mixture was heated under reflux for 30 min. The residue was filtered through a sintered glass n°3. Finally, the precipitate was washed with distilled water and was dried at 105 °C during 24 h. The reactivity was calculated as follows:

$$SI\ (\%) = A/B \qquad (21)$$

A: dry weight of precipitate
B: dry weight of tannin extract

Annex V: Characterization of the resins

V.1.1 Viscosity

Shear viscosity was measured using a viscometer Alfa (Fungilab) with a small sample adapter (APM/B), and a TL5 spindle. Samples of 6mL were placed in the portable sampler and the viscosity was measured using the suitable rotation speed. Several measurement were taken over time until the values became constant.

V.1.2 Non-volatile content (NVC)

Procedure ASTM D4426-01. Standard Test Method for Determination of Percent Nonvolatile Content of Liquid Phenolic Resins Used for Wood Laminating.

V.2 Determination of the hydroxyl number

Procedure ASTM D4274-99. Standard Test Method for Testing Polyurethane Raw Materials: Determination of Hydroxyl Numbers of Polyols.

V.3 Determination of the acid/alkalinity number

Procedure ASTM D974-04. Standard Test Method for Polyurethane Raw materials: Determination of Acid and Alkalinity Numbers of Polyols.

V.4 Differential Scanning Calorimetry analysis (DSC)

This analysis was carried out in a TA instrument (DSC Q500) under dynamic nitrogen flow rate of 60 mL min^{-1}. Samples between 4-8 mg were placed in a sealed aluminum pan of high pressure and heated in the range 30-525 ºC at a constant heating rate of 10 °C min^{-1} under nitrogen atmosphere.

Annex VI: Assessment of the performance of the coatings

VI.1 Calorimetry pump analysis

This test was carried out by means of a Parr 6200 Calorimeter in isoperibolic mode. The combustion of the samples was performed in a Parr 1108 oxygen bomb. The samples were prepared with a size of 20x20x3 mm so that they could fit into the circular sample holder of the oxygen bomb. Then a tungsten filament was connected between the two poles of the oxygen bomb, in which the current was applied to produce the spark leading to the combustion. It was assured that the filament was in contact to the sample, which was subjected to combustion. Then the oxygen bomb was hermetically close and it was pressurized with oxygen. Following to this, the bomb was meticulously introduced into an oval bucket, which was filled with 2 L of water, and in the calorimeter. After that, the wires producing the current were connected from the calorimeter to the poles of the oxygen bomb and the machine was closed. Then the analysis was started through the interface of the machine and after a period of 6 minutes, the results of the High Heating Values (HHV) of the samples were presented in the screen. The measurements for this analysis were done in triplicate. Besides a calibration was performed before analyzing any samples by using benzoic acid, which has a known HHV (26.454 $MJ \cdot Kg^{-1}$). After every measurement, the bomb was depressurized and then open to clean the inside wall and the lid, and to remove the pieces of the remaining filament. After each combustion, no sample was remaining inside the oxygen bomb.

VI.2 Flammability analysis

Procedure UNE-EN 60695-11-10:2014. Ensayos relativos a los riesgos del fuego. Parte 11-10: Llamas de ensayo. Métodos de ensayo horizontal y vertical a la llama de 50W.

VI.3 Conductivity analysis

This test was performed with conductivity meter instrument "Hot Disk TPS 1500" and a probe Kapton Ref. 5456 of 3.189 mm radius. First, the wood samples were prepared with dimensions 30x20x10 mm. Two symmetrical parts of each sample were cut to set them in the upper and the lower part of the probe. Prior to the measure of the conductivity, different parameters (power and time of discharge) were set appropriately to ensure the accuracy of the results. Besides the temperature of both parts of the sample was measured and set as another input parameter of the machine. The conductivity was measured in triplicate for each of the samples.

Annex VII: List of figures

Annex VIII: List of tables